Analyse temporelle de la dynamique de communautés végétales à l'aide de modèles individus-centrés

Théophile Lohier

N d'ordre: D.U : 2686
EDSPIC : 750

UNIVERSITÉ BLAISE PASCAL
U.F.R. Sciences et Technologies

ÉCOLE DOCTORALE DES SCIENCES POUR L'INGÉNIEUR

THÈSE

présentée pour obtenir le grade de

DOCTEUR D'UNIVERSITÉ

Spécialité: Informatique

par Théophile LOHIER

Analyse temporelle de la dynamique de communautés végétales à l'aide de modèles individus-centrés.

Temporal analysis of plant community dynamics using individual-based models.

Soutenue le 24 mars 2016

Rapporteurs :	Sabrina GABA Chargée de recherches, Institut National de la Recherche Agronomique, Dijon
	Jacques GIGNOUX Chargé de recherches, Université Pierre et Marie Curie, Paris
Directeur de thèse :	Guillaume DEFFUANT Directeur de recherche, Irstea, Clermont-Ferrand
Examinateurs :	Nicolas MOUQUET Directeur de recherche, Institut des Sciences de l'Évolution, Montpellier
	Pierre BERTRAND Professeur, Université Blaise Pascal, Clermont-Ferrand
Encadrant :	Franck JABOT IPEF, Irstea, Clermont-Ferrand

Avant-propos

Cette thèse a été réalisée à IRSTEA (Institut National de Recherche en Sciences et Technologies pour l'Environnement et l'Agriculture)[1] de Clermont-Ferrand au sein du Laboratoire d'Ingénierie pour les Systèmes Complexes (LISC)[2].

Cette thèse a pu être réalisée grâce au soutien financier de la région Auvergne[3] dans le cadre de sa politique de participation au développement de la recherche, notamment à travers le financement d'allocations de recherche.

[1] www.irstea.fr
[2] http://motive.cemagref.fr/lisc/presentation
[3] www.auvergne.fr

Remerciements

La route a été longue et parsemée d'embuches. Heureusement, durant ce voyage initiatique qu'est la thèse je n'ai jamais été isolé. J'aimerais ici remercier ceux qui ont accepté de faire un petit bout de chemin avec moi et qui m'ont aidé à relever la tête dans les moments difficiles.

J'ai eu la chance d'être entouré pendant mon voyage de vieux briscards de la recherche qui arpentent ses voies depuis plusieurs années. Ils m'ont accueillis à bras ouvert au sein de leur petite communauté et n'ont pas hésité à partager avec moi leurs expériences avec simplicité et bonne humeur. Je me suis senti chez moi parmi vous et pour cela un grand merci.

Un grand merci également à Franck qui m'a guidé tout au long de ce périple. Plus que ses connaissances et ses conseils grâce auxquels j'ai pu éviter bien des ecueils, c'est sa vision de la recherche et sa façon d'être au quotidien que je veux saluer ici.

Lorsque la journée s'achève, il est essentiel de trouver un havre pour se reposer. Au moment de retirer mes godasses de thésard pour me chauffer les arpions au coin du feu, j'ai toujours bénéficié d'une compagnie de qualité. Pour cela, je remercie maître Cadot, toujours prompt à embarquer ses hôtes dans des discussions animés, le docteur Bombrun et ses anecdotes scientifiques croustillantes, le baron Fouki dont les largesses resteront fameuses à Romagnat et le capitaine Rackham le Roux, toujours partant pour mettre les voiles vers des terres plus verdoyantes. Merci également aux voyageurs de passage qui m'ont aidé par leur présence et leurs rires à oublier la fatigue et les coups de blues.

Cultiver une relation amoureuse tout en maintenant le cap est loin d'être chose aisée mais j'ai eu la chance d'être accompagné pendant les moments les plus difficiles de cette thèse par une compagne compréhensive et attentionée qui a toujours répondu présente quand ça n'allait pas et m'a aidé à touver un équilibre entre vie professionnelle et vie sentimentale. Toute mes pensées vont vers elle.

Enfin, j'aimerais exprimer ma gratitude envers mes parents et ma fraterie. Aucune métaphore bancale, aucune anecdote évocatrice ne saurait suffire à mettre en lumière tout ce que je leur dois, ni tout l'amour que je leur porte.

Résumé

Les communautés végétales constituent des systèmes complexes au sein desquels de nombreuses espèces, pouvant présenter une large variété de traits fonctionnels, interagissent entre elles et avec leur environnement. En raison de la quantité et de la diversité de ces interactions les mécanismes qui gouvernent les dynamiques des ces communautés sont encore mal connus. Les approches basées sur la modélisation permettent de relier de manière mécaniste les processus gouvernant les dynamiques des individus ou des populations aux dynamiques des communautés qu'ils forment. L'objectif de cette thèse était de développer de telles approches et de les mettre en oeuvre pour étudier les mécanismes sous-jacents aux dynamiques des communautés.

Nous avons ainsi développés deux approches de modélisation. La première s'appuie sur un cadre de modélisation stochastique permettant de relier les dynamiques de populations aux dynamiques des communautés en tenant compte des interactions intra- et interspécifiques et de l'impact des variations environnementale et démographique. Cette approche peut-être aisément appliquée à des systèmes réels et permet de caractériser les populations végétales à l'aide d'un petit nombre de paramètres démographiques. Cependant nos travaux suggèrent qu'il n'existe pas de relation simple entre ces paramètres et les traits fonctionnels des espèces, qui gouvernent pourtant leur réponse aux facteurs externes. La seconde approche a été développée pour dépasser cette limite et s'appuie sur le modèle individu-centré Nemossos qui représente de manière explicite le lien entre le fonctionnement des individus et les dynamiques de la communauté qu'ils forment. Afin d'assurer un grand potentiel d'application à Nemossos, nous avons apportés une grande attention au compromis entre réalisme et coût de paramétrisation. Nemossos a ainsi pu être entièrement paramétré à partir de valeur de traits issues de la littérature , son réalisme a été démontré, et il a été utilisé pour mener des expériences de simulations numériques sur l'importance de la variabilité temporelle des conditions environnementales pour la coexistence d'espèces fonctionnellement différentes.

La complémentarité des deux approches nous a permis de proposer des éléments de réponse à divers questions fondamentales de l'écologie des communautés incluant le rôle de la compétition dans les dynamiques des communautés, l'effet du filtrage environnementale sur leur composition fonctionnel ou encore les mécanismes favorisant la coexistence des espèces végétales. Ici ces approches ont été utilisées séparément mais leur couplage peut offrir des perspectives intéressantes telles que l'étude du lien entre le fonctionnement des plantes et les dynamiques des populations. Par ailleurs chacune des approches peut être utilisée dans une grande variété d'expériences de simulation susceptible d'améliorer notre compréhension des mécanismes gouvernant les communautés végétales.

Mots clés: Modèle individu-centré, modèle stochastique, analyse de séries temporelles, sélection de modèle, inférence statistique, écophysiologie, dynamique des communautés végétales, prairie, traits fonctionnels, théorie de l'allocation optimale.

Abstract

Plant communities are complex systems in which multiple species differing by their functional attributes interact with their environment and with each other. Because of the number and the diversity of these interactions the mechanisms that drive the dynamics of theses communities are still poorly understood. Modelling approaches enable to link in a mechanistic fashion the process driving individual plant or population dynamics to the resulting community dynamics. This PhD thesis aims at developing such approaches and to use them to investigate the mechanisms underlying community dynamics.

We therefore developed two modelling approaches. The first one is based on a stochastic modelling framework allowing to link the population dynamics to the community dynamics whilst taking account of intra- and interspecific interactions as well as environmental and demographic variations. This approach is easily applicable to real systems and enables to describe the properties of plant population through a small number of demographic parameters. However our work suggests that there is no simple relationship between these parameters and plant functional traits, while they are known to drive their response to extrinsic factors. The second approach has been developed to overcome this limitation and rely on the individual-based model Nemossos that explicitly describes the link between plant functioning and community dynamics. In order to ensure that Nemossos has a large application potential, a strong emphasis has been placed on the tradeoff between realism and parametrization cost. Nemossos has then been successfully parameterized from trait values found in the literature, its realism has been demonstrated and it has been used to investigate the importance of temporal environmental variability for the coexistence of functionally differing species.

The complementarity of the two approaches allows us to explore various fundamental questions of community ecology including the impact of competitive interactions on community dynamics, the effect of environmental filtering on their functional composition, or the mechanisms favoring the coexistence of plant species. In this work, the two approaches have been used separately but their coupling might offer interesting perspectives such as the investigation of the relationships between plant functioning and population dynamics. Moreover each of the approaches might be used to run various simulation experiments likely to improve our understanding of mechanisms underlying community dynamics.

Keywords: Individual based modelling, stochastic modelling, time series analysis, model selection, statistical inference, ecophysiology, plant community dynamics, grassland, functional traits, optimal allocation theory.

Table des matières

I. Objectifs de la thèse et démarche adoptée

L'objectif scientifique de cette thèse est de montrer que l'information contenue dans les traits fonctionnels des espèces végétales prairiales peut être intégrée au sein de modèles mécanistes et que ces nouvelles approches de modélisation peuvent être utilisées pour améliorer notre compréhension des mécanismes gouvernant les dynamiques des communautés végétales.
Le choix de cette démarche est argumenté par une analyse bibliographique, présentée en partie II du document, dont nous exposons ici rapidement les points principaux. Puis, cette partie introductive présente une vue d'ensemble des différents modèles développés et des principaux résultats de cette thèse, exposés dans les chapitres III à VI.

Une pléiade d'études théoriques et empiriques se sont intéressées aux communautés végétales mais malgré de grandes avancées de nombreux patterns n'ont pas encore été expliqués. Au cours des deux dernières décennies l'écologie des communautés végétales a connu un changement de paradigme, délaissant les approches taxonomiques au profit d'approches plus fonctionnelles. Ce changement de paradigme offre une opportunité d'améliorer significativement notre compréhension des mécanismes gouvernant les dynamiques des communautés. Cependant la plupart des travaux menés jusqu'à présent se sont concentrés sur la recherche de corrélations empiriques ou se sont basés sur des modèles nuls (Swenson, 2013). Un moyen de dépasser la recherche de patterns et de remonter aux mécanismes qui structurent les communautés consiste à intégrer les informations apportées par les traits fonctionnels au sein d'approches plus mécanistes. Marks & Lechowicz (2006) ou encore VanWijk (2007) ont amorcé ce virage vers une écologie fonctionnelle plus englobante en

développant des modèles individus centrés axés sur le lien entre les traits et les processus physiologiques qui gouvernent le développement des végétaux. Marks & Lechowicz (2006) se sont concentrés sur les communautés forestières, tandis que VanWijk (2007) a proposé un modèle pour les communautés arctiques. Récemment Soussana et al. (2013) ont introduit une approche basée sur le même principe pour étudier le fonctionnement des communautés prairiales. Cependant la complexité de ce modèle (132 équations, 187 variables et 100 paramètres par défaut) rend sa paramétrisation à partir des traits fonctionnels couramment mesurés difficile et est susceptible d'altérer notre capacité à tracer les mécanismes à l'origine des dynamiques simulées. Par ailleurs ce modèle n'intègre pas la dynamique de l'eau à travers le continuum sol-plante-atmosphère, alors qu'il s'agit d'une ressource critique pour le développement des végétaux.

Notre analyse bibliographique suggère que des modèles mécanistes fondés sur des traits fonctionnels des plantes pourraient apporter des prédictions plus précises des patterns de communautés de plantes et une compréhension renouvelée de leurs causes. C'est le défi que ce travail de thèse cherche à relever. Deux approches de modélisation complémentaires ont ainsi été développées et mises en oeuvre pour identifier et quantifier ces mécanismes sous-jacents. Un premier modèle stochastique de dynamique de population basé sur l'analyse de séries temporelles de biomasse a été développé en s'appuyant sur les travaux de de Mazancourt et al. (2013). L'idée est de mettre en place un outil aisément traçable, permettant d'analyser l'impact des facteurs biotiques et abiotiques sur les dynamiques des communautés prairiales. Ce modèle a notamment permis de mettre en évidence l'importance des interactions compétitives sur les dynamiques des communautés indépendamment des variations des conditions environnementales et démographiques. Cependant les paramètres agrégés du modèle, bien qu'étant biologiquement pertinents, ne semblent pas directement reliés aux traits

fonctionnels des espèces, suggérant que l'échelle de la population n'est pas suffisamment fine pour distinguer les mécanismes sous-jacents. Un second modèle, axé sur l'individu et sur une représentation mécaniste des processus physiologiques qui déterminent son développement a alors été construit. La démarche adoptée pour développer ce modèle s'inscrit dans la dynamique amorcée par Marks & Lechowicz (2006), les traits fonctionnels occupant une place centrale dans la représentation des processus physiologiques. Par ailleurs une grande attention a été apportée à la complexité des modules utilisés pour décrire les processus physiologiques. Le modèle peut ainsi être entièrement paramétré à partir de traits fonctionnels couramment mesurés sur le terrain.

I.1. Analyser les mécanismes structurant les communautés à l'aide d'un modèle stochastique de dynamique des populations

Les modèles de dynamique de population basés sur les équations de Lotka-Volterra on été largement utilisés en écologie des communautés pour étudier l'effet des interactions interspécifiques sur la dynamique des communautés (May & Leonard, 1975; Weiner & Thomas, 1986). Dans leur forme la plus classique ces modèles décrivent les dynamiques de N populations interagissant au sein d'une communauté à l'aide de N équations différentielles du premier ordre. La dynamique d'une population dépend uniquement de son taux de croissance intrinsèque et des interactions intra- et interspécifiques. Ces modèles ont été complexifiés de manière à intégrer les effets de facteurs abiotiques tels que la disponibilité des ressources au sein de l'habitat sur le taux de croissance de la population (Armstrong & McGehee, 1980; Tilman, 1985). Théoriquement, il est possible d'intégrer un nombre illimité de ressources dans ce modèle, cependant cela implique de connaître la forme de la relation entre le taux de croissance de la population et la disponibilité des différentes ressource. Un moyen de

contourner ce problème consiste à décrire l'effet des conditions environnementales sur le taux de croissance de la population à l'aide d'une unique variable aléatoire (Ives et al., 2000). Cette approche a par la suite été complexifiée de manière à intégrer les effets de la variabilité démographique sur le taux de croissance (Loreau et al., 2008).

Dans ce cadre, les dynamiques des populations sont décrites à travers leur densité. Cet indicateur est pertinent pour des populations d'individus facilement dénombrables, comme c'est le cas pour la plupart des populations animales ou des populations d'arbres. Cependant pour la majorité des populations composant les communautés prairiales la densité est difficile à estimer. De plus les taux de reproduction des populations végétales dépendent de leur densité mais aussi de la quantité de ressources que les individus ont été en mesure d'extraire de l'habitat, qui peut se traduire en termes de biomasse produite. De même l'intensité des interactions compétitives au sein des populations et de la communauté est conditionnée par la densité mais également et surtout par la quantité de biomasse produite par chaque individu. Ainsi une espèce produisant une grande quantité de biomasse va souvent avoir un impact plus grand sur ses concurrents à travers par exemple une forte interception de la lumière. Pour ces raisons, l'étude des communautés végétales repose souvent sur la quantification de la biomasse des différentes populations (Roscher et al., 2011). Watkinson (1980) a été l'un des premiers à mettre en avant l'idée selon laquelle les modèles de dynamique de population seraient plus pertinents pour l'étude des communautés végétales s'ils décrivaient l'évolution de la biomasse plutôt que celle de la densité. De Mazancourt et al. (2013) ont ainsi proposé d'adapter le modèle stochastique de dynamiques introduit par Loreau et al. (2008) de manière à décrire les dynamiques des populations à travers leur biomasse et non plus leur densité. Cependant comme cette adaptation consiste simplement à remplacer la densité par la biomasse dans l'équation décrivant les dynamiques des populations, leur approche est

susceptible de mésestimer certains aspects fondamentaux des dynamiques des communautés végétales.

Le modèle développé par de Mazancourt et al. (2013) décrit la dynamique de la biomasse des populations avec un pas de temps saisonnier, ainsi la réduction de la production de biomasse pendant la saison *T* induite par les interactions intra- et interspécifiques est conditionnée par la biomasse produite pendant la saison (*T*-1). Pour les populations végétales, et plus particulièrement pour les populations des communautés prairiales qui subissent des réductions drastiques de leur biomasse entre deux saisons consécutives, dues notamment aux fauches ou à la période hivernale, l'influence de la biomasse à la fin d'une saison sur le taux de croissance de la population durant la saison suivante est susceptible de n'être que marginale. Pour ce type de population, le taux de croissance diminue tout au long de la saison à mesure que la biomasse des individus des différentes espèces augmente tandis que le niveau de ressource de l'habitat diminue. Afin de décrire l'impact des interactions compétitives sur les dynamiques des populations de manière plus réaliste, nous avons construit un nouveau modèle stochastique de dynamique de population ayant une résolution temporelle plus fine. En raison de cette modification de la structure du modèle les techniques de paramétrisation et d'analyse proposées par de Mazancourt et al. (2013) ne peuvent être appliquées. Par conséquent une méthode d'inférence permettant d'estimer les paramètres spécifiques à partir de séries temporelles réunissant des données sur les variations de la biomasse de communautés prairiales monospécifiques a été développée. A l'aide de cette approche nous avons mis en évidence l'importance des interactions intra- et interspécifiques dans les dynamiques des communautés. Par ailleurs nous avons étudié les corrélations entre les traits fonctionnels des différentes espèces et les paramètres du modèle qui caractérisent le taux de croissance intrinsèque d'une population ainsi que sa sensibilité aux variations environnementale et

démographique. Aucune corrélation significative n'a été trouvée, suggérant que les propriétés spécifiques résultent d'interactions entre plusieurs traits fonctionnels. Pour comprendre comment ces interactions façonnent la réponse des populations, il est nécessaire de développer des modèles plus mécanistes liant explicitement les traits fonctionnels aux processus physiologiques qui déterminent la réponse des espèces végétales.

I.2. Remonter aux mécanismes gouvernant les réponses individuelles pour comprendre les dynamiques des communautés.

Pour relier le fonctionnement des individus aux dynamiques de la communauté qu'ils forment, un modèle individu centré spatialement explicite a été développé. Les traits constituant un bon moyen de relier les propriétés fonctionnelles individuelles aux dynamiques des communautés, les modules décrivant les processus physiologiques ont été sélectionnés de manière à pouvoir être entièrement paramétrés à partir de traits couramment mesurés sur le terrain. Notre démarche de modélisation s'est alors décomposée en deux temps. Nous avons construit un premier modèle de croissance végétale qui nous a permis de sélectionner un module pour l'allocation du carbone, processus essentiel dans le fonctionnement de la plante. Puis ce modèle a été spatialisé, enrichi de plusieurs processus physiologiques connus pour jouer un rôle clé dans le fonctionnement des végétaux et relier à un modèle de sol qui décrit les dynamiques de l'eau et de l'azote. La cohérence des prédictions de ce modèle avec les observations empiriques a été testée à travers un ensemble d'expériences de simulation. Enfin ce modèle a été utilisé pour étudier les mécanismes favorisant la coexistence des espèces végétales ainsi que le lien entre traits fonctionnels et coexistence.

I.2.1. Un cadre mécaniste pour prédire l'allocation du carbone

Le développement des espèces végétales est fortement contraint par la quantité de ressources qu'elles sont capables d'extraire de leur habitat. La biomasse aérienne conditionne la fixation du carbone atmosphérique à travers la photosynthèse tandis que la biomasse souterraine détermine la quantité de ressources que l'individu est capable d'extraire du sol (eau, nutriments). Comprendre comment les végétaux répartissent les carbohydrates produits durant la photosynthèse entre leurs parties aériennes et souterraines est donc un prérequis au développement de modèles mécanistes susceptibles de prédire la réponse individuelle des espèces végétales. Cependant comme cette répartition résulte de l'interactions de plusieurs processus (Cannell & Dewar, 1994) et dépend fortement des conditions environnementales (Chapin, 1980; Poorter et al., 2012), il est difficile de la décrire à l'aide d'un modèle mécaniste.

Plusieurs approches ont toutefois été proposées pour décrire l'allocation du carbone entre les différents compartiments des végétaux (Génard et al., 2008; Franklin et al., 2012). Une première approche repose sur l'utilisation des relations allométriques qui permettent de relier les quantités de biomasse de deux compartiments différents (B_1 et B_2) à partir d'une relation de la forme $B_1 = \alpha.(B_2)^{\beta}$ où α et β sont des coefficients estimés empiriquement. Cette approche, bien que conceptuellement et techniquement simple, nécessite un grand nombre de données empiriques puisque les coefficients allométriques sont susceptibles de varier avec les conditions environnementales. Une seconde approche consiste à décrire le transport des carbohydrates depuis le lieu de la photosynthèse jusqu'aux différents compartiments de la plante (Thornley, 1998). Cette approche est basée sur la mécanique de la plante mais nécessite une description précise des processus de transport et de régulation interne qui sont difficiles à quantifier à partir de données empiriques. Enfin de nombreux modèles s'appuient sur divers

principes d'optimisation. Ces approches sont généralement basées sur l'hypothèse que les espèces végétales allouent les ressources disponibles de manière à maximiser leur valeur adaptative, quantifiée à travers un proxy tel que le taux de croissance relative ou la production de graines (Charles-Edwards *et al*., 1976; Reynolds and Chen, 1996). Elles ont parfois été enrichies à l'aide de méthodes issues de la théorie des jeux afin d'intégrer l'impact des interactions compétitives sur l'allocation des carbohydrates (Franklin *et al*., 2012; McNickle and Dybzinski, 2013). Cette dernière approche constitue un candidat idéal pour notre modèle individu centré puisqu'elle intègre une base mécaniste qui permet de décrire les effets des conditions environnementales sur l'allocation du carbone, sans toutefois faire appel à des traits difficilement mesurables sur le terrain. Cependant l'hypothèse d'allocation optimale est loin de faire consensus et plusieurs études empiriques ont remis sa pertinence en question (recensées par Poorter et al., 2012).

Une première étape dans le développement de notre modèle individu centré a donc été de chercher à savoir si l'hypothèse d'allocation optimale devait être rejetée ou si, complétée par des mécanismes susceptibles d'expliquer les différences entre prédictions et observations elle pouvait être utilisée comme base pour modéliser l'allocation des carbohydrates. Pour cela nous avons développé un modèle de croissance végétale basé sur l'hypothèse de l'allocation optimale et intégrant les processus de photosynthèse et d'extraction de l'azote du sol, ces processus étant contraints par les traits fonctionnels des espèces. Le modèle a par la suite été enrichi avec divers mécanismes susceptibles d'expliquer la différence entre les schémas d'allocation prédits et observés. Ces mécanismes incluent l'appauvrissement du sol en azote au cours du développement de la plante, la diminution de la capacité d'extraction des racines avec l'âge ainsi que l'existence de contraintes ontogénétiques pendant les premiers jours de croissance. Ces travaux ont permis de montrer que l'hypothèse d'allocation optimale n'était

pas incompatible avec les observations empiriques à condition que l'impact des contraintes ontogéniques s'exerçant sur la plante pendant les premiers jours de croissance soit pris en compte.

I.2.2. Implémentation et réalisme du modèle individu centré Nemossos

Le modèle de croissance végétale utilisé pour étudier la validité de l'hypothèse d'allocation optimale a été spatialisé de manière à pouvoir décrire la croissance d'une communauté au sein d'une parcelle. La spatialisation couplée à la représentation individu-centrée des plantes permet notamment une description mécaniste de la compétition pour la lumière et les ressources du sol. De plus le modèle, baptisé Némossos, a été enrichi de plusieurs processus physiologiques connus pour jouer un rôle clé dans le fonctionnement des végétaux. Ces processus permettent de décrire l'extraction des quatre ressources fondamentales pour le développement des végétaux: l'eau, l'azote, la lumière et le carbone, ainsi que leur utilisation par la plante. De nombreuses approches de modélisation, ou modules, ont été développées pour décrire ces processus physiologiques et la manière dont ils sont contraints par les facteurs abiotiques. Nemossos a été développé pour explorer les mécanismes gouvernant les dynamiques des communautés végétales prairiales. Par conséquent il doit être capable de simuler les dynamiques de communautés variant à la fois par leur composition spécifiques et par l'habitat dans lequel elles se développent. Pour satisfaire à ces exigences, le choix des modules s'est basé sur deux critères: 1) chaque module doit reproduire fidèlement l'impact des facteurs externes sur les processus physiologiques pour des niveaux de ressources et des conditions abiotiques similaires à ceux observés dans la nature; et 2) les modules doivent nécessiter le moins de paramètres possibles, ces paramètres devant majoritairement être des traits fonctionnels couramment mesurés sur le terrain. Pour être certain de remplir ces deux conditions, les différentes options de modélisation relatives aux processus physiologiques

intégrés dans Nemossos ont été comparées selon leur complexité, définie comme le nombre de paramètres requis par les différents modules. Par ailleurs, afin de prendre en compte les interactions entre la communauté et son environnement un modèle de sol décrivant les dynamiques de l'eau et de l'azote a été développé et relié au modèle de croissance individu-centré.

La première étape a été de s'assurer que le modèle Nemossos était capable de reproduire de manière réaliste le développement d'une communauté monospécifique dans différentes conditions environnementales. Le modèle a d'abord été utilisé pour simuler la réponse d'une communauté constituée d'une espèce moyenne présentant des traits fonctionnels caractéristiques des espèces prairiales le long de trois gradients environnementaux: un d'azote, un de précipitation et un de température. La réponse de la communauté à ces gradients a été quantifiée à travers sa production saisonnière de biomasse et comparée à des données empiriques issues de la littérature. La capacité du modèle à reproduire l'impact des interactions intraspécifiques sur la réponse individuelle a ensuite été testé en simulant la dynamique saisonnière d'une monoculture de densité initiale élevée. L'effet de la compétition intraspécifique a ainsi été étudié à travers la loi du "self-thinning" qui relie la production moyenne des individus à la densité au sein de la communauté (Yoda, 1963). Enfin la capacité du modèle à reproduire le lien entre les conditions environnementales et la composition fonctionnelle des communautés végétales a été testée à travers la simulation des dynamiques de communautés plurispécifiques pour différents niveaux de précipitation et de disponibilité du sol en azote. Pour ce faire nous avons simulé la dynamique saisonnière d'une communauté polyspécifique composées d'espèces variant par leur stratégie, ces dernières étant définies à l'aide d'un ensemble de traits corrélés (Reich et al., 2003a; Maire et al., 2009), a travers deux

gradients environnementaux. Les variations de la composition fonctionnelle de la communauté le long de ces gradients ont ensuite été analysées.

I.2.3. Utilisation de Nemossos pour explorer les mécanismes à l'origine de la coexistence

Une question fondamentale en écologie des communautés soulevée par le principe d'exclusion compétitive (Gause, 1935) est: comment des espèces végétales, qui ont besoin des mêmes ressources et qui les acquiert au moyen de mécanismes similaires, sont capables de coexister au sein de communautés pouvant abriter une très forte diversité spécifique? L'explication classique repose sur la différentiation de niche (Hutchinson, 1957) et plusieurs études empiriques se sont attachées à montrer que la composition des communautés végétales dépendait de facteurs abiotiques comme le niveau de précipitation ou de lumière (Hector et al., 2002; Fridley, 2003), de différences structurelle comme la profondeur des racines (Schenk, 2008) ou encore de l'affinité des espèces pour la symbiose microbienne (Reynolds et al., 2003) qui joue un rôle important dans l'acquisition des nutriments minéraux. Cependant même si la différentiation de niche est un mécanisme important pour la coexistence, il ne suffit pas à expliquer comment des dizaines d'espèces peuvent coexister au sein d'une même communauté (Silvertown, 2004).

Plusieurs mécanismes ont été proposés comme cause plausible de la coexistence de multiples espèces au sein des communautés végétales (Bengtsson, 1994; Chesson, 2000; Barot, 2004). Parmi ces mécanismes, il a été démontré à la fois théoriquement (Chesson & Warner, 1981; Pacala & Tilman, 1994) et empiriquement (Adler et al., 2006) que la variabilité temporelle des conditions environnementales était un mécanisme clé pour la coexistence des espèces. Cependant la plupart des modèles théoriques utilisés sont basés sur les équations de Lotka-

Volterra et représentent donc la variabilité fonctionnelle interspécifique de manière très grossière. Récemment quelques modèles plus mécanistes s'appuyant sur des traits fonctionnels ont été proposés pour étudier les mécanismes favorisant la coexistence (Warren & Topping, 2004; Lehsten & Kleyer, 2007). Toutefois ces modèles ne considèrent qu'un petit nombre de traits et ne cherchent pas à relier les processus physiologiques contrôlant la croissance des végétaux aux dynamiques des communautés. Pour comprendre comment variabilité environnementale et diversité fonctionnelle interagissent et conduisent à la coexistence de multiples espèces partageant les mêmes besoins, on se propose d'utiliser le modèle Nemossos.

En utilisant les corrélations entre traits fonctionnels définies à travers le "leaf economic spectrum" (Wright et al., 2004), 10 espèces de plantes prairiales réalistes ont été générées. Ces espèces virtuelles ont ensuite été utilisées pour assembler 45 mixtures de 2 espèces, dont les dynamiques ont été simulées pendant 10 ans. Pour explorer l'impact de la variabilité temporelle des conditions environnementales sur les dynamiques de ces communautés virtuelles, trois scénarios ont été implémentés. Dans le premier, les conditions environnementales sont maintenues constantes à travers les 10 saisons simulées. Dans le second les conditions environnementales varient au sein d'une saison mais sont identiques à travers les saisons. Et dans le dernier, les conditions environnementales varient à la fois au sein et à travers les saisons.

I.3. Structure du document

La seconde partie de ce manuscrit est dédiée à une synthèse bibliographique à travers laquelle sont résumés: 1) les connaissances relatives aux principaux mécanismes gouvernant les

dynamiques des communautés végétales; 2) les connaissances relatives aux liens entre traits fonctionnels et dynamique des communauté végétales; et 3) les approches de modélisation qui on été mises en oeuvre pour analyser ces dynamiques.

Les parties III à VI décrivent, à travers quatre articles, les approches de modélisation développées, la manière dont elles ont été mises en oeuvres pour aborder sous un angle nouveau des problématiques courantes en écologie des communautés, et leurs apports par rapport aux approches existantes. La partie III est consacrée à notre cadre de modélisation stochastique. Les parties IV et V retracent les étapes clés de la construction du modèle individu-centré Nemossos. Enfin la partie VI montre comment Nemossos peut être utilisé pour améliorer notre compréhension des mécanismes favorisant la diversité au sein des communautés végétales prairiales.

La dernière partie propose une discussion générale sur les travaux réalisés et les perspectives offertes par les approches de modélisation développées. La littérature citée dans les articles est donnée au sein du chapitre tandis que la littérature citée dans le reste de ce document est regroupée à la fin du manuscrit. Les tables et les figures sur lesquelles s'appuient les différents articles sont placées à la fin de chaque chapitre à la suite de la bibliographie. Par ailleurs l'article constituant le coeur de la partie IV s'accompagne de deux appendices placées à la fin du chapitre.

II. Synthèse bibliographique

Le concept de communauté végétale est utilisé pour diviser des paysages complexes en entités discrètes distinctes et permet ainsi de faciliter significativement l'étude de ces paysages. Cette discrétisation est la plupart du temps arbitraire et dépend fortement du problème abordé. De manière générale, une communauté végétale peut être définie comme un ensemble d'espèces végétales partageant une même zone géographique qui interagissent entre elles et avec leur environnement. Les communautés végétales constituent des systèmes dynamiques dont la composition et la structure varient au cours du temps. Un des grands chantiers de l'écologie des communautés est donc de comprendre et de quantifier l'importance des mécanismes à l'origine des dynamique temporelles des communautés végétales.

Dans cette synthèse bibliographique, nous proposons tout d'abord un tour d'horizon des mécanismes connus pour jouer un rôle dans les dynamiques des communautés végétales ainsi que des approches, à la fois théoriques et empiriques, mises en oeuvre pour comprendre et quantifier l'impact de ces mécanismes. Puis nous nous concentrons sur l'approche dite fonctionnelle, qui consiste à s'appuyer sur les traits des espèces végétales, définis comme n'importe quelle caractéristique morphologique, physiologique ou phénologique mesurable au niveau de l'individu, pour décrire et analyser les dynamiques des communautés qu'elles forment. Enfin divers approches basées sur la modélisation et destinées à l'étude des dynamiques des communautés végétales sont présentées. A l'issue de cette synthèse nous détaillons la problématique de la thèse et les approches de modélisation développées pour y répondre.

II.1. De la compréhension des mécanismes écologiques à la prédiction des dynamiques temporelles des communautés végétales

Pour qu'une espèce se maintienne et abonde au sein d'une communauté, elle doit être capable de se régénérer, i.e. de produire des descendants viables. L'efficacité du processus de régénération d'une espèce dépend d'une part de la quantité de descendants qu'elle est capable de produire et d'autre part de la capacité de ces descendants à se développer dans les conditions environnementales propres à la communauté à laquelle ils appartiennent. Chez les espèces végétales prairiales, la production de descendants est principalement déterminée par les propriétés intrinsèques des espèces et par la quantité de ressources acquises au cours de la phase de croissance végétative. Cette dernière dépend de divers processus physiologiques qui interagissent entre eux et peuvent être influencés par les facteurs abiotiques d'une part et par les interactions interspécifiques d'autre part. Les travaux présentés ici s'intéressent principalement à la phase végétative et aux mécanismes qui gouvernent le développement de plantes déjà établies dans une communauté.

II.1.1. L'impact des facteurs abiotiques

L'idée selon laquelle la composition des communautés végétales est étroitement liée aux conditions abiotiques dans lesquelles elles se développent remonte au début du XXème siècle. Les communautés végétales sont alors vues comme des entités constituées d'un groupe d'espèces qui, à travers des processus de sélection, se sont adaptés de manière à pouvoir coexister les unes avec les autres. Dans ce cadre, un gradient abiotique unidimensionnel théorique peut être découpé en sections distinctes, chaque section étant occupée par une communauté particulière et identifiable à travers les espèces qui la compose (Fig. 1.A, Braun-Blanquet 1932). A cette vision holistique des communautés végétales, Gleason (1926) oppose une vision individualiste dans laquelle "chaque individu est distribué indépendamment selon

ses caractéristiques génétiques, physiologiques et historiques et selon ses interactions avec les autres espèces; ainsi deux espèces distinctes ne peuvent présenter la même distribution". Cette vision individualiste est à l'origine du principe de communauté continue, énoncé par Whittaker (1975): "Le chevauchement et la dispersion des distributions des espèces le long d'un gradient implique que la plupart des communautés s'entremêlent de manière continue le long de gradients environnementaux plutôt que de former des zones distinctes clairement séparées" (Fig. 1.B).

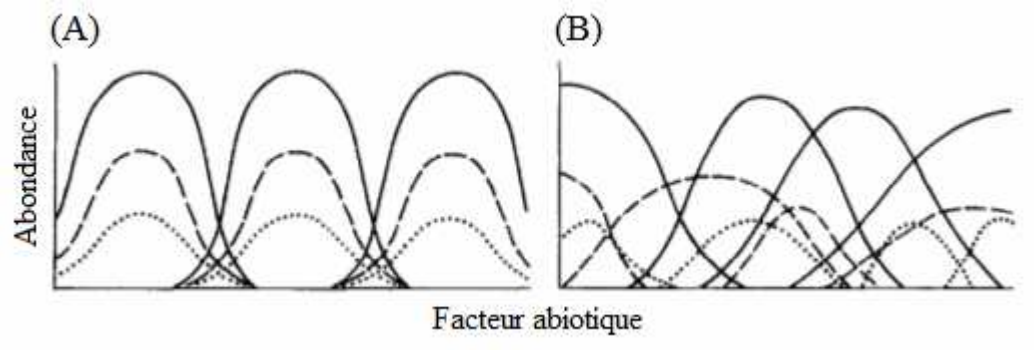

Fig.1. (A) Vision discrète des communautés: chaque communauté est constituée d'espèces ayant des distributions similaires le long d'un gradient environnemental. (B) Vision continue des communautés: chaque espèce est indépendamment distribuée le long d'un gradient environnemental.

Le débat provoqué par l'opposition de ces deux visions a conduit à la mise en place de nombreuses expériences de terrain et au développement de méthodes mathématiques facilitant l'étude de la composition des communautés végétales. Des approches telles que l'analyse de gradient (Whittaker, 1956) ou les méthodes d'ordination (Curtis & McIntosh, 1951; Goodall, 1954; Bray & Curtis, 1957) ont ainsi été introduites. Les méthodes d'ordination permettent de répartir des échantillons végétaux représentatifs de la composition des communautés selon un ou plusieurs axes de composition de telle sorte que la distance entre échantillons est

proportionnelle à la similarité floristique des échantillons. L'analyse de gradient est quant à elle une méthode graphique permettant de représenter la distribution des espèces le long de gradients environnementaux. En s'appuyant sur ces approches, de nombreuses études suggèrent que les distributions des espèces se croisent sans qu'il n'y ait de frontière claire entre les différentes communautés (Whittaker, 1951; McIntosh, 1967; Austin et al., 1990). Même s'ils ne constituent pas une preuve formelle en soit (Daubenmire, 1966), ces travaux ont mené à l'acceptation du concept de continuum au sein de la communauté des écologues. Pour autant la vision clementsienne n'a pas été complètement abandonnée et reste un des fondements de la phytosociologie (Braun-Blanquet, 1918).

Le lien entre les conditions abiotiques et la distribution des espèces végétales a été formalisé de manière théorique à travers le concept de niche écologique (Elton, 1927). Selon Hutchinson (1957), la niche écologique d'une espèce est définie comme l'ensemble des ressources nécessaires à sa croissance et à sa reproduction. Elle peut ainsi être représentée à l'aide d'un hypervolume à N dimensions, chaque dimension correspondant à un facteur abiotique distinct. En théorie chaque point de cet hypervolume, appelé niche fondamentale, définit un ensemble de facteurs abiotiques pour lequel l'espèce considérée est capable de se maintenir indéfiniment si aucun autre facteur externe ne vient affecter son développement (e.g. maladie, herbivorie). La forme et la taille de la niche fondamentale d'une espèce dépend de la forme et de l'amplitude de sa réponse aux variations des facteurs abiotiques. Plusieurs dizaines de facteurs abiotiques sont susceptibles d'affecter la forme des niches fondamentales des espèces végétales et il est donc difficile de tous les prendre en compte. De plus, en milieu naturel, les facteurs abiotiques interagissent entre eux et il est souvent impossible d'isoler l'effet d'un facteur singulier sur la valeur adaptative des espèces. Le cadre conceptuel utilisant les niches écologiques reste donc majoritairement théorique même si quelques méthodes ont

été développées pour estimer grossièrement la forme des niches (Whittaker, 1956; 1960; Austin et al., 1990; Guisan et Thuiller, 2005). Pour pouvoir utiliser ce cadre théorique pour analyser la composition des communautés végétales et leurs dynamiques temporelles, il est nécessaire de décrire et de quantifier la réponse des espèces aux variations des différents facteurs abiotiques ainsi que les interactions entre ces facteurs.

Certains facteurs sont connus pour avoir un effet majeur sur la valeur adaptative des espèces végétales et quantité de travaux se sont attachés à quantifier ces effets et à décrire la forme des réponses des espèces (Lambers et al. 2008). Ici on ne cherchera donc pas à dresser une liste exhaustive des facteurs abiotiques déterminant la niche fondamentale des espèces végétales mais plutôt à isoler quelques facteurs dont le rôle est prépondérant et l'effet sur le développement des plantes connu. Trois ressources essentielles au fonctionnement des végétaux, c'est-à-dire sans lesquelles les plantes ne peuvent pas compléter leur développement normalement (Epstein, 1972), sont: 1) la lumière captée par les feuilles qui apporte l'énergie nécessaire à la photosynthèse; 2) l'eau qui occupe une place centrale dans tous les processus physiologique et assure le transport des substances chimiques nécessaire au développement des plantes d'un organe à l'autre; et 3) divers nutriments minéraux incluant notamment le phosphore, le potassium et l'azote. Dans les communautés prairiales naturelles, l'azote est le nutriment qui limite le plus souvent le développement des individus (Cleveland et al., 1999). Une multitude d'expériences ont été menées pour documenter la relation entre la quantité de lumière captée par les feuilles d'une plante (PAR) et son efficacité photosynthétique (Björkman, 1981; Ögren, 1993; Landhausser & Lieffers, 2001). En s'appuyant sur ces travaux, plusieurs modèles de complexité variable ont été proposés pour décrire cette relation (Jassby & Platt, 1976), le plus répandu et le mieux documenté étant l'hyperbole non rectangulaire. De même la relation entre la capacité photosynthétique et la concentration en

azote foliaire a été étudié intensivement (Evans, 1989; Reich et al., 1997), mettant en évidence une augmentation linéaire de la capacité photosynthétique avec la concentration en azote foliaire. Enfin il a été démontré que la disponibilité en eau contraignait la capacité photosynthétique des plantes à travers la conductance stomatique. En cas de limitation en eau les stomates se ferment pour réduire la perte d'eau induite par la transpiration, limitant ainsi les échanges gazeux entre les feuilles et l'atmosphère (Schulze, 1991) et donc la capacité photosynthétique.

Par ailleurs les processus physiologiques à l'origine du développement des plantes sont sensibles aux conditions atmosphériques. On peut notamment mentionner la température qui influence fortement les processus physiologiques mettant en jeu une ou des catalyse enzymatiques tels que la photosynthèse (Atkin et al., 2006), l'humidité relative qui est susceptible de déclencher la fermeture des stomates (Oren et al., 1999) ou encore la concentration atmosphérique en dioxyde de carbone qui peut avoir un effet sur les échanges gazeux entre les feuilles et l'atmosphère (Bowes, 1996).

Bilan. Les expériences de terrain ont remis en question la vision holistique des communautés végétales et conduit à l'acceptation du concept de continuum. Le cadre conceptuel des niches écologiques a été développé afin de pouvoir relier la composition des communautés et leurs dynamiques aux facteurs abiotiques. Cependant en raison du grand nombre de variables à prendre en compte, ce cadre reste théorique et ne peut être utilisé que moyennant des simplifications. Par ailleurs en milieu naturel les différents facteurs abiotiques dépendent fortement les uns des autres de telle sorte qu'il est difficile d'isoler l'effet d'un facteur singulier. Pour contourner ces problèmes il est nécessaire de réduire le nombre de variables considérées en fonction de leur effet sur les espèces végétales et de quantifier cet effet.

II.1.2. L'impact des interactions interspécifiques

La compétition interspécifique est définie comme une interaction entre deux ou plusieurs espèces conduisant à l'augmentation de la densité ou de la biomasse d'une espèce au détriment de celle d'une autre. L'intensité de la compétition interspécifique peut être quantifiée à travers l'importance de la réduction de la croissance d'une espèce induite par la présence d'une autre. De nombreuses études de terrains se sont appuyées sur cette méthode de quantification pour montrer que la survie et la croissance d'un individu pouvait être significativement affectées par la compétition avec les individus de son voisinage (Wilson & Keddy, 1986; Goldberg, 1987). La compétition occupe un place centrale dans de nombreuses théories en écologie végétale (Hutchinson, 1957; Grime, 1979; Tilman, 1982) et son importance dans la composition des communautés végétales est largement acceptée.

Le taux de croissance d'une espèce est la plupart du temps déterminé par la ou les ressources dont la disponibilité est la plus faible relativement aux besoins de l'espèce. On parle alors de ressources limitantes. Gregory Gause fut l'un des premiers à mettre en place une série d'expériences en conditions contrôlées pour déterminer l'impact de la compétition pour les ressources sur la dynamique de communautés de paramécies. Ces expériences l'ont conduit à proposer une loi, souvent référencée comme le "principe d'exclusion compétitive", affirmant que deux espèces étant en compétition pour une même ressource limitante ne peuvent coexister indéfiniment si les autres facteurs écologiques sont maintenus constants. Plusieurs modèles théoriques, dont les modèles de type Lotka-Volterra (Volterra, 1928; Lotka, 1932) et les modèles basés sur le ratio des ressources (Armstrong & McGehee, 1980; Tilman, 1982), corroborent le principe d'exclusion compétitive avec l'extinction de l'espèce dont la capacité d'extraction de la ressource limitante est la plus faible. Dans ce cadre, deux espèces ayant des

niches écologiques strictement similaires ne peuvent donc coexister au sein d'une même communauté.

Comme toutes les plantes terrestres ont besoin de lumière, d'eau et de nutriments pour pouvoir se développer, elles entrent nécessairement en compétition pour ces ressources lorsqu'elles sont en quantité insuffisante pour satisfaire la demande de l'ensemble des individus. De plus le nombre de mécanismes grâce auxquels elles acquièrent ces ressources est limité. Par conséquent le principe d'exclusion compétitive prédit que différentes espèces végétales ne devraient pas pouvoir coexister au sein d'une même communauté. Pourtant la plupart des communautés végétales présentent un forte diversité spécifiques, comme par exemple certaines prairies au sein desquelles on recense jusqu'à 40 espèces au mètre carré ou les forêts tropicales qui peuvent abriter jusqu'à 1000 espèces différentes sur un hectare. Cette divergence entre les observations de terrain et la théorie recquiert des explications.

Dans le cadre théorique développé par Hutchinson (1957), les niches écologiques sont définies comme des hypervolumes de dimension N, chaque dimension (ou axe) correspondant à un facteur écologique. Dans ce cadre, la compétition interspécifique est censée réduire le volume des niche écologiques. Hutchinson établit ainsi une distinction entre la niche fondamentale d'une espèce qui décrit l'ensemble des facteurs abiotiques permettant à cette espèce de se maintenir indéfiniment en l'absence d'interactions biotiques et la niche réalisée qui intègre les effets des interactions biotiques. Cette approche de la compétition est attirante mais présente un sérieux inconvénient empêchant son application à des systèmes réels: il n'existe pas de méthode a priori permettant d'identifier les dimensions de la niche pertinentes pour l'étude d'une communauté singulière (Silvertown, 1987). Et étant donné le grand nombre de facteurs susceptibles d'affecter le développement des espèces végétales, certaines

dimensions de la niche ont nécessairement été négligées lors des études empiriques et théoriques sur la coexistence.

D'autre part de nombreux modèles théoriques ont été développés pour mettre en évidence les mécanismes permettant de réconcilier la théorie de la compétition et les observations empiriques. La plupart de ces modèles sont basés sur des hypothèses similaires à celles utilisées dans le modèle de Lotka-Volterra mais intègrent des axes de niches supplémentaires, comme les niches de régénération (Grubb, 1977), ou des conditions particulières comme l'hétérogénéité spatiale (Tilman, 1982) ou temporelle (Chesson, 1994) de l'environnement. Ces travaux ont permis de mettre en évidence plusieurs mécanismes susceptibles d'expliquer la coexistence des espèces végétales (Bengtsson et al., 1994; Chesson, 2000). Certains de ces mécanismes, comme la réduction de la compétition due à l'hétérogénéité spatiale, ont été largement explorés à travers des études aussi bien empiriques (Stein et al., 2014) que théoriques (Holt, 1984; Amarasekare, 2003), tandis que d'autres, tel que le "storage effect", n'ont été le sujet que d'un petit nombre de travaux (e.g. Adler et al., 2006).

Outre la compétition interspécifique, un second type d'interactions, appelé facilitation, a été mis en évidence (Bertness & Callaway, 1994; Brooker & Callaghan, 1998; Bruno et al., 2003). La facilitation désigne des interactions entre individus qui bénéficient à au moins l'un des individus sans porter préjudice aux autres. Ces interactions positives peuvent se produire lorsqu'une des espèces rend l'environnement local plus favorable à une autre soit directement par exemple par une réduction du stress thermique, hydrique ou nutritif à travers l'ombrage ou la symbiose, soit indirectement à travers la suppression des compétiteurs ou des prédateurs. Par exemple les légumineuses sont capables de fixer l'azote atmosphérique et augmentent ainsi la richesse des sols, favorisant le développement des espèces qui extraient l'azote par

l'intermédiaire de leurs racines. Même si dans certains cas ces interactions peuvent être très spécifiques et localisées (Dickie et al., 2005), elles sont susceptibles de jouer un rôle majeur dans les dynamique des communautés végétales (Holzapfel & Mahall, 1999; Schenck & Mahall, 2002).

Il a été montré que l'intensité de la compétition interspécifique (Grime, 1979; Tilman, 1988) aussi bien que celle de la facilitation (Bertness & Callaway, 1994, Callaway, 1998) variaient le long de gradients de ressource. Les interactions entre plantes sont donc dynamiques et leur issue, en termes de productivité ou de valeur adaptative, dépend des facteurs abiotiques. Cependant aucune relation claire entre interactions interspécifiques et facteurs abiotiques n'a été établie. Plusieurs étude de terrains ont montré qu'il peut y avoir un déplacement des interactions interspécifiques de la facilitation vers la compétition lorsque le stress abiotique augmente (Bertness & Hacker, 1994; Greenlee & Callaway, 1996; Pugnaire & Luque, 2001) tandis que d'autres suggèrent que la forme de la relation entre stress abiotiques et intensité des interactions interspécifiques tend à varier selon le système considéré (Goldberg et al., 1999).

Bilan. S'il est communément admis que les interactions entre espèces, qu'elles soient positives (facilitation) ou négatives (compétition), jouent un rôle majeur dans les dynamiques des communautés végétales, la forme et l'amplitude des relations liant interactions et dynamiques restent méconnues. Cette méconnaissance résulte principalement de la variabilité de l'intensité des interactions avec les conditions environnementales auxquelles sont soumises les communautés. Pour améliorer notre compréhension des dynamiques des communautés végétales il est donc nécessaire de tenir compte de l'impact des facteurs abiotiques sur le développement des individus mais aussi sur l'intensité des interactions interspécifiques.

II.1.3. Intégrer les mécanismes écologiques pour comprendre et prédire les dynamiques des communautés.

Dans le cadre théorique développé par Hutchinson (1957), la présence et l'abondance d'une espèce au sein d'une communauté sont entièrement déterminées par les conditions abiotiques et les interactions interspécifiques. Dans ce contexte, il est théoriquement possible d'une part de relier une espèce à un type d'habitat, l'habitat étant défini comme l'ensemble des conditions abiotiques dans lesquelles une communauté se développe, et d'autre part de déterminer les effets des interactions au sein de la communauté sur cette espèce. Plusieurs cadres théoriques s'appuyant sur le concept des niches écologiques ont été développés pour essayer de produire des règles générales concernant la structure des communautés végétales et leurs dynamiques. De manière générale, l'objectif de ces approches est de répartir les espèces le long de gradients environnementaux tout en établissant une hiérarchie compétitive entre ces espèces.

Deux de ces cadres ont suscité de vifs débats: la théorie CSR introduite par Grime (1979) et la théorie basée sur le "ressource ratio" introduite par MacArthur (1972) et développée par la suite par Tilman (1980, 1982, 1988). Ces deux approches prennent en compte deux gradients environnementaux: un gradient de productivité qui traduit la disponibilité des ressources et un gradient de perturbation. Dans l'approche de Tilman, la survie d'une espèce est déterminée par ses besoins en ressource par rapport à la quantité de ressource disponible. La compétition résulte de la déplétion des ressources et en cas de limitation l'espèce ayant les besoins les plus importants voit sa valeur adaptative diminuer puis est exclue de la communauté. Ce cadre théorique a été traduit par un modèle couplant la dynamique des populations au sein d'une communauté et le niveau de ressource disponible. Grime quant à lui s'appuie sur les traits fonctionnels, c'est-à-dire sur les caractéristiques morphologiques, physiologiques et phénologiques intrinsèques, des espèces, pour définir trois stratégies: 1) Les espèces capables

de maintenir une croissance soutenue aux prix d'un taux élevé de renouvellement des tissus sont qualifiées de compétitives (C). Cette stratégie est supposée dominer les milieux productifs et peu perturbés. 2) Les espèces ayant un taux de croissance modéré voire faible, associé à un faible taux de renouvellement des tissus qui permet le maintient des ressources au sein de la plante sont qualifiées de tolérantes au stress (S). Cette stratégie est associée aux milieux peu productifs et peu perturbés. Enfin 3) les espèces ayant un cycle de vie court et investissant la majeur partie de leurs ressources dans la reproduction sont définies comme rudérales (R) et dominent les milieux très perturbés.

Ces approches ont toutes deux mis en évidence l'existence de compromis évolutifs permettant de distinguer les différentes espèces végétales. Elles ont également contribué à mettre l'accent sur l'importance des traits fonctionnels, des processus d'acquisition et de perte des ressources ainsi que des effets des perturbations sur les individus pour notre compréhension des dynamiques des communautés végétales. Par ailleurs elles ont permis d'étudier l'impact des facteurs abiotiques sur l'intensité de la compétition interspécifique, conduisant à deux visions différentes. La théorie développée par Tilman prédit que l'intensité de la compétition reste constante le long de gradients de productivité avec un déplacement des interactions des parties aérienne aux parties souterraines de la plante lorsque la productivité de l'habitat diminue. Au contraire le cadre théorique de Grime prédit que la compétition souterraine est négligeable dans les habitats peu productifs. Ces deux hypothèses ont été confrontées à travers des mesures de l'intensité de la compétition le long de gradients de productivités, mais les résultats de ces études sont très variables et ne permettent pas de trancher (Goldberg & Barton, 1992; Twolan-Strutt & Keddy, 1996, Carlyle, 2010).

La classification CSR établie par Grime a continué à être développée, conduisant à la mise en place d'une procédure d'attribution des stratégies aux espèces végétales basée sur des traits fonctionnels aisément mesurables (Hodgson et al., 1999). Cette classification, initialement conçue pour les espèces herbacées présentes dans le nord de l'Angleterre, a été étendue à travers l'Europe (Caccianiga et al., 2006; Pierce et al., 2007; Yildirim et al., 2012) et il a été montré que la méthode développée par Hodgson et al. (1999) pouvait être appliquée avec succès en dehors de la zone géographique initiale (Cerabolini et al., 2010). De plus cette méthode a été étendue de manière à autoriser la classification des espèces ligneuses (Pierce et al., 2013). Au cours de la dernière décennie elle a été majoritairement utilisée dans un but descriptif, permettant notamment de décrire le développement, la valeur écologique et la restauration de la végétation au sein d'écosystèmes gérés (Pywell et al., 2003; Boatman et al., 2011) ainsi que l'écologie et l'historique d'invasion des espèces exotiques (Pysek et al., 2003; Lambdon et al., 2008). Quelques travaux axés sur la prédiction de la réponse de la végétation aux changement climatiques se sont également appuyés sur la classification CSR (Grime et al., 2000; Abrahams, 2008). Cependant comme les concepts développés dans le cadre théorique de Grime ne sont pas synthétisés à travers une formulation mathématique, les prédictions qu'il est susceptible de produire ne sont que qualitatives.

Le cadre théorique de Tilman a également continué à être développé au cours des dernières décennies. Ces développements ont permis d'une part d'étendre son champ d'application, avec par exemple les travaux de Holt & Lawton (1994) qui ont intégré au cadre original les perturbations induites par la prédation, ou encore ceux de Tilman (2004) qui permettent à travers la théorie des niches stochastiques de relier le niveau de consommation d'une ressource par les espèces établies à la probabilité de colonisation de l'habitat par une nouvelle espèce. Et d'autre part ils ont permis de confronter différentes hypothèses théoriques sur les

mécanismes gouvernant les dynamiques des communautés. Ce type de démarche a notamment conduit à l'identification de processus susceptibles d'affecter la relation entre biodiversité et productivité (Abrams, 1988) et de mécanismes pouvant expliquer la co-existence d'espèces partageant les mêmes caractéristiques au sein d'une même communauté (Chesson, 1990; Leibold, 1998). Certaines des prédictions produites par le modèle de Tilman (1982) et ses dérivés ont été testées à travers des études empiriques, améliorant notre compréhension des processus gouvernant la dynamique des communautés (Miller et al., 2005). Cependant ce modèle repose sur l'hypothèse centrale selon laquelle l'espèce ayant les plus faibles besoins par rapport à la ressource limitante est systématiquement la meilleure compétitrice. Or il a été montré que cette hypothèse n'est pas toujours valide (Craine, 2005; Fargione & Tilman, 2006). En effet, l'extraction des ressources par les plantes fait intervenir différents processus physiologiques susceptibles d'interagir et résumer la capacité d'extraction aux besoins d'une espèce peut être trompeur. Le modèle de Tilman (1982) ne repose donc pas sur des bases mécanistes suffisamment solides pour pouvoir produire des prédictions fiables sur les dynamiques des communautés à travers différents types d'habitat (Craine, 2007).

Bilan. Le débat engendré par les prédictions contradictoires produites par les cadres théoriques de Grime (1979) et Tilman (1982) a suscité la mise en place de nombreuses expériences qui ont permis d'améliorer significativement notre compréhension des mécanismes déterminant l'intensité des interactions compétitives le long de gradient environnementaux. Par ailleurs la théorie CSR a permis de mettre au point une classification largement utilisée pour décrire la structure des communautés, tandis que l'approche de Tilman est encore utilisée pour produire des hypothèses théoriques sur les mécanismes gouvernant les dynamiques des communautés. Cependant l'approche de Grime est purement qualitative et celle de Tilman manque d'une base mécaniste. Malgré ces limites, les deux théories ont

apportées des idées novatrices qui, intégrées au sein d'un cadre mathématique mécaniste, ont le potentiel de significativement améliorer notre compréhension et notre capacité à prédire les dynamiques des communautés végétales (Jabot & Pottier, 2012).

II.2. Vers une écologie plus fonctionnelle

Etant donné la multitude d'espèces végétales et d'habitats viables pour ces espèces, il est peu probable que des études s'attachant au comportement de quelques espèces singulières dans des conditions environnementales particulières produisent des règles générales (Rigler, 1982; Keddy, 1992). Pour contourner cette difficulté, plusieurs écologues ont proposé d'aborder les questions relatives aux dynamiques des communautés végétales sous un angle nouveau, passant d'études basées sur la composition taxonomique des communautés à des études basées directement sur leur composition fonctionnelle (Shipley et al., 1989; Diaz et al., 1998; Reich et al, 2003; Westoby & Wright, 2006). Cette approche fonctionnelle fournit une mesure objective des caractéristiques des différentes espèces et permet donc de les comparer à travers diverses communautés (Lavorel & Garnier, 2002; McGill et al., 2006).

II.2.1. Traits fonctionnels et stratégies végétales

Les traits fonctionnels des plantes déterminent leur capacité à s'établir dans un habitat, à en extraire les ressources, et la manière dont ces ressources sont utilisées pour soutenir leur croissance et leur reproduction. La distribution de ces traits à travers différents types d'habitat n'est pas aléatoire et l'idée selon laquelle les conditions environnementales sont à l'origine de la sélection des combinaisons de traits propre aux différentes espèces est depuis longtemps un des principes fondamentaux de l'écologie (Lamarck, 1809; Darwin, 1859). Il découle de ce principe que pour chaque type d'habitat, il existe un nombre fini de combinaisons de traits, ou

stratégies végétales, permettant aux espèces d'assurer leur survie et leur reproduction. Autrement dit il devrait être possible de déterminer la niche fondamentale d'une espèce à partir de ses traits fonctionnels. En se concentrant sur ces stratégies plutôt que sur des espèces singulières, il devrait être possible d'identifier les mécanismes à travers lesquels les interactions entre environnement et traits fonctionnels déterminent les dynamiques des communautés (Grime, 1979; Southwood, 1988). La première étape de cette démarche consiste à définir les stratégies végétales en fonction des traits fonctionnels.

L'idée d'utiliser les stratégies des espèces végétales pour analyser les dynamiques des communautés n'est pas récente et plusieurs travaux empiriques ont suggéré que ces stratégies étaient susceptibles d'être réparties le long d'un spectre. D'un coté de ce spectre se trouvent des espèces ayant un taux élevé de renouvellement des tissus, un fort potentiel d'extraction des ressources et une croissance à court terme rapide. Ces espèces ont été qualifiées d'espèces "exploitatrices" ou dispendieuses. A l'autre extrémité de ce spectre se trouvent des espèces dites conservatrices ayant un faible taux de renouvellement des tissus associé à une forte capacité de conservation des ressources (Grime, 1977; Chapin, 1980; Poorter et al., 1990). Il a été montré à travers des études empiriques locales que ces stratégies végétales étaient reliées à un ensemble de traits fonctionnels corrélés entre eux (Field & Mooney, 1986; Reich et al., 1999; Niinemets, 1999). Ainsi les stratégies conservatives sont associées à des espèces ayant une faible surface spécifique foliaire (SLA), une grande longévité foliaire et une faible teneur en azote foliaire (LNC) ainsi qu'une faible capacité photosynthétique (A_{max}) et un faible taux de respiration (R_d). Cette combinaison de traits conduit généralement à un faible taux de croissance (RGR). Par opposition, les espèces dispendieuses présentent des traits fonctionnels favorisant un fort taux de croissance, incluant un SLA, un LNC et un A_{max} élevés associé à une longévité foliaire faible ainsi qu'un R_d élevé. Récemment, la mise en place de procédures

standardisées de mesure des attributs fonctionnels des espèces végétales (Cornelissen et al., 2003), et la constitution de base de données telles que Glopnet (Wright et al., 2004) ou Try (Kattge et al., 2011) ont rendu possible l'étude du spectre des stratégies végétales à une échelle globale. Ainsi Diaz et al. (2004) ont confirmé, à travers une comparaison de 12 traits fonctionnels mesurés sur 640 espèces végétales réparties à travers trois continents, l'existence d'un compromis entre deux stratégies, l'une privilégiant l'acquisition rapide des ressources et l'autre favorisant la conservation des ressources au sein de tissus résistants. Dans la même logique Wright et al. (2004) se sont intéressés aux corrélations entre les traits foliaires de 2548 espèces végétales réparties sur 175 sites à travers les cinq continents. Ils ont ainsi démontré que la majorité des stratégies foliaires, définies comme l'union de six traits caractéristiques des propriétés foliaires, varient le long d'un axe de spécialisation unique. Ces études ont permis: 1) de démontrer la puissance de l'utilisation des traits fonctionnels pour définir les stratégies végétales; 2) de confirmer l'existence d'un spectre des stratégies végétales reflétant le compromis entre acquisition et conservation des ressources à l'échelle globale; 3) d'établir que la répartition des stratégies le long de ce spectre est continue.

L'existence d'un spectre des stratégies végétales corrobore l'hypothèse selon laquelle les propriétés intrinsèques des plantes résultent de multiples compromis évolutifs. Dès lors, il semble probable que différentes stratégies végétales soient adaptées à différents types d'habitats. La seconde étape de l'approche fonctionnelle est de comprendre comment les facteurs abiotiques influencent la répartition des stratégies le long de gradients environnementaux. De nombreuses études empiriques se sont attachées à décrire ce lien entre conditions environnementales et traits fonctionnels, la plupart du temps en mesurant les traits d'espèces à travers différents types d'habitat. Les nutriments présents dans le sol étant la principale ressource limitant la productivité des habitats (Chapin, 1980; Aerts & Chapin,

2000), plusieurs études ont été menées pour essayer de comprendre comment ils contraignaient la distribution des traits fonctionnels (Beadle, 1966; Monk, 1966; Chapin, 1980). Cependant les preuves empiriques de la relation entre nutriments et traits fonctionnels sont rares, principalement en raison de la difficulté de mesurer la concentration en nutriments du sol. Quelques études ont tout de même tenté de quantifier cette relation, ainsi plusieurs études de terrain ont montré que le SLA diminuait avec la concentration en phosphore du sol (Cunningham et al., 1999; Wrigth & Westoby, 1999; Fonseca et al., 2000). Par ailleurs les travaux de Craine et al. (2001) ont démontré que les espèces se développant dans des habitats pauvres en azote avaient généralement des tissus plus denses (e.g. un SLA plus faible) que les espèces caractéristiques des habitats riches en azote. Si les études reliant directement la concentration du sol en nutriments aux traits fonctionnels des plantes sont peu courantes, certaines études descriptives corroborent l'hypothèse selon laquelle les habitats pauvres en nutriments favorisent les stratégies conservatrices (Wedin & Tilman, 1990; Reich et al., 1997; Craine et al., 2002). Les espèces caractéristiques des habitats très ombragés présentent elles aussi des traits caractéristiques d'une stratégie conservative avec de grandes longévités foliaires (Coley, 1988; Williams et al., 1989) ainsi que de faibles SLA (Veneklaas & Poorter, 1998), de faibles A_{max} (Chazdon & Field, 1987; Williams et al., 1989) et de faibles R_d (Walter et al., 1993; Valladares et al., 2000). C'est également le cas des habitats dans lesquels le niveau de précipitation est faible. On retrouve effectivement une diminution du SLA avec le niveau de précipitation (Specht & Specht, 1989; Cunningham et al., 1999; Fonseca et al., 2000) suggérant un déplacement vers des stratégies plus conservatives.

Par ailleurs il a été montré que ces stratégies pouvaient s'écarter significativement de l'axe de spécialisation défini à l'échelle globale. Par exemple les espèces se développant dans des habitats xériques présentent une longévité foliaire plus faible et un LNC plus élevé que ceux

prédits par le "leaf economic spectrum" (Wright et al., 2004) pour une valeur de SLA donnée (Reich et al., 1999; Wright et al., 2003). Ces résultats suggèrent que même si l'impact des facteurs abiotiques sur les axes des spécialisations est difficilement visible à l'échelle globale, ces derniers sont susceptibles d'être un facteur clé dans le filtrage local de ces stratégies.

Bilan. L'analyse fonctionnelle des communautés a permis de confirmer l'existence à l'échelle globale de compromis évolutifs, conduisant à la définition d'un spectre continu des stratégies végétales. Chaque stratégie présente des caractéristiques particulières qui déterminent le type d'habitat dans lequel elle est susceptible d'être favorisée.

II.2.2. Des traits fonctionnels aux dynamiques des communautés

En raison de leur généralité à travers les différentes espèces et les différents habitats, les stratégies végétales peuvent devenir un outil fiable et puissant pour prédire les dynamiques des communautés. Mais pour cela il est nécessaire de comprendre comment la distribution des traits fonctionnels au sein d'une communauté détermine sa structure et sa composition. Plusieurs travaux se sont appuyés sur les stratégies végétales pour décrire les dynamiques des communautés (Tilman, 1990; Pysek et al., 1995; Garnier et al., 2004). Elles ont par exemple été utilisées pour analyser les dynamiques de succession: on sait ainsi que les espèces présentes au début de la succession possèdent un ensemble de traits caractéristiques, incluant une forte fécondité, une forte capacité de dispersion, une croissance rapide lorsque le niveau des ressources est élevé et un fort taux de mortalité lorsqu'il ne l'est pas. Ces espèces sont remplacées petit à petit et la fin de la succession est généralement dominée par des espèces qui possèdent des traits opposés avec une fécondité et une capacité de dispersion relativement faibles ainsi qu'un taux de survie et des capacités compétitives importants dans les milieux pauvre en ressources. Cependant la plupart des approches utilisées pour relier les traits

fonctionnels aux dynamiques des communautés s'appuient sur des modèles conceptuels et ne peuvent produire que des prédictions qualitatives (MacArthur & Wilson, 1967; Tilman, 1988; Westoby, 1998; Grime, 2001). Elles mettent ainsi en lumière l'existence d'un lien entre la distribution des traits et les dynamiques des communautés mais ne permettent pas de prédire quantitativement la composition et la structure de la communauté.

Récemment des approches permettant de relier quantitativement les traits fonctionnels des espèces constituant une communauté à leurs abondances respectives ont été introduites. En s'appuyant sur l'hypothèse du "mass ratio", selon laquelle les propriétés des communautés à un instant *t* sont principalement déterminées par la valeur des traits fonctionnels des espèces dont la biomasse est la plus importante (Grime, 1998), Shipley et al. (2006) ont ainsi développé une approche qui utilise le maximum d'entropie pour prédire l'abondance des espèces à partir des valeurs de traits agrégés à l'échelle de la communauté. Ce modèle prédit que les espèces ayant des traits dont les valeurs moyennes sont proches des valeurs agrégées à l'échelle de la communauté sont les plus abondantes (Laughlin et al., 2011; Shipley et al., 2011). Il a été montré que cette approche permettait de prédire avec une bonne précision la composition de diverses communautés végétales (Shipley et al., 2006; Frenette-Dussault et al., 2013). Cependant comme cette approche s'appuie sur des valeurs de traits moyennées à travers les populations composant les communautés, elle ne permet pas de prendre en compte la variabilité intraspécifique alors que cette dernière est susceptibles de modifier significativement la distribution des traits au sein des communautés (Albert et al., 2010; Messier et al., 2010). Pour remédier à ce problème, Laughlin et al. (2012) ont proposé de s'appuyer sur des méthodes d'inférence bayésiennes pour estimer l'abondance des espèces au sein des communautés à partir de valeurs de traits individuels. Ces deux approches se basent sur la distribution des traits au sein de la communauté pour estimer l'abondance des

différentes espèces. La distribution des traits est supposée résulter de la superposition de filtres environnementaux et est estimée à l'aide de modèle linéaires généralisés prenant en entrée plusieurs facteurs abiotiques connus pour affecter la distribution des traits. Par conséquent les mécanismes par lesquels les filtres environnementaux contraignent la distribution des traits ne sont pas décrits explicitement. De même les méthodes utilisées pour déduire l'abondance des espèces de la distribution des traits reposent sur des outils statistiques qui ne permettent pas de remonter aux mécanismes sous-jacents. Ils ont donc un bon pouvoir prédictif à court terme pour des systèmes dont les propriétés sont connues. En revanche, leurs prédictions à long terme sur des communautés soumis à des changements environnementaux importants sont très peu fiables.

Pour aller au delà de ces approches statistiques, il est nécessaire de définir un cadre conceptuel permettant de relier explicitement la distribution des traits fonctionnels individuels aux contraintes environnementales, puis à la structure de la communauté (Suding et al., 2003; Gross et al., 2009). Un moyen d'aborder cette problématique consiste à distinguer plusieurs niveaux d'organisation au sein de la communauté. Par exemple Suding et al. (2003) proposent de distinguer 4 niveaux de réponse: le premier niveau décrit les propriétés intrinsèques des espèces, définies par des contraintes génétiques et physiologiques. Ces propriétés définissent la réponse d'un individu de l'espèce lorsque les conditions environnementales sont optimales. Le second niveau décrit la manière dont chacun des facteurs biotiques ou abiotiques modifie la réponse optimale de l'individu. Ces facteurs sont nombreux et variés et l'effet de leurs interactions sur la réponse des individus ne peut être aisément prédit à partir des effets des facteurs singuliers. Le troisième niveau de réponse décrit donc les conséquences de ces interactions entre facteurs biotiques et abiotiques pour l'individu. Enfin le quatrième niveau décrit les dynamiques des communautés à l'échelle de la population. Suding et al. (2003) ont

mis en évidence que ces différents niveaux de réponse étaient reliés les uns aux autres et que ces liens pouvaient permettre de déduire la composition et la structure des communautés (dernier niveau de réponse) à partir du premier niveau de réponse. Initialement ce cadre a été conçu pour analyser des données empiriques. Les liens entre les différents niveaux de réponse sont alors déterminés à l'aide d'outils statistiques et ne décrivent pas explicitement les mécanismes sous-jacents. Toutefois, ce cadre conceptuel identifie plusieurs niveaux d'organisation au sein des communautés qui peuvent être utilisés pour développer des approches plus mécanistes.

Bilan. De nombreuses études empiriques ont démontré qu'il existait un lien entre la composition fonctionnelle et la structure des communautés. Quelques approches ont tenté d'intégrer cette relation au sein de cadres prédictifs basés sur des méthodes statistiques, permettant notamment de prédire la relation entre les traits fonctionnels et l'abondance des différentes espèces. Mais pour comprendre comment les distributions des traits conduisent aux patterns observés, il est nécessaire d'identifier et de quantifier les mécanismes qui déterminent la relation entre les traits fonctionnels des espèces et leur réponse individuelle dans un habitat donné.

II.3. La modélisation, un outil pour comprendre et prédire les dynamiques des communautés végétales.

La modélisation est un outil permettant de résumer, d'organiser et de synthétiser les connaissances relatives à un système, puis d'utiliser ces connaissances pour proposer des prédictions quantitatives, déterministes ou probabilistes quant à l'état futur du système.

Lorsque le système étudié présente une forte complexité, il n'est pas rare que les connaissances des mécanismes sous-jacents ne soit que partielle, et même lorsque tous les mécanismes ont été élucidés il est très difficile, voire impossible, d'intégrer l'ensemble des connaissances disponibles dans un modèle. Les dynamiques des communautés végétales dépendent d'une pléiade de facteurs biotiques et abiotiques qui interagissent de manière a priori imprévisible. Dans ce cas il est nécessaire de faire des choix de modélisation, i.e. d'intégrer dans le modèle uniquement les variables pertinentes pour répondre à une problématique préalablement définie.

En écologie des communautés végétales, il existe une multitude de modèles variant par leur structure, leur complexité mais aussi par leur vocation. Plusieurs classifications basées sur ces différents aspects ont été proposées (Holling, 1966; Evans et al., 2013; Mouquet et al., 2015). Nous diviserons ici les modèles en deux catégories: les modèles basés sur les dynamiques de populations et les modèles basés sur les dynamiques individuelles.

II.3.1. Des modèles basés sur les dynamiques de population

Les modèles de populations cherchent à décrire les variations de la taille et de la distribution des âges au sein d'une population en fonction des caractéristiques intrinsèques des espèces et des contraintes extrinsèques telles que les facteurs abiotiques et les interactions avec les organismes d'autres espèces.

Les modèles matriciels de population (Encadré 1.1), dans lesquels les individus sont divisés en classes distinctes basées sur leur taille, leur âge ou encore leur phase de développement, sont largement utilisés dans les études démographiques sur les plantes pour quantifier les performances des populations. Ils permettent notamment d'estimer le taux de croissance à

long terme d'une population à partir de données individuelles sur la survie, la croissance et la fécondité des espèces (Caswell, 2001). Ces modèles sont principalement utilisés pour mener des analyses de viabilité de population (Menges, 2000) mais aussi pour analyser l'impact de facteurs environnementaux tels que les inondations (Smith et al., 2005) ou l'abondance des pollinisateurs (Ramula et al., 2007) sur les dynamiques de population, pour produire des recommandations relatives aux récoltes et à la conservation (Freckleton et al., 2003; Linares et al., 2008) et pour évaluer différentes stratégies de gestion des espèces invasives (Ramula et al., 2008). Malgré leur popularité, les modèles matriciels présentent des limites susceptibles d'affecter la précision de leurs prédictions. Une des principales limites vient de la structure même du modèle qui implique la division d'une variable d'état, souvent continue (e.g. âge, masse, longueur des feuilles), en classes distinctes qui sont déterminées arbitrairement la plupart du temps. Se pose alors le problème du nombre de classes à considérer: si trop peu de classes sont définies, le réalisme biologique du modèle diminue puisque des individus ayant des caractéristiques différentes sont traités comme s'ils étaient identiques. A l'inverse l'utilisation d'un trop grand nombre de classes peut conduire à des problèmes de paramétrisation, chaque classe nécessitant un nouvel ensemble de paramètres caractérisant sa fécondité, sa croissance et sa mortalité.

Les modèles de projection intégral (ou "Integral Projection Model"; Encadré 1.2) apportent une solution aux problèmes de classification liés à l'approche matricielle. Ces modèles partagent plusieurs propriétés avec les modèles matriciels et peuvent être paramétrés à partir du même type de données (Easterling et al., 2000a). Dans ces modèles, les taux démographiques sont décrits par une fonction continue, appelée noyau de projection, dépendant de l'état de l'individu plutôt que de son appartenance à une classe. Ainsi au lieu de devoir estimer les taux démographiques pour chacune des classes, il suffit de déterminer le

noyau de projection de la population, ce qui permet d'améliorer significativement la précision de l'approche lorsqu'on ne dispose que d'une faible quantité de données individuelles. Il est par exemple préférable d'utiliser ce type d'approche pour étudier les dynamiques des population d'espèces invasives ou rares, sur lesquelles peu de données sont disponibles (Ramula et al., 2009). Lorsque les données sont suffisamment détaillées, il a été montré que les deux approches produisent des résultats similaires (Easterling et al. 2000b). Si les approches s'appuyant sur les modèles intégrales améliorent significativement celles basées sur les modèles matriciels et constituent des outils fonctionnels pour les gestionnaires, elles présentent toutefois d'importantes limitations. Tout d'abord les modèles intégrales, tout comme les modèles matriciels, ne permettent pas de prendre en compte la variabilité démographique résiduelle inter individus, i.e. tous les individus de même état (taille, âge…) ont les mêmes taux démographiques (Caswell, 2001). Par ailleurs ce type d'approche ne permet de prendre en compte ni les interactions intraspécifiques, ni les interactions interspécifiques, chaque population étant supposée indépendante des autres.

Plusieurs modèles, souvent répertoriés comme modèles de compétition, ont été développés pour essayer de relier les dynamiques des communautés aux dynamiques des populations qui les composent. Les premiers modèles de compétition à avoir été utilisés en écologie des communautés se basaient sur les équations de Lotka-Volterra (Volterra, 1928; Lotka, 1932). Dans ces modèles les interactions compétitives se résument aux effets négatifs qu'une population exerce sur la croissance des autres populations de la communauté, sans que les mécanismes sous-jacents soient explicitement décrits. Deux approches ont été privilégiées pour rendre ces modèles plus mécanistes. Une première approche consiste à intégrer l'impact des ressources dans l'estimation des paramètres de compétition du modèle (MacArthur & Levin, 1967; Schoener, 1974). La principale difficulté de cette approche est de quantifier le

lien entre l'utilisation des ressources d'une population et la manière dont elle affecte les autres populations à travers les interactions compétitives (May, 1975). La seconde approche consiste à intégrer les mécanismes gouvernant la compétition directement dans le modèle. L'exemple le plus connu est le modèle basé sur l'hypothèse du "resource ratio" introduit par Tilman (1982). Ce modèle suppose que l'issue de la compétition entre deux populations est entièrement déterminée par les ressources disponibles et les besoins en ressource des populations. De nombreux autres modèles basés sur les équations de Lotka-Volterra et tentant d'intégrer les mécanismes induisant des phénomènes compétitifs ont été développés, chacun présentant des spécificités relatives aux espèces et aux habitats considérés (e.g. Stewart & Levin, 1973; Holt, 1983).

Une approche alternative consiste à considérer les dynamiques de populations comme des processus stochastiques. Dans ce cadre, la dynamique d'une population peut être décrite à l'aide d'un processus autorégressif (Encadré 1.4) dont le terme stochastique est supposé représenter la variabilité environnementale (Ives et al., 2000). En utilisant des séries temporelles sur la dynamique des populations il est alors possible d'estimer les paramètres du modèle autorégressif ainsi que les caractéristiques de la distribution des variables environnementales (généralement supposée normale). En intégrant des coefficients de compétition interspécifique, il est possible d'utiliser ce type d'approche pour prédire la dynamique d'une communauté à l'aide de modèles autorégressifs multidimensionnels (Ives, 2003). Ce type de modèle permet notamment de dériver des indicateurs sur les propriétés de la communauté telles que la stabilité (Ives et al., 2000). Loreau et al. (2008) ont récemment raffiné l'approche de Ives en distinguant trois composantes stochastiques: une composante environnementale, une composante démographique, qui décrit l'impact de la variabilité intraspécifique sur le taux de croissance des populations, et une composante intégrant l'erreur

d'observation commise lors du recensement des populations. Ce modèle permet notamment d'isoler et de quantifier les effets induits par les variabilités environnementales et démographiques ainsi que par les erreurs d'observations sur des propriétés de la communauté telles que la stabilité et la productivité.

Encadré 1. Modèles basés sur les dynamiques de population.

1.1. Modèles matriciels de populations

Les modèles matriciels de populations permettent de décrire les dynamiques temporelles de populations contenant un nombre J_k d'individus, $k = 1,...,N$. Ces individus sont répartis en classes distinctes, généralement définies selon leur phase de développement (e.g. établissement, croissance végétative, reproduction) ou leurs caractéristiques morphologiques (e.g. diamètre du tronc). Pour chaque population les effectifs, i.e. le nombre d'individus, de chacune des classes sont regroupés dans un vecteur $\boldsymbol{n}_k$, appelé vecteur population. A chaque pas de temps, les individus de la classe *i* sont susceptibles de modifier l'effectif de la classe *j*. Les variations de l'effectif de la classe *j* induites par les individus de la classe *i* sont quantifiées à travers un coefficient déterminé empiriquement. Les coefficients caractérisant les effets d'une classe sur une autre sont regroupés au sein d'une matrice, appelée matrice de projection de la population $\boldsymbol{A}$, de telle sorte que la composition de la population *k* à l'instant $t+1$, caractérisée par le vecteur population $\boldsymbol{n}_k(t+1)$, peut être calculée à partir de $\boldsymbol{n}_k(t)$ selon:

$$n_k(t+1) = A_k n_k(t) \qquad \text{(eq. 1.1)}$$

Dans leur forme classique les modèles matriciels de population supposent que les interactions entre individus d'espèces différentes n'influencent pas la dynamique de la communauté, ainsi chaque population évolue indépendamment des autres selon l'équation (eq.1).

1.2. Modèles de projection intégrale

Les modèles de projection intégrale sont basés sur le même principe que les modèles matriciels de population, mais la dynamique de la population est décrite par une variable d'état continue x et non un ensemble de classes distinctes. Ainsi le vecteur population $\boldsymbol{n}$ est remplacé par une fonction de distribution $n(x,t)$ telle que le nombre d'individus dont la variable d'état est dans l'intervalle $[x, x+dx]$ est donné par $n(x,t)dx$. La matrice de projection $\boldsymbol{A}$ est quant à elle remplacée par un noyau de projection $K(y,x) = P(y,x) + F(y,x)$ où P décrit le taux de survie et de croissance de l'état x à l'état y et F décrit le taux de production de descendants dont la variable d'état est y par des parents dont la variable d'état vaut x. La dynamique d'une population est alors décrite par:

$$n(y,t+1) = \int_{L}^{U} K(y,x) \cdot n(x,t)dx \qquad \text{(eq. 1.2)}$$

où $[L,U]$ est l'intervalle des états possibles. Le noyau de projection peut être estimé à partir de données similaires à celle employé pour construire la matrice de projection $\boldsymbol{A}$.

1.3. Modèle de Lotka-Volterra

Le modèle de Lotka-Volterra repose sur un ensemble d'équations différentielles ordinaires. Chaque équation décrit la dynamique temporelle d'une population en intégrant le taux de croissance intrinsèque de la population et l'impact des autres populations sur ce taux de croissance. Considérant une communauté composée de N populations, la dynamique de l'espèce i peut être décrite par l'équation différentielle suivante:

$$\frac{dx_i}{dt} = x_i \cdot f_i(x) \qquad \text{(eq. 1.3)}$$

Avec x_i la densité de l'espèce i, $\boldsymbol{x}$ un vecteur dont chaque élément correspond à la densité d'une des populations de la communauté et f_i le i-ème élément du vecteur $\boldsymbol{f}$ tel que:

$$f = r + Ax \qquad \text{(eq. 1.4)}$$

Ou $\boldsymbol{r}$ est un vecteur contenant les taux de reproduction ou de sénescence de chacune des populations composant la communauté et $\boldsymbol{A}$ est une matrice décrivant les relations entre les différentes espèces. L'élément de la i-ème ligne, j-ème colonne a_{ij} représente l'impact de l'espèce *j* sur l'espèce *i*. L'intensité de cet impact est proportionnelle aux densités de population des deux espèces x_i et x_j.

1.4. Modèles autorégressifs

Les modèles autorégressifs permettent de décrire un processus aléatoire dans lequel la valeur de la variable modélisée à l'instant $t+1$, X_{t+1} dépend linéairement de sa valeur à l'instant t, X_t et d'un terme stochastique ε_t. Le modèle se résume donc à une équation de différence stochastique de la forme:

$$X_{t+1} = a + b \cdot X_t + \varepsilon_t \qquad \text{(eq. 1.5)}$$

En écologie ces modèles peuvent être utilisés pour décrire la dynamique de la densité d'une population. Plusieurs modèles déterministes établissent une relation entre la densité d'une population à l'instant $t+1$, n_{t+1} et sa densité à l'instant t, n_t (e.g. Gompertz model). Certains de ces modèles peuvent se mettre sous une forme linéaire (e.g. transformation logarithmique du modèle de Gompertz) à laquelle il suffit ensuite d'ajouter un terme stochastique. Ces modèles de dynamique de population peuvent être généralisés de manière à décrire la dynamique d'une communauté contenant *N* populations. La version étendue de l'équation (eq.2) prend la forme d'un système matriciel:

$$X_{t+1} = A + BX_t + \mathrm{E}_t \qquad \text{(eq. 1.6)}$$

où $\boldsymbol{X_t}$ est un vecteur de taille *N* x 1 contenant l'abondance des différentes espèces à l'instant *t*, $\boldsymbol{A}$ est un vecteur de taille *N* x 1 de termes constants, $\boldsymbol{B}$ est une matrice de taille *N* x *N* dont les élément b_{ij} décrivent l'impact de la population *j* sur le taux de croissance de la population *i* et $\boldsymbol{E_t}$ est un vecteur de taille *N* x 1 contenant des variables aléatoires suivant une distribution normale multidimensionnelle de moyenne nulle et de matrice de covariance $\boldsymbol{\Sigma}$. Les vecteurs

$\boldsymbol{E}_t$ représentent la variabilité environnementale et sont supposés indépendants à travers le temps. En revanche les éléments de $\boldsymbol{E}_t$ ne sont pas indépendants les un des autres et leur covariation est décrite par les éléments non diagonaux de $\boldsymbol{\Sigma}$. Tous les paramètres du modèle peuvent être déterminés à partir de séries temporelles d'abondance.

Bilan. Les modèles basés sur les dynamiques de populations constituent des outils prédictifs facilement paramétrables et pouvant être aisément mis en oeuvre sur des systèmes réels. Par ailleurs ils fournissent une base de modélisation à laquelle divers mécanismes peuvent être aisément intégrés et ils représentent donc un bon moyen de tester des théories relatives au dynamiques des communautés végétales. Cependant ils reposent sur une représentation grossière, souvent empirique, du processus de croissance. Il est donc difficile d'utiliser un même modèle sur différents systèmes. De plus ces modèles ne permettent pas d'analyser finement la relation entre processus physiologiques des plantes et dynamiques des communautés.

II.3.2. Des modèles spatialement explicites basés sur l'individu

Un moyen de prendre en compte la structure spatiale dans les modèles de dynamique de communauté consiste à discrétiser l'espace en plusieurs parcelles, chaque parcelle contenant un petit nombre d'individus ou un unique individu (modèles individus centrés). Les dynamiques du ou des individus d'une parcelle sont décrites à l'aide de fonctions plus ou moins mécanistes, et les parcelles peuvent interagir les unes avec les autres. Par ailleurs les modèles individus centrés permettent d'intégrer la variabilité intraspécifique de manière explicite. Dans cette section on détaille quatre types de modèle spatialement explicites couramment utilisés en écologie des communautés végétales.

Une des approches de modélisation spatiale des dynamiques des communauté la plus utilisée au cours des deux dernière décennies s'appuie sur la théorie neutre. Cette théorie, développée par Hubbell (1979, 1997, 2001) est dite neutre car elle repose sur l'idée que tous les individus d'une communauté ont des taux de reproduction et de mortalité strictement équivalents (Encadre 3.1). Hubbell (2001) a montré que sa théorie est capable de reproduire un grand nombre de patterns observés sur le terrain, incluant la distribution des abondances des espèces au sein d'une communauté, la relation entre l'extension spatiale de la communauté et sa richesse spécifique ou encore la diversité bêta, i.e. la probabilité que deux individus appartiennent à la même espèce, connaissant la distance qui les sépare. Parce qu'ils reposent sur l'hypothèse d'équivalence des espèces et ignorent ainsi les contraintes spécifiques induites par la théorie des niches, les modèles neutres ont été sujet à une forte controverse (Whitfield, 2002; Chave, 2004; Alonso et al., 2006) et un grand nombre de travaux se sont attachés à tester empiriquement les prédictions produites par ces modèles. La plupart de ces travaux ont cherché à déterminer si les patterns d'abondance, de diversité et de distribution des espèces observés sur le terrain sont cohérents avec ceux produits par les modèles neutres (Condit et al., 2002; McGill, 2003; Volkov et al., 2003). Les résultats de ces études sont contrastés et ont conduit plusieurs écologues à rejeter la théorie neutre. Cependant même si elle ne s'appuie pas sur une description réaliste de la nature, la théorie neutre intègre des aspects importants des dynamiques de communautés que d'autres approches ignorent. Ainsi elle accorde une place centrale à la stochasticité démographique dans la modélisation des processus de recrutement et de mortalité, elle permet la prise en compte d'un grand nombre d'individus d'espèces différentes et propose des hypothèses sur la manière dont ces individus interagissent. Comme ils n'intègrent qu'un petit nombre de mécanismes communs à la majorité des communautés écologiques, les modèles neutres ont un rôle important à jouer en tant que modèles nuls et

sont susceptibles d'améliorer significativement notre compréhension des mécanismes gouvernant les dynamiques des communautés végétales.

Tout comme les modèles neutres, les modèles de loterie (Sale, 1977; Chesson & Warner, 1981) reposent sur une hypothèse centrale selon laquelle l'issue de la compétition pour l'établissement entre propagules est déterminée par le hasard (Encadre 2.2). Cependant à la différence des modèles neutres, chaque individu possède des caractéristiques spécifiques qui déterminent ses taux de reproduction, de croissance et de mortalité. Ce type de modèle a parfois été utilisé comme modèle nul pour tester l'importance des attributs fonctionnels sur la dynamique des communautés. Par exemple (Leishman & Murray, 2001) ont mis en évidence l'importance de la taille des graines sur la structure spatiale de la communauté en comparant les prédictions d'un modèle de loterie et d'un modèle plus mécaniste. Par ailleurs ils ont souvent été utilisés comme base pour confronter des hypothèses théoriques sur les mécanismes susceptibles d'expliquer la coexistence des espèces au sein des communautés (Chesson, 2000; Muko & Iwasa, 2000, 2003; Mouquet et al., 2002). Dans leur forme la plus classique ces modèles ne cherchent pas à décrire de manière précise les processus physiologiques gouvernant le développement des individus, et les interactions compétitives ne sont prises en compte qu'à travers la production de propagules. Cependant la prise en compte de la structure spatiale de la communauté et de la stochasticité démographique constitue une base intéressante pour la modélisation des communautés végétales.

Plusieurs approches de modélisation se sont appuyées sur les automates cellulaires, qui permettent de décrire à l'aide de règles simples la dynamique des individus ainsi que leurs interactions avec les autres individus de la communauté. Les automates cellulaires sont des systèmes dynamiques où le temps et l'espace sont discrétisés et dans lesquels la distribution

d'une espèce à travers une grille environnementale en deux dimensions est déterminée par des règles traduisant des processus biologiques tels que la dispersion des graines, l'expansion clonale et les interactions entre individus voisins (Encadré 2.2). Ils ont été utilisés pour étudier des questions théoriques comme l'influence sur les dynamiques des communautés des stratégies d'utilisation des ressources (Colsanti & Grime, 1993; van Wijk & Rodriguez-Iturbe, 2002) et de reproduction (Crawley & May, 1987; Silvertown et al., 1992). Mais ils peuvent également servir à produire des prédictions sur les variations de la composition des communautés végétales induite par des changements d'utilisation des sols (Wilkie & Finn, 1988; Soares-Filho, 2002), par la destruction d'habitat (Dytham, 1995) ou encore par les changements climatiques (Carey, 1996). Généralement ces modèles sont développés pour une application précise dans un contexte donné et de par leur structure, ils ne peuvent être appliqués en dehors de ce cadre. En effet les règles de transition définies dépendent à la fois des espèces considérées et des conditions environnementales et pour des espèces et des habitats différents, ces règles sont susceptibles de changer. Par ailleurs la variabilité démographique inter individus n'est généralement pas prise en compte.

Les modèles de trouées (ou "gap model") sont plus axés sur la compréhension des mécanismes que les modèles précédemment décrits. Le processus de recrutement est ainsi favorisé par la création d'une trouée dans la canopée qui correspond à une libération d'espace et de ressources. D'autre part le processus de croissance est généralement modélisé à l'aide d'une fonction spécifique à l'espèce qui tient compte des facteurs biotiques et abiotiques. Le détail de cette fonction varie à travers les différents modèles de trouée (Shugart & Smith, 1996; Bugmann, 2001). Les processus de reproduction et de mortalité sont essentiellement stochastiques même si certains modèles s'appuient sur des attributs fonctionnels pour contraindre ces processus. Initialement développé pour une application aux communautés

forestières, le cadre conceptuel des modèles de trouée à été étendu aux communautés prairiales (Coffin & Lauenroth, 1990), aux alpages (Humphries et al., 1996) et aux savanes (Gignoux et al., 1995). De plus il a été modifié de manière à pouvoir simuler la dynamique de communautés comprenant plusieurs types de végétation (e.g interface prairie/forêt, Smith et al., 1989). Ils ont été notamment utilisés pour étudier l'impact des changements climatiques sur la dynamique des forêts (Bowes & Sedjo, 1993; Fischlin et al., 1995; Lindner et al., 2000), pour étudier l'impact des perturbations comme les incendies (Keane et al., 1990) mais aussi pour l'aide au développement de politiques de gestion (Mohren & van de Veen, 1991). Si quelques modèles de trouée ont des bases mécanistes solides (Kellomäki & Kolström, 1992), la plupart de ces modèles utilisent des fonctions de réponse phénoménologiques fortement dépendante des espèces et des habitats considérés.

Encadré 2. Modèles spatialement explicites basés sur l'individu.

2.1. Modèles neutres

Dans leur forme la plus classique les modèles neutres décrivent une communauté locale contenant J individus. A chaque pas de temps, un de ces individus, choisi aléatoirement, meurt et est remplacé. Le remplaçant est un descendant d'un autre individu choisi aléatoirement soit dans la communauté locale avec une probabilité m, soit dans un ensemble d'espèces extérieures à la communauté, désigné comme la métacommunauté, avec une probabilité $(1-m)$. Le paramètre m caractérise donc la limitation de la dispersion. La métacommunauté contient J_M individus et la distribution des abondances des espèces est supposée constante à l'échelle temporelle de la communauté locale. Un processus similaire à celui décrivant la dynamique de la communauté locale détermine la distribution des abondances dans la métacommunauté, les remplaçants des espèces mourantes étant toujours des descendants des individus de la métacommunauté, sauf dans le cas d'un événement de

spéciation. La spéciation correspond à l'apparition d'une nouvelle espèce dans la métacommunauté et la probabilité qu'un tel événement se produise est noté υ. La théorie neutre caractérise la distribution d'échantillonnage des abondances des espèces dans une métacommunauté de taille J_M et de taux de spéciation υ à l'aide d'un unique paramètre agrégé $\theta = J_M.\upsilon / (1- \upsilon)$. Plusieurs variantes de ce modèle existent.

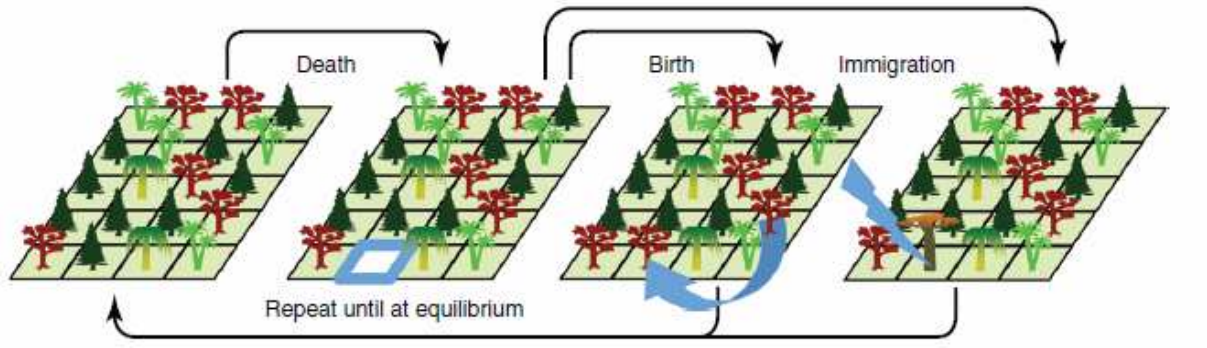

2.2. Modèles de loterie

Dans leur forme la plus classique les modèles de loterie décrivent une communauté locale contenant *N* populations. L'espace est divisé en *K* parcelles, chaque parcelle étant occupée de manière exclusive par un unique individu. Entre les instants *t* et *t+1* une proportion $\delta_i(t)$ des individus de l'espèce *i* meurent, libérant ainsi les parcelles qu'ils occupaient. Ces parcelles sont colonisées par de nouveaux individus appartenant aux populations présentes au sein de la communauté. Le système de loterie postule que la probabilité qu'une espèce *i* colonise une parcelle libre est donnée par le ratio entre le nombre de descendants produit par l'espèce *i* et le nombre total de descendants produit par l'ensemble des espèces de la communauté. Le nombre de descendants produit par l'espèce *i* est déterminé par le taux individuel net de reproduction $\beta_i(t)$. Dans ce cadre la proportion de parcelles occupées par l'espèce *i* à l'instant *t+1*, $P_i(t+1)$ peut s'exprimer à partir de la proportion de parcelles occupées par l'espèce *i* à l'instant *t*, $P_i(t)$ selon:

$$P_i(t+1) = \left(1-\delta_i(t)\right)\cdot P_i(t) + \left(\sum_{j=1}^{N}\delta_j(t)\cdot P_j(t)\right)\cdot\frac{\beta_i(t)\cdot P_i(t)}{\sum_{j=1}^{N}\beta_j(t)\cdot P_j(t)} \qquad \text{(eq. 2.1)}$$

2.3. Modèles à automate cellulaire

Les automates cellulaires sont des modèles dynamiques discrets en temps, en espace et en état. Un automate cellulaire simple est défini par un maillage L, un ensemble des états Q, un modèle de voisinage δ et une fonction de transition locale f. Chaque cellule de L peut être dans un état discret appartenant à Q. Les cellules peuvent être reliées de différentes façons, avec dans le cas le plus simple une connexion géométrique (e.g. grille carrée, parcelles hexagonales). Les cellules sont susceptibles de changer d'état à chaque pas de temps. Généralement les automates cellulaires sont synchrones, i.e toutes les cellules changent d'état simultanément. La dynamique d'une cellule dépend de son voisinage et de la fonction de transition f, qui peut être déterministe aussi bien que stochastique.

2.4. Modèles de trouées

Les modèles de trouées décrivent l'établissement, la croissance et la mort des individus d'une communauté au sein d'une parcelle de petite taille avec une résolution temporelle annuelle. Lorsqu'un des individus meurt, il libère un espace (ou gap) au sein du patch, augmentant ainsi le niveau de ressource disponible pour les individus concurrents ainsi que le taux de recrutement. La manière dont sont estimés le taux d'établissement, la croissance et la mortalité des individus varie largement à travers les différents "gap models" avec différents niveaux de détails et d'intégration des mécanismes sous-jacents. Les processus d'établissement et de mortalité sont souvent décrits par des processus stochastiques tandis que la croissance est déterministe. Ces processus peuvent être contraints par des caractéristiques connus des espèces (e.g. production de graines, taux de croissance maximal, longévité), par les facteurs abiotiques (e.g. niveau de nutriments dans le sol, température) et par la compétition pour l'accès au ressource (e.g. nutriments, eau, lumière).

Bilan. Se placer à l'échelle de l'individu plutôt qu'à celle de la population permet une description plus fine des processus dirigeant la croissance. Par ailleurs comme la structure spatiale des communautés végétales modélisées est explicitement représentée, il est possible d'utiliser ces modèles pour étudier l'impact des hétérogénéités spatiales de l'environnement ou de la disposition des individus sur la dynamique des communautés. Toutefois bon nombre de ces modèles reposent sur une représentation simpliste du processus de croissance et ne prennent en compte que quelques facteurs environnementaux. Les quelques modèles cherchant à représenter plus finement le processus de croissance s'appuient souvent sur des paramètres spécifiques à la communauté étudiée ou à la problématique abordée. Ils manquent donc de généralité pour explorer des questions comme l'impact de gradients environnementaux sur les dynamiques de communautés et ne peuvent être utilisés pour relier les processus physiologiques sous-jacents aux dynamiques des communautés.

II.3.3. Vers une modélisation basée sur les traits fonctionnels

Il a été suggéré que les traits fonctionnels pouvaient être utilisés pour relier la réponse individuelle des espèces végétales constituant une communauté à la dynamique de cette communauté (Suding et al., 2003; Gross et al., 2009). Le modèle basé sur la maximisation de l'entropie développé par Shipley et al. (2006) constitue une des premières tentatives d'intégration de cette relation entre traits fonctionnels et dynamique des communautés au sein d'un cadre mathématique prédictif. Ce modèle repose sur la convergence des traits sous l'effet du filtrage environnemental, ainsi le modèle prédit une dominance des espèces dont les traits ont des valeurs moyennes proches des valeurs des traits moyens pondérés au niveau de la communauté ("community-weighted mean traits" (CWMT) en anglais). Il a été montré que cette approche permettait de prédire avec précision la composition de diverses communautés végétales lorsque les CWMT étaient connus (Shipley et al., 2006; Frenette-Dussault et al.,

2013), cependant les pouvoirs prédictifs de ce modèle sont sujets à débat (Marks & Muller-Landeau, 2007; Roxburgh & Mokany, 2007). Récemment, Laughlin et al. (2012) ont proposé un nouveau cadre de modélisation bayésien pour relier les dynamiques des communautés aux traits fonctionnels, tout en évitant une partie des problèmes soulevés par l'approche de Shipley et al. (2006). Ces approches sont intéressantes, d'une part parce qu'elles constituent un outil prédictif qui peut permettre d'anticiper les variations de la composition des communautés végétales sous l'effet de changements environnementaux, et d'autre part parce qu'elles mettent en évidence l'existence d'un lien fort entre traits fonctionnels et dynamiques des communautés. Toutefois comme elles sont basées sur des modèles statistiques elles ne peuvent être utilisées pour étudier la nature de ce lien. Pour mieux comprendre et quantifier la relation entre traits fonctionnels et dynamique des communautés il est donc nécessaire de développer des modèles plus dynamiques.

Au cours des quinze dernières années, quelques modèles dynamiques basés sur les traits fonctionnels ont été développés. Ainsi Norberg et al. (2001) ont dérivé une équation de croissance pour décrire les dynamiques de la biomasse ou de la taille d'une population en fonction d'un unique trait et des conditions environnementales. Cette approche a par la suite été enrichie par Savage et al. (2007) de manière à pouvoir intégrer l'effet de plusieurs traits sur les dynamiques des communautés. Puis plus récemment par Enquist et al. (2015) à travers la "trait driver theory" (TDT). La TDT couple l'approche de Norberg et al. (2001) avec d'une part l'hypothèse du ratio de masse (en anglais "mass ratio hypothesis"; Grime, 1998) qui postule que le fonctionnement des communautés est déterminé par les traits des espèces dominantes, et d'autre part avec la "metabolic scaling theory" qui permet de relier les traits fonctionnels associés au métabolisme à la réponse individuelle (croissance et utilisation des ressources), puis au fonctionnement de la communauté (Enquist et al., 1998, 2003, 2009). Ces

approches ont permis d'analyser le rôle des traits fonctionnels, de leur diversité, de leur niveau de corrélation et de leur plasticité sur le fonctionnement de la communauté. Cependant comme la relation entre traits fonctionnels, facteurs abiotiques et réponse individuelle est décrite par une fonction empirique, ce type de modèle ne permet pas de remonter aux mécanismes qui déterminent la distribution des traits fonctionnels au sein des communautés végétales. Pour analyser ces mécanismes, il est nécessaire de mettre en place des approches qui font le lien entre traits fonctionnels et processus physiologiques tout en prenant en compte les interactions de ces processus entre eux et avec l'environnement.

Les traits fonctionnels sont depuis longtemps utilisés pour modéliser les processus physiologiques des plantes. Farquhar et al. (1980) ont ainsi développé un modèle de photosynthèse qui dépend des taux de carboxylation et de régénération du RuBP ainsi que du point de compensation, la loi de la diffusion de Fick permet d'exprimer le taux de transpiration potentiel des feuilles en fonction de la conductance stomatique (Farquhar & Sharkey, 1982) et la relation de Hane permet de relier la capacité potentielle d'extraction de l'azote d'un individu à la concentration en azote du sol (Engels et al., 2000). Pour la plupart des processus physiologiques il existe une grande diversité de modèles, phénoménologiques ou mécanistes, qui intègrent des traits fonctionnels plus ou moins facilement mesurables sur le terrain. Pour autant la plupart des modèles utilisés pour étudier les dynamiques des communautés ne s'appuient pas sur la modélisation des processus physiologiques pour décrire l'utilisation des ressources et la croissance des individus (section III.1 et III.2). L'intérêt porté aux traits au cours des dernières années et la mise en évidence de leur utilité pour la compréhension et la prédiction des dynamiques des communautés ont incité les chercheurs à intégrer des modèles physiologiques dans leurs modèles de dynamique. Marks & Lechowicz (2006) ont ainsi adopté cette démarche et ont proposé un modèle de dynamique forestière axé

sur les traits fonctionnels. Ces derniers contraignent la réponse des individus à travers l'utilisation de quatre ressources essentielles à la croissance des végétaux: la lumière, l'eau, l'azote et le carbone. Van Wijk (2007) a utilisé une démarche similaire pour modéliser les dynamiques de communautés arctiques, la croissance des individus dépend ainsi de la valeur de leurs traits et des quantités de lumière et d'azote auxquelles ils ont accès. Enfin Soussana et al. (2013) ont récemment proposé un modèle pour les communautés prairiales basé sur les processus physiologiques des végétaux et paramétrable à partir de traits fonctionnels. Ce modèle permet de simuler la croissance d'un individu moyen pour chaque population d'une communauté multispécifique de plantes C_3 tout en tenant compte de l'impact des facteurs abiotiques et de la compétition pour la lumière et l'azote. Cependant les modules utilisés dans ce modèle pour décrire les processus physiologiques sont très détaillés et il en résulte un coût de paramétrisation très élevé.

Bilan. L'utilisation des traits fonctionnels dans les modèles de dynamique des communautés permettent de relier la distribution des traits au sein de la communauté à son fonctionnement et à sa composition, soit à l'aide de fonction phénoménologiques de croissance, soit à l'aide d'une modélisation plus fine des processus physiologiques et de leurs interactions entre eux et avec l'environnement. Ce type d'approche est donc susceptible d'améliorer significativement notre compréhension du lien entre réponse individuelle des espèces et dynamique des communautés. Cependant, encore peu de modèles intègrent les traits, et le seul modèle de dynamique de communautés prairiales développé dans ce cadre présente une grande complexité (Soussana et al., 2013).

III. Analyser les mécanismes structurant les communautés à l'aide d'un modèle stochastique de dynamique des populations.

Manuscrit correspondant:

Lohier, T., Jabot, F., Weigelt, A., Schmid, B., & Deffuant, G. (in review). Predicting stochastic community dynamics in grassland under the assumption of competitive symmetry.

Predicting stochastic community dynamics in grasslands under the assumption of competitive symmetry

Théophile Lohier, Franck Jabot, Alexandra Weigelt, Bernhard Schmid & Guillaume Deffuant

Submitted to Journal of Theoretical Biology

Jabot, F. (Corresponding author, franck.jabot@m4x.org)[1]

Lohier, T. (theophile.lohier@gmail.com)[1]

Weigelt, A. (alexandra.weigelt@uni-leipzig.de)[2]

Schmid, B. (bernhard.schmid@ieu.uzh.ch)[3]

Deffuant, G. (guillaume.deffuant@irstea.fr)[1]

[1]LISC - Laboratoire d'Ingénierie pour les Systèmes complexes, IRSTEA, 9 avenue Blaise Pascal, CS 20085, 63178 Aubière, France.

[2]Institute of Biology, University of Leipzig, Johannisallee 21-23, 04103, Leipzig, Germany.

[3]Institute of Evolutionary Biology and Environmental Studies, University of Zurich, Winterthurerstrasse 190, CH-8057, Zurich, Switzerland.

ABSTRACT

Community dynamics is influenced by multiple ecological processes such as environmental spatiotemporal variation, competition between individuals and demographic stochasticity. Quantifying the respective influence of these various processes and making predictions on community dynamics require the use of a dynamical framework encompassing these various components. We here demonstrate how to adapt the framework of stochastic community dynamics to the peculiarities of herbaceous communities, by using a short temporal resolution adapted to the time scale of competition between herbaceous plants, and by taking into account the seasonal drops in plant aerial biomass following winter, harvesting or consumption by herbivores. We develop a hybrid inference method for this novel modelling framework that both uses numerical simulations and likelihood computations. Applying this methodology to empirical data from the Jena biodiversity experiment, we find that environmental stochasticity has a larger effect on community dynamics than demographic stochasticity, and that both effects are generally smaller than observation errors. We further evidence that plant intrinsic growth rates and carrying capacities are moderately predictable from plant vegetative height, specific leaf area and leaf dry matter content. We do not find any trade-off between demographical components, since species with larger intrinsic growth rates tend to also have lower demographic and environmental variances. Finally, we find that our model is able to make relatively good predictions of multi-specific community dynamics based on the assumption of competitive symmetry.

1. INTRODUCTION

Plant community dynamics is driven by intra- and interspecific interactions, and by environmental factors such as climatic conditions or soil composition. The way these processes influence community dynamics is of utmost importance for understanding community assembly (Ackerly 2003; Ejrnaes et al. 2006; Chase 2010), productivity (Mouquet et al. 2002) and stability (Sprugel 1991; Hector et al. 2010). Studies based on static descriptors of community structure have provided tests for predictions of ecological theories (Stubbs & Wilson 2004; Cornwell et al. 2006; Norden et al. 2009; Gonzalez et al. 2010). The next step is to quantitatively relate empirical observations to the underlying dynamical processes (Jabot & Chave 2011; de Mazancourt et al. 2013). In this vein, a growing number of studies aim at building dynamical models of community dynamics based on explicit ecological processes, and at calibrating these models with field data (Lande et al. 2003; Beaumont 2010), thereby belonging to the more general trend towards a more predictive ecology (Mouquet et al. 2015).

To build models of plant community dynamics, the framework of stochastic population dynamics is particularly appealing (Lande et al. 2003). This approach consists in modelling the joint effects of competitive interactions, demographic and environmental stochasticities on community dynamics. Although the role of environmental stochasticity in community dynamics has been recognized for a long time (Chesson & Warner 1981), it has been neglected in many recent analyses by community ecologists (Chisholm et al. 2014; Kalyuzhny et al. 2015). There is therefore a renewing interest in better taking into account this component of community dynamics in dynamical models (de Mazancourt et al. 2013, Kalyuzhny et al. 2015).

This general framework has been mainly applied to easily countable organisms, such as animals (Lande et al. 2003) or trees (Chisholm et al. 2014, Kalyuzhny et al. 2015). To be applied to herbaceous plants, it has been proposed to model the dynamics of plant biomass instead of population sizes (de Mazancourt et al. 2013). But two additional specificities of herbaceous plant communities have been mainly overlooked in previous studies. First, the time scale of variation in competition between plants is short, due to the temporal variability of resources and to the rapid modification of vertical community structure following plant growth (Wilson and Tilman 1993, Silvertown et al. 2015). Second, herbaceous plant communities face frequent major disturbance events leading to sudden aerial biomass drops, such as winter mortality of aerial plant tissues or agricultural harvests by mowing or grazing (Jouven et al. 2006, Jabot and Pottier 2012). These disturbance events periodically reset aerial biomass to low levels, and therefore need to be taken into account in dynamical models of community dynamics.

The present study aims at developing a model of stochastic dynamics for herbaceous plant communities based on biomass rather than population sizes, and at taking into account both the short temporal scale of between plant competition and the frequent biomass drops encountered by herbaceous plant communities. We detail an inference method to calibrate the daily time step model parameters from biomass measurements in the field at seasonal time steps, coming from the Jena biodiversity experiment (Weigelt et al. 2010). This methodological development enables us to answer to four questions on herbaceous plant community dynamics: 1) what is the respective influence of demographic and environmental variabilities on community dynamics? 2) is there an equalizing trade-off between species intrinsic growth rates and their temporal stability as would be expected for species coexistence (Chesson 2000)? 3) are species demographical characteristics predictable from

plant functional traits? 4) are multi-specific community dynamics predictable from species individual dynamics?

2. METHODS

2.1. A new biomass-based model of plant stochastic community dynamics

The model describes the dynamics of species aboveground biomass within a growing season and the way competition, demographic and environmental stochasticities affect species growth. In the following, we call "season" a temporal period during which plants are growing without experiencing a strong biomass decrease or removal (due to winter, harvests or consumption by herbivores). At the end of each season, the aboveground biomass is assumed to drop and this reduced biomass is used to initialize the species dynamics in the following season (Fig. 1). A community is here defined as a group of plants of the same or of different species growing in the same plot *p*. The intra-seasonal dynamics of plant growth is modelled with a daily time step. The biomass of species *i* during season *T* in plot *p* after *t* days of growth, $B_i(t,p,T)$, is modelled with the following difference equation:

$$B_i(t+1,p,T) = B_i(t,p,T) + \left(r_{mi} + \sigma_{ei} u_{ei}(T) + \frac{\sigma_{di} u_{di}(T,p)}{\sqrt{B_i(0,p,T)}} \right) \cdot B_i(t,p,T) \cdot \left(1 - \frac{B_i(t,p,T) + \sum_{j \neq i} \alpha_{ij} B_j(t,p,T)}{K_i} \right) \quad \text{(eq.1)}$$

where r_{mi} is the intrinsic growth rate of species *i*, K_i is its carrying capacity and α_{ij} is the inter-specific competition coefficient describing the effect of species *j* on species *i*. Environmental stochasticity encompasses the inter-seasonal variability in species growth rates stemming from environmental variability. It is modelled through $\sigma_{ei} u_{ei}(T)$ where σ_{ei}^2 is the environmental variance, and $u_{ei}(T)$ are drawn from a normal distribution with zero mean and unit variance. For each species *i*, $u_{ei}(T)$ are assumed to be constant across all plots *p* during season *T*. Demographic stochasticity encompasses intra-specific variability. It is incorporated

through $\sigma_{di}u_{di}(T,p)$ where σ_{di}^2 is the demographic variance, and $u_{di}(T,p)$ are drawn from a normal distribution with zero mean and unit variance, and are thus assumed to vary across the plots p. Consequently, the growth rate of a given species is likely to differ across plots because of demographic stochasticity and across seasons because of both demographic and environmental stochasticities. The last logistic term represents intra- and inter-specific competition for resources which decreases the plant growth rate. This growth reduction due to competition increases as plants grow during the season.

The biomass at the start of the growing season $B_i(0,p,T)$ is used in the scaling of the demographic variance in equation (eq.1) as being a proxy of the number of growing individuals in season T. $B_i(0,p,T)$ is assumed to be constant across seasons and equal to $B_0 = 2$ g.m^{-2} for monocultures while in species mixtures, B_0 is equally divided between species.

2.2. Field data

We used data from the long-term grassland biodiversity experiment in Jena (Weigelt et al. 2010). In this dataset, 60 plant species were grown in monocultures from 2002 to 2010, with each monoculture replicated in 2 plots. In each monoculture plot, biomass was measured twice a year in June and September, in 2 samples per plot. Half of the monocultures (i.e 60 plots) were given up in 2006. Additionally, 16 mixtures of 2, 4 and 8 plant species, 14 mixtures of 16 plant species and 4 mixtures of all 60 plant species were grown from 2002 to 2008. In each polyculture plot, biomass of all plant species was measured twice a year in June and September, in 4 samples per plot. After each biomass measurement, both monoculture and polyculture plots were mown (Weigelt et al. 2010). We therefore consider in the

following that there are two growing seasons per year, from April to June, and from July to September (Fig.1).

2.3. Inference based on monoculture data

The daily time step model parameters encompasses species characteristics (r_{mi}, K_i, σ_{ei}, σ_{di}) as well as environmental and demographic seasonal variables $u_{ei}(T)$ and $u_{di}(T,p)$. We present in the following how all these parameters can be estimated using field biomass data of species grown in monoculture for several years, as in the Jena experiment. It is worth noting at this point that there is a mismatch of time scale between the modelled processes of plant growth occurring at a daily time step, and the available biomass data collected at a seasonal time step, at the end of each growing season. This mismatch of time scales requires developing an adapted estimation method detailed below.

The sampling procedure used to collect biomass data generates an observation error. We model this observation error with a lognormal distribution, meaning that observed biomass $B_i^{obs}(T,p,s)$ of species i in season T, plot p, sample s, is the real biomass $B_i(T,p)$ in season T, plot p, plus a random variable representing observation error:

$$\ln\left(B_i^{obs}(T,p,s)\right) = \ln\left(B_i(T,p)\right) + \sigma_{oi} \cdot u_{oi}(T,p,s) \qquad \text{(eq.2)}$$

where σ_{oi}^2 is the observation variance, and $u_{oi}(T,p,s)$ are independent normal variables with zero mean and unit variance. The real biomass is therefore estimated as the average of observed log-transformed biomass across samples:

$$\hat{B}_i(T,p) = \exp\left(\frac{1}{N_s}\sum_{s=1}^{N_s}\ln\left(B_i^{obs}(T,p,s)\right)\right) \qquad \text{(eq.3)}$$

where N_s is the number of samples harvested in a plot. Note that we used here the notation $\hat{B}_i(T,p)$ to designate our estimates of the true values $B_i(T,p)$. We keep this convention for estimates in the following of this paragraph.

The observation variance is estimated as the empirical variance of observed biomass across samples:

$$\hat{\sigma}_{oi}^{2} = \frac{1}{N_T \cdot N_p \cdot (N_s - 1)} \cdot \sum_{T,p,s} \left(\ln\left(B_i^{obs}(T,p,s)\right) - \ln\left(\hat{B}_i(T,p)\right) \right)^2 \qquad \text{(eq.4)}$$

The estimated real biomass data $\hat{B}_i(T,p)$ according to equation 3 (eq.3) are then used in the following.

The carrying capacity K_i of species i is assumed to be linearly related to the maximal biomass of species i across seasons, and is therefore estimated as:

$$\hat{K}_i = a \cdot \max_{T,p} \hat{B}_i(T,p) \qquad \text{(eq.5)}$$

In the following, a will be arbitrarily fixed to 2. We checked that alternative choices for a did not change the results qualitatively by repeating the analyses with values of a equal to 1.5 and 3 (data not shown).

We then estimated the intra-seasonal growth rates $r_i(T,p)$ of species i for plot p and season T, defined as:

$$r_i(T,p) = r_{mi} + \sigma_{ei} \cdot u_{ei}(T) + \frac{\sigma_{di} \cdot u_{di}(T,p)}{\sqrt{B_0}} \qquad \text{(eq.6)}$$

For a given value of $r_i(T,p)$, the biomass dynamics can be estimated with the following difference equation (see eq. 1):

$$B_i^{sim}(t+1,p,T) = B_i^{sim}(t,p,T) + r_i(T,p)\cdot B_i^{sim}(t,p,T)\cdot\left(1-\frac{B_i^{sim}(t,p,T)}{\hat{K}_i}\right) \qquad \text{(eq.7)}$$

We used an optimization algorithm to estimate $\hat{r}_i(T,p)$ that minimizes the difference between the simulated and real biomass at the end of the growing season $\left|B_i^{sim}(60,p,T) - \hat{B}_i(T,p)\right|$.

Then the set of model parameters (r_{mi}, σ_{ei}, σ_{di}) are estimated from the estimated intra-seasonal growth rates $\hat{r}_i(T,p)$ with a maximum likelihood procedure: let $\hat{r}$ be the vector of previously estimated intra-seasonal growth rates then the likelihood function $L(\{r_{mi},\sigma_{ei},\sigma_{di}\}|\hat{r})$ can be defined up to a multiplicative constant as:

$$L(\{r_{mi},\sigma_{ei},\sigma_{di}\}|\hat{r}) = \prod_{T,p}\int_{-\infty}^{+\infty}\frac{1}{2\pi\sigma_{ei}\sigma_{di}}\exp\left[-\frac{1}{2}\cdot\left(\left(\frac{t}{\sigma_{ei}}\right)^2+\left(\frac{\hat{r}_i(T,p)-r_{mi}-t}{\sigma_{di}}\sqrt{B_0}\right)^2\right)\right]dt \qquad \text{(eq.8)}$$

This equation (eq. 8) is obtained by writing down the probability of generating the estimated intra-seasonal growth rates $\hat{r}_i(T,p)$ from random draws of $u_{ei}(T)$ and $u_{di}(T,p)$ in normal distributions with zero mean and unit variance.

The set of model parameters (r_{mi}, σ_{ei}, σ_{di}) are estimated as:

$$\{\hat{r}_{mi},\hat{\sigma}_{ei},\hat{\sigma}_{di}\} = \arg\max L(\{r_{mi},\sigma_{ei},\sigma_{di}\}|\hat{r}) \qquad \text{(eq.9)}$$

Finally the estimation of the realized values of environmental and demographic variables $u_{ei}(T)$ and $u_{di}(T,p)$ is based on a maximum likelihood procedure. Let $\hat{r}(T,.) = \left(\hat{r}(T,1),...,\hat{r}(T,p)\right)$ be the vector of previously estimated intra-seasonal growth rates across plots for season T and $\boldsymbol{u(T)} = (u_{ei}(T), \boldsymbol{u_{di}(T,.)})$ with $\boldsymbol{u_{di}(T,.)}$ the vector of demographic random draws across plots for season T. From (eq.6), the likelihood $L(u(T)|\hat{r}(T,.),\hat{r}_{mi},\hat{\sigma}_{ei},\hat{\sigma}_{di})$ is given by:

$$L(u(T)\,|\,\hat{r}(T,.),\hat{r}_{mi},\hat{\sigma}_{ei},\hat{\sigma}_{di}) =$$

$$(2\cdot\pi)^{-(Np+1)/2}\cdot\exp\left[-\frac{1}{2}\cdot\left(u_{ei}(T)^2+\sum_{p}^{Np}\left(\frac{\hat{r}_i(T,p)-\hat{r}_m-\hat{\sigma}_{ei}\cdot u_{ei}(T)}{\hat{\sigma}_{di}}\sqrt{B_0}\right)^2\right)\right] \qquad \text{(eq.10)}$$

Maximisation of the likelihood function enables to estimate $\hat{u}_{ei}(T)$. The demographic values $\hat{u}_{di}(T,.)$ are then deduced from (eq.6). All optimization procedures were performed with the "optim" R function using the Nelder and Mead (1965) algorithm. In the following, we do not distinguish the notation of estimated values from that of true values to keep the notations simple.

2.4. Model checking

To assess the ability of our model to reproduce observed biomass dynamics in monocultures, we performed several model checks. First, we assessed, for each of the 60 species in monocultures, whether fitted realized values of environmental variables $u_{ei}(T)$, demographic variables $u_{di}(T,p)$ and observation errors $u_{oi}(T,p,s)$ significantly deviated from normal distributions using a Kolmogorov-Smirnov test (Kolmogorov, 1933). Second, we simulated the monospecific biomass dynamics using our stochastic model with fitted parameters (r_{mi}, K_i, σ_{ei}, σ_{di}, σ_{oi}) and variables (u_{ei}, u_{di}, u_{oi}) randomly drawn in normal distribution with zero mean and unit variance and compared the outputs of these simulations with observed biomass dynamics to assess whether systematic deviations between the two were present. More precisely, for each of the 60 species, we simulated virtual data, following the Jena experimental setup: each monoculture was replicated in two plots, and two subsamples by plot were harvested during 17 seasons. Each such monoculture simulation was replicated 100 times, and for each replication, the average and standard deviation of community biomass across plots, subsamples and seasons were computed. The ability of the model to reproduce

the observed values of these indicators for species *i* was assessed through the p-value p_i computed as the rank of the observed value within the set of simulated values. The model was considered to pass the model checking test when the p-value was comprised between 0.025 and 0.975.

2.5. Quantifying the sources of biomass variability

For each species, we assessed the effects of environmental stochasticity, demographic stochasticity and observation error on observed biomass variances. To do this, we simulated monoculture biomass dynamics using fitted parameters (r_{mi}, K_i, σ_{ei}, σ_{di}, σ_{oi}) and variables (u_{ei}, u_{di}, u_{oi}) randomly drawn in normal distribution with zero mean and unit variance in a virtual plot sampled once during 1000 seasons. This biomass time series was used to compute the reference biomass variance V_{ref}. We then replicated this procedure, shutting down sequentially observation error, demographic stochasticity, and environmental stochasticity. The contributions of these three sources of variability to observed biomass variability were then computed as the relative decrease in biomass variance caused by the suppression of these sources of variability in the simulations. More precisely, the effect of observation error was computed as $\Sigma_o = (V_{ref} - V_{e+d}) / V_{ref}$, where V_{e+d} stands for the biomass variance in simulations with environmental and demographic stochasticity only. The effect of demographic stochasticity was computed as $\Sigma_d = (V_{e+d} - V_e) / V_{ref}$, where V_e stands for the biomass variance in simulations with environmental stochasticity only. The effect of environmental stochasticity was finally computed as $\Sigma_e = V_e / V_{ref}$.

2.6. Analyzing species demographical characteristics

We assessed whether species with larger intrinsic growth rates r_{mi} have also larger demographic σ_{di}^2 and environmental σ_{ei}^2 variances by correlation analyses. We also assessed

whether species demographical characteristics (r_{mi}, K_i, σ_{ei}, σ_{di}) could be predicted from three functional traits: plant vegetative height, specific leaf area (SLA) and leaf dry matter content (LDMC). Trait data were extracted from the LEDA trait database (Kleyer et al., 2008). When multiple entries for a given species were available, we used average values.

2.7. Predicting multi-specific community dynamics based on the assumption of competitive symmetry

We finally assessed whether knowledge of species individual demographical characteristics was sufficient to predict the multi-specific community dynamics in mixtures. Predictions in mixtures were based on the assumption of competitive symmetry, meaning that the coefficients α_{ij} in equation 1 were fixed to 1. This assumption is rather strong, but it represents a first step in order to predict complex community dynamics, in the spirit of neutral community models (Rosindell et al. 2011) and their extensions (Jabot and Chave 2011, Kalyuzhny et al. 2015). All other species demographical parameters (r_{mi}, K_i, σ_{ei}, σ_{di}, σ_{oi}) were set to their estimates from monoculture data (see section 2.3).

We performed several sets of predictions for mixtures to assess the gain in prediction accuracy brought by several components of species demography. In the first set of simulations, we used the realized values of environmental variables $u_{ei}(T)$ estimated from monoculture data. The demographic and observation variables, $u_{di}(T,p)$ and $u_{oi}(T,p,s)$ are however likely to vary from one plot to another. We therefore run 100 simulations for each mixture with $u_{di}(T,p)$ and $u_{oi}(T,p,s)$ randomly drawn in normal distributions with zero mean and unit variance, and using the same sampling protocol as in the Jena experiment (see section 2.2). This set of simulation incorporates both the demographical specificities of each species in the mixtures, and the temporal asynchrony of species responses to environmental

variability through $u_{ei}(T)$. We additionally performed a second set of simulations in which the observed temporal asynchrony was not taken into account anymore. Concretely, in this set of simulations, instead of using the realized values of environmental variables $u_{ei}(T)$ fitted on monoculture data, we randomly drew them in normal distributions with zero mean and unit variance. In doing this, species are assumed to respond independently to environmental variability.

For each set of simulations, we computed the average $\overline{B}$ and standard deviation σ_B of community biomass across seasons and subsamples, as well as the Simpson's concentration index defined as:

$$\lambda = \sum_{i=1}^{N} \overline{p}_i^2 \qquad \text{(eq.11)}$$

For each mixture, the distribution across replicates of $\overline{B}$, σ_B and λ was compared with observed values and the ability of the model to reproduce community dynamics was assessed through the p-value computed as the rank of the observed value within the set of simulated values. For each species richness level, we defined an aggregated indicator N_{dev}, which describes the proportion of mixtures for which the p-value is smaller than 0.025 or higher than 0.975. Moreover the average of $\overline{B}$, σ_B and λ across replicates were computed and the correlation between predicted averages and observed values across mixtures was quantified.

Finally, the overall discrepancy between observed values in mixtures and predicted averages is not necessarily indicative of a failure of the assumption of competitive symmetry. Indeed, it may be due solely to demographic stochasticity and observation errors, which are averaged out in predicted averages but not in observed values. We therefore computed the correlation coefficient across mixtures between the predicted average and one simulation value randomly

picked among the 100 replicates for each mixture, R^2_{samp}. This procedure is repeated 100 times and the validity of the assumption of competitive symmetry is assessed through the p-value, computed as the rank of the correlation coefficient between observed and predicted values within the set of R^2_{samp} obtained through the sampling procedure. The assumption of competitive symmetry is rejected when the p-value is smaller than 0.025 or larger than 0.975.

All R scripts to perform the different analyses are included in the Supporting Information (see Appendix S1-2).

3. RESULTS

3.1. Model checking and inference based on monoculture data

Our model passed most model checking tests successfully. Indeed, only three out of the 60 species had not normally distributed environmental variables u_{ei} according to the Kolmogorov-Smirnov test (Fig.2.A): *Cardamine pratensis*, *Luzula campestris* and *Trifolium fragiferum*. Model failure for these three species can be explained by the fact that they were frequently not found in the plots: *C. pratensis* was not found for 13 of the 14 seasons, *L. campestris* for 8 of the 14 seasons and *T. fragiferum* was found in only one of the two plots in which it was sown. These multiple null values in the datasets further caused biased estimates of model parameters for these three species (Table 1) so that they should not be considered as reliable. They were excluded from the subsequent analyses. Model failure was also detected for six additional species on other model checks (Fig. 2, Table S4). These species were however kept in the subsequent analyses because model failure was more marginal in these cases. For the remaining 57 species, we were able to estimate the four species demographical parameters (r_{mi}, K_i, σ_{ei}, σ_{di}) (Table 1).

3.2. Sources of biomass variability

Our analysis revealed that the variance in community biomass σ_B^2 was mainly due to observation error with an average proportion of explained variance equal to 46%, followed by environmental stochasticity (33%) and demographic stochasticity (21%). More precisely, observation error was the main cause of biomass variance for 30 out of the 57 species, while environmental stochasticity was the main cause for 23 out of the 57 species (Table 1). We further detected variations in this hierarchy depending on the functional group considered, with the effect of environmental stochasticity being especially large for grasses, especially low for legumes, and intermediate for tall and small herbs. In contrast, the effect of observation error was more consistently large, while the one of demographic stochasticity more consistently low across the different functional groups (Fig. 3).

3.3. Analysis of species demographical characteristics

Overall, we did not find any support for the idea of an equalizing trade-off in the plant demographical components. Intrinsic growth rates (r_m) tended to be negatively correlated with environmental (σ_e), demographic (σ_d) and observation (σ_o) variance while observation variance tended to be positively correlated with environmental and demographic variance (Table S5). The correlations were weak when the functional types were not distinguished ($R^2 < 0.25$). But we observed a strong negative correlation between r_m and σ_e as well as between r_m and σ_o for grass species ($R^2 = 0.67$). There was also a significant negative correlation between r_m and σ_o for small herbs, between r_m and σ_d for tall herbs and between σ_d and σ_o for legumes ($R^2 > 0.4$).

We found that some plant demographical characteristics (r_m and K) were moderately predictable from the functional traits examined. When all plant functional groups were considered, both intrinsic growth rate r_m and carrying capacity K were positively correlated

with plant height and LDMC, and negatively with plant SLA (Table 2). Three of these correlations were significant (r_m – Height, r_m – SLA, K – SLA, K – LDMC), and one marginally significant (K – Height). However, depending on the functional group considered, the link between plant functional traits and these demographical parameters varied: plant height and LDMC were mostly influential for grasses, while SLA mostly influenced herbs and legumes. In contrast, the plant functional traits examined had little explanatory power on both environmental and demographic variances, neither on observation errors (Table 2).

3.4. Predicting multi-specific community dynamics based on the assumption of competitive symmetry

We obtained a good predictive ability of multi-species community dynamics under the assumption of competitive symmetry (Fig. 4), with coefficient of determinations between predicted and observed values equal to 0.58 and 0.39 for biomass averages and standard deviations, and to 0.78 for community composition (Simpson's concentration index). We further found that our predictive ability tended to decrease when considering mixtures of increasing diversity (Fig. 4, Table 3). Surprisingly, we found that taking into account the asynchrony between species in their response to environmental variations did not improve our predictive ability of these summary statistics (Supplementary Table S6).

In these comparisons between predicted and observed community dynamics, predictions are computed from averages over 100 simulated community dynamics, while observed values are based on single realizations of this dynamics and single realizations of observation errors. We therefore assessed whether the discrepancy between observations and predictions was due to model error or whether it may only be due to demographic stochasticity and observation error using two complementary tests. First, we assessed for each mixture, whether observed values

fell within the distribution of the 100 simulated values. We found that only about one third of mixtures significantly deviated from the simulated distributions (N_{dev} in Table 3). We again observed that the quality of the predictions decreased in more diverse communities, with N_{dev} progressively rising in more diverse mixtures (Table 3). Second, to obtain a more synthetic picture of the magnitude of model error, we assessed whether the coefficient of determination between observed and predicted values across communities significantly deviated from the null distribution based on simulated communities. Using this approach, our model was not rejected regarding its predictions on biomass averages and standard deviations, but it was rejected regarding its predictions on community composition (Simpson's concentration index) that overestimated the species abundance evenness of the communities.

4. DISCUSSION

The analysis of stochastic community dynamics has been mainly carried on easily countable organisms (Lande et al. 2003, Chisholm et al. 2014, Kalyuzhny et al. 2015). The present study aimed at extending such analyses to herbaceous plants which are easier to monitor in terms of aerial biomass, which experience inter-individual competition at short time scales, and which suffer from sudden seasonal collapses due to winter mortality or agricultural management. We therefore proposed a novel model of stochastic community dynamics, inspired by the recent work of de Mazancourt et al. (2013). We further developed an original inference method based on both numerical simulations and likelihood computing so as to tackle the mismatch of time scales between modelled processes occurring at a daily time step and field observations gathered at a seasonal time step (Fig. 1). This inference method further has the advantage of being very flexible, so that alternative modelling assumptions can be easily explored within the same quantitative framework.

Our simple model was sufficient to reproduce most observed monoculture data of the Jena biodiversity experiment (Fig. 2). We further found that we could predict multi-specific community dynamics with a relatively good precision using species demographical parameters estimated from monoculture data and assuming competitive symmetry, the fact that intraspecific and interspecific competitions have the same magnitude (Fig. 4, Table 3). Still, further improvements of our predictive ability should be sought in relaxing this simplifying assumption of competitive symmetry. In particular, the fact that our model predictions overestimated the species abundance evenness of the communities indicates that some level of asymmetry cannot be ignored to fully understand the dynamics of these herbaceous communities. This result is in accord with previous knowledge on plant competitive asymmetry (Begon, 1984, Cannell et al., 1984). It further provides clues on how to proceed to improve the model in the future. For instance, competitive asymmetry between a pair of plant species might be predicted from their difference in functional trait values, so that plant functional traits may be included in the model, as drivers of competition coefficients.

Our approach further revealed that environmental stochasticity had a larger impact on population temporal variance than demographic stochasticity (Fig. 3). The importance of environmental stochasticity on community dynamics has recently received a renewed interest (Chisholm et al. 2014, Kalyuzhny et al. 2015). Our results are perfectly in line with these findings in other types of plant communities. While environmental variability is likely to foster species coexistence by favoring in turn different sets of species (Chesson and Warner 1981), our analysis revealed that it was unlikely to be involved in an equalizing trade-off among species between their intrinsic growth rate and their temporal stability. Indeed, we found the contrary result that species with larger growth rates also tended to have both lower demographic variance and lower environmental variance (Table S5).

We finally found that the plant functional traits examined only had modest predictive ability of the species demographical characteristics (Table 2). This result recalls the recent findings of Kraft et al. (2015) on pairwise competition between annual plants. As previously argued, plant functional traits may however be informative on the competitive strength between pairs of species. This clearly constitutes a promising perspective to improve the present state of modelling of the stochastic dynamics of herbaceous plant communities.

More generally, among the growing literature on stochastic community dynamics (Freckleton *et al.* 2000; Keith *et al.* 2008; Loreau and de Mazancourt 2008; Chase *et al.* 2010; Fowler *et al.* 2012), our approach is original in that it jointly uses simulation-based and analytical inference methods to study more complex models of stochastic community dynamics than those commonly used. By using more detailed and realistic representations of biological processes, such hybrid inference approaches should contribute to the development of complex models of ecosystem dynamics (Evans *et al.* 2013) that can be informed by field data.

ACKNOWLEDGEMENTS

T.L was funded by the Institut national de Recherche en Sciences et Technologie pour l'Environnement et l'Agriculture (IRSTEA) and the Regional Council of Auvergne.

REFERENCES

Ackerly, D.D. 2003. Community assembly, niche conservatism, and adaptive evolution in changing environments. *International Journal of Plant Sciences* 164(S3): S165-S184.

Beaumont, M.A. 2010. Approximate Bayesian computation in population genetics. *Annu. Rev. Ecol. Evol. Syst.* 41: 379-406.

Begon, M. 1984. Density and individual fitness: asymmetric competition. In: Shorrocks, B. (ed.). Evolutionary ecology. Blackwell, Oxford.

Cannell, M.G.R., Rothery, P., Ford, E.D. 1984. Competition within stand of *Picea sitchensis* and *Pinus contorta*. *Annals of Botany* 53: 349-362.

Chase, J.M. 2010. Stochastic community assembly causes higher biodiversity in more productive environments. *Science* 328: 1388-1391.

Chesson, P.L. & Warner, R.R. 1981. Variability promotes coexistence in lottery competitive systems. *The American Naturalist* 117(6): 923-943.

Chesson, P.L. 2000. Mechanisms of maintenance of species diversity. *Annual review of ecology and systematics*. 31: 343-538.

Chisholm, R.A., Condit, R., Abd. Rahman, K., Baker, P.J., Bunyavejchewin, S., Chen, Y.-Y., Chuyong, G. 2014. Temporal variability of forest communities: empirical estimates of population change in 4000 tree species. *Ecology Letters* 17(7): 855-865.

Cornwell, W.K., Schwilk, D.W. & Ackerly D.D. 2006. A trait-based test for habitat filtering: convex Hull volume. *Ecology* 87(6): 1465-1471.

De Mazancourt, C., Isbell, F., Larocque, A., Berendse, F., De Luca, E., Grace, J.B., Haegeman, B., Polley, H.W., Roscher, C., et al. 2013. Predicting ecosystem stability from community composition and biodiversity. *Ecology Letters* 16: 617-625.

Ejrnaes, R., Bruun, H.H. & Graae, B.J. 2006. Community assembly in experimental grasslands: suitable environment or timely arrival. *Ecology* 87(5): 1225-1233.

Evans, M. R., Grimm, V., Johst, K., et al. 2013. Do simple models lead to generality in ecology? *Trends in ecology & evolution* 28(10): 578-583.

Fowler, M. S., Laakso, J., Kaitala, V., Ruokolainen, L., Ranta, E. 2012. Species dynamics alter community diversity–biomass stability relationships. *Ecology letters* 15(12): 1387-1396.

Freckleton, R.P., Watkinson, A.R., Dowling, P.M., Leys, A.R. 2000. Determinants of the abundance of invasive annual weeds: community structure and non-equilibrium dynamics. *Proceedings of the Royal Society of London B: Biological Sciences* 267(1448): 1153-1161.

Gonzalez, M.A., Roger, A., Courtois, E.A., Jabot, F., Norden, N., Paine, C.E.T., Baraloto, C., Thébaud, C. & Chave, J. 2010. Shifts in species and phylogenetic diversity between sapling and tree communities indicate negative density dependence in a lowland rain forest. *Journal of Ecology* 98(1): 137-146.

Hector, A., Hautier, Y., Saner, P., Wacker, L., Bagchi, R., Joshi, J., Scherer-Lorenzen, M. et al. 2010. General stabilizing effects of plant diversity on grassland productivity through population asynchrony and overyielding. *Ecology* 91(8): 2213-2220.

Jabot, F. & Chave, J. 2011. Analyzing tropical forest tree species abundance distributions using a nonneutral model and through approximate Bayesian inference. *The American Naturalist* 178(2): E37-E47.

Jabot, F., Pottier, J. 2012. A general modelling framework for resource-ratio and CSR theories of plant community dynamics. *Journal of ecology* 100(6): 1296-1302.

Jouven, M., Carrere, P., Baumont, R. 2006. Model predicting dynamics of biomass, structure and digestibility of herbage in managed permanent pastures. 2. Model evaluation. *Grass and forage science* 61(2): 125-133.

Kalyuzhny, M., Kadmon, R., Shnerb, N.M. 2015. A neutral theory with environmental stochasticity explains static and dynamic properties of ecological communities. *Ecology letters* 18(6): 572-580.

Keith, D. A., Akçakaya, H. R., Thuiller, W., et al. 2008. Predicting extinction risks under climate change: coupling stochastic population models with dynamic bioclimatic habitat models. *Biology Letters* 4(5): 560-563.

Kolmogorov, A. 1933. Sulla determinazione empirice di una legge di distribuzione. G. Ist. Ital. Attuari 4:83-91.

Kraft, N.J., Gofoy, O., Levine, J.M. 2015. Plant functional traits and the multidimensional nature of species coexistence. Proceedings of the National Academy of Sciences, 112(3), 797-802.

Lande, R., Engen, S. & Saether, B.-E. 2003. *Stochastic population dynamics in ecology and conservation*. Oxford University Press, New York.

Loreau, M. & de Mazancourt, C. 2008. Species synchrony and its driver: neutral and nonneutral community dynamics in fluctuating environments. *The American Naturalist* 172: E48-E66.

Mouquet, N., Moore, J.L. & Loreau, M. 2002. Plant species richness and community productivity: why the mechanism that promotes coexistence matters. *Ecology Letters* 5: 56-65.

Mouquet, Nicolas, et al. 2015. Improving predictive ecology in a changing world. *Journal of Applied Ecology*: in-press.

Nelder, J. A. & Mead, R. 1965. A simplex algorithm for function minimization. *Computer Journal* 7: 308-313.

Norden, N., Chazdon, R.L., Chao, A., Jiang, Y.-H. & Vilchez-Alvardo, B. 2009. Resilience of tropical rain forests: tree community reassembly in secondary forests. *Ecology Letters* 12: 385-394.

Rosindell, J., Hubbell, S.P. & Etienne, R.S. 2011. The unified neutral theory of biodiversity and biogeography at age ten. *Trends in Ecology & Evolution* 26(7): 340-348.

Silvertown, J., Araya, Y., Gowing, D. 2015. Hydrological niches in terrestrial plant communities: a review. *Journal of Ecology* 103(1): 93-108.

Sprugel, D.G. 1991. Disturbance, equilibrium, and environmental variability: what is 'natural' vegetation in a changing environment? *Biological Conservation* 58(1): 1-18.

Stubbs, W.J. & Wilson, J.B. 2004. Evidence for limiting similarity in a sand dune community. *Journal of Ecology* 92: 557-567.

Weigelt, A., Marquard, E., Temperton, V.M., Roscher, C., Scherber, C., Mwangi, P.N., Felten, S., Buchmann, N., Schmid, B., Schulze, E.-D. & Weisser, W.W. 2010. The Jena experiment: six years of data from a grassland biodiversity experiment. *Ecological Archives* E091-066.

Wilson, S. D., Tilman, D. 1993. Plant competition and resource availability in response to disturbance and fertilization. *Ecology*, 74(2): 599-611.

TABLES

Tab. 1. Species demographical characteristics estimated from monoculture data including the intrinsic growth rate (r_m), the carrying capacity (K), the environmental (σ_e), demographic (σ_d) and observation (σ_o) standard deviations as well as the relative effects of environmental (Σ_e) and demographic (Σ_d) stochasticities and observation error (Σ_o) on community biomass variance.

Species*	r_m	K	σ_e	σ_d	σ_o	Σ_e	Σ_d	Σ_o
Grasses								
Alo.pra	0.0769	1011.494	0.0165	0.0082	0.3098	0,504	0,176	0,32
Ant.odo	0.0567	668.1089	0.0295	0.0147	0.3603	0,489	0,179	0,331
Arr.ela	0.0824	1510.984	0.0142	0.0079	0.304	0,461	0,211	0,328
Ave.pub	0.0677	1267.008	0.0232	0.0057	0.4186	0,543	0,069	0,388
Bro.ere	0.0808	2039.401	0.0159	0.0089	0.2634	0,495	0,26	0,245
Bro.hor	0.0515	964.4861	0.0315	0.0187	0.4243	0,355	0,235	0,411
Cyn.cri	0.0306	204.025	0.0271	0.0071	0.6365	0,317	0,048	0,636
Dac.glo	0.0802	1225.749	0.0138	0.0058	0.2182	0,628	0,167	0,205
Fes.pra	0.0652	1250.319	0.0162	0.0157	0.5562	0,135	0,248	0,617
Fes.rub	0.0722	1129.696	0.0179	0.0096	0.1933	0,585	0,267	0,148
Hol.lan	0.0812	1186.745	0.0124	0.0069	0.2652	0,49	0,214	0,296
Luz.cam	0.0189	42.2128	0.0519	0	0.5378	0,475	0	0,525
Phl.pra	0.0682	1383.776	0.0231	0.0141	0.5054	0,283	0,185	0,533
Poa.pra	0.0524	652.0373	0.0247	0.0073	0.4385	0,498	0,092	0,409
Poa.tri	0.0371	419.0995	0.0295	0.0149	0.7988	0,134	0,07	0,795
Tri.fla	0.0712	1125.347	0.0244	0.0044	0.25	0,775	0,051	0,173
Small herbs								
Aju.rep	0.0205	68.62	0.0125	0.0161	0.3567	0,163	0,451	0,387
Bel.per	0.0188	162.4894	0.0182	0.0112	1.1326	0,027	0,025	0,948
Gle.hed	0.0414	367.4765	0.027	0.0105	0.4903	0,399	0,117	0,484
Leo.aut	0.0634	692.4243	0.0188	0.0101	0.2864	0,507	0,229	0,264
Leo.his	0.0729	824.3441	0.0129	0.0085	0.2244	0,481	0,295	0,224

Pla.lan	0.06	510.7189	0.006	0.0246	0.1738	0,031	0,834	0,135
Pla.med	0.075	869.5729	0.0194	0.0047	0.3254	0,63	0,059	0,311
Pri.ver	0.0453	656.356	0.0198	0.023	0.591	0,085	0,282	0,633
Pru.vul	0.0464	936.7887	0.0244	0.0119	0.6608	0,208	0,125	0,666
Ran.rep	0.047	445.0211	0.019	0.0123	0.746	0,121	0,097	0,782
Tar.off	0.0684	547.478	0.0166	0.0052	0.4059	0,472	0,069	0,459
Ver.cha	0.0559	465.6701	0.0228	0.0104	0.3834	0,472	0,151	0,377
Tall herbs								
Ach.mil	0.0699	1229.282	0.0173	0.0053	0.1936	0,731	0,136	0,133
Ant.syl	0.0566	1113.886	0.0254	0.0135	0.6877	0,182	0,109	0,709
Cam.pat	0.0149	968.5991	0.0255	0.0163	0.1763	0,278	0,599	0,123
Car.pra	0	4.1	0	2.00E-04	NA	NA	NA	NA
Car.car	0.0465	721.2159	0.0142	0.0131	0.3874	0,194	0,396	0,41
Cen.jac	0.0733	1506.494	0.0189	0.0067	0.0735	0,787	0,184	0,029
Cir.ole	0.0597	696.1138	0.0187	0.0155	0.3988	0,274	0,306	0,419
Cre.bie	0.0607	1134.767	0.0267	0.0144	0.8056	0,125	0,066	0,809
Dau.car	0.0583	1502.602	0.0264	0.0136	0.4784	0,329	0,199	0,472
Gal.mol	0.0779	635.7595	0.0072	0.0099	0.3056	0,177	0,384	0,439
Ger.pra	0.0534	705.6141	0.0086	0.0235	0.7644	0,01	0,188	0,802
Her.sph	0.0474	603.7538	0.0208	0.0158	1.0586	0,03	0,037	0,933
Kna.arv	0.0825	1549.742	0.0147	0.0056	0.2242	0,651	0,148	0,201
Leu.vul	0.0701	1558.09	0.0231	0.0111	0.2492	0,564	0,24	0,196
Pas.sat	0.0576	459.9719	0.0168	0.0073	0.4402	0,394	0,121	0,485
Pim.maj	0.0687	714.5135	0.0118	0.0084	0.2771	0,397	0,293	0,31
Ran.acr	0.0653	590.1405	0.0148	0.0076	0.2485	0,545	0,217	0,238
Rum.ace	0.0577	749.9891	0.0165	0.019	0.6108	0,094	0,232	0,674
San.off	0.0738	941.0103	0.0183	0.0113	0.386	0,384	0,199	0,417
Tra.pra	0.0499	837.5519	0.0189	0.0177	0.6891	0,087	0,185	0,728
Legumes								
Lat.pra	0.0706	665.9246	0.0143	0.0085	0.2763	0,478	0,231	0,291
Lot.cor	0.0754	853.2408	0.0128	0.0128	0.1936	0,359	0,463	0,179
Med.lup	0.0361	478.2948	0.0216	0.0203	0.8347	0,051	0,118	0,83

Med.var	0.0938	1269.795	0.0075	0.0062	0.2437	0,335	0,269	0,395
Ono.vic	0.0912	2446.729	0.0261	0.0105	0.6382	0,258	0,052	0,69
Tri.cam	0.0146	176.4898	0.0223	0.0074	0.4644	0,447	0,137	0,416
Tri.dub	0.0194	405.3371	0.0254	0.0191	0.4901	0,172	0,338	0,49
Tri.fra	0.0539	880.4678	0	0.0418	0.2149	0	0,839	0,161
Tri.hyb	0.0484	959.1322	0.0282	0.0169	1.2199	0,02	0,016	0,964
Tri.pra	0.0641	963.3051	0.012	0.0285	0.5761	0,03	0,331	0,639
Tri.rep	0.0683	695.8475	0.0162	0.0181	0.5577	0,139	0,219	0,642
Vic.cra	0.0521	713.2172	0.0119	0.0201	0.4787	0,059	0,414	0,527

*Full species names corresponding to each code are given in Table S3.

Tab.2. Correlations between demographical parameters including the intrinsic growth rate (r_m), the carrying capacity (K), the environmental (σ_e), demographic (σ_d) and observation (σ_o) standard deviations and three plant functional traits: the plant height, the specific leaf area (SLA) and the leaf dry matter content (LDMC). The correlations were computed either for all species together or separately for each functional group. Significance at the 0.05 level are indicated in bold.

		Height		**SLA**		**LDMC**	
		R	p-value	R	p-value	R	p-value
$\boldsymbol{r_m}$	All	**0.30**	**0.029**	**-0.39**	**0.003**	0.21	0.134
	Grass	0.37	0.188	-0.15	0.581	0.29	0.284
	Small herb	0.30	0.376	-0.50	0.141	0.15	0.660
	Tall herb	0.08	0.726	**-0.45**	**0.028**	-0.12	0.642
	Legumes	0.20	0.561	-0.47	0.174	0.07	0.851
$\boldsymbol{K}$	All	0.25	0.071	**-0.45**	**0.001**	**0.31**	**0.023**
	Grass	0.35	0.225	-0.35	0.207	0.45	0.089
	Small herb	0.03	0.926	-0.46	0.133	0.04	0.897
	Tall herb	-0.12	0.616	-0.45	0.051	-0.01	0.960
	Legumes	-0.09	0.807	**0.78**	**0.001**	0.22	0.548
$\boldsymbol{\sigma_e}$	All	-0.15	0.271	0.16	0.226	0.19	0.171
	Grass	-0.49	0.077	0.08	0.768	-0.03	0.913
	Small herb	0.14	0.676	0.38	0.224	0.27	0.421
	Tall herb	0.13	0.587	0.25	0.296	-0.16	0.523
	Legumes	-0.58	0.077	-0.17	0.645	0.19	0.600
$\boldsymbol{\sigma_d}$	All	-0.17	0.206	0.09	0.499	-0.17	0.223
	Grass	-0.46	0.094	0.37	0.169	-0.10	0.710
	Small herb	-0.16	0.637	-0.35	0.265	0.23	0.494
	Tall herb	-0.01	0.977	0.25	0.294	-0.01	0.967
	Legumes	-0.04	0.907	0.13	0.716	-0.53	0.112
$\boldsymbol{\sigma_o}$	All	-0.01	0.930	0.17	0.209	-0.15	0.272
	Grass	-0.14	0.641	0.29	0.288	-0.35	0.194
	Small herb	-0.44	0.177	0.11	0.735	-0.18	0.588
	Tall herb	0.42	0.075	0.20	0.400	-0.01	0.964
	Legumes	-0.30	0.392	0.01	0.989	0.05	0.891

Tab.3. Assessment of model predictive ability in species mixtures. R^2 between observed and predicted values, proportion of mixtures N_{dev} significantly deviating from model predictions and overall deviation significance p from predictions for the studied summary statistics. Results regarding the community biomass average ($\overline{B}$) and standard deviation (σ_B) across seasons and subsamples as well as the Simpson's concentration index (λ) are reported both for all the empirical mixtures, and for each diversity level separately.

		All	2 species	4 species	8 species	16 species
$\overline{B}$	R^2	0.58	0.73	0.58	0.55	0.82
	N_{dev}	0.37	4/16	1/11	5/10	6/6
	p	0.06	0.35	0.25	0.09	0.17
σ_B	R^2	0.39	0.38	0.71	0.47	0.40
	N_{dev}	0.33	3/16	1/11	5/10	5/6
	p	0.11	0.06	0.27	0.10	0.46
λ	R^2	0.78	0.50	0.00	0.00	0.22
	N_{dev}	0.35	7/16	3/11	5/10	0/6
	p	0.00	0.01	0.00	0.00	0.41

FIGURES

Fig. 1. Model description and relationships with data used for calibration. Only end of season biomass $B_i(t=60,T)$ is known.

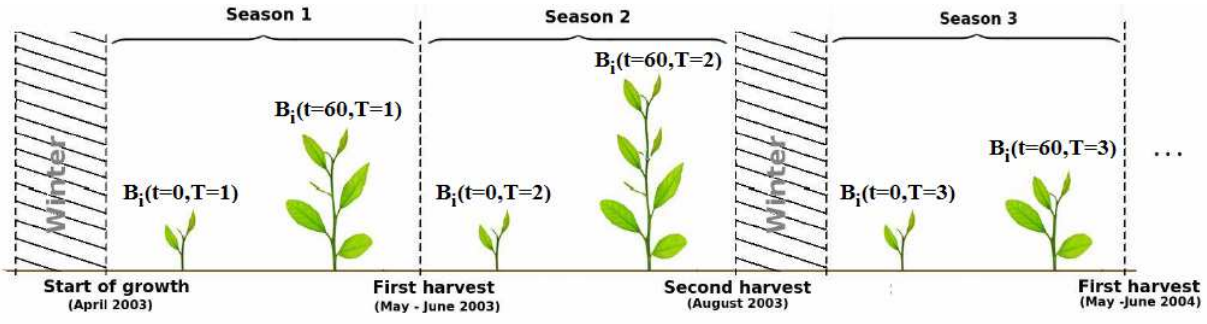

Fig.2. Model checking results. Normality test p-values of environmental variables u_{ei} (A), demographic variables u_{di} (B) and observation variables u_{oi} (C) obtained for each species. And model checking p-values based on biomass averages (D) and standard deviations (E) obtained for each species. The solid blue lines represent the one-tail 0.05 threshold for the first three panels, and the two-tail 0.025 and 0.975 thresholds for the last two panels.

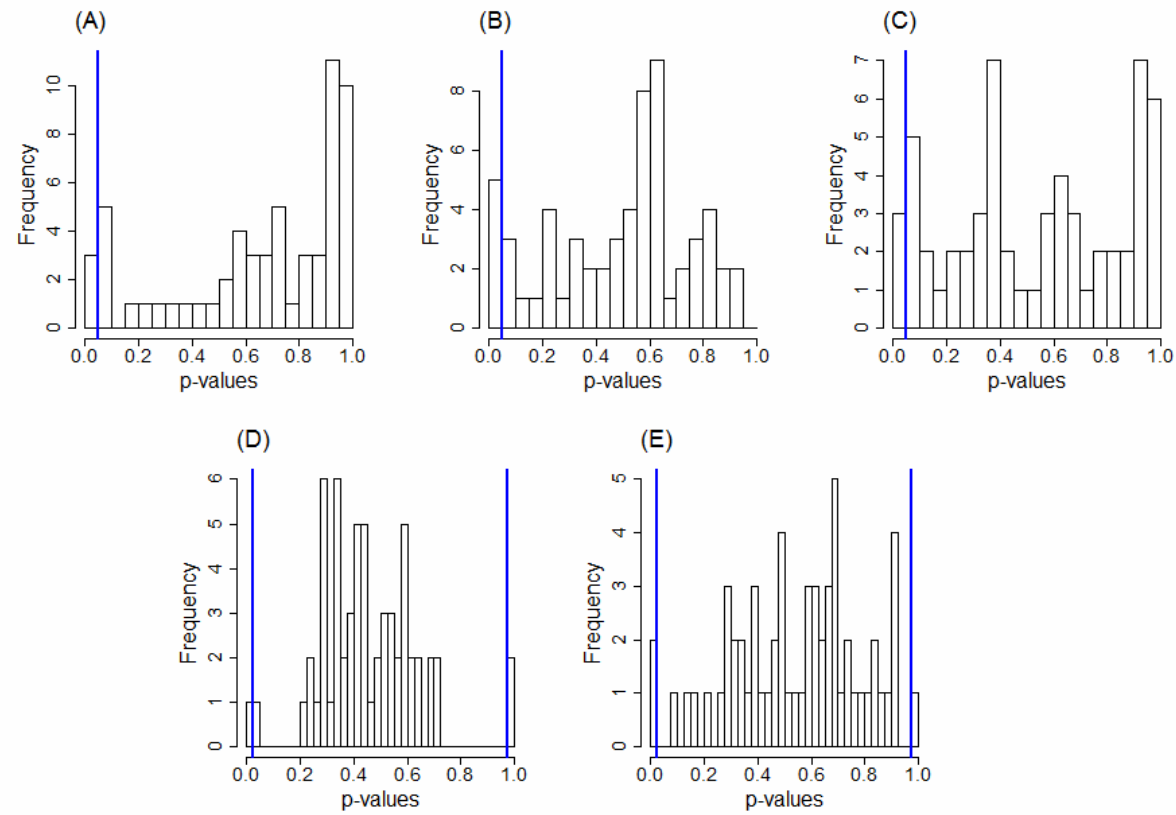

Fig.3. Effects of observation error (Σ_o), environmental (Σ_e) and demographic (Σ_d) stochasticities on the variance of community biomass σ_B^2 for (A) grasses; (B) small herbs; (C) tall herbs; (D) legumes.

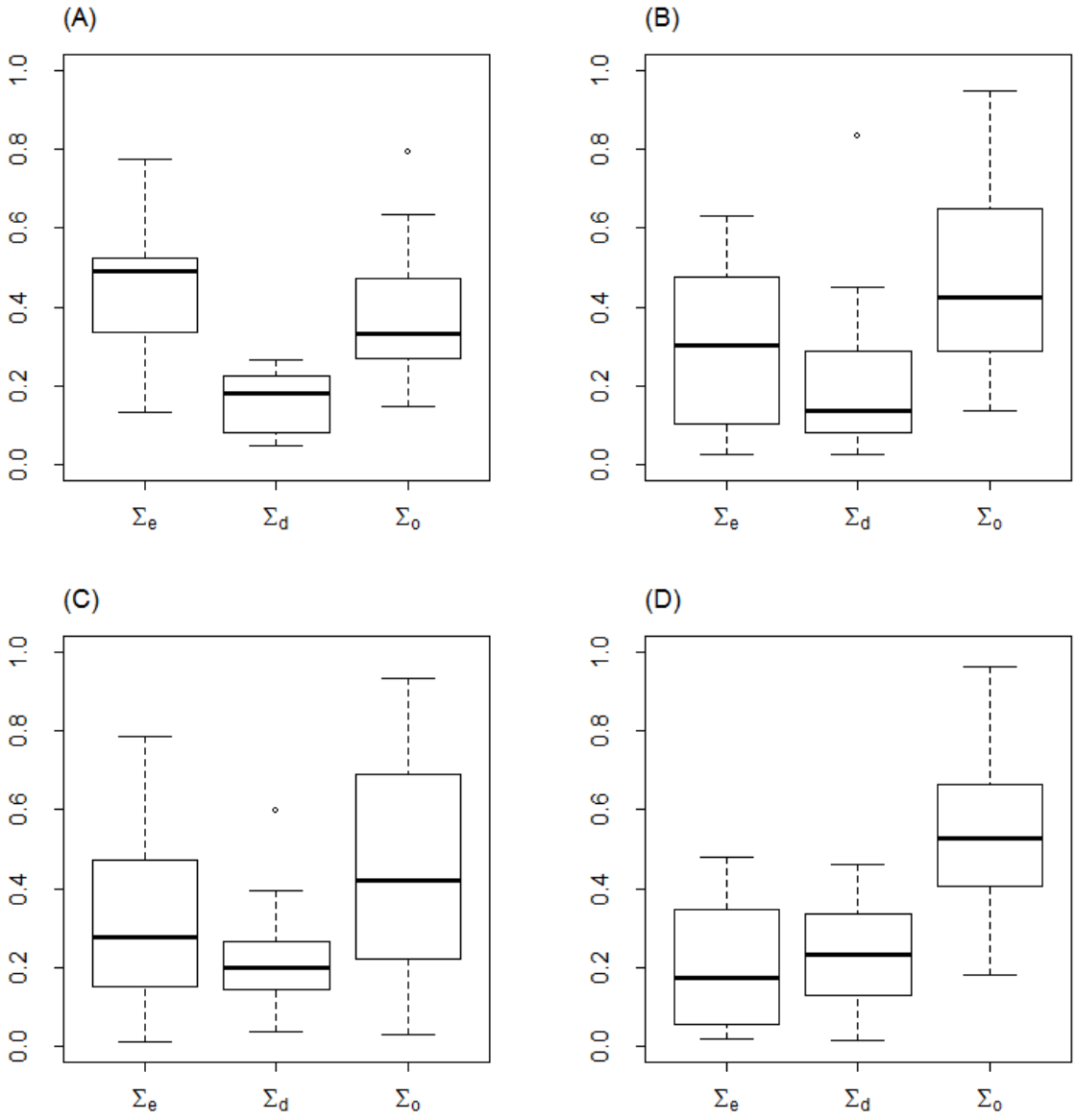

Fig.4. Comparison between predicted and observed multi-species community dynamics, based on their log-transformed average biomass $\overline{B}$ (panel A), their log-transformed standard deviation σ_B (panel B) and their Simpson's concentration index λ (panel C). Black circles, red squares, blue diamonds and green triangles represent respectively 2-, 4-, 8- and 16-species mixtures. Solid lines represent the y=x function.

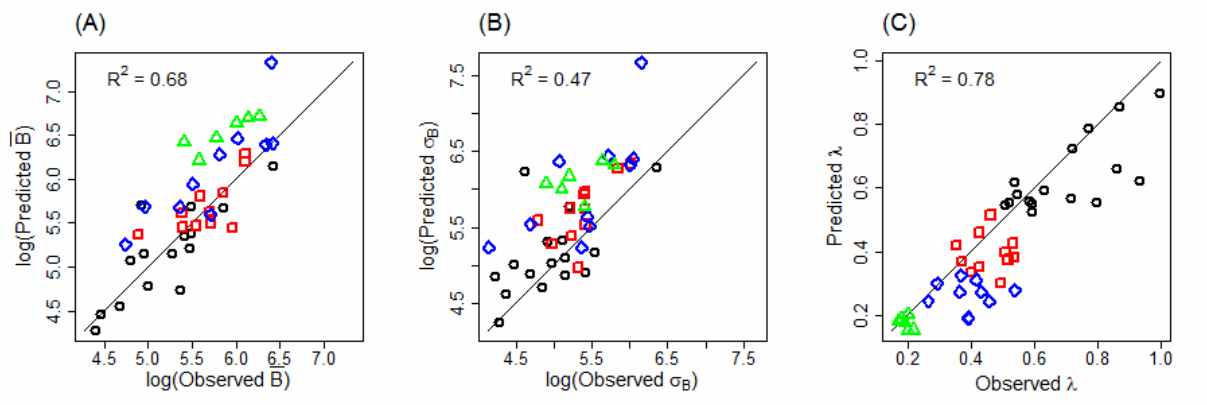

IV. Un cadre mécaniste pour prédire l'allocation du carbone.

Manuscrit correspondant:

Lohier, T., Jabot, F., Meziane, D., Shipley, B., Reich, P. B., & Deffuant, G. (2014). Explaining ontogenetic shifts in root–shoot scaling with transient dynamics. *Annals of botany*, *114*(3), 513-524.

Explaining ontogenetic shifts in root-shoot scaling with transient dynamics

Théophile Lohier[1], Franck Jabot[1,*], Driss Meziane[2], Bill Shipley[3], Peter Reich[4,5] and Guillaume Deffuant[1]

[1]LISC - Laboratoire d'Ingénierie pour les Systèmes complexes, IRSTEA, 9 avenue Blaise Pascal, CS 20085, 63178 Aubière, France.

[2]Université Sidi Mohamed Ben Abdellah, Faculté des sciences Dhrar El Mehraz, Département de biologie, BP 1796, Fès, Atlas, Maroc.

[3]Département de biologie, Université de Sherbrooke, Sherbrooke (Qc), Canada J1K 2R1.

[4]Department of Forest Resources, University of Minnesota, St. Paul MN 55108, USA.

[5]Hawkesbury Institute for the Environment, University of Western Sidney.

Running title: Explaining ontogenetic root-shoot scaling with transient dynamics

[*]For correspondence. E-mail: franck.jabot@irstea.fr

ABSTRACT

• *Backgrounds and Aims* Simple models of herbaceous plant growth based on optimal partitioning theory predict, at steady state, an isometric relationship between shoot and root biomass during plant ontogeny: i.e. a constant root-shoot ratio. This prediction has received mixed empirical support, suggesting either that optimal partitioning is too coarse an assumption to model plant biomass allocation, or that additional processes need to be modelled to account for empirical findings within the optimal partitioning framework. Here simulations are used to compare quantitatively two potential explanations for observed non-isometric relationships, namely nutrient limitation during the experiments and initial developmental constraints.

• *Methods* A simple plant growth model was built, based on optimal partitioning theory combined with empirically measured plant functional traits. We assessed its ability to reproduce plant relative growth rate and final root weight ratio. Predicted root-shoot ratios during plant ontogeny were compared to experimental observations. The effects of nutrient limitation and initial developmental constraints on root-shoot ratios were then tested.

• *Key Results* The model was found to accurately reproduce overall plant growth patterns, but failed, in its simplest form, at explaining non-isometric growth trajectories. Both nutrient limitation and ontogenetic developmental constraints were further shown to cause a transient dynamics resulting in a deviation from isometry. Nitrogen limitation alone was not sufficient to explain observed trajectories of most plant species. The inclusion of initial developmental constraints enabled to reproduce the observed trajectories and were consistent with observed initial root-shot ratios.

• *Conclusions* This study highlights that considering transient dynamics enables to reconcile theoretical predictions based on optimal partitioning with empirically measured ontogenetic

root-shoot allometries. This transient dynamics cannot be solely explained by nutrient limitation during the experiments, pointing to a likely role of initial developmental constraints in the observed non-isometric growth trajectories.

Key words: allometry, functional trait, grassland, model selection, optimal partitioning theory, transient dynamics.

INTRODUCTION

Plants both fix atmospheric carbon in their leaves by photosynthesis and capture soil water and nutrients by their roots. The way these basic resources are allocated among different plant organs during plant growth is of utmost importance to understanding such basic ecological phenomena as competition between plants (Tilman, 1988; Grime, 2001), the global carbon cycle and the consequences of rising atmospheric carbon dioxide (Hungate *et al*., 1997; Mokany *et al*., 2006; Bonan, 2008). Allocation of biomass between roots and shoots in plants has received much attention (Poorter *et al*., 2012). This allocation strongly depends on environmental conditions (Chapin, 1980; Poorter *et al*., 2012), so that it constitutes a major difficulty for plant growth modelling (Thornley, 1995; Le Roux *et al*., 2001).

Many approaches have been used to model allocation in plants (Génard *et al*., 2008; Franklin *et al*., 2012). Allometric relationships (Niklas, 1994; West *et al*., 1999) can be used to constrain the growth of different plant parts so that allometric equations are always satisfied during plant ontogeny (Taubert *et al*., 2012). Although this approach is conceptually and technically simple, it requires empirical measurements of allometric coefficients in multiple environmental conditions. As a result, this approach cannot predict how allometric relationships are likely to vary depending on the environmental conditions encountered by the plant (Bloom *et al*., 1985). A second approach is to represent the capture of basic resources by the plant and their transport across different plant organs (Thornley, 1998). This approach aims at being mechanistic, but it requires the quantification of mechanistic properties such as the resistance to nutrient flow in the plant, as well as processes of internal regulation. A third type of approach relies on various optimization principles. Studies of this type generally consider that allocation in the plant aims at maximizing some criterion, used as a proxy for

plant fitness, such as plant relative growth rate (Charles-Edwards *et al*., 1972; Reynolds and Chen, 1996). They sometimes also make use of game-theoretic or adaptive dynamics methods to take into account the ecological and evolutionary impacts of competition between plants (Franklin *et al*., 2012; McNickle and Dybzinski, 2013).

The idea that plants may allocate their assimilates among organs so as to balance their root activity of water and nutrient uptake and their shoot activity of photosynthesis dates back at least to the work of Brouwer (1962). Since then, this hypothesis has been variously called "optimal partitioning", "functional equilibrium" or the "balanced growth hypothesis" (Poorter *et al*., 2012). This simple idea has proven powerful at qualitatively explaining how environmental conditions and perturbations affect patterns of root-shoot allocation (Iwasa and Roughgarden, 1984; Bloom *et al*., 1985; Poorter *et al*., 2012). Optimal partitioning is thus used in a large number of plant growth models (Shipley and Meziane, 2002; Franklin *et al*., 2012).

Some simple models of plant growth that assume optimal partitioning predict an isometric relationship between shoot and root biomass during the exponential phase of growth in non-limiting conditions; i.e. root and shoot biomass remain proportional (Charles-Edwards, 1976; Robinson, 1986; Shipley and Meziane, 2002). This prediction has received mixed empirical support. According to the meta-analysis of Poorter et al. (2012), ontogenetic shifts in root-shoot ratios are variable across experiments performed so far. For instance, McConnaughay and Coleman (1999) explored the impact of resource gradients on three annual species and found that the root-shoot ratio decreases during plant development. Müller et al. (2000) studied allocation patterns of 27 herbaceous plant species and also found a decreasing root-

shoot ratio for 14 species. In contrast, Shipley and Meziane, (2002) studied 22 herbaceous plant species during 35 days and found a preferential allocation to roots during plant ontogeny in general, although deviations from isometry were weak in most cases. Arredondo *et al.* (1998) also found an increase in root-shoot ratio during plant ontogeny. The variable root-shoot ratios evidenced in these studies question the validity of the optimal partitioning hypothesis.

However, rather than a fundamental flaw in the assumption of optimal partitioning, the discrepancies between data and model predictions could also be due to the requirement for additional model assumptions beyond optimal partitioning. For instance, Reynolds and Thornley (1982), Johnson (1985) and Johnson and Thornley (1987) made the point that optimal partitioning implied that plants should be equally limited by shoot and root activities, which do not need to be constant over time, but rather depend on dynamical environmental conditions and potential disturbances. In this vein, Shipley and Meziane (2002) argued that non-isometric relationships may be explained by a progressive nitrogen limitation of plant growth during their experiments or by a decrease of intrinsic root uptake capacity with their age. These two features are susceptible to cause a transient phase of preferential allocation to roots (Ingestad and Ågren 1991). An alternative explanation for non-isometric trajectories might be that root-shoot partitioning is ontogenetically constrained, especially during the early stages of growth (Gedroc et al., 1996). If allocation is ontogenetically constrained, the shoot-root ratio is likely to differ from the ratio predicted by optimal partitioning. Importantly, even if developmental constraints cease early during plant ontogeny, they are likely to have persistent effects on plant growth trajectories during a transient phase of root-shoot ratio adjustment by the plant. This will be tested here by considering that the initial

shoot-root ratio may differ from the one predicted by optimal partitioning, but that subsequent dynamics is controlled by optimal partitioning equations. Transient dynamics, either due to nutrient limitation or to some initial developmental constraints, could potentially explain the discrepancy between steady-state predictions based on optimal partitioning theory and experimental findings. This study aims at quantitatively testing these potential explanations.

The study is structured in three main parts. First, a simple plant growth model is built, which is based on the optimal partitioning hypothesis and on plant functional traits that can be measured in the field. This model represents the basic processes of photosynthesis, nutrient uptake, and root-shoot carbon and nitrogen allocation. Second, we investigate the ability of such a simple model to reproduce patterns of relative growth rate (RGR) and final root weight ratio (RWR) experimentally measured for 25 species by Reich *et al*. (2003). This particular study was chosen because most plant traits used in the model were measured during the experiments. The other model parameters, which were not experimentally measured, are estimated so as to maximize the model fit to the two growth indicators (RGR and RWR). Model goodness of fit is then assessed, as well as the realism of fitted parameter values. This part of the study served to determine if the simple model considered is a realistic approximation of plant growth dynamics. Third, armed with this simple but realistic plant growth model, the experiments of Shipley and Meziane (2002) are re-analyzed. In these experiments, root and shoot biomass trajectories of 22 plant species were measured experimentally in varying environmental conditions. The simple model is shown not to be able to explain the observed non-isometric root-shoot biomass relationships when model parameters are constrained so that the model accurately fits overall plant growth data. It has then been tested whether adding nitrogen limitation and a decrease of root uptake capacity

with root age may lead to the observed non-isometric relationships. It has finally been explored whether considering ontogenetic constraints through variations in initial shoot-root ratio may improve the model fit to data. Fitted initial shoot-root ratios were finally compared to observed ones by re-analyzing the data of Shipley and Meziane (2002).

MODEL DESCRIPTION

The model simulates the growth of herbaceous species in non-limiting conditions of water supply. In this model, a plant is described by its total biomass B(t) at time t. This biomass is divided into above- (B_s) and below-(B_r) ground biomass, so that:

$$B\,(t) = B_s\,(t) + B_r\,(t) \qquad (1)$$

Four growth processes are modelled: i) shoot photosynthesis, ii) nitrogen uptake by roots, iii) nitrogen allocation among roots and shoots, and iv) carbon allocation among roots and shoots. Leaves and stems are not distinguished in the shoot component for two reasons. First, since both leaves and stems contribute to photosynthesis in herbaceous plants (Nilsen, 1995), pooling these two plant components makes sense functionally. Second, distinguishing these two plant components would increase model complexity by adding leaf- and stem-specific activity rates (photosynthesis and respiration) and two additional leaf-stem allocation rules for carbon and nitrogen, while these processes are poorly documented. Certainly, increasing the complexity of the model with both stem and leaves components could be easily achieved for cases in which additional information is available.

Plant Development

A simple difference equation is used with one time step representing one hour. The plant biomass at t+1 is given by:

$$B\,(t+1) = B\,(t) + \Delta B\,(t) = B\,(t) + P_{net}\,(t) \quad (2)$$

where P_{net} (t) is the net primary production at time t.

The increases of shoot and root biomass between times t and t+1 are described by equations (3) and (4) respectively:

$$\Delta B_s\,(t) = a\,(t) \times P_{net}\,(t) \quad (3)$$

$$\Delta B_r\,(t) = (\,1 - a\,(t)\,) \times P_{net}\,(t) \quad (4)$$

where a (t) is the portion of net primary production allocated to shoot. The computations of P_{net} (t) and a (t) are detailed below.

Photosynthesis

Grasses perform photosynthesis both in their leaves and stems (Aschan and Pfanz 2003). Although stem photosynthetic rate may differ from leaf photosynthetic rate, as well as mass-surface ratios, it will be assumed here for simplicity that these quantities are equal among stems and leaves and thus that net primary production P_{net} (t) can be modelled by:

$$P_{net}\,(t) = C \times A_N\,(t) \times SLA \times B_s\,(t) \quad (5)$$

where A_N (t) is the leaf net photosynthetic rate, SLA is the specific leaf area, B_s (t) is the shoot biomass and C is a constant accounting for the conversion of assimilated CO_2 into dry matter content. C is calculated from the stochiometry of photosynthetic reactions: to synthesize one mole of glucose ($C_6H_{12}O_6$) weighting 180g, six moles of carbon dioxide (CO_2) are needed, hence $C = 180/6 = 30$ (Kikuzawa and Lechowicz, 2006). Equation (5) has been abundantly used in plant growth modelling (see for instance Foley (2007)). Note that this approach is still valid if less strong assumptions are used, namely that the stem-leaf ratio is constant during plant ontogeny and that the stem photosynthetic rate responds similarly to light conditions and

plant nitrogen status as leaf photosynthetic rate. In this case, A_N (t) should be understood as an effective shoot net photosynthetic rate.

Net photosynthetic rate A_N (t) has been shown to be linearly related to the nitrogen content of shoot (Lambers *et al*., 1998). Following Konings *et al*. (1989), the following relationship is used:

$$A_N(t) = (A_{max}(t) / LNC_{max}) \times (N_s(t) / B_s(t)) \quad (6)$$

where LNC_{max} is the maximal leaf nitrogen content, N_s (t) is the nitrogen content of shoot and A_{max} (t) is the net maximal leaf photosynthetic rate in given light conditions:

$$A_{max}(t) = A_{sat} \times f(I_r(t)) - R_d \quad (7)$$

where A_{sat} is the light saturated gross photosynthetic rate, R_d is the dark respiration, I_r (t) is the incoming irradiance at time t and $f(I_r)$ is a function varying between zero when I_r is null and one when it is optimal. This function accounts for the impact of ambient light on photosynthesis. In the following the irradiance is assumed to be constant during the photoperiod and therefore A_{max} (t) is also constant. Overnight the irradiance I_r is null, so f is null and A_{max} (t) equals - R_d. As we are interested in the first stages of plant growth the decrease of net photosynthetic rate caused by self-shading and the resulting variations in root-shoot scaling is likely to be negligible. So self-shading will be neglected in the following.

Nitrogen uptake

When nutrient supply is non-limiting, nitrogen uptake is only limited by plant physiology and root biomass. So at time t, a plant is able to absorb at most:

$$N_p = U_{max} \times B_r(t) \quad (8)$$

where U_{max} is the mass-based root effective uptake capacity.

Roots are assumed to be able to adjust nitrogen uptake so as to match the nitrogen demand of the plant N_d (Schippers and Kropff, 2001). The latter corresponds to the amount of nitrogen required for the leaf content of new leaf biomass to be equal to LNC_{max}. N_d is thus given by:

$$N_d = (LNC_{max} \times \Delta B_s (t)) / a_N (t) \quad (9)$$

where ΔB_s (t) is the shoot biomass produced between t and t+1 and a_N (t) is the fraction of nitrogen captured between t and t+1 which is allocated to shoot. Thereafter, assimilated nitrogen N_u equals the minimum of N_p and N_d:

$$N_u (t) = \min (N_p (t) , N_d (t)) \quad (10)$$

Nitrogen allocation

Following Dybzinski *et al*. (2011), it is assumed that a fixed fraction of assimilated nitrogen is allocated to the shoot: a_N (t) = a_N. An alternative way for modelling nitrogen partitioning would be to use optimal partitioning theory (Mäkelä *et al*., 2008). But to apply this theory, it would be necessary to know the relationship between root uptake efficiency and root nitrogen content or to make some assumptions on the relationship between shoot and root nitrogen content (Mäkelä *et al*., 2008; Valentine and Mäkelä, 2012).

Carbon allocation

An optimal allocation model is used for carbon allocation (Dewar *et al*., 2009), in which plants are assumed to allocate assimilates so as to maximize their relative growth rate. Assuming that biomass and leaf nitrogen content at time t are known, we look for an allocation to shoot *a* (t) such that *RGR* (t+1) is maximal. *RGR* (t+1) is given by:

$$RGR (t+1) = \Delta B (t+1) / B (t+1) = P_{net} (t+1) / B (t+1) \quad (11)$$

From equations (5) and (6), *RGR* (t+1) maximization is equivalent to maximize:

$$C \text{ x } (A_{max} \text{ (t+1)} / LNC_{max}) \text{ x } (N_s \text{ (t+1)} / B_s \text{ (t+1)}) \text{ x } SLA \text{ x } B_s \text{ (t+1)} \quad (12)$$

Given that:

$$N_s \text{ (t+1)} = N_s \text{ (t)} + N_u \text{ (t)} \quad (13)$$

RGR (t+1) is maximal when N_u (t) is maximal. In other words *RGR* (t+1) is maximal when the nitrogen demand at t+1 is equal to the potential uptake N_p (t):

$$LNC_{max} \text{ x } a \text{ (t) x } P_{net} \text{ (t)} = N_p \text{ (t)} \quad (14)$$

Hence the shoot allocation factor a(t) is given by:

$$a \text{ (t)} = N_p \text{ (t)} / (LNC_{max} \text{ x } P_{net} \text{ (t)}) \quad (15)$$

In summary, the model takes as input six parameters (A_{max} , R_d, LNC_{max}, *SLA*, U_{max} and a_N). Most of the parameters are commonly measured plant functional traits (Kattge *et al*., 2011). A_{max} , R_d, LNC_{max} and *SLA* were measured in the experiments of Reich *et al*. (2003), and LNC_{max} and *SLA* in the experiments of Meziane and Shipley (1999). Note that plant senescence was neglected, since we are interested here in the first stages of plant development.

PARAMETER ESTIMATION AND MODEL SELECTION

In this section, the data set used to test the model ability to reproduce real plant growth dynamics is first presented. The fitting procedure of the remaining unmeasured model parameters is then detailed. The results of this model-data comparison procedure are presented in the last subsection.

Plant growth data

An experiment performed by Reich *et al*. (2003) is used, in which 25 herbaceous plant species were grown in monoculture under controlled environmental conditions, for nine weeks after germination. Beginning two weeks after sowing, pots received 30 ml of half strength Hoagland's solution three times per week. Pots were watered as needed between treatment applications to maintain soils near field capacity. Supplemental lighting provided an additional 130 - 170 $\mu mol.m^2.s^{-1}$ above ambient light levels during a 14 h. photoperiod. Each three weeks, plants were harvested and the biomass of the different plant components (leaves, stem and roots) were measured. From these measurements, several quantities were computed: the root weight ratio RWR equal to the root biomass divided by the total plant biomass; and the relative growth rate *RGR* computed as in Evans (1972):

$$RGR = [\ \ln(B\ (t_2)) - \ln(B\ (t_1))\ ] / (\ t_2 - t_1\ ) \qquad (16)$$

where t_1 and t_2 are harvesting dates.

Several plant functional traits were also measured: the light saturated photosynthetic rate A_{sat} the dark respiration R_d, the leaf nitrogen content *LNC*, the root nitrogen content *RNC* and the specific leaf area *SLA*. RNC is not a model parameter, but it enables to compute the nitrogen allocation coefficient a_N with the following equation:

$$a_N = (\ N_s\ (t_{end}) / B_s\ (t_{end})\ ) / [\ (\ N_s\ (t_{end}) / B_s\ (t_{end})) + RNC \times (B_r\ (t_{end}) / B_s\ (t_{end}))\ ] \qquad (17)$$

This data set enables to assess the model ability to explain observed plant growth patterns, when it is strongly constrained by empirically measured plant traits.

Fitting the model on experimental data

Following Goudriaan and Van Laar (1994), the initial shoot-root ratio was set to one. Initial root and shoot biomass values do not affect the computed growth indicator, so they are arbitrarily set to 0.5mg. The maximal nutrient uptake efficiency U_{max} was not measured in the experiments of Reich *et al*. (2003) and thus had to be estimated. Besides, the maximal photosynthetic efficiency A_{max} was measured for an irradiance of 1000 µmol.m^2.s^{-1}, while plants were not grown under constant light conditions. The effective A_{max} during the experiments, resulting from the variable light conditions, was therefore estimated. These two parameters were estimated by fitting the plant growth model to the growth data of the experiments of Reich *et al*. (2003). A distance ε between model predictions and experimental data was defined. It was based on two experimentally measured growth indicators: the plant relative growth rate RGR, and the final root weight ratio RWR. ε was defined as:

$$\varepsilon = \sqrt{\frac{1}{2} \times \frac{\sum_{i=1}^{2} (X_i^{obs} - X_i^{sim})^2}{(X_i^{obs})^2}} \qquad (18)$$

where $X^{sim} = (RGR_{sim}, RWR_{sim})$ and $X^{obs} = (RGR_{obs}, RWR_{obs})$ are the growth indicators of the simulations and of the experimental data respectively.

This distance ε was computed on a 50x190 grid of parameter values described in Table 1 and the parameter set that minimized this distance was retained. The parameter space was chosen so as to include the reported parameter values found in the literature (Table 1). Note that the interval chosen for A_{max} does not include the largest values measured by Reich *et al*. (2003). In this experiment, the photosynthetic efficiency was measured in optimal light conditions ($f(I_r) = 1$). But plants were not grown in optimal light conditions, so that the effective photosynthetic efficiency is necessarily smaller than light saturated photosynthetic efficiency.

Empirical growth indicators have been measured with observation errors of 5 to 10% (Reich et al. 2003). Therefore all sets of parameters leading to ε values smaller than 0.05 are retained. They form an interval of likely values for A_{max} and U_{max}, which were relatively narrow (Table 2).

Results

The coefficients of variation of the two model parameters A_{max} and U_{max} were smaller than 5 and 10% respectively (Table 2), which means that the growth data used were sufficiently informative to obtain accurate parameter estimates of the minimal version of the model. Model parameter estimates are realistic compared to the range of values reported in the literature (Table 1). Importantly, the remaining lack-of-fit of the model to data, leading to a residual error ε_{min} (Table 2), was negligible compared to the observed interspecific variations of growth indicators (Figure 1, average NRMSE=3.47%). This means that this simple trait-based model was sufficient to capture interspecific differences in growth rates as well as in root-shoot carbon and nitrogen partitioning.

The growth dynamics predicted by the fitted minimal version of the model consists of a short transient phase during which carbon allocation a (t) varies, followed by a steady-state regime of exponential growth during which carbon allocation is constant (Figure 2A) and root and shoot growth rates scale proportionally (Figure 2B), leading to an allometric coefficient β equal to one (Figure 2C). The predicted duration of the transient phase depends on the species identity, but never exceeds 15 days (Figure 2C). In the 35-day experiments of Shipley and Meziane (2002), the first measurements occurred 15 days after germination (shown by the

dashed lines in Figure 2B-C). So the duration of transient dynamics in the minimal version of the model is insufficient to explain the observed deviations from isometry observed in the 35-day experiments of Shipley and Meziane (2002). These authors suggested that the observed deviation from isometry could come from a progressive appearance of nitrogen limitation in the experimental setting in which nitrogen was added in fixed amounts. They also discussed that a decrease of intrinsic root uptake capacity with root age could contribute to non-isometric growth trajectories. These two additional processes were included in the model to assess their ability to explain observed patterns. It has been further assessed whether a modification of the initial (ontogenetically constrained) shoot-root ratio could significantly contribute to observed non-isometric trajectories.

ALLOMETRIC PREDICTIONS

In this section, the data set used to test the model predictions on root-shoot allometry is first presented. Two additional model ingredients are then introduced: the consideration of nitrogen consumption during the experiment potentially causing some nitrogen limitation for plants, especially at the end of the experiment; and the inclusion of a decrease in root uptake capacity as they age. The impact of initial shoot-root ratio on allometric patterns was also investigated. Third, the model-data fitting procedure was detailed, as well as the associated test of whether the different models studied are able to reproduce the empirical root-shoot allometries. Fourth, the results of this model-data comparison procedure are presented.

Plant growth data

Given that Reich et al. (2003) did not perform detailed measures of allometric relationships (they only performed three sequential harvests), a second data set collected by Meziane and

Shipley (1999) and Shipley and Meziane (2002) is used. In this experiment, a total of 1150 plants from 22 different herbaceous plant species were grown in hydroponic sand monoculture in factorial combinations of high (1100 $\mu mol.m^2.s^{-1}$ PAR) and low (200 $\mu mol.m^2.s^{-1}$ PAR) irradiance crossed with a full strength and a 1/6 dilution of Hoagland's hydroponic solution. Each plant grew in a separate 1.3 dm^3 container in a growth chamber with 15/9 h light:dark cycles. Each plant grew in one of four resource environments: high (L, 1100 $\mu mol.m^2.s^{-1}$) and low (l, 200 $\mu mol.m^2.s^{-1}$) irradiance combined with high (N, full-strength Hoagland's nutrient solution) and low (n, 1/6 dilution) external nutrient concentrations. These four experimental treatments are termed LN, Ln, lN and ln treatments respectively. Each container was filled to field capacity with the nutrient solution three times a day. Plants were harvested and biomass of leaves, stems and roots measured at 15, 20, 25, 30 and 35 days post-germination. Two plant functional traits were measured: *LNC* and *SLA*. RWR was computed, as well as average RGR, computed as the slope of a regression of the natural logarithm of plant dry mass on harvest date. Allometric relationships between shoot and root biomass along plant ontogeny was further measured, using an equation of the form:

$$B_s = \alpha \times B_r^{\ \beta} \quad (19)$$

which can be re-written as:

$$\ln(B_s) = \ln(\alpha) + \beta \times \ln(B_r) \quad (20)$$

The allometric coefficient β was thus computed as the slope of a regression of the natural logarithm of shoot dry mass on the natural logarithm of root dry mass. This second data set was not used for model checking, since less plant functional traits have been measured empirically, and thus it would have been a less conservative test of the model with a larger number of unmeasured model parameters and a smaller number of growth indicators to

match. Rather, it was used to confront the model predictions with empirically-measured allometric data.

Adding nitrogen consumption by plants in the containers

Following Engels *et al.* (2000), Hane's relationship was used to model the dependency of uptake rate $U(t)$ to substrate concentration:

$$U(t) = U_{max} \times [N]_{soil}(t) / (K_m + [N]_{soil}(t)) \quad (21)$$

where K_m is the substrate affinity and $[N]_{soil}(t)$ is the nitrogen concentration in soil at time t. Initially soil nitrogen content equals:

$$N_{soil}(t_0) = [N]_{Hoagland} \times V \times C_{soil} \quad (22)$$

where $[N]_{Hoagland}$ is the nitrogen concentration in the hydroponic solution used in the experiment (0.210 $g.L^{-1}$ for full strength solution, 1/6 of this value in the low nitrogen treatment), V is the container volume (1.3 L) and C_{soil} is the volumetric soil moisture content remaining at field capacity (about 5% according to Tucker 1999). Then soil nitrogen content is computed at each time step as:

$$N_{soil}(t) = N_{soil}(t - 1) - N_u(t - 1) \quad (23)$$

where $N_u(t)$ is the amount of nitrogen absorbed by the plant at time t (eq. 12). Every 8 hours each container is filled to field capacity with the nutrient solution, so this dynamics of nitrogen concentration decrease in the container is restarted.

Adding a decrease of root uptake capacity with root age

The model of decrease in root uptake efficiency as they age is based on the observations of Volder *et al*. (2005). Root biomass is divided in several layers. Each layer has its own biomass, age and nitrogen uptake capacity. At the beginning of each time step *t*, a root layer is

added with a biomass corresponding to the newly produced root biomass ΔB_r (t - 1). A root layer *i* will have a varying with time nitrogen uptake capacity U_i (t) given by:

$$U_{max,i}(t) = U_{max} \times (1 + 2 \times e^{-\rho (t - ti)}) / 3 \qquad (24)$$

where ρ is the decay rate of root nitrogen uptake efficiency, and t_i is the time of appearance of the root layer *i*. Following Volder *et al.* (2005), it is assumed that after some days root uptake efficiency stabilizes around one third of maximal efficiency.

Adding variation in initial root-shoot ratio

Since first measurements in the experiment of Shipley and Meziane (2002) occurred 15 days after germination, no information is available on growth trajectories during the very first days of the experiment. Two hypotheses were compared regarding allocation patterns during these first 15 days. (H_0) Biomass is optimally allocated, so that the shoot root ratio at first measurement, called initial shoot-root ratio R_0 in the following, is the ratio required for optimal partitioning, R_{opt}. (H_1) Because of ontogenetic developmental constraints, the initial shoot-root ratio R_{ont} differs from the optimal one:

$$(H_0) \ : \ B_s(t_0) = R_{opt} \times B_r(t_0) \qquad (H_1) \ : \ B_s(t_0) = R_{ont} \times B_r(t_0) \qquad (25)$$

These additional model ingredients are used to build three models. The first one does not include nitrogen limitation and assumes that initial shoot-root ratio corresponds to the ratio predicted by optimal partitioning (M_0). The second one additionally includes nitrogen consumption and decrease in root uptake capacity with age (M_1). The third one additionally authorizes initial shoot-root ratios differing from the optimal one (M_2). Each model was fitted to the same data of Shipley and Meziane (2002) which have been obtained in four resource environments: high and low irradiance combined with high and low external nitrogen

concentration. Importantly, all modelled dynamics are based on optimal partitioning theory: in model M_2, developmental constraints cease after the first 15 days and only affect the initial conditions.

Fitting models to experimental data

Four parameters, the photosynthetic efficiency A_{max}, the dark respiration R_d, the nitrogen allocation a_N and the maximal nutrient uptake efficiency U_{max} were not measured in the experiments of Meziane and Shipley (1999). An average dark respiration R_d^{mean} was computed from the data of Reich *et al*. (2003), and this average value $R_d^{mean} = 80$ nmol.g^{-1}.s^{-1} was used for all the species studied in Meziane and Shipley (1999). It thus remains three parameters to estimate in the minimal version of the model: A_{max} , a_N and U_{max}. Up to three additional parameters, ρ, K_m and R_0, need to be estimated in the additional versions of the model described above.

A 25x26x5x7x9x19 grid of parameter values was used (Table 3). The parameter space has been chosen so as to include the reported parameter values found in the literature (Table 3). In M_0, parameters ρ and K_m were set to zero. In models M_0 and M_1, initial shoot-root ratio R_0 was equal to the ratio predicted by optimal partitioning.

The same distance ε between model predictions and experimental data is used. This time, between four and six model parameters have to be estimated with only two growth indicators. Consequently, a large array of parameter sets can lead to model predictions matching the two growth indicators. Therefore, rather than trying to estimate the model parameters, the model simulations are filtered so that they fit the available growth indicators (Jabot and Bascompte

2012). As previously, model parameter sets leading to ε values smaller than 0.05 are retained. These retained realistic simulations are then used to explore the range of allometric relationships between root and shoot biomass that the three models are able to predict. To this end, for each model simulation, the same procedure as in Shipley and Meziane (2002) was used to compute the allometric coefficient β: plant biomass was simulated at 15, 20, 25, 30 and 35 days post-germination and β was computed as the slope of a regression of the natural logarithm of shoot dry mass on root dry mass. To quantify the predictive ability of the models, the relative distance between simulated and empirical values of allometric coefficients β is computed for every retained parameters sets and the sets which lead to the smallest distance, called $d_{\min}$ are kept:

$$d_{\min} = \min\left(\sqrt{\left(\frac{(\beta_{obs} - \beta_{sim})^2}{(\beta_{obs})^2}\right)}\right) \quad (26)$$

where β_{obs} and β_{sim} are empirical and simulated values of the allometric coefficients.

Results

Model M_0 was found (as in the first section) to produce β values equal to one (Figure 3A). Adding a decrease in root uptake efficiency with age and nitrogen consumption (model M_1) caused plants to become progressively limited in nitrogen and to allocate an increasing amount of biomass to roots as they grow. This lead to β values smaller than one (Figure 3B). When initial shoot-root ratio was large, plants also allocated more biomass to roots until an optimal ratio was reached (model M_2). This also lead to β values smaller than one (Figure 3C), although it affected the beginning of the growth dynamics rather than the end as observed with nutrient limitation (Figure 3B). These two processes were found to enforce each other, since they acted at different growth stages (Figure 3D).

The three models were fitted to the data of Shipley and Meziane (2002). Some models failed at reproducing some of the growth indicators with an average relative error ε smaller than 0.05. Model M_0 did not succeed in reproducing RGR and RWR of 8, 14, 18 and 21 out of the 22 species in the LN, lN, Ln and ln treatments respectively (Figure 4). When the effects of nitrogen limitation were included in the model (model M_1), the number of accurately reproduced growth patterns strongly increased: the growth indicators of 18, 20, 20 and 22 out of the 22 species could be reproduced in the lN, LN, Ln and ln treatments respectively. The full model (M_2) was able to accurately reproduce the growth indicators of all species, except in the LN treatment (20 of the 22 species).

When models succeeded in reproducing the plant growth indictors, the allometric coefficients β that they predicted were compared to observed ones. Model M_0 failed at reproducing such allometric coefficients, irrespective of the environmental treatments. Adding nitrogen limitation weakly increased the predictive ability of the model: the relative distance d_{min} between empirical and simulated allometric coefficients was equal to zero for only seven species across all treatments, i.e in 8% of the cases. In contrast, model M_2 succeeded in reproducing observed allometric coefficients with d_{min} values almost always equal to zero, except for *Rumex acetosa* (β = 0.748) in the LN treatment, *Deschampsia cespitosa* (β = 1.261) in the Ln treatment and S*ilene cucubalus* (β = 0.804), *Polygonum lapathifolium* (β = 0.906), *Plantago major* (β = 0.948) and P*anicum capillare* (β = 1.000) in the lN treatment (Figure 4).

Even if a model fails at accurately predicting the empirical allometric coefficients, it may still make close predictions. β values simulated with model M_1 were closer to empirical values of

Shipley and Meziane (2002) than those simulated with model M_0 for all species with β values smaller than one (Figure 4). The relative distance d_{min} between empirical and simulated β values was larger than 0.10 in 83% of the cases for model M_0, while for model M_1, d_{min} was smaller than 0.025 in 26% of the cases and smaller than 0.10 in 50% of the cases. The full model (M_2) had relative errors d_{min} on β values smaller than 0.10 for all species in all treatments, except for *Rumex acetosa* in the LN treatment.

Model validation

The modelling results make an additional prediction: in cases in which allometric coefficients β are significantly different from one, this should be due to the difference between the initially constrained shoot-root ratio and the ratio required for optimal partitioning. If β is smaller than one, the initial shoot-root ratio should be larger than the optimal ratio and vice versa (**[Supplementary information]**, Figure S2) This final prediction was tested by re-analyzing the data of Shipley and Meziane (2002). The average initial shoot-root ratio and the standard deviation were computed from available biomass data, and a weighted least square regression was used to assess the accuracy of model predictions (Figure 5).

For the LN and ln treatments, the initial shoot-root ratio predicted by the full model (M2) fits the biomass raw data with a good accuracy (r = 0.87 for the LN treatment and r = 0.53 for the ln treatment). For the Ln and lN treatments, model predictions are not so good (r = 0.12 for the lN treatment and r = 0.33 for the Ln treatment). In these treatments only 5 (respectively 6) species out of 21 had a β value significantly different from 1 (Shipley and Meziane 2002). When the regression was performed solely on species with an allometric coefficient significantly smaller than one, the regression coefficient sharply increased to 0.80 for the lN

treatment and to 0.63 for the Ln treatment. This means that model predictions regarding initial root-shoot ratios were close to observations in cases in which this ontogenetic constraint was necessary to explain root-shoot trajectories. In cases in which a simpler model was sufficient to account for observations, the uncertainty of the initial root-shoot ratio estimation obscured the predictions (Figure 5).

DISCUSSION

This study aimed at testing whether observed root-shoot allometries during plant development could be explained by the hypothesis of optimal partitioning. The approach was thus twofold. First, a simple model of plant growth was built based on commonly measured plant functional traits, and it has been tested whether this model was a sufficiently detailed account of plant growth to reproduce various growth indicators of experimental studies. The model succeeded in reproducing these indicators with a very good accuracy (Figure 1). Two plant traits were not empirically measured during the experiments and were estimated to reproduce the two plant growth indicators. Fitted trait values were within the ranges reported in the literature, and were thus realistic. This first study part was essential to discard the possibility that the discrepancy between theoretical predictions and empirical allometries would be due to a poor modelled representation of plant growth.

The second part of the study aimed at using this simple model to predict root-shoot allometry during plant development. The results of previous simpler models were recovered: the optimal partitioning hypothesis lead to an isometric growth of roots and shoot (Charles-Edwards *et al*., 1972; Shipley and Meziane, 2002), in contrast with the empirical findings of Shipley and Meziane (2002). This steady-state isometry was further found to be preceded by a

short transient period of non-isometric growth, during which plants were dynamically adjusting their allocation coefficient if initial root-shoot ratio were not optimal (Figure 2). It has been then tested whether adding complementary model ingredients could lengthen the duration of this transient phase and change the shape of the root-shoot allometry. Root senescence was added in the model, as well as the nitrogen consumption by plants in the experimental containers. These first two ingredients improved the ability of the models to reproduce growth indicators when light and nitrogen were limiting. However they were insufficient to explain the results of Shipley and Meziane (2002) on allometric trajectories. The initial shoot-root ratio was then varied to represent initial developmental constraints. With this third ingredient, most empirical findings of Shipley and Meziane (2002) could be reproduced (Figure 4).

These simulation results show that to be a reasonable approximation of plant allocation scheme, the optimal partitioning framework needs to be complemented by a number of complementary processes which lead to transient phases of allocation adjustment by the plant. A combination of these processes was found to be necessary to recover the empirical findings of Shipley and Meziane (2002). More precisely, initial shoot-root ratio had to be different from the ratio predicted by optimal partitioning to recover most allometric coefficients which were significantly different from one. Gedroc *et al*. (1996) already evidenced that ontogenetic constraints were likely to play a role in allometric trajectories by statistically analyzing plant growth trajectories. The modelling approach proposed here enables to incorporate mechanistically various processes that have been suggested in the literature to cause shifts in root-shoot scaling during plant ontogeny, and to test their respective influences quantitatively. Furthermore, this approach demonstrates that although adding some initial developmental

constraints may be needed to recover experimental findings, such developmental constraints are no longer needed during the subsequent plant growth dynamics which were controlled by optimal partitioning equations in this study.

The hypothesis that initial shoot-root ratios may differ from the ratio required for optimal partitioning is supported by the re-analysis of the experiments of Shipley and Meziane (2002) (Figure6). Moreover the finding that initial shoot-root ratio should be larger than 1 during the very first days of plant growth after germination is consistent with observations (Jurado and Westoby 1992; Leishman and Westoby, 1994). The hypothesis that this initial shoot-root ratio should be at least partially developmentally constrained is also consistent with observations (Evans, 1977; Kitajima, 2002) and the biological fact that initial plant growth is ensured by the consumption of seed reserves. The explanation modelled here for non-isometric root-shoot trajectories is hence uniquely based on a transient dynamics controlled by optimal partitioning equations. The model proved powerful in the non-constant nutrient conditions of Shipley and Meziane (2002)'s experiments (when looked at an hourly resolution). This model could hence similarly be used to quantitatively predict root-shoot dynamics in response to disturbances (Mäkelä 1999).

The model proposed here does not take into account self-shading, shoot senescence nor water use by the plant. It is thus not able in its present form to assess potential explanations for observed ontogenetic shifts in root-shoot scaling evidenced in longer term experiments (e.g., Mueller et al. 2000) for which these three effects could play an additional role. It can neither be used in its present form to assess the potential role of temperature increase or water shortage in biomass allocation. Since these last two environmental pressures are likely to be

important according to current climate change scenarios, further model refinements to add temperature and water effects constitute very interesting perspectives. Such future model developments will be eased by the general approach of progressive model building through quantitative assessment that has been developed in this study.

.

In this study, optimal allocation equations were based on the idea that relative growth rate should be a good proxy for plant fitness and thus should be optimized by evolution. However, plants have evolved in competitive environments, so that for a plant, maximizing its growth in isolation is not necessarily the best strategy to maximize its growth in competitive conditions (McNickle and Dybzinski, 2013). Future work addressing this issue would be valuable. They would require the consideration of below-ground competition for soil resources and of above-ground competition for light (Tilman, 1988; Schieving and Poorter, 1999; Gersani *et al*., 2001; O'Brien and Brown, 2008). Such work would enable to understand whether the use of new plant fitness proxies in optimal partitioning modelling could also produce the long-lasting transient dynamics that have been here evidenced.

AKNOWLEDGEMENTS

Théophile Lohier was funded by the Institut national de Recherche en Sciences et Technologies pour l'Environnement et l'Agriculture (IRSTEA) and the region Auvergne.

LITERATURE CITED

Aschan G, Pfanz H. 2003. Non-foliar photosynthesis - a strategy of additional carbon acquisition. *Flora* 198: 81-97.

Bloom A, Chapin F, Mooney H. 1985. Resource limitation in plants - an economic analogy. *Annual Review of Ecology and Systematics* 16: 363-392.

Bonan G. 2008. Forests and climate change: forcings, feedbacks, and the climate benefits of forests. *Science* 320: 1444-1449.

Brouwer R. 1962. Nutritive influences on the distribution of dry matter in the plant. *Netherlands Journal of Agricultural Science* 10: 399-408.

Chapin F. 1980. The mineral nutrition of wild plants. *Annual Review of Ecology and Systematics* 11: 233-260.

Charles-Edwards D. 1976. Shoot and root activities during steady-state plant growth. *Annals of Botany* 40: 767-772.

Charles-Edwards D, Charles-Edwards J, Sant F. 1972. Models for mesophyll cell arrangement in leaves of ryegrass (lolium perenne l.). *Planta* 104: 297-305.

Dewar R, Franklin O, Mäkelä A, McMurtrie R, Valentine H. 2009. Optimal function explains forest responses to global change. *BioScience* 59: 127-139.

Dybzinski R, Farrior C, Wolf A, Reich P, Pacala S. 2011. Evolutionarily stable strategy carbon allocation to foliage, wood, and fine roots in trees competing for light and nitrogen: an analytically tractable, individual-based model and quantitative comparisons to data. The *American Naturalist* 177: 153-166.

Engels C, Neumann G, Gahoonia TS, George E, Schenk MK. 2000. *Assessing the ability of roots for nutrients acquisition*. in Springer, editor. Root Methods. A handbook.

Evans G. 1972. *The quantitative analysis of plant growth*. University of California press.

Evans PS. 1977. Comparative root morphology of some pasture grasses and clovers. *New Zeland Journal of Agricultural Research* 20: 331-335.

Foley J. 2007. Net primary productivity in the terrestrial biosphere: the application of a global model. *New Phytologist* 174:811-822.

Franklin O, Johansson J, Dewar R *et al.* 2012. Modeling carbon allocation in trees: a search for principles. *Tree Physiology* 00: 1-19.

Gedroc J, McConnaughay K, Coleman J. 1996. Plasticity in root/shoot partitioning: optimal, ontogenetic, or both ? *Functional Ecology* 10: 44-50.

Gersani M, Bown J, O'Brien E, Maina G, Abramsky Z. 2001. Tragedy of the commons as a result of root competition. *Journal of Ecology* 89: 660-669.

Goudriaan J, Van Laar H. 1994. *Modelling potential crop growth processes*. Kluwer Academic Publishers, Dordrecht, The Netherlands

Grime, J.P. 2001. *Plant strategies, vegetation processes, and ecosystem properties*, 2nd. ed. Wiley, Chichester, UK.

Génard M, Dauzat J, Franck N *et al*. 2008. Carbon allocation in fruit trees: from theory to modelling. *Trees* 22: 269-282.

Hungate B, Holland E, Jackson R, Chapin F, Mooney H. 1997. On the fate of carbon in grasslands under carbon dioxide enrichment. *Nature* 579: 388-576.

Iwasa Y, Roughgarden J. 1984. Shoot/root balance of plants: Optimal growth of a system with many vegetative organs. *Theoretical Population Biology* 25: 78-105.

Jurado E, Wetoby M, 1992. Seedling growth in relation to seed size among species of arid Australia. *Journal of ecology* 80, 407-416.

Kattge J, Diaz S, Lavorel S *et al*. 2011. Try - a global database of plant traits. *Global change biology* 17: 2905-2935.

Kikuzawa K, Lechowicz M. 2006. Toward synthesis of relationships among leaf longevity, instantaneous photosynthetic rate, lifetime leaf carbon gain, and the gross primary production of forests. *The American Naturalist* 168: 373-383.

Kitajima K. 2002. Do shade-tolerant tropical tree seedlings depend longer on seed reserves? Functional growth analysis of three Bignoniaceae species. *Functional Ecology* 16: 433-444.

Konings H, Koot E, De Wolf A. 1989. Growth characteristics, nutrient allocation and photosynthesis of carex species from floating fens. *Oecologia* 80: 111-121.

Lambers H, Chapin F, Pons T. 1998. *Plant physiological ecology*. Springer-Verlag, New York.

Leishman M.R., Westoby M. 1994. The role of large seed size in shaded conditions: experimental evidence. *Functional ecology* 8: 205-214.

Le Roux X, Lacointe A, Escobar-Gutiérrez A, Le Dizes S. 2001. Carbon-based models of individual tree growth: a critical appraisal. *Annals of Forest Science* 58: 469-506.

Maire V, Gross N, Da Silveira Pontes L, Picon-Cochard C, Soussana J. 2009. Trade-off between root nitrogen acquisition and shoot nitrogen utilization across 13 co-occurring pasture grass species. *Functional Ecology* 23: 668-679.

Mäkelä A, Valentine H, Helmisaari H. 2008. Optimal co-allocation of carbon and nitrogen in a forest stand at steady state. *New Phytologist* 180: 114-123.

Mäkelä A. 1999. Acclimatation in dynamic models based on structural relationships. *Functional Ecology* 13: 145-156.

McConnaughay KDM, Coleman JS. 1999. Biomass allocation in plant: ontogeny or optimality? A test along three resource gradients. *Ecology* 80: 2581-2593.

McNickle G, Dybzinski R. 2013. Game theory and plant ecology. *Ecology Letters* 16:545–555.

Meziane D, Shipley B. 1999. Interacting components of interspecific relative growth rate: constancy and change under differing conditions of light and nutrient supply. *Functional Ecology* 13: 311-622.

Mokany K, Raison R, Prokushkin A. 2006. Critical analysis of root: shoot ratios in terrestrial biomes. *Global Change* 12: 84-96.

Morris JT. 1980. The nitrogen uptake kinetics of *spartina alterniflora* in culture. *Ecology* 61(5): 1114-1121.

Müller I, Schmid B, Weiner J. 2000. The effect of nutrient availability on biomass allocation patterns in 27 species of herbaceous plants. *Perspectives in plant ecology, evolution and systematics* 3: 115-127.

Niklas K. 1994. *Plant Allometry The scaling of Form and Process*. Chicago University Press.

Nilsen E. 1995. *Plant Stems: Physiology and Functional Morphology*. Ed. B.L. Gartner. Academic Press, New York.

O'Brien E, Brown J. 2008. Games roots play: effects of soil volume and nutrients. *Journal of Ecology* 96: 438-446.

Poorter H, Niklas K, Reich P, Oleksyn J, Poot P, Mommer L. 2012. Biomass allocation to leaves, stems and roots: meta-analyses of interspecific variation and environmental control. *New Phytologist* 193: 30-50.

Reich P, Buschena1 C, Tjoelker M *et al*. 2003. Variation in growth rate and ecophysiology among 34 grassland and savannah species under contrasting n supply: a test of functional group differences. *New Phytologist* 157: 617-631.

Reynolds JF, Thornley JHM. 1982. A shoot:root partitioning model. *Annals of botany* 49: 585-597.

Reynolds J, Chen J. 1996. Modeling whole-plant allocation in relation to carbon and nitrogen supply: Coordination versus optimization. *Plant and Soil* 185: 65-74.

Robinson D. 1986. Limits to nutrient inflow rates in roots and root systems. *New Phytologist* 68: 551-559.

Schieving F, Poorter H. 1999. Carbon gain in a multispecies canopy: the role of specific leaf area and photosynthetic nitrogen-use efficiency in the tragedy of the commons. *New Phytologist* 143: 201-211.

Schippers P, Kropff MJ. 2001. Competition for light and nitrogen among grassland species: a simulation analysis. *Functional Ecology* 15: 155-164.

Shipley B, Meziane D. 2002. The balanced-growth hypothesis and the allometry of leaf and root biomass allocation. *Functional Ecology* 16: 326-331.

Taubert F, Frank K, Huth A. 2012. A review of grassland models in the biofuel context. *Ecological Modelling* 245: 84-93.

Thornley J. 1995. Shoot: root allocation with respect to c, n and p: an investigation and comparison of resistance and teleonomic models. *Annals of Botany* 75: 391-405.

Thornley J. 1998. *Grassland Dynamics: An Ecosystem Simulation Model*. Wallingford, UK: CAB International.

Tilman D. 1988. *Plant strategies and the dynamics and structure of plant communities*. Princeton University Press.

Tomlinson KW, Sterck FJ, Bongers F, Da Silva DA, Barbosa ERM, Ward D, Bakker FT. 2012. Biomass partitioning and root morphology of savanna trees across a water gradient. *Journal of Ecology* 100: 1113-1121.

Tucker MR. 1999. Clay minerals: their importance and function in soils. Soil Fertility Note 13, NCDA&CS Agronomic Division. Downloadable at www.ncagr.gov/agronomi/pdffiles/sfn13.pdf .

Valentine HT, Mäkelä A. 2012. Modeling forest stand dynamics from optimal balances of carbon and nitrogen. *New Phytologist* 194: 961-971.

Volder A, Smart D, Bloom A, Eissenstat D. 2005. Rapid decline in nitrate uptake and respiration with age in fine lateral roots of grape: implications for root efficiency and competitive effectiveness. *New Phytologist* 165: 493-502.

West G, Brown J, Enquist B. 1999. The fourth dimension of life: Fractal geometry and allometric scaling of organisms. *Science* 284: 1677-1679.

TABLES

TABLE 1. *Parameter ranges reported in the literature and those used for model calibration with the experiments of Reich et al. (2003).*

	A_{max} nmol.g^{-1}.s^{-1}	U_{max} mg.g^{-1}.h^{-1}
Range reported in the literature	150 - 900[1]	0.22 – 0.92[2]
Range used for model calibration	100 - 600	0.10 – 2.00
Grid step used for model calibration	10	0.01

[1] *(Reich et al., 2003)* ; [2] *(Maire et al., 2009)*

TABLE 2. *Average estimates of model parameters and associated minimal distance between model predictions and empirical data. Standard deviations of parameter estimates which lead to an ε smaller than 5% are indicated inside the parentheses.*

Species	A_{max} $nmol.g^{-1}.s^{-1}$	U_{max} $mg.g^{-1}.h^{-1}$	ε_{min} **%**
Achillea millefolium (AcM)	262 (9.85)	0.87 (0.064)	0.6
Anemone cylindrica (AnC)	184 (5.06)	0.75 (0.048)	1.4
Asclepias tuberosa (AsT)	200 (7.62)	0.55 (0.039)	0.2
Aster azureus (AsA)	282 (9.37)	1.64 (0.104)	0.8
Coreopsis palmata (CoP)	269 (7.93)	0.90 (0.058)	0.0
Liatris aspera (LiA)	154 (4.99)	1.29 (0.063)	3.0
Monarda fistulosa (MoF)	259 (7.93)	0.85 (0.062)	0.3
Rudbeckia hirta (RuH)	261 (9.85)	0.73 (0.056)	0.3
Solidago nemoralis (SoN)	-	-	11.2
Agropyron repens (AgR)	183 (4.83)	0.55 (0.038)	0.8
Agropyron smithii (AgS)	170 (0.00)	0.59 (0.045)	0.6
Bromus inermis (BrI)	228 (11.38)	0.31 (0.031)	0.8
Calamagrostis canadensis (CaC)	217 (7.35)	0.77 (0.051)	0.8
Elymus canadensis (ElC)	191 (7.03)	0.55 (0.039)	0.7
Koeleria cristata (KoC)	259 (7.73)	1.06 (0.068)	0.2
Leersia oryzoides (LeO)	291 (7.72)	0.64 (0.040)	1.0
Stipa comata (StC)	153(4.89)	0.49 (0.035)	1.4
Andropogon gerardii (AnG)	215 (5.11)	0.49 (0.037)	1.7
Bouteloua curtipendula (BoC)	229(7.55)	0.80 (0.050)	0.6
Bouteloua gracilis (BoG)	180 (0.00)	1.17 (0.079)	0.0
Buchloe dactyloides (BuD)	240 (7.84)	0.44 (0.034)	0.3
Panicum vigatum (PaV)	194 (5.08)	0.68 (0.043)	2.1
Schyzarchyrium scoparium (ScC)	184(5.06)	0.76 (0.046)	2.3
Sorghastrums nutans (SoNb)	224 (5.03)	0.50 (0.033)	1.0
Sporobolus cryptandrus (SpC)	213 (4.71)	1.17 (0.066)	0.8

TABLE 3. *Parameter ranges reported in the literature and those used for model calibration with the experiments of Shipley and Meziane (2002).*

	A_{max}	U_{max}	a_N	ρ	K_m	R_0
	nmol.g^{-1}.s^{-1}	mg.g^{-1}.h^{-1}	%	mg.g^{-1}.h^{-1}	mg.L^{-1}	-
Range reported in the literature	150 - 900[1]	0.22 – 0.92[2]	50 - 70[1]	0.025[3]	0.06 - 0.56[4]	1.0[5]
Range used for model calibration	100 - 700	0.10 – 2.50	50 - 90	0.0 - 0.030	0.0 – 2.0	0.5 – 5.0
Grid step used for model calibration	25	0.10	10	0.005	0.25	0.25

[1](Reich *et al*., 2003) ; [2](Maire *et al*., 2009) ; [3](Volder *et al*., 2005) ; [4](Morris 1980) ; [5](Goudriaan and Van Laar, 1994).

FIGURES

FIG. 1. (A) Computed relative growth rates against measured relative growth rates. (B) Computed root weight ratios against measured root weight ratios. (C) Computed root nitrogen contents against measured root nitrogen contents. (D) Computed shoot nitrogen contents against measured shoot nitrogen contents. The solid line represents y = x. Each circle represents a plant species. NRMSE: normalized root mean square error.

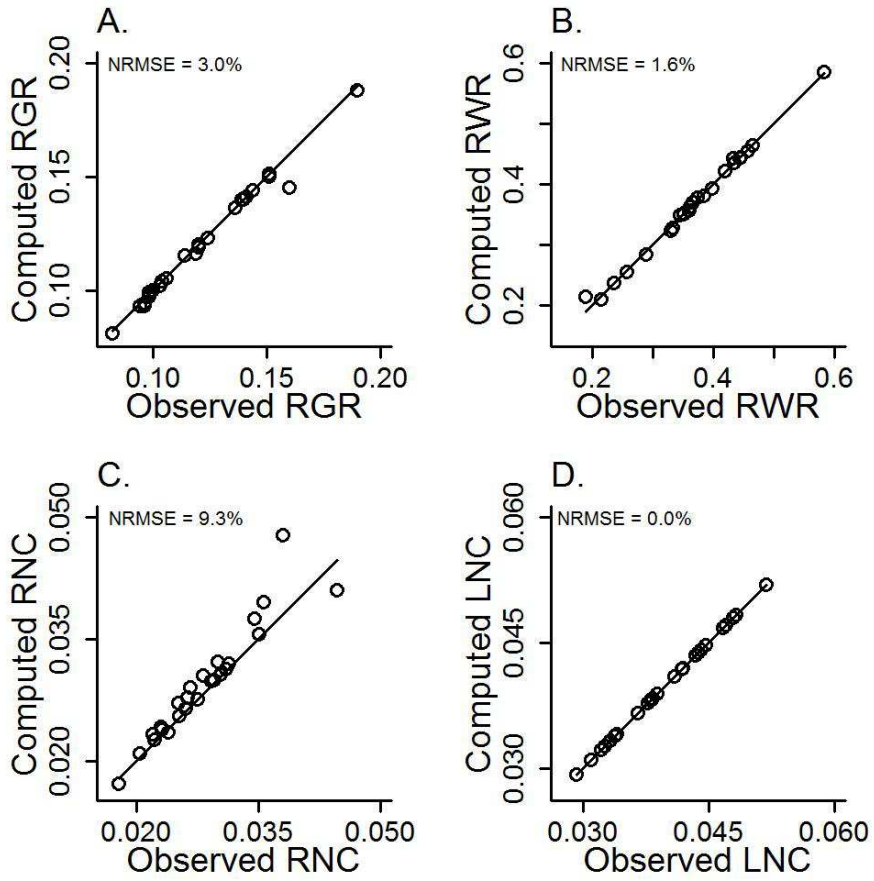

FIG. 2. (A) Simulated dynamics of the carbon fraction allocated to above-ground biomass. (B) Bivariate plots of shoot and root simulated dynamics. (C) Simulated dynamics of the allometric coefficient β. Each symbol stands for a particular species: *Achillea millefolium* (○), B*romus inermis* (□), C*alamagrostis canadensis* (◊) and *Buchloe dactyloides* (Δ). Best-fit parameters were used in the simulations of the minimal model. The first harvest in the experiment of Shipley and Meziane (2002) is shown by a vertical dashed line.

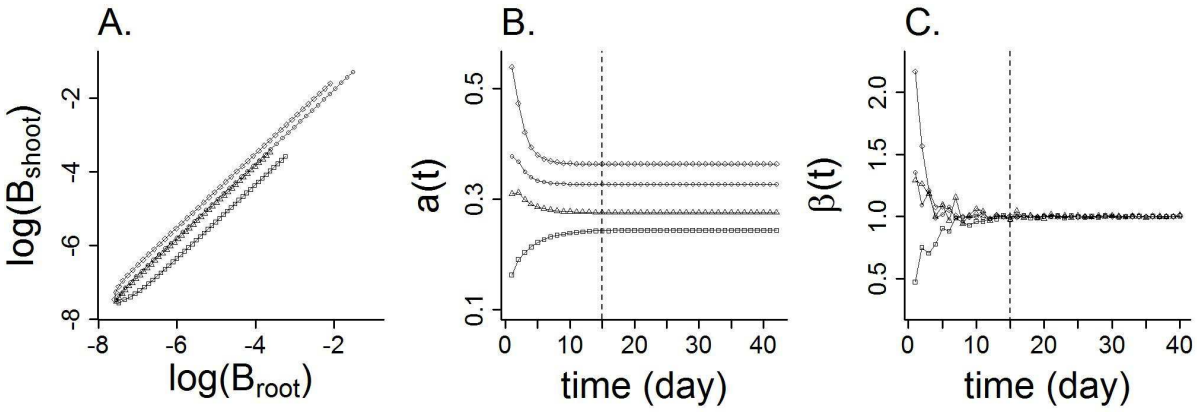

FIG. 3. Root-shoot trajectories of *Eupatorium maculatum* simulated with (A) the reference model M_0, (B) a model including nitrogen limitation resulting from root senescence and the decrease of soil nitrogen concentration, (C) a model including a small nitrogen limitation and a large initial shoot-root ratio, (D) a model including a large nitrogen limitation and a large initial shoot-root ratio. The dashed line represents y = x. Crosses on the different trajectories represent root and shoot biomass at the harvesting dates, which are used to compute the allometric coefficient β. These various trajectories do not fit overall plant growth patterns, but are used here to illustrate the effects of the various model ingredients on root-shoot trajectories.

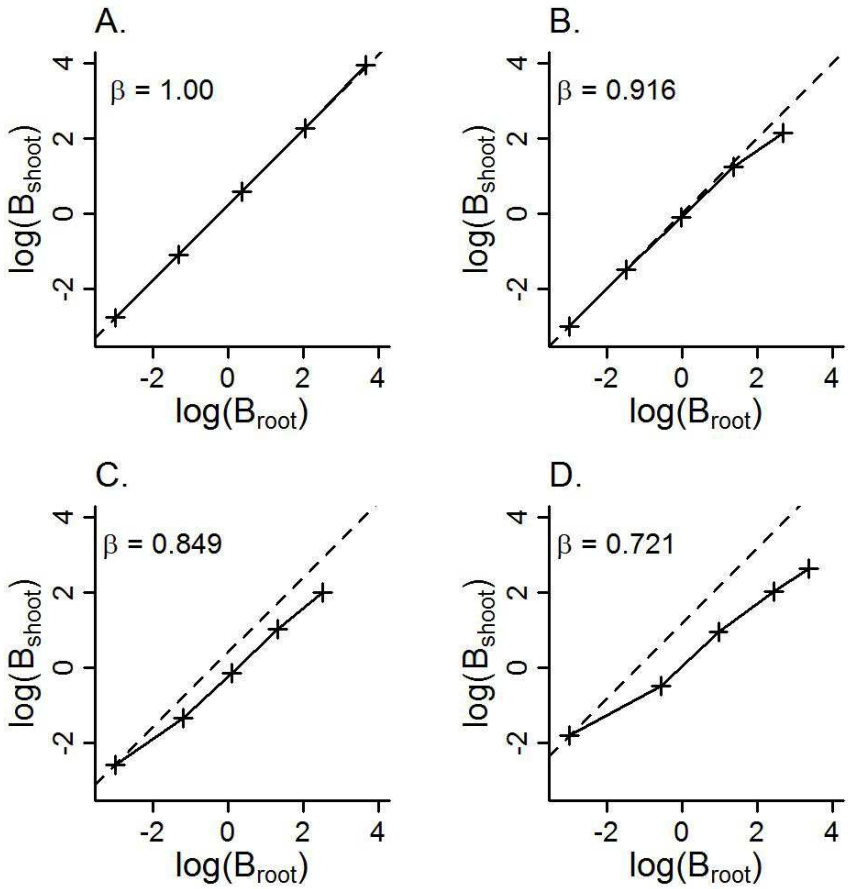

FIG. 4. Minimal relative distance d_{min} between empirical and simulated allometric coefficients β for each species studied in Shipley and Meziane (2002). (A) LN treatment. (B) lN treatment. (C) Ln treatment. (D) ln treatment. Species are sorted by increasing β values. Each symbol corresponds to a model. When a model did not succeed in reproducing growth indicators with a good accuracy, its corresponding point was not shown. The solid line represents a threshold d_{min} of 2.5%.The abbreviations for species names used in the x-axis are detailed in Table S1.

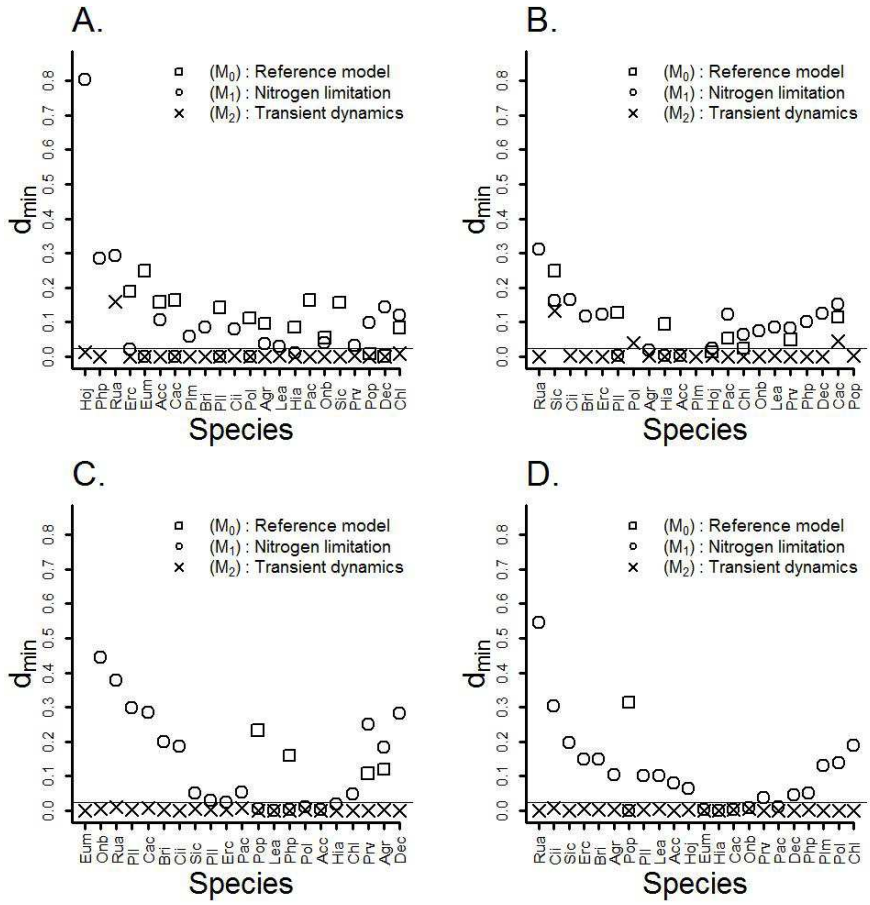

FIG. 5. Fitted initial shoot-root ratios against initial shoot-root ratios computed from the biomass raw data of Shipley and Meziane (2002) in (A) the LN treatment, (B) the lN treatment, (C) the Ln treatment and (D) the ln treatment. Each circle represents a species with β significantly (●) or not significantly (○) different from one. Standard deviations are drawn in dotted lines. Weighted least square regression coefficients were computed from all data (r) and from data with β significantly different from one (r_s).

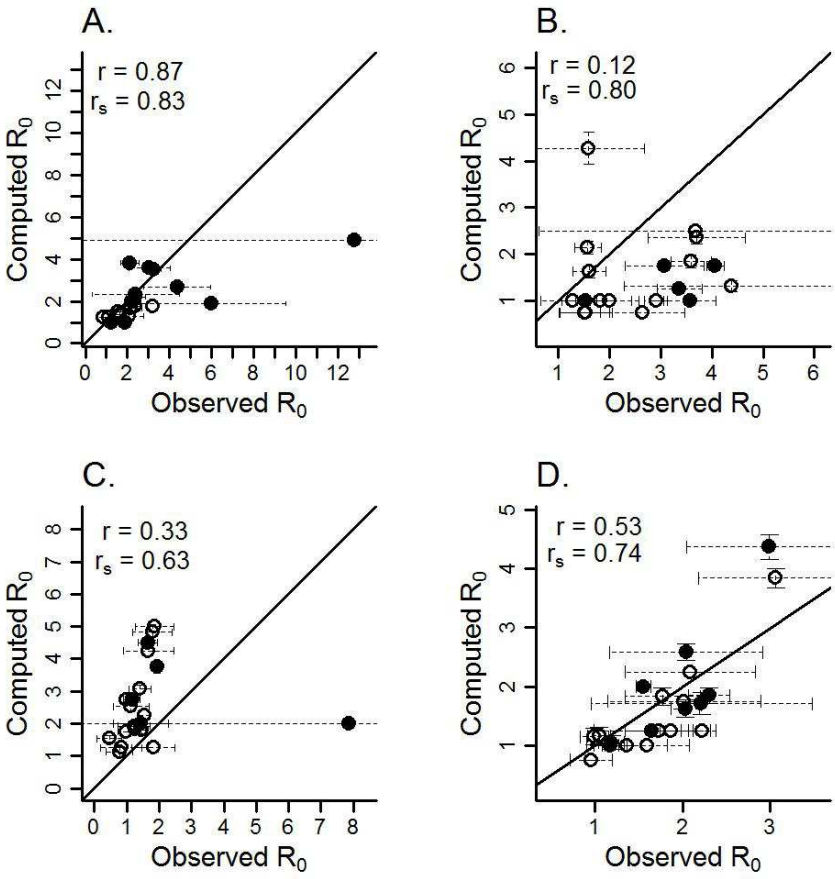

SUPPLEMENTARY INFORMATIONS

TABLE S1. List of abbreviations used for the species studied by Shipley and Meziane (2002).

Abbreviation	Species
Acc	*Acorus calamus*
Agr	*Agropyron repens*
Bri	*Bromus inermis*
Cac	*Carex crinita*
Chl	*Chrysanthemum leucanthemumu*
Cii	*Cichorium intybus*
Dec	*Deschampsia cespitosa*
Erc	*Erysimum cheirantoides*
Eum	*Eupatorium maculatum*
Hia	*Hieracium aurantiacum*
Hoj	*Hordeum jubatum*
Lea	*Leontodon autumnalis*
Onb	*Oenothera biennis*
Pac	*Panicum capillare*
Php	*Phleum pratense*
Pll	*Plantago lanceolata*
Plm	*Plantago major*
Pop	*Poa pratensis*
Pol	*Polygonum lapathifolium*
Prv	*Prunella vulgaris*
Rua	*Rumex acetosa*
Sic	*Silene cucubalus*

FIG. S2. Shoot-root ratio required for optimal partitioning (+) and shoot-root ratio minimizing the distance between empirical and simulated allometric coefficients (○) in (A) the LN treatment,. (B) the Ln treatment., (C) the lN treatment and. (D) the ln treatment. Species are sorted by increasing β values. The abbreviations for species names used in the x-axis are detailed in Table S1.

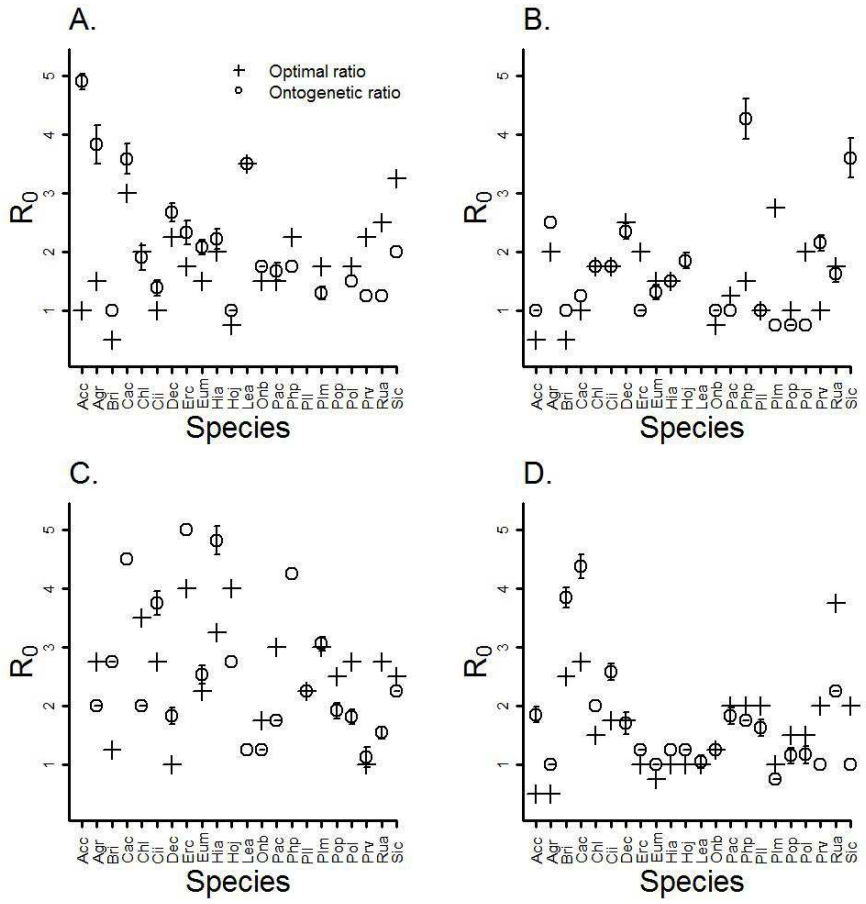

V. Implémentation et réalisme du modèle indvidu-centré Nemossos

Manuscrit correspondant:

Lohier, T., Jabot, F., & Deffuant G. (in prep). Mechanistic traits-based plant community dynamics: The Nemossos model.

Mechanistic trait-based plant community dynamics: the Nemossos model.

Théophile Lohier[1*], Franck Jabot[1,] and Guillaume Deffuant[1]

Imminent submission in *Ecological Modelling*

[1]LISC - Laboratoire d'Ingénierie pour les Systèmes complexes, IRSTEA, 9 avenue Blaise Pascal, CS 20085, 63178 Aubière, France.

*Corresponding author: theophile.lohier@gmail.com

ABSTRACT

Understanding the ecological drivers of plant community dynamics thanks to plant functional traits is one major focus of community ecology. Most works on this topic have used correlative analyses. To further advance the field of plant functional ecology, a critical step to cross is to understand the underlying mechanics subtending the links between the set of plant functional traits and their response to their abiotic and biotic environment. The present contribution describes the model Nemossos, a mechanistic model of herbaceous community dynamics that is parametrized with a limited number of measurable plant functional traits. A particular attention has been paid to keep the model as simple as possible. We therefore provide a detailed comparison of the chosen model components with those of previous grassland models. We demonstrate that Nemossos is able to reproduce observed patterns of plant responses to their abiotic environment, as well as observed competitive hierarchies between plants in given environmental conditions. Nemossos is both relatively simple and realistic. It therefore opens exciting perspectives towards a fuller understanding of community assembly and dynamics.

1. INTRODUCTION

A promising way to understand plant community dynamics rely on plant functional trait analysis (Lavorel and Garnier, 2002; McGill et al., 2006). Over the past decades, a large number of studies have therefore been focused on the statistical analysis of co-occurring traits within communities, in the search of general rules of community assembly, including the effect of competition (Gaudet and Keddy, 1988) and habitat filtering (Ackerly, 2003; Cornwell et al., 2006; Kraft et al., 2008) on plant communities. These static approaches have led to important findings, including the general covariations between plant traits (Wright et al. 2004), the effects of environmental conditions on these traits (Poorter et al. 2009, Maire et al. 2015), and the resulting effects of plant traits on ecosystem functioning (Diaz et al. 2007, Cornwell et al. 2008). However, such approaches do not enable to quantitatively relate empirical observations to the underlying dynamical processes.

To move beyond this descriptive knowledge and go towards a more quantitative understanding of processes shaping plant communities, several approaches based on dynamical models have been developed. Most of these models attempt to link one or a few functional traits to plant dynamics (Warren and Topping, 2004; Jabot, 2010; Herben and Wildova, 2012; Enquist et al., 2015; Kraft et al. 2015). These models have proven useful to quantify the role of some plant traits in community dynamics. However, they are not well suited to take into account the interactions between the various physiological processes determining plant responses to environmental conditions (Marks and Lechowicz, 2006; Kraft et al. 2015).

To overcome these limitations, we need more detailed models, which would represent the effects of environmental forcing on various physiological processes, and would account for

the interactions between these processes. Some works have already been made in this direction, including works on forest seedlings (Marks and Lechowicz, 2006), and grasslands (Soussana et al., 2012). These contributions have made use of a large number of model parameters to finely represent available biological knowledge on the processes affecting the plant life cycle. This high level of details comes with important costs of parametrization and analysis, which limit the transferability and use of such models (Evans et al. 2013).

We therefore developed the Nemossos model, a novel individual-based model of plant community dynamics, that is parametrized with easily measurable plant functional traits, and that is kept as parsimonious as possible to broaden its application potential. The aim of this model is to assess our ability to derive pertinent integrated measure of plant performance in given environmental conditions from commonly measured plant functional traits. In this paper, we first describe the submodels used for each biological process and compare them to alternative modelling choices previously made in the literature. We then assess the ability of the Nemossos model to reproduce observed patterns of plant responses to their abiotic environment, as well as observed competitive hierarchies between plants in given environmental conditions. We finally discuss the exciting perspectives opened by Nemossos towards a fuller understanding of community assembly and dynamics.

2. MODEL DESCRIPTION

2.1. Model structure

Nemossos is a spatially-explicit individual-based model designed to simulate the vegetative growth of grassland communities within a plot of finite dimension with toroidal boundary conditions. It runs on a daily time step, and it can be easily linked to a climate simulator. The model describes the basic process of carbon assimilation by leaves and its dependency to

abiotic conditions. To account for the impact of nitrogen and water availability on photosynthesis, the dynamics of these resources in the soil and in the plant are explicitly modelled. All the process submodels are based on commonly measured functional traits. Competition between individuals occurs through resource depletion in the soil and through shading between plants.

Individual positions in the plot are described by two dimensional coordinates. Each individual is described by its above- and below-ground biomass and the spatial extension of these two compartments is represented by two distinct cylinders (Figure A1). The height and radius of these cylinders increases with compartment biomass according to species-specific allometric rules. In total, Nemossos contains 30 parameters per individual corresponding to measurable plant functional traits (Table 1) 22 of these traits are used to compute basic physiological processes including photosynthesis, transpiration, resource uptake and allocation of assimilates. The 8 remaining parameters enable to determine above- and below-ground plant part geometry. On top of these parameters, Nemossos needs as inputs 34 atmospheric and soil variables. In the following, we introduce the different process submodels, and describe how they interact between each other, as well as with abiotic factors. All the equations of the different submodels of Nemossos are provided in Appendix A. We also compare the complexity of the retained submodels with those used in alternative grassland models previously proposed in the literature (Table 2). This complexity comparison is summarized in Table 3, and alternative modelling choices for each submodel are extensively reviewed in Appendix B. The commented R code of Nemossos is provided in Appendix C.

2.2. Photosynthesis

The ability of plants to fix CO_2 in optimal conditions is parametrized by their maximal photosynthetic efficiency A_{max}. This maximal photosynthetic activity is decreased by five limiting factors: the amount of photosynthetically active radiation (PAR) captured by the plant, the leaf nitrogen content (*LNC*) which is not a fixed model parameter but an output of Nemossos (see section 2.6), the temperature T_l of the leaves, the soil water content θ which may trigger stomatal closure, and atmospheric CO_2 concentration C_a.

The relationship between the photosynthetic efficiency A actually realized by the plant and PAR have been extensively studied in the literature, leading to the development of several submodels (see Jassby and Platt (1976) for a review). The most parsimonious submodel consists in assuming that A increases linearly with PAR (as in models [2], [3], [5], [6], see Tab.2). Because of its simplicity, this submodel is not able to capture extreme behaviors like the saturation of photosynthetic efficiency at high PAR levels. At the other extreme, some complex submodels describe the biochemical processes underlying photosynthesis to capture the effects of PAR (e.g., [9]). These very detailed submodels make use of several trait values that are difficult to measure in the field (Tab.B1). We therefore used a semi-empirical submodel that is based on a nonrectangular hyperbola. It accounts for the saturation of A at high PAR levels, and only requires two parameters on top of A_{max} (eq.A7).

It has been evidenced that A increases linearly with *LNC* (Pons et al., 1994; Reich et al., 1997) and most of the grassland models integrate the effects of nitrogen availability on photosynthesis efficiency through a linear function ([1], [4], [6], [7]), which most often requires two parameters (Tab.B2). More mechanistic submodels have also been developed, but their complexity and the associated cost in terms of parameterization are much larger ([9],

Tab.B2). We therefore used a linear function between A and LNC, with two additional plant functional traits, LNC_{max} and LNC_{min}, which correspond to the boundaries of the observed range of LNC for a given species (eq.A6).

As photosynthesis results from a sequence of enzymatically catalyzed reactions, its efficiency depends on the temperature of the leaves T_l. The response of A to T_l can be modelled from the optimal temperature for photosynthesis T_{opt}, which is generally close to the usual growth temperature of the individual (Berry and Björkman, 1980; Yamori et al., 2005). The most parsimonious submodels assume a linear dependency of the gross CO_2 assimilation rate A_g to the temperature ([1]) with a plateau for highest temperatures ([5]). In this case the response function only requires two parameters (Tab.B3). But as it describe the effects of temperature on A_g, the effects of temperature on the respiration rate must be accounted for separately. We used this approach that required two plant traits: the optimal temperature for photosynthesis T_{opt}, and the temperature below which photosynthesis is null T_{min} (eq. A8). Alternative approaches that are more costly are described in Table B3.

The flux of CO_2 into the leaves is controlled by the stomatal opening, which modulates the stomatal conductance g_{CO2}, and by the CO_2 concentration gradient between the atmosphere (C_a) and the leaf intercellular space (C_i). We used the Fick's law of diffusion to estimate the maximal net CO_2 assimilation rate allowed when stomata are fully open (eq.A10). If this rate is larger than the one previously computed from photosynthetic efficiency A, the CO_2 enters the leaves faster than it can be fixed by the plant, which triggers the closing of stomata to limit water loss through transpiration, and leads to a decrease of g_{CO2}. Otherwise, photosynthesis is limited by stomatal opening, which depends on the soil water content (see section 2.10). One of the great benefits of this modelling approach is thus that it integrates the photosynthesis

dependency to water availability through the stomatal conductance, providing a more mechanistic representation than empirical response functions used in most of the grassland models reviewed ([3], [4]. [5], [7], [8], Tab.B4). This approach is furthermore very parsimonious, since it enables to express the effects of both drought and atmospheric CO_2 concentration on photosynthesis with only the three traits used to compute the leaf intercellular CO_2 concentration C_i according to the actual conductance g_{CO2}. Indeed, we used an empirical relationship derived from the works of Norman (1982) and Baldocchi (1994) to relate the leaf intercellular CO_2 to the stomatal conductance (eq.A11).

In total, our modelling of photosynthesis requires 10 parameters, and enables to account for the effects of PAR, leaf nitrogen content, leaf temperature, soil water availability and atmospheric CO2 concentration. Previously proposed submodels made use of a least 16 parameters to cover all these abiotic effects ([7]). Further submodel simplifications would have led to incomplete representations of the effects of abiotic constraints on photosynthesis.

2.3. Respiration

Approximately half of the carbohydrates assimilated by a plant during its photosynthetic activity are lost through respiration during the same period (Van der Werf et al., 1992). The rate of respiration R may be decomposed into three major processes: maintenance of biomass, growth and ion transport. In most plant growth models (but see [4]), respiratory costs induced by ion transport are implicitly integrated in the maintenance respiration rate and we followed this strategy.

The maintenance respiration accounts for the cost of repairing and maintaining biomass so that the maintenance respiration rate R_m increases with plant biomass. It is often modelled

through a linear function with a slope corresponding to a reference maintenance respiration rate (Tab.B5). Moreover R_m depends on both plant protein content (Ryan, 1991) and atmospheric temperature (McCree, 1974), which is often accounted for with response functions ([2], [4], [6], [7], [8], [9]). In our model, R_m is also computed as a linear function of plant biomass (eq.A12) and the effects of temperature on R_m are integrated through an empirical function (eq.A13). As the stomatal conductance which determines plant water demand is computed from the net CO_2 exchange rate of the shoot, we distinguish the shoot respiration rate, which is likely to impact plant water demand, from the root respiration rate which has no effect on plant water demand. For simplicity, Nemossos does not take into account the dependency of R_m on nitrogen availability.

Growth respiration corresponds to the cost associated with biomass synthesis from carbohydrates. The growth respiration rate R_g is therefore directly related to the amount of carbohydrates fixed during photosynthesis. As in models [1], [4], [7], and [9], we followed Johnson and Thornley (1985), and assumed that R_g depends linearly on the total daily gross primary production (eq.A12).

Our modelling approach of respiration integrates the dependency of the respiration rate to the amount of biomass that the plant needs to maintain, and to the amount of carbohydrates fixed during a time step, while accounting for the effects of temperature on maintenance respiration. The parameterization cost of this submodel is one of the lowest among reviewed models with only 4 needed parameters (Tab.1). It is worth noting however that this priority concern on parsimony led us to ignore the effects of nitrogen availability on the respiration rate.

2.4. Transpiration

Because of stomatal opening needed to maintain the photosynthetic activity of the leaves, more than 99% of water extracted by the roots of a plant is lost by its shoot through transpiration (Lambers et al., 2008). In most of the grassland models reviewed ([3], [5], [7], [8]), the transpiration rate is estimated as the potential transpiration rate, which is often computed with a meteorological submodel, weighted by an empirical response function depending on the extractable soil water content (Tab.B7). Although this approach is parsimonious, it is not well suited to take into account the potential coupling between transpiration and photosynthetic rates through stomatal opening. We therefore adopted a more mechanistic approach similar to that used in [2]. It is based on the Fick's law of diffusion which enables to estimate the potential transpiration rate from the stomatal conductance and the difference in water vapor concentration between the leaf and the atmosphere Δw (eq.A15). The effective transpiration rate is then estimated as the minimum between the potential transpiration rate and the potential water uptake rate (eq.A19). This modelling approach enables: 1) to take into account the effects of water shortage on the transpiration rate; 2) to account for the effects of the atmospheric temperature and humidity on the transpiration rate through the leaf to air vapor pressure (eq.A16, A17 and A18) and 3) to explicitly describe the effects of water shortage on stomatal conductance, which in turn constrains the CO_2 availability for photosynthesis (see section 2.2 above). Finally, this approach does not require extensive parametrization since it is based on only one additional plant functional trait: the maximal root water uptake rate $U_{W,max}$, and on some abiotic parameters as soil characteristics and atmospheric variables (Tab.A5).

2.5. Nitrogen uptake

For most species, the primary way of nitrogen acquisition is the root uptake from the soil (Cleveland et al., 1999). We therefore ignored the process of atmospheric nitrogen fixation in Nemossos (but see [7]). Nitrogen is present in the soil in both organic and ionic (nitrate and ammonium) forms. Nemossos considers that plants are able to extract the ionic forms of nitrogen, which are in direct contact with their root surface. The nitrogen available for root uptake therefore corresponds to the nitrogen included in the cylinder delineating the root biomass. Nitrogen enters this area thanks to water movements induced by soil water extraction by the roots.

The rate at which plants are able to extract the nitrogen ionic forms from the soil depends on the root surface area, the uptake properties of this surface and the nitrogen concentration in the vicinity of this surface. Moreover plants are able to regulate their nitrogen uptake in order to match the whole plant demand and thus to avoid nitrogen toxicity. A common modelling approach consists in separately estimating root potential uptake and plant requirement. The effective nitrogen uptake equals the minimum of the two ([6], [7], [8], [9], Tab.B8). Here, we used a similar approach: the potential uptake rate variation with the nitrogen concentration in the rooting zone is described with a Michaelis-Menten equation (eq.A23) while the plant requirement depends on the produced biomass and on LNC_{max} (eq.A24). The parametrization cost of our submodel is among the lowest with only 4 parameters required (Tab.1).

2.6. Allocation of assimilates

Carbon allocation. The atmospheric carbon fixed by the leaves during photosynthesis is then partitioned among above- and belowground plant parts. Despite the crucial importance of carbon allocation in plant dynamics, the underlying mechanisms are still misunderstood and

the relative importance of functional equilibrium versus ontogeny is still discussed (Gedroc et al., 1996, Lohier et al., 2014). The grassland models reviewed reflect this lack of knowledge: some models are based on ontogeny with individuals trying to reach a determined root-shoot ratio ([3], [7], [8]) while other ones assume a functional equilibrium ([1], [2], [4], [6]). Model [9] incorporates both functional equilibrium and ontogenetic constrains, which results in high parametrization costs (Tab. B9). In our model, we assume that plants try to reach a functional equilibrium (eq.A25 and A26), which is the most parsimonious choice (Tab.1).

Nitrogen allocation. Little is known about the biochemical processes driving the nitrogen allocation between above- and below-ground plant parts, but it has been evidenced that the leaf nitrogen content *LNC* of plants is likely to vary depending on their habitat. For example, it is well-known that species from xeric habitat have a larger *LNC* suggesting a trade-off between water use efficiency and nutrient use efficiency (Reich et al., 2003a). Model [2] integrates this empirical knowledge in its nitrogen allocation submodel through response functions accounting for water and temperature effects (Tab.B10). When environmental conditions do not exhibit broad variations, *LNC* is often assumed to remain approximately constant during plant growth in such a way that the amount of nitrogen translocated from root to shoot may be assumed proportional to the newly produced biomass. Under this hypothesis the proportion of nitrogen allocated to the aboveground plant parts λ_N may be deduced either from the proportion of carbon allocated to the aboveground plant parts λ_C ([1], [4]) or from the shoot-root ratio ([7]). Finally, in models [6] and [8], only the nitrogen requirement of the shoot is estimated and root demand is implicitly assumed to be satisfied, while [9] does not distinguish above- and belowground tissues for nitrogen (but it distinguishes labile and stable reserves). Our nitrogen partitioning submodel simply consists in allocating a constant part of the nitrogen captured by roots to the shoot.

2.7. Phenology

A convenient modelling approach for plant life cycle, common to several grassland models ([1], [3], [4], [7]), consists in expressing the life phases through discrete states. The transition between stages may be governed either by elapsed time ([1], [4], [7]) or by an environmental variable based on temperature ([3]). The life class of the tissues may be used to account for the effects of aging on some physiological processes ([1], [4]) or on the allocation of assimilates ([3], [7]). This modelling approach significantly increases the parametrization cost since dependence of the growth processes on tissue age must be described. Alternatively, [6] assumed that resource allocation depends on the amount of stored assimilates. Similarly to [2] and [9], we do not explicitly model plant developmental stages but tissue senescence is accounted for. The senescence of above and belowground tissues is modelled as a continuous process following an exponential function of elapsed time (eq.A27).

2.8. Nitrogen resorption

It has been evidenced that approximately half of the nitrogen content of leaves is resorbed during senescence and is used to support further plant growth (Bausenwein et al., 2001; Kazakou et al., 2007). Despite the importance of this process in plant nitrogen budget, most of the grassland models reviewed do not take it into account. Model [2] integrates nitrogen resorption indirectly by using a lower death rate for shoot nitrogen than for shoot carbon. Models [7] and [9] explicitly account for nitrogen resorption through a nitrogen remobilization rate. In these models, it is assumed that nutrient resorption occurs for both shoot and root despite the lack of empirical support for root nitrogen resorption (Nambiar, 1987; Aerts, 1990). In Nemossos, we account for nitrogen resorption from senescing shoot tissues by allocating a fixed part of their nitrogen to newly produced biomass (eq.A29). For

parsimony, we assumed that it was a species-specific constant (but see e.g., Huang et al. 2008).

2.9. Storage of assimilates

A part of the nutrients and carbohydrates acquired by a plant may be stored. These reserves are mobilized when plant growth demand is large and resource availability is low, such as in early spring. They can also enable a rapid recovery after dramatic loss of leaves or roots due to fire, herbivores or other disturbances (Chapin et al., 1990, Volenec et al., 1996). Finally, these reserves may be used to rapidly shift from a vegetative to a reproductive phase, even when resource availability is low (Below et al., 1981; Chapin et al., 1990). Storage is often ignored in grassland models. Notable exceptions include [6] that assumes that perennials invest all the extracted resources to storage until reaching an empirical threshold; and [9] which assumes a constant storage rate. In Nemossos, as in most of the models reviewed ([1], [2], [3], [4], [5], [7]), storage is not accounted for and assimilates are partitioned between above and belowground plant parts. Still, it is worth noting that regrowth of aerial tissues after a disturbance event is already indirectly facilitated in Nemossos, because of the functional equilibrium hypothesis used to model allocation: after a disturbance event, all the newly fixed carbon will be allocated to aerial tissues, thereby stimulating aerial growth until the functional equilibrium is reached.

2.10. Resource dynamics

Light environment. As plants are growing, the shoot cover increases and upper layers of the canopy intercept a part of the incoming PAR. The total amount of PAR received by an individual is estimated by integrating the Beer's law on shoot height (eq.A30-32). When two or several shoot cylinders are intersecting, the light extinction increases according to the

height of the individuals and to their cover assessed through the leaf area index, LAI (eq.A.33 and A.34). To determine if cylinders are intersecting and the area of this intersection, space is discretized in the form of voxels (Fig.A.2).

Nitrogen cycle. The model developed by Johnsson *et al.* (1987) was used to simulate nitrogen cycle in a two dimensional layered soil. This model includes the major processes that determine inputs, transformation and outputs of nitrogen in the soil (Fig. A.3). The soil is divided in two principal organic matter pools: a fast cycling pool (litter), and a slow-cycling pool (humus). The humus is divided in layers of equal size, the number of layers being set by the user. In the following use of Nemossos, we used 2 such layers. At each time step, the nitrogen transformations and movements are simulated in each layer. Nitrate is considered to be wholly in solution and move from one layer to another and from soil to the rooting zone depending on water flow rates. Ammonium is assumed immobile.

Water cycle. The basic processes of precipitation, evaporation, drainage and capillary rise are modelled. Drainage and capillary rise from one layer to the other depend on the soil hydraulic conductivity and on the difference in soil water content between the two layers (Philip, 1960). The water flow is always orientated from the layer of smallest water content to the layer of higher water content (eq.A41). Horizontal movements of water from the soil to the rooting zone induced by the water depletion are also modelled (eq.A42), which enables to compute mass flows. The evaporation rate is computed using the Penman-Monteith equation (eq.A35) and only occurs for the first soil layer.

3. SIMULATION EXPERIMENTS

In this section, we detail the design of simulation experiments used to assess the behavior of Nemossos. First, we assessed whether Nemossos captures the effects of abiotic factors and intra-specific competition on plant growth. We then assessed whether the relative efficiency of eight distinct plant strategies along the acquisition-conservation continuum (Wright et al. 2004) was depending on environmental conditions. Soil properties remained constant across these numerical experiments (Tab. A10-18).

3.1. Effects of abiotic factors on plant growth

We considered an average grass virtual species with average trait values similar to that found in the literature (Tab. 1). The vegetative growth of twenty seedlings of this virtual species was simulated for a growing season of 180 days in a plot of 20x20 cm^2 with soil depth of 50cm. PAR values remained constant during the 14h photoperiod and equaled 750 $\mu mol.m^{-2}.s^{-1}$, while it was null during the night. The atmospheric humidity remained constant throughout the growing season and equaled 65%. The effects of seasonal precipitations *SPPT* (E1), total soil nitrogen concentration in the beginning of the season (E2) and atmospheric temperature (E3) on the seedling growth were investigated by varying the corresponding environmental variables. Daily precipitation amount were drawn from truncated to zero normal distributions with a variance equal to 25 and a mean varying between 1 and 4.5 $mm.d^{-1}$ with a step of 0.5 $mm.d^{-1}$. These values are in accordance with the observations made in the Cedar Creek Ecosystem Science Reserve (experiment 080, XX citation) and yielded seasonal precipitation amounts between 400 and 950 mm. In order to account for the impact of the precipitation distribution across the season on plant growth (Swemmer et al., 2007), three replicates were made for each precipitation level The soil nitrogen levels were varied between 0.02, and 0.24 $mg.cm^{-3}$ with a step of 0.01 $mg.cm^{-3}$. This corresponds to the range observed in the long term

nitrogen deposition experiment in the Cedar Creek Ecosystem Science Reserve (experiment 001, XX citation). Finally, the daily atmospheric temperature was assumed to remain constant during the season and was varied between 7.5 and 25°C with a step of 2.5°C. When not varied, the daily precipitation amount was drawn from a truncated to zero normal distribution with variance equal to 25 and mean of 3.5 $mm.d^{-1}$, the soil nitrogen concentration at the beginning of the growing season was 0.15 $mg.cm^{-3}$ ensuring that the individuals were not limited by nitrogen and the atmospheric temperature was equal to 16°C, which was close to the average daily temperature reported for the Cedar Creek Ecosystem Science Reserve. The effects of these abiotic factors on plant growth was assessed through the aboveground net primary production in the plot (ANPP in $g.m^{-2}$). The form of the relationships between abiotic factors and plant performance predicted by the model was compared to empirical observations drawn from the literature. Moreover, the accuracy of the model was tested on a more quantitative basis by comparing the model predictions to empirical observations from the literature. For (E1), the model predictions were compared with the results of the experiments conducted by Knapp et al. (2006) in which the relationship between ANPP and seasonal precipitation was investigated in the Konza Prairie Biological Station. For (E2), the model predictions were compared with the results of the meta-analysis performed by Xia & Wan (2008), which explored the general response patterns of terrestrial plant species to nitrogen additions. For (E3), the model predictions were compared to the survey of Smit et al. (2008), who reported and analyzed the spatial distribution of grassland productivity in Europe in relation to some abiotic factors, including atmospheric temperature.

3.2. Effects of intra-specific competition on plant growth

After an initial period of growth with no mortality, plant populations of large density enter a phase of self-thinning, that is a density-dependent mortality due to resource competition. The

self-thinning rule (Yoda et al., 1963) describes the relationship between the average biomass of individual plants and the density of surviving seedlings. This relationship might take the form:

$$\overline{B} = K \cdot N^{\gamma} \quad \text{(eq.1)}$$

where $\overline{B}$ is average individual biomass (in grams), N is plant density (in individuals per square meter), γ = -3/2, and K is a constant.

In this simulation experiment, we aim at testing the ability of the Nemossos model to reproduce this empirical self-thinning law. The vegetative growth of the virtual species used in the previous section was simulated during 180 days for 50 seedlings in a plot of 10x10 cm^2 with soil depth of 50cm in the following conditions: 14h day duration, temperature of 16°C, PAR of 750 $\mu mol.m^{-2}.s^{-1}$, and atmospheric relative humidity of 65%. The soil water content was held constant at field capacity and the soil nitrogen concentration at the beginning of the growth was equal to 0.75 $mg.cm^{-3}$. The conditions during the 10h night were the same except for PAR which was null. We investigated the form of the relationship between the average individual biomass and the seedling density in the plot and compared the value of the exponent γ to the theoretical value of - 3/2 proposed by Yoda et al. (1963).

3.3. Context-dependent optimal plant strategies

In this numerical experiment, we generated eight realistic virtual grass species with strategies ranging from high resource acquisition to high resource conservation (Tab. 4). The traits values of these eight virtual species were determined as follows: shoot lifespan was varied between 60 and 130 days, and the 6 other trait values were computed using the interspecific linear regressions of Reich et al. (2003b) and Maire et al. (2009). We compared the efficiency of these strategies in variable environmental conditions to assess whether a single strategy

was always optimal or whether the optimal strategy depended on environmental conditions.. We considered a plot of 20x20 cm^2 with soil depth of 50cm containing five seedlings of each species. The position of the seedlings were randomly drawn in a grid with cell size equal to 2.5mm. The temporal dynamics of this virtual community was simulated for a growing season of 180 days. In order to account for the impact of species spatial position in the plot on the community dynamics, two replicates were simulated for each environmental condition. The length of the photoperiod was 14h with PAR values equal to 750 $\mu mol.m^{-2}.s^{-1}$ while it was null at night. The atmospheric temperature was held constant at 16°C and the relative humidity equaled 65%. The seasonal precipitation amount and the soil nitrogen content were varied independently. The daily precipitation amounts were drawn from a truncated to zero normal distribution with a variance equal to 25 and a mean varying between 1 and 4 $mm.d^{-1}$ with a step of 0.5 $mm.d^{-1}$. The soil nitrogen levels were varied between 0.01, and 0.15 $mg.cm^{-3}$ with a step of 0.02 $mg.cm^{-3}$. When not varied, daily precipitation amounts were drawn from a truncated to zero normal distribution with a variance equal to 25 and a mean of 3.5 $mm.d^{-1}$, while the nitrogen inorganic content was equal to 0.15 $mg.cm^{-3}$. For each simulation, we computed the community weighted mean shoot lifespan *CWM*, computed as:

$$CWM = \sum_{i=1}^{N} p_i \cdot SL_i \qquad \text{(eq.2)}$$

where N is the number of species in the community, p_i is the relative abundance of species i and SL_i is the shoot lifespan of species i. The shoot lifespan was selected because it is a good proxy for plant strategies with conservative species having high shoot lifespan while exploitative species tend to have low shoot lifespan.

4. RESULTS

4.1. Effects of abiotic factors on plant growth

Water. Nemossos predicted that the relationship between seasonal precipitations and ANPP is accurately described by the following linear model: $ANPP = 267 + 0.49 \cdot SPPT$ (R^2=0.73, Fig. 1.A) where *SPPT* is seasonal precipitation in millimeters and 0.49 represents the average water-use efficiency of the community ($g.m^{-2}.mm^{-1}$). This value is in close agreement with that of 0.51 reported by Knapp et al. (2006) for the Konza Prairie Biological Station. Moreover, the residual variance of this relationship was found to be relatively large in the virtual experiment (Fig. 1A). This residual variance was due to the varying intra-seasonal precipitation patterns across the three simulation replicates. This result is in accordance with the empirical study of Swemmer et al. (2007) who evidenced the importance of precipitation timing on aboveground productivity, beyond the total seasonal precipitation amount.

Soil nitrogen. The asymptotic form of the relationship between soil nitrogen content and ANPP predicted by the model is in accordance with the empirical observations of Tilman & Wedin (1991) (Fig. 1.B). The increase of biomass production induced by nitrogen addition strongly depends on the initial soil N concentration. For instance, the biomass response to a nitrogen addition of $15g.m^{-2}$ ranges from 4.5% for large initial soil N concentration to 537 % for low initial soil N concentration. The average biomass response to this nitrogen addition across initial soil N levels is equal to 130%., which is of the same order of magnitude as the result of the meta-analysis of N addition studies conducted by Xia & Wan (2008), where ANPP increased by 54% under similar N fertilization.

Temperature. Nemossos predicted that the relationship between ANPP and the mean daily temperature is well described by a bell-shaped curve (Fig. 1.C), which is in accordance with

the empirical observations of Smit et al. (2008). Moreover, when the daily temperature is smaller than 10°C, the ANPP is negligible, which is consistent with the definition of the growing season proposed by Smit et al. (2008). As the effects of atmospheric temperature and precipitation on ANPP strongly interact through evapotranspiration, no further quantitative comparison can be made with the result of the European scale study of Smit et al. (2008).

4.2. Self-thinning

The average individual shoot mass of the virtual species increased as the seedling density in the plot decreased due to density-dependent mortality following a power law ($R^2 = 0.95$, Fig. 2). The exponent γ of the self-thinning equation (eq.1) computed from simulated data equals -1.46, which is in close agreement with the theoretical value of -3/2 proposed by Yoda et al. (1963).

4.3. Context-dependent optimal plant strategies

The community weighted mean shoot lifespan was significantly negatively correlated with both the soil nitrogen content ($R^2 = 0.84$, Fig. 3.A) and the seasonal precipitation amount ($R^2 = 0.95$,Fig. 3.B). This suggests that the increase in soil resource availability led to a change in the optimal strategy from conservative to exploitative strategy, which is in accordance with multiple empirical studies (Diaz et al., 1997; Reich et al., 2003a; Maire et al., 2015). The relative position of individuals in the plot slightly impacts the species proportion at the end of the simulation, but it does not modify the form of the relationship between *CWM* and soil resource levels.

5. DISCUSSION

We have developed an individual-based model of vegetative growth for grassland species which enables to explicitly link the fundamental physiological processes driving plant development to intrinsic and extrinsic constrains. All these processes interact in a mechanistic way to shape the plant response. Submodels describing plant physiological processes have been selected according to their ability to reproduce empirically observed behaviors, while limiting their parameterization cost (Tab.3). This approach based on parsimony ensures that the model can be entirely parameterized from commonly measured functional traits. To account for the effects of soil composition on plant performance, a soil submodel which integrates nitrogen and water dynamics has been developed. Finally, the model Nemossos can be easily linked to a meteorological model to integrate the effects of atmospheric constrains.

When parameterizing Nemossos using average functional trait values found in the literature for grassland species (Tab.1), we evidenced its ability to reproduce well-known relationships between plant performance and abiotic constrains for monoculture stands (Fig. 1), as well as the effects of intra-specific competition giving rise to the self-thinning empirical law (Fig. 2). When assessing the consequences of interspecific competition in Nemossos, we also recovered empirically supported behaviors, with the progressive replacement of conservative species by exploitative ones along two gradients of resource availability, precipitation and soil nitrogen concentration (Fig. 3, Chapin et al., 1993; Reich et al., 2003a).

In the past decades, the relationship between plant functional traits and ecosystem function has been extensively investigated across broad environmental gradients (Diaz et al., 1998; Reich et al., 2003a). Less work has been devoted to the development of mechanistic models allowing to quantitatively relate functional traits to plant performance (Van Wijk, 2007;

Soussana et al., 2012; Enquist et al, 2015). Besides, the diffusion and transferability of such mechanistic models has been often limited by their inherent complexity (Evans et al. 2013, Mouquet et al. 2015). We therefore paid particular attention to design a model of minimal complexity, so as to maximize its transferability.

Nemossos opens numerous exciting perspectives in plant functional ecology research. By providing a both parsimonious and realistic simulation platform, Nemossos may be used to make testable predictions on a plant performance in given environmental conditions based on its measured functional traits (Lavorel and Garnier 2002). It could be used to design grassland species mixtures in silico rather than in natura (e.g., Prieto et al. 2015) or to assess the community-wide consequences of particular physiological processes (Bazzaz 1996). Nemossos also brings novel perspectives for more theoretically-oriented researches, by providing a realistic simulation platform to assess the robustness of theoretical predictions on community assembly and dynamics (e.g., Chesson 2000).

Further improvements of Nemossos might also be the focus of future studies. The most important simplifying assumption within our model is the absence of reproductive stage in plant phenology. Since vegetative reproduction largely outweighs seed reproduction in most grasslands (e.g., Benson and Hartnett 2006), this simplification is amply justified. Still, the inclusion of seed reproduction in Nemossos would enable to perform complementary investigations mobilizing the role of seed banks in vegetation dynamics, particularly following disturbances (Bossuyt and Honnay 2008). Additional potential lines of improvement concern the inclusion of reserves and of sink-driven formalizations of plant growth (Körner 2015). These improvements may further refine the realism of Nemossos,

provided that they are performed with the same care of parsimony that has driven our model building strategy.

AKNOWLEDGEMENTS

T.L was funded by the Institut national de Recherche en Sciences et Technologie pour l'Environnement et l'Agriculture (IRSTEA) and the Regional Council of Auvergne.

REFERENCES

Ackerly, D.D. 2003. Community assembly, niche conservatism, and adaptative evolution in changing environments. *Int. J. Plant Sci.* 164(S3): S165-S184.

Aerts, R. 1990. Nutrient use efficiency in evergreen and deciduous species from heathlands. *Oecologia* 84(3): 391-397.

Baldocchi, D. 1994. An analytical solution for coupled leaf photosynthesis and stomatal conductance models. *Tree Physiol.* 14: 1069-1079.

Bausenwein, U., Millard, P., & Raven, J.A. 2001. Remobilized old−leaf nitrogen predominates for spring growth in two temperate grasses. *New Phytol*. 152(2): 283-290.

Bazzaz, F. A. 1996. *Plants in changing environments: linking physiological, population, and community ecology*. Cambridge University Press.

Below, F.E., Christensen, L.E., Reed, A.J., & Hageman, R.H. 1981. Availability of reduced N and carbohydrates for ear development of maize. *Plant Physiol.* 68(5): 1186-1190.

Benson, E. J., & Hartnett, D. C. 2006. The role of seed and vegetative reproduction in plant recruitment and demography in tallgrass prairie. *Plant Ecol.* 187(2): 163-178.

Berry, J., & Björkman, O. 1980. Photosynthetic response and adaptation to temperature in higher plants. *Ann. Rev. Plant Physiol.* 31: 491-543.

Bossuyt, B., & Honnay, O. 2008. Can the seed bank be used for ecological restoration? An overview of seed bank characteristics in European communities. *Journal of Vegetation Science* 19(6): 875-884.

Chapin III, F.S., Schulze, E.-D., & Mooney, H.A. 1990. The ecology and economics of storage in plants. *Ann. Rev. Ecol. Syst.* 21: 423-444.

Chesson, P. (2000). Mechanisms of maintenance of species diversity. *Annual review of Ecology and Systematics*, 343-366.

Cleveland, C.C., Townsend, A.R., Schimel, D.S. et al. 1999. Global patterns of terrestrial biological nitrogen (N2) fixation in natural ecosystems. Ecosystem and Conservation Science Faculty Publications. Paper 7.

Cornwell, W.K., Schwilk, D.W., & Ackerly D.D. 2006. A trait-based test for habitat filtering: convex Hull volume. *Ecology* 87(6): 1465-1471.

Diaz, S., Cabido, M., & Casanoves, F. 1998. Plant functional traits and environmental filters at a regional scale. *J. Veg. Sci.* 9(1): 113-122.

Enquist, B.J., Norberg, J., Bonser, S.P., et al. 2015. Scaling from traits to ecosystems: developing a general trait driver theory via integrating trait-based and metabolic scaling theories. *Adv. Ecol. Res.*

Evans, G.C., & Hughes, A.P. 1961. Plant growth and the aerial environment. *New Phytol.* 60(2): 150-180.

Evans, M. R., Grimm, V., Johst, K., Knuuttila, T., de Langhe, R., Lessells, C. M., ... & Wilkinson, D. J. 2013. Do simple models lead to generality in ecology?. *TREE*, 28(10): 578-583.

Gaudet, C.L., & Keddy, P.A.1988. A comparative approach to predicting competitive ability from plant traits. *Nature* 334: 242-243.

Gedroc , J.J., McConnaughay, K.D.M., & Coleman, J.S. 1996. Plasticity in root/shoot partitioning: optimal, ontogenetic or both? *Fun. Ecol.* 10 (1): 44-50.

Herben, T., & Wildova, R. 2012. Community-level effects of plant traits in a grassland community examined by multispecies model of clonal plant growth. *Ecol. Mod.* 234: 60-69.

Huang, J.Y., Zhu, X.G., Yuan, Z.Y., Song, S.H., Li, X., & Li, L.H. 2008. Changes in nitrogen resorption traits of six temperate grassland species along a multi-level N addition gradient. *Plant and Soil* 306(1-2): 149-158.

Jabot, F. 2010. A stochastic dispersal-limited, trait-based model of community dynamics. *J. Theor. Biol.* 262(4): 650-661.

Johnson, I.R., & Thornley, J.H.M. 1985. Dynamic model of the response of a vegetative grass crop to light, temperature and nitrogen. *Plant, Cell Environ.* 8(7): 485-499.

Johnsson, H., Bergstrom, L., Jansson, P.E., & Paustian, K. 1987. Simulated nitrogen dynamics and losses in a layered agricultural soil. *Agric., Ecosyst. Envir.* 18(4): 333-356.

Kazakou, E., Garnier, E., Navas, M.L., Roumet, C., Collin, C., & Laurent, G. 2007. Components of nutrient residence time and the leaf economics spectrum in species from Mediterranean old‐fields differing in successional status. *Fun.l Ecol.* 21(2): 235-245.

Kraft, N.J.B., Valencia, R., & Ackerly, D.D. 2008. Functional traits and niche-based tree community assembly in an Amazonian forest. *Science* 332(5901): 580-582.

Körner, C. 2015. Paradigm shift in plant growth control. *Curr. Opin. Plant Biol*. 25: 107-114.

Lambers, H., Chapin III, F.S., & Pons, T.L. 2008. *Plant water relation*. In: Plant physiological ecology, 2nd edition. Springer-Verlag, New York, pp 164.

Lavorel, S., & Garnier, E. 2002. Predicting changes in community composition and ecosystem functioning from plant traits: revisiting the holy grail. *Fun. Ecol.* 16: 545-556.

Lohier, T., Jabot, F., Meziane, D., Shipley, B., Reich, P.B., & Deffuant, G. 2014. Explaining ontogenetic shifts in root-shoot scaling with transient dynamics. *Anna. Bot.* 114(3): 513-524.

Maire, V., Gross, N., da Silveira Pontes, L., Picon‐Cochard, C., & Soussana, J.F. 2009. Trade−off between root nitrogen acquisition and shoot nitrogen utilization across 13 co−occurring pasture grass species. *Fun. Ecol.* 23(4): 668-679.

Maire, V., Wright, I.J., Prentice, I.C., Batjes, N.H., Bhaskar, R., Bodegom, P.M., ... & Reich, P.B. 2015. Global effects of soil and climate on leaf photosynthetic traits and rates. *Glob. Ecol. Biogeo.* 24(6), 706-717.

Marcks, C.O., & Lechowicz, M.J. 2006. Alternative designs and the evolution of functional diversity. *Am. Nat.* 167 (1): 55-66.

McCree, K.J. 1974. Equations for the rate of dark respiration of white clover and grain sorghum, as functions of dry weight, photosynthetic rate, and temperature. *Crop Sci.* 14(4): 509-514.

McGill, B.J., Enquist, B.J., Weiher, E., & Westoby, M. 2006. Rebuilding community ecology from functional traits. *Trends Ecol. Evol.* 21(4): 178-185.

Meziane, D., & Shipley, B. 1999. Interacting components of interspecific relative growth rate: constancy and change under differing conditions of light and nutrient supply. *Fun. Ecol.* 13(5): 611-622.

Mouquet, N., Lagadeuc, Y., Devictor, V., Doyen, L., Duputié, A., Eveillard, D., ... & Jabot, F. 2015. Predictive ecology in a changing world. *J. Appl. Ecol.* 52(5): 1293-1310..

Nambiar, I.K.S. 1987. Do nutrients retranslocate from fine roots? *Can. J. For. Res.* 17: 913-918.

Philip, J.R. 1960. Absolute thermodynamic functions in soil-water studies. *Soil Science*, 89(2): 111.

Pons, T.L. 1977. An ecophysiological study in the field layer of ash coppice. II Experiments with Geum urbanum and Cirsium palustre in different light intensities. *Acta Bot. Neerl.*, 26(1): 29-42.

Pons, T.L., Van der Werf, A., & Lambers, H. 1994. *Photosynthetic nitrogen use efficiency of inherently slow and fast growing species: possible explanation for observed differences*. In: A whole-plant perspective of carbon nitrogen interactions, J. Roy and E. Garnier (eds.). SPB Academic Publishing, The Hague, pp 61-67.

Prieto, I., Violle, C., Barre, P., Durand, J. L., Ghesquiere, M., & Litrico, I. (2015). Complementary effects of species and genetic diversity on productivity and stability of sown grasslands. *Nature Plants*, *1*(4).

Reich, P.B., Walters, M.B., & Ellsworth, D.S. 1997. From tropics to tundra: global convergence in plant functioning. *Ecology* 94: 13730-13734.

Reich, P.B., Wright, I.J., Cavender-Bares, Craine, J.M., Oleksyn, J., Westoby, M., & Walters, M.B. 2003a. The evolution of plant functional variation: traits, spectra and strategies. *Int. J. Plant Sci.* 164 (S3): S143-S164.

Reich, P.B., Buschena, C., Tjoelker, M.G., Wrage, K., Knops, J., Tilman, D., & Machado, J. L. 2003b. Variation in growth rate and ecophysiology among 34 grassland and savanna species under contrasting N supply: a test of functional group differences. *New Phyto.*, 157(3): 617-631.

Ryan, M. G. 1991. Effects of climate change on plant respiration. *Ecol. App.*, 1(2): 157-167.

Soussana J.-F., Maire, V., Gross, N. et al. 2012. Gemini: a grassland model simulating the role of plant traits for community dynamics and ecosystem functioning. Parameterization and evaluation. *Ecol. Mod.* 231: 134-145.

Swemmer, A.M., Knapp, A.K., & Snyman, H.A. 2007. Intra−seasonal precipitation patterns and above−ground productivity in three perennial grasslands. *J. Ecol.* 95(4), 780-788.

Tilman, D., & Wedin, D. 1991. Plant traits and resource reduction for five grasses growing on a nitrogen gradient. *Ecology*, 685-700.

Van de Werf, A., Welschen, R., & Lambers, H. 1992. *Respiratory losses increase with decreasing inherent growth rate of a species and with decreasing nitrate supply: a search for explanations for these observations*. In: Molecular, biochemical and physiological aspects of plant respiration, H. Lambers and L.H.W Van der Plas (eds.). SPB Academic Publishing, The Hague, pp. 483-492.

Volenec, J.J., Ourry, A., & Joern, B.C. 1996. A role for nitrogen reserves in forage regrowth and stress tolerance. *Physiologia Plantarum* 97(1): 185-193.

Warren, J., & Topping, C. 2004. A trait specific model of competition in a spatially structured plant community. *Ecol. Mod.* 180: 477-485.

White, J. 1980. *Demographic factors in populations of plants*. In: Demography and evolution in plant populations. O.T. Solbrig (ed.). University of California Press, Berkeley, California, USA, pp 21 - 48.

Wright, I.J., Reich, P.B., Westoby, M., et al. 2004. The worldwide leaf economics spectrum. *Nature* 428: 821-827.

Yamori, W., Noguchi, K., & Terashima, I. 2005. Temperature acclimation of photosynthesis in spinach leaves: analyses of photosynthetic components and temperature dependencies of photosynthetic partial reactions. *Plant Cell Envir.* 28, 536-547.

Yoda, K., Kira, T., Ogawa, H. & Hozumi, K. 1963. Self-thinning in overcrowded pure stands under cultivated and natural conditions. *Journal of Biology, Osaka City University*, 14: 107-129.

TABLES

Tab.1. Plant functional traits used in Nemossos with the corresponding model equations (see Appendix A), mean values reported in the literature and associated references.

Symbols	Meaning	Equation	Mean values	References
	Plant structural traits			
$B_{r,0}$	Initial root biomass	-	0.02 g	Shipley & Meziane (2002)
SRR_0	Initial shoot-root ratio	-	2.5	Shipley & Meziane (2002)
ρ_r, ρ_s	Root and shoot density	A.1	0.15; 0.40 $g.cm^{-3}$	Craine et al. (2002)
a_r, b_r	Allometric coefficients for rooting zone volume	A.2	4; 1	Fox et al. (1984)
a_s, b_s	Allometric coefficients for shoot volume	A.2	10; 1	Andariese & Covington (1986)
	Aboveground plant traits			
A_{max}	Gross CO2 assimilation rate in optimal conditions	A.6	13.5 $\mu mol.m^{-2}.s^{-1}$	Reich et al. (2003)
g_{low}	Conductance threshold below which the ratio $C_i(t)/C_a(t)$ decreases	A.11	0.010 mol. $m^{-2}.s^{-1}$	Baldocchi (1994)
k	Light extinction coefficient	A.30	0.5	Anten et al. (1998)
LNC_{max}	LNC inducing optimal photosynthesis	A.6	3.85 %	Reich et al. (2003)
LNC_{min}	LNC below which photosynthetic activity stops	A.6	2.25 %	Sage & Pearcy (1987)
$R_{d,r}$	Root maintenance respiration rate	A.12	36 $nmol.g^{-1}.s^{-1}$	Reich et al. (2003)
$R_{d,sh}$	Shoot maintenance respiration rate	A.12	34.5 $nmol.g^{-1}.s^{-1}$	Reich et al. (2003)
SLA	Specific leaf area	A.5	320 $cm^2.g^{-1}$	Reich et al. (2003)
SLL	Shoot lifespan	A.27	60 d	Ryser & Urbas (2000)
T_{min}	Temperature threshold below which photosynthesis efficiency is null	A.8	0 °C	-
T_{opt}	Temperature threshold above which photosynthesis efficiency is maximal	A.8	20 °C	-
Y	Growth efficiency	A.12	0.8	Johnson (2008)
α	Photosynthetic efficiency	A.7	0.05 $\mu mol.\mu mol^{-1}$	Ehleringer & Pearcy (1983)
β	Curvature parameter for the light response curve	A.7	0.85	Jones (1988)
λ_N	Nitrogen fraction allocated to aboveground organs	A.24	0.6	Reich et al. (2003)
χ	Value of the ratio $C_i(t)/C_a(t)$ when $g_{CO2}(t)$ is larger than g_{low}	A.11	0.6	Baldocchi (1994)

χ_{up}	Value of the ratio $C_i(t)/C_a(t)$ when $g_{CO2}(t)$ equals g_{min}	A.11	2	Baldocchi (1994)
	Belowground plant traits			
K_N	Michaelis-Menten constant for nitrogen uptake	A.23	$3.5.10^{-4}$ mg.cm^{-3}	Leadley et al. (1997)
RLL	Root lifespan	A.27	650 d	Tjoelker et al. (2005)
NRE	Nitrogen resorption efficiency	A.29	60%	Huang et al. (2008)
$U_{N,max}$	Nitrogen uptake rate in optimal conditions	A.23	0.515 mg.g^{-1}.h^{-1}	Maire et al. (2009)
$U_{W,max}$	Water uptake rate in optimal conditions	A.19	6 cm^3.g^{-1}.d^{-1}	Hunt et al. (1991)

Tab.2. List of the 9 grassland models used for comparison.

Reference	Model	Literature
[1]	HP model	Thornley el al. (1989)
[2]	GEM	Hunt et al. (1991)
[3]	GRAZPLAN	Moore et al. (1997)
[4]	PaSim	Riedo et al. (1998)
[5]	Lingra	Schapendonck et al. (1998)
[6]	-	Schippers and Kropff (2001)
[7]	SGS	Johnson et al. (2008)
[8]	GRASSMIND	Taubert et al. (2012)
[9]	GEMINI	Soussana et al. (2012)

Tab.3. Parsimony of grassland models. For each submodel, the number of parameters of our model (Φ) is compared to the minimal (Φ_{min}) and maximal (Φ_{max}) number of parameters among the reviewed models, with the corresponding model references in parenthesis.

	Φ	**Φ_{min}**	**Φ_{max}**
Photosynthesis	10	5 ([5])	31 ([9])
Respiration	4	4 ([6], [7], [8])	14 ([9])
Transpiration	1	2 ([4], [5], [8])	5 ([3])
Nitrogen uptake	4	4 ([7], [8])	10 ([9])
Carbon allocation	2	2 ([8])	14 ([9])
Nitrogen allocation	1	1 ([1], [4])	9 ([2])
TOTAL	22	18 ([6])	69 ([9])

Tab.4. Plant functional traits of the eight virtual species used in the virtual experiment on interspecific competition. The values of the other plant traits are those of Table 2.

Sp	**SL** (day)	A_{max} ($\mu mol.m^{-2}.s^{-1}$)	SLA ($cm^2.g^{-1}$)	LNC_{max} ($mg.g^{-1}$)	$R_{d,r}$ ($nmol.g^{-1}.s^{-1}$)	$R_{d,sh}$ ($nmol.g^{-1}.s^{-1}$)	$U_{N,max}$ ($mg.g^{-1}.d^{-1}$)
1	60	15.3	286	348	30.9	31.8	0.61
2	70	14.4	267	325	28.3	30.8	0.456
3	80	13.7	248	307	25.8	29.6	0.36
4	90	13.0	229	291	23.1	28.5	0.29
5	100	12.5	210	278	20.6	27.4	0.23
6	110	12.1	191	267	18.0	26.3	0.20
7	120	11.7	172	257	15.4	25.1	0.17
8	130	11.3	153	248	12.8	24.0	0.14

FIGURES

Fig.1. Effects of seasonal precipitation amounts SPPT (panel A), soil nitrogen concentration (panel B) and daily atmospheric temperature (panel C) on aboveground net primary production (ANPP). The solid line in panel (A) corresponds to the regression line described by: ANPP = 227 - 0.49xSPPT, $R^2 = 0.73$.

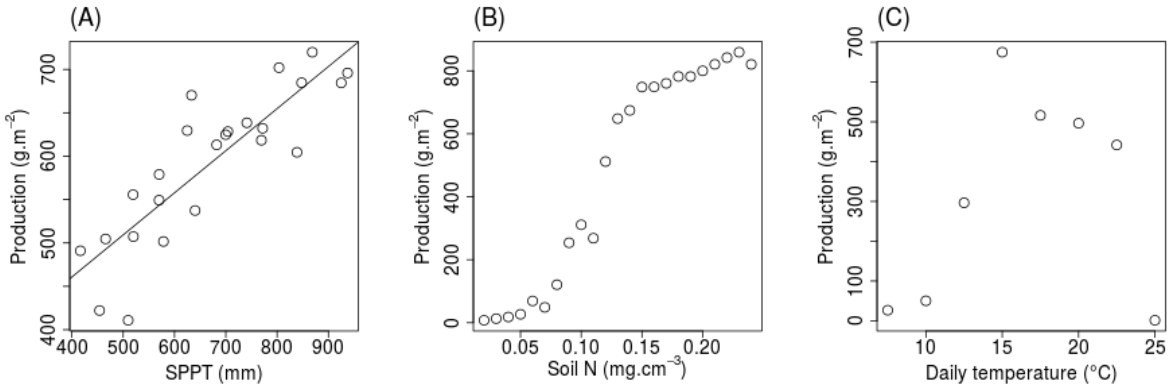

Fig.2. Self-thinning law. Relationship between seedling density and mean individual biomass of the surviving individuals. The dotted line corresponds to the regression line:

$\log(\overline{B}) = 12.52 - 1.46 \times \log(N)$, $R^2 = 0.95$.

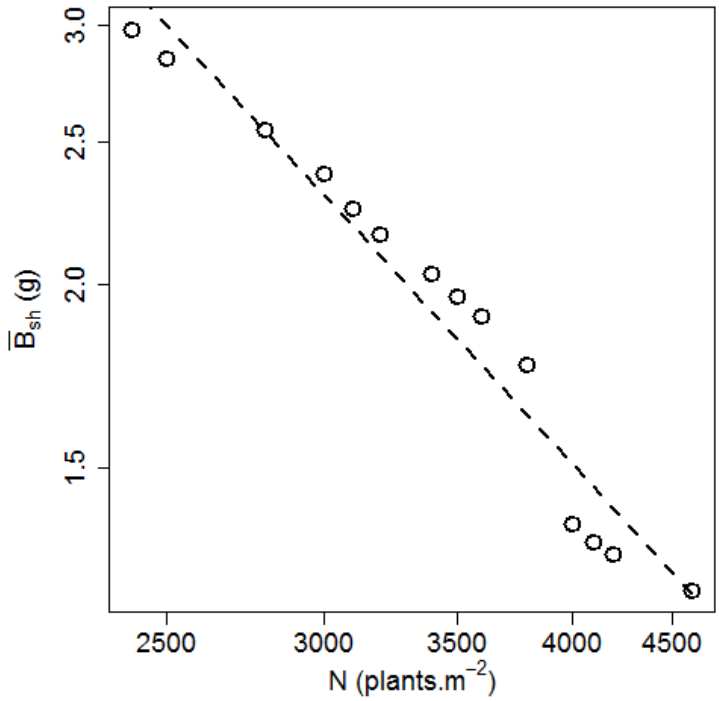

Fig.3. Relationship between the community weighted mean shoot lifespan (CWM) and (A) the soil nitrogen content, and (B) the seasonal precipitation amount (SPPT). The solid lines correspond to regression lines described by the following equations: $CWM = 92.06 - 85.2 \times N$, $R^2 = 0.84$ for soil N; $CWM = 97.1 - 0.021 \times SPPT$, $R^2 = 0.95$ for seasonal precipitation.

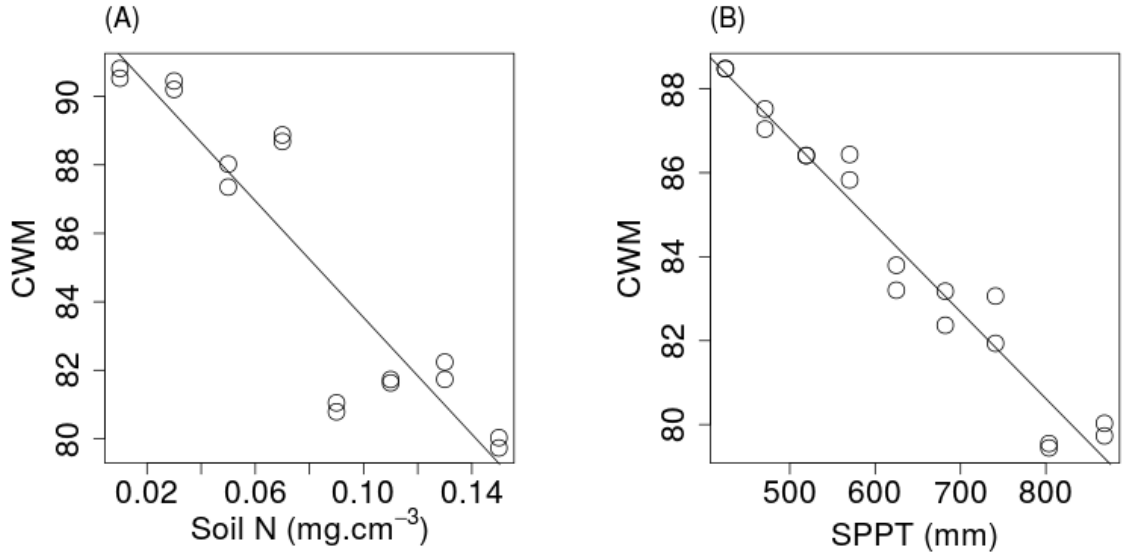

APPENDIX A. MODEL EQUATIONS

The model simulates individual plants growth and interactions in a patch on a daily basis. Plant growth depends on species functional traits, soil profile and atmospheric conditions. The model is then divided in three sections: *Atmosphere*, *Plant* and *Soil* (Fig. A.1).

The section *Atmosphere* includes the following atmospheric variables:

- photosynthetically active radiation (PAR) on top of the canopy;
- air temperature;
- wind speed;
- precipitation;
- volume fraction of carbon dioxide in air;
- vapor pressure deficit (VPD), which quantify the relative humidity in air.

and the routine allowing the computation of PAR received by plants shoot when self-shading and light competition are taken into account.

The section *Soil* includes soil water and nitrogen profile and soil characteristics (e.g. permanent wilting point, saturated nitrification rate). The model used these variables to compute:

- the evaporation from the soil;
- the horizontal and vertical water movements in the soil;
- the nitrogen cycling;
- the nitrogen movements with water.

The section *Plant* includes functional and architectural traits describing an individual plant so as its position in the patch. The *Plant* section access to *Atmosphere* and *Soil* variables to compute:

- the shoot photosynthetic rate;
- the shoot transpiration rate;
- the root water uptake;
- the root nitrogen uptake;
- the carbon allocation between above- and belowground plant parts;
- the senescence of above- and belowground plant parts.

A.1. Plant growth and development

A.1.1. Spatial growth

The position of an individual is described by its Cartesian coordinates in the patch. Both shoot and root are modelled by cylinders centered in the individuals coordinate (Johnson et al., 1988; Taubert *et al.*, 2012) and described by a height $h(t)$ and a radius $r(t)$ (Figure A.2). At each time step, the volume increment of a cylinder $\Delta V(t)$ is computed according to the plant biomass increment $\Delta B(t)$ and the species specific density ρ:

$$\Delta V(t) = \frac{\Delta B(t)}{\rho} \tag{A.1}$$

The height $h(t+1)$ and radius $r(t+1)$ are deduced from the cylinder volume at $t+1$ $V(t+1) = V(t) + \Delta V(t)$ using an allometric relationship between height and radius. We then obtained the following linear system:

$$\begin{cases} V(t) + \Delta V(t) &= \pi \cdot h(t+1) \cdot r(t+1)^2 \\ h(t+1) &= a \cdot r(t+1)^b \end{cases} \tag{A.2}$$

which may be easily solve by substitution leading to the following analytical expressions for height and radius in time $t+1$:

$$\begin{cases} r(t+1) &= \left(\frac{V(t)+\Delta V(t)}{a\cdot\pi}\right)^{\frac{1}{b+2}} \\ h(t+1) &= a\cdot\left(\frac{V(t)+\Delta V(t)}{a\cdot\pi}\right)^{\frac{b}{b+2}} \end{cases} \quad \text{(A.3)}$$

Initially the volume cylinders are computed from the initial plant biomass and the species specific density using equation (A.1) and the linear system (A.2). When biomass is lost by senescence the cylinder volumes are assumed to remain constant whereas the density decreases below the species specific density.

Figure A.1. Representation of a single individual plant using cylinders for above- and belowground plant parts.

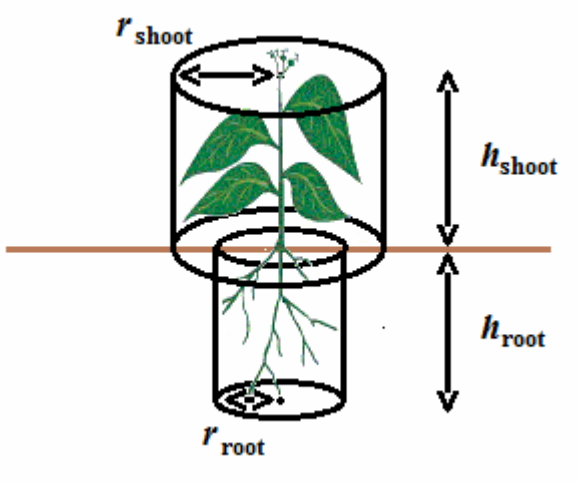

Table A.1. Parameters, input and output variables required for modelling the spatial growth of individual plants.

Parameters	Meaning	Units	Values
a_r	Allometric coefficient for root development	-	5
a_s	Allometric coefficient for shoot development	-	5
b_r	Allometric coefficient for root development	-	0.25
b_s	Allometric coefficient for shoot development	-	0.5
ρ_r	Specific root density	$g.cm^{-3}$	0.01

ρ_s	Specific shoot density	g. cm^{-3}	0.01
Input	**Meaning**	**Units**	**Values**
$B_r(t)$	Root biomass	g	-
$B_s(t)$	Shoot biomass	g	-
Output	**Meaning**	**Units**	**Values**
$h_r(t)$	Height of the cylinder surrounding root biomass	cm	-
$h_s(t)$	Height of the cylinder surrounding shoot biomass	cm	-
$r_r(t)$	Radius of the cylinder surrounding root biomass	cm	-
$r_s(t)$	Radius of the cylinder surrounding shoot biomass	cm	-

A.1.2. Growth rate

At each time step the biomass increment $\Delta B(t)$ is computed from the difference between the daily gross primary production $GPP(t)$ and growth respiration rate $R(t)$ in time t:

$$\Delta B(t) = GPP(t) - R(t) \cdot \Delta t \quad \text{(A.4)}$$

where $GPP(t)$ is computed from the gross CO_2 assimilation rate $A_g(t)$:

$$GPP(t) = b_{NPP} \cdot 10^{-6} \cdot A_g(t) \cdot B_s(t) \cdot SLA(t) \cdot \Delta t \quad \text{(A.5)}$$

where $SLA(t)$ is the specific leaf area and b_{NPP} is a constant approximating the amount of biomass produced from a given amount of fixed carbon. b_{NPP} is computed from the stochiometry of photosynthetic reactions: to synthesize one mole of glucose ($C_6H_{12}O_6$) weighting 180g, six moles of carbon dioxide (CO_2) are needed, hence $b_{NPP} = 180/6 = 30$ (Kikuzawa and Lechowicz, 2006).

Table A.2. Parameters, input and output variables required for the computation of the growth rate of individual plants.

Parameters	**Meaning**	**Units**	**Values**

b_{NPP}	Conversion factor from carbon assimilated during photosynthesis to biomass	g. g^{-1}	30
SLA	Specific leaf area	$m^2.g^{-1}$	0.01 - 0.05
Input	**Meaning**	**Units**	**Values**
$A_g(t)$	Photosynthetic rate	$\mu mol.m^{-2}.s^{-1}$	-
$B_s(t)$	Shoot biomass	g	-
R(t)	Respiration rate	$g.d^{-1}$	-
Output	**Meaning**	**Units**	**Values**
$\Delta B(t)$	Biomass increment	g	-

A.1.3. Gross CO_2 assimilation rate

The intrinsic ability of a species to synthesized carbohydrates from atmospheric CO_2 in optimal conditions may be described with the maximum photosynthetic efficiency A_{max}. Photosynthesis efficiency can be limited by both leaf nitrogen content *LNC* (Lambert et al.,1998), PAR received by shoots (Perchorowicz et al., 1981) and leaf temperature. The photosynthetic rate limitation due to leaf nitrogen content is modelled according to Anten et al. (1998). We assumed a linear decrease of the photosynthetic rate with the shoot nitrogen content $LNC(t)$ from A_{max} when the shoot nitrogen content equals LNC_{max} to zero when the shoot nitrogen content equals LNC_{min}:

$$A_N(t) = \frac{LNC(t) - LNC_{min}}{LNC_{max} - LNC_{min}} \cdot A_{max} \quad \text{(A.6)}$$

Once the maximal photosynthetic efficiency under the current nitrogen plant status $A_N(t)$ has been computed, we estimated the effects of PAR received by the leaves using a non-rectangular hyperbola (Johnson and Thornley, 1984):

$$A_{N,PAR}(t) = \frac{A_N(t) + \alpha \cdot I(t) - \sqrt{\left(A_N(t) + \alpha \cdot I(t)\right)^2 - 4 \cdot A_N(t) \cdot \alpha \cdot \beta \cdot I(t)}}{2 \cdot \beta} \quad \text{(A.7)}$$

where α is the quantum yield and β is a curvature factor.

We then integrate the effects of leaf temperature T on photosynthesis using an empirical response function f_T which increases linearly with the leaf temperature between T_{min} and T_{opt}, is null if T is smaller than T_{min} and equals 1 if T is higher than T_{opt}:

$$f_T(T) = \begin{cases} 0 & if \quad T < T_{min} \\ \dfrac{T - T_{min}}{T_{opt} - T_{min}} & if \quad T_{min} < T < T_{opt} \\ 1 & if \quad T > T_{opt} \end{cases} \tag{A.8}$$

The potential photosynthetic efficiency for given LNC, PAR and T, $A_{pot}(t)$ is then equals to:

$$A_{pot}(t) = A_{N,PAR}(t) \cdot f_T(T) \tag{A.9}$$

On the other hand the net CO_2 assimilation rate $A_n(t)$ is constrained by the stomatal conductance $g_{CO2}(t)$ which may limit the amount of CO_2 incoming the leaves. The Fick's law of diffusion gives:

$$A_n(t) = g_{CO2}(t) \cdot \left(C_a(t) - C_i(t)\right) \tag{A.10}$$

where $C_a(t)$ is the atmospheric CO_2 concentration and $C_i(t)$ is the leaf intercellular CO_2 concentration. Following Norman (1982) and Baldocchi (1994) we assumed that the ratio $C_i(t)/C_a(t)$ remains constant while stomatal conductance is higher than a threshold values g_{low}. When $g_{CO2}(t)$ becomes smaller than g_{low}, the ratio $C_i(t)/C_a(t)$ increases linearly until reaching a maximal values χ_{up} which depend on the species:

$$\begin{cases} \dfrac{C_i(t)}{C_a(t)} = \chi & if \quad g_{CO2}(t) > g_{low} \\ \dfrac{C_i(t)}{C_a(t)} = \dfrac{\chi - \chi_{up}}{g_{low}} \cdot g_{CO2}(t) + \chi_{up} & otherwise \end{cases} \tag{A.11}$$

The value χ is a species dependant parameter.

If the net CO_2 assimilation rate $A_n(t)$ allowed by the stomatal conductance $g_{CO2}(t)$ is higher than the net CO_2 assimilation rate computed from the potential photosynthetic efficiency $A_{pot}(t)$, the plant is assumed to close its stomata in order to reduce water loss induced by transpiration in such a way that $A_g(t) = A_{pot}(t)$. We then update the stomatal conductance value using (eq.A.8) and (eq.A.9).

Table A.3. Parameters, input and output variables required for computation of the gross CO_2 assimilation rate $A_g(t)$of individual plants.

Parameters	**Meaning**	**Units**	**Values**
A_{max}	Specific photosynthetic rate	$\mu mol.m^{-2}.s^{-1}$	10 - 50
g_{low}	Conductance threshold below which the ratio $C_i(t)/C_a(t)$ decreases	$mol.\ m^{-2}.s^{-1}$	
LNC_{max}	LNC for which photosynthesis is maximal	$g.\ g^{-1}$	0.01 - 0.05
LNC_{min}	LNC for which photosynthesis is null	$g.\ g^{-1}$	0.005
T_{min}	Temperature threshold below which photosynthesis efficiency is null	°C	0
T_{opt}	Temperature threshold above which photosynthesis efficiency is maximal	°C	25
α	Initial slope of the photosynthesis vs. light relationship	$\mu mol.mol^{-1}$	0.01 - 0.1
β	Convexity of the photosynthesis vs. light relationship	-	0.5 - 0.95
χ	Value of the ratio $C_i(t)/C_a(t)$ when $g_{CO2}(t)$ is higher than g_{low}	-	0.4-0.7
χ_{up}	Value of the ratio $C_i(t)/C_a(t)$ when $g_{CO2}(t)$ equals 0	-	1.1-1.5
Input	**Meaning**	**Units**	**Values**
$C_a(t)$	Atmospheric CO_2 concentration	$\mu mol.mol^{-1}$	200 - 1000
$C_i(t)$	Volume fraction of CO_2 in the leaf intercellular spaces	$\mu mol.mol^{-1}$	200 - 300
$g_{CO2}(t)$	Stomatal conductance for CO_2	$mol.\ m^{-2}.s^{-1}$	
$I(t)$	PAR received by shoot	$\mu mol.m^{-2}.s^{-1}$	0 - 1200
$LNC(t)$	Leaf nitrogen content	$g.\ g^{-1}$	0 - LNC_{max}
$R(t)$	Respiration rate	$\mu mol.m^{-2}.s^{-1}$	
		Units	**Values**

Output	Meaning		
$A_g(t)$	Potential photosynthetic rate	$\mu mol.m^{-2}.s^{-1}$	0 - A_{max}
$g_{CO2}(t)$	Stomatal conductance for CO_2	mol. $m^{-2}.s^{-1}$	

A.1.4. Respiration rate

The rate of respiration rate $R(t)$ may be decomposed into three major processes: maintenance of biomass, growth and ion transport. In our model respiratory costs induced by ion transport are implicitly integrated in the maintenance respiration rate and $R(t)$ is computed using the widely-used McCree-Thornley (1970) approach:

$$R(t) = \left(\frac{1-Y}{Y}\right) \cdot \Delta B(t) + \left(R_{d,sh} \cdot B_s(t) + R_{d,r} \cdot B_r(t)\right) \cdot \Delta t \qquad \text{(A.12)}$$

where the first term corresponds to the growth respiration rate, which is associated with the respiratory cost induced by carbohydrates synthesis during photosynthesis. The growth respiration rate increases linearly with the amount of biomass produced in day t, $\Delta B(t)$ according to the efficiency with which new tissues are synthesized Y. The second and third terms correspond to the maintenance respiration rates for shoot and root respectively, which accounts for the cost of repairing and maintaining biomass. It therefore depends on the shoot and root biomass $B_s(t)$ and $B_r(t)$ and on maintenance respiration coefficients $R_{d,s}$ and $R_{d,r}$. The maintenance process involves enzymatic reactions and is therefore temperature dependant. The increase of maintenance respiratory costs is modelled in the same way for root and shoot using a Q10 relation such that:

$$R_d = R_{d,20} \cdot Q_{10,m}^{\frac{1}{10}\cdot(T-20)} \qquad \text{(A.13)}$$

Table A.4. Parameters, input and output variables required for the computation of the respiration rate of individual plants.

Parameters	Meaning	Units	Values
$R_{d,r,20}$	Maintenance respiration coefficient for root at the reference temperature of 20°C	$nmol.g^{-1}.s^{-1}$	15 - 75
$R_{d,sh,20}$	Maintenance respiration coefficient for shoot at the reference temperature of 20°C	$nmol.g^{-1}.s^{-1}$	25 - 65
$Q_{10,m}$	Response of $k_{m,20}$ to a 10-degree change	-	1-3
Y	Growth efficiency	-	0.7-0.9
Input	**Meaning**	**Units**	**Values**
$B(t)$	Total plant biomass	g	-
T	Atmospheric temperture	°C	-
$\Delta B(t)$	Biomass produced in day t	g	-
Output	**Meaning**	**Units**	**Values**
$R(t)$	Respiration rate	$g.d^{-1}$	-

A.1.5. Transpiration rate and water uptake

The transpiration rate *TR* depends on the difference in water vapor concentration between leaf and air and is regulated by the stomata opening. The effects of stomata opening on *TR* may be quantified through the stomatal conductance for water $g_{H2O}(t)$ which can be computed from the stomatal conductance for CO_2, $g_{CO2}(t)$ using the following relationship:

$$g_{H2O}(t) = a \cdot g_{CO2}(t) \tag{A.14}$$

where a = 1.6 is the ratio between the diffusivities of water vapor and CO_2 in air. TR may then be described by Fickian diffusion (Farquhar and Sharkey, 1982):

$$TR = g_{H2O}(t) \cdot \left(w_i(t) - w_a(t)\right) \tag{A.15}$$

where $w_i(t)$ and $w_a(t)$ are the mole fraction of water vapor in shoot and in air respectively. According to Kramer and Boyer (1983), we assumed that the vapor pressure of water in the cell wall surfaces is that of pure water and we used the Antoine equation to determine the vapor pressure in the shoot e_i:

$$e_i = 0.133322 \cdot \exp\left(20.386 - \frac{5132}{(T + 273.3)}\right) \tag{A.16}$$

The vapor pressure in air is estimated from the relative humidity of air *RH* and from the saturation vapor pressure e_{as}:

$$e_a = \frac{RH}{e_{as}} \tag{A.17}$$

The difference in water vapor concentration between leaf and air is then computed by dividing the difference in water vapor pressure between leaf and air by the atmospheric pressure P_a:

$$w_i(t) - w_a(t) = \frac{e_i - e_a}{P_a} \tag{A.18}$$

When the plants are water stressed, stomatal conductance $g_{H2O}(t)$ is computed based on the assumption that the leaf is saturated with water vapor and that the stomata regulates water loss in order to balance transpiration and water uptake rates (Fiscus, 1983; Davies et al., 1994).

The rate at which roots are able to extract water from the soil $U_{w,pot}(t)$ depends on the maximal rate of water uptake $U_{w,max}$ and on the soil water content $\theta(t)$ according to the formulation of Feddes et al. (1988):

$$U_{w,pot}(t) = U_{w,\max} \cdot f_w(\theta(t)) \tag{A.19}$$

where $f_w(\theta(t))$ is an empirical response function describing the effects of $\theta(t)$ on root water uptake. When the soil water content is higher than θ_{an} (anaerobic point) or smaller than θ_{wp} (wilting point), the water uptake is null. Between θ_{sat} and θ_{an} (reduction point) the water uptake is maximal and between θ_{sat} and θ_{wp} increases from 0 to 1 (see figure A.3):

$$f_w(\theta(t)) = \begin{cases} 0 & if \quad \theta(t) < \theta_{wp} \quad or \quad \theta(t) > \theta_{sat} \\ \dfrac{\left((\theta(t) - \theta_{res})^{-1/\lambda} - (\theta_{wp}(t) - \theta_{res})^{-1/\lambda}\right)}{\left((\theta_{sat}(t) - \theta_{res})^{-1/\lambda} - (\theta_{wp}(t) - \theta_{res})^{-1/\lambda}\right)} & if \quad \theta_{wp} < \theta(t) < \theta_{fc} \\ 1 & if \quad \theta_{fc} < \theta(t) < \theta_{sat} \end{cases} \tag{A.20}$$

where the parameter λ is the pore-size distribution index of the soil (Brooks and Corey, 1974).

Plants were assumed to avoid water stress by reducing their stomatal conductance: if the potential water uptake rate $U_{w,pot}(t)$ is smaller than the transpiration rate TR, the effective water uptake rate $U_w(t)$ equals $U_{w,pot}(t)$ and the stomatal conductance $g_{H2O}(t)$ is updated in such a way that $U_{w,pot}(t)$ match TR:

$$\begin{cases} g_{H2O}(t) = \dfrac{U_{w,pot}(t)}{w_i(t) - w_a(t)} \\ U_w(t) = U_{w,pot}(t) \end{cases} \quad \text{(A.21)}$$

Conversely if $U_{w,pot}(t)$ is higher than TR, the plants are assumed to reduce their water uptake rate in such a way that the effective water uptake rate $U_w(t)$ equals the transpiration rate. The model does not account for water storage.

Table A.5. Parameters, input and output variables required for the computation of the transpiration rate of individual plants.

Parameters	**Meaning**	**Units**	**Values**
a	Ratio between the diffusivities of water vapor and CO_2 in air	-	1.6
$U_{w,max}$	Maximal root water uptake rate	$mol.g^{-1}.d^{-1}$	0.5-1.5
λ	Pore-size distribution index	-	0.378
θ_{fc}	Soil water content at field capacity	$cm^3.cm^{-3}$	0.25
θ_{res}	Residual soil water content	$cm^3.cm^{-3}$	0.05
θ_{sat}	Saturated soil water content	$cm^3.cm^{-3}$	0.30
θ_{wp}	Soil water content at permanent wilting point	kPa	1500
Input	**Meaning**	**Units**	**Values**
$g_{CO2}(t)$	Stomatal conductance for CO_2	$mol.\ m^{-2}.s^{-1}$	-
P_a	Atmospheric pressure	kPa	101.325

RH	Relative humidity of air	-	-
T	Atmospheric temperature	°C	-
$w_a(t)$	mole fraction of water vapor in air	$mol.mol^{-1}$	-
$w_i(t)$	Mole fraction of water vapor in shoot	$mol.mol^{-1}$	-
$\theta(t)$	Soil water content in the rooting zone	$cm^3.cm^{-3}$	-
Output	**Meaning**	**Units**	**Values**
$g_{H2O}(t)$	Stomatal conductance for H_2O	$mol.\ m^{-2}.s^{-1}$	-
TR(t)	Transpiration rate	$mol.m^{-2}.d^{-1}$	-
U_w	Effective root water uptake rate	$mol.g^{-1}.d^{-1}$	0 - $U_{w,max}$

A.1.6. Nitrogen uptake

The ability of plants to extract ionic nitrogen from soil is modelled through the maximal nitrogen uptake rate $U_{N,max}$. The main factor likely to impair this extraction rate is the shortage of ionic nitrogen in the vicinity of the roots. Moreover as plants are able to regulate their nitrogen uptake in order to match the whole plant demand and thus avoid nitrogen toxicity, we assumed that the effective nitrogen uptake rate $U_N(t)$ is the minimum between the potential uptake rate in given soil nitrogen conditions $U_{N,pot}(t)$ and the uptake rate needed to satisfy the plant demand $U_{N,dem}(t)$:

$$U_N(t) = \min\left(U_{N,pot}(t), U_{N,dem}(t)\right) \quad \text{(A.22)}$$

Following Engels et al. (2000), Hane's relationship (Michaelis-Menten transformed equation) was used to model the dependency of $U_{N,pot}(t)$ to the concentration in ionic nitrogen in the rooting zone $N_r(t)$:

$$U_{N,pot}(t) = \frac{U_{N,max} \cdot N_r(t)}{K_N + N_r(t)} \quad \text{(A.23)}$$

where K_m is the substrate affinity. As plant roots are able to uptake both ammonium (NH_4^+) and nitrate (NO_3^-), we use a global specific uptake rate and $N_r(t)$ is the concentration of both NH_4^+ and NO_3^- in the rooting zone.

We consider that plant demand corresponds to the amount of nitrogen required for the nitrogen content of new shoot biomass produced in Δt to be equal to LNC_{max}, assuming that all the newly produced biomass is allocated to shoot. $U_{N,dem}(t)$ is thus given by:

$$U_{N,dem}(t) = \frac{1}{B_r(t) \cdot \Delta t} \cdot \left(\frac{LNC_{max} \cdot \Delta B(t) - N_{res}(t)}{\lambda_N} \right) \quad \text{(A.24)}$$

where $N_r(t)$ is the nitrogen withdrawn via resorption during senescence and λ_N is the proportion of captured nitrogen allocated to aboveground plant parts, which is assumed constant.

Table A.6. Parameters, input and output variables required for computation of the nitrogen uptake rate of individual plants.

Parameters	**Meaning**	**Units**	**Values**
λ_N	Fraction of captured nitrogen allocated to shoot	%	0.5 - 0.8
K_m	Michaelis constant	mg. cm^{-3}	0.05
LNC_{max}	Leaf nitrogen content for which photosynthesis is maximal	g. g^{-1}	0.01 - 0.05
$U_{N,max}$	Specific nitrogen uptake rate	$mg.g^{-1}.h^{-1}$	0.1 - 1.0
Input	**Meaning**	**Units**	**Values**
$B_r(t)$	Root biomass	g	-
$\Delta B(t)$	Newly produced biomass	g	-
$N_r(t)$	Ionic nitrogen concentration in the rooting zone	mg. cm^{-3}	-
$N_{res}(t)$	Nitrogen withdrawn during senescence	mg	-
		Units	**Values**

Output	Meaning		
$U_N(t)$	Effective nitrogen uptake rate	mg	-

A.1.7. Allocation of assimilates

Carbon allocation. The general idea is to compute a carbon allocation coefficient $\lambda_C(t)$ which determines the amount of carbon allocated to above- and belowground plant parts $\Delta B_s(t)$ and $\Delta B_r(t)$ respectively so that:

$$\begin{cases} \Delta B_s(t) = & \lambda_C(t) \cdot \Delta B(t) \\ \Delta B_r(t) = & (1 - \lambda_C(t)) \cdot \Delta B(t) \end{cases} \quad \text{(A.25)}$$

The computation of $\lambda_C(t)$ is based on the hypothesis of functional equilibrium between photosynthesis and nitrogen uptake (Brouwer, 1963). We assumed that while the root are able to satisfy the nitrogen demand of the shoot, all the newly produced biomass is allocated to aboveground plant parts in order to maximize the relative growth rate of the plant. When nitrogen is limiting, carbon allocation to shoot decreases so that the nitrogen provided by the root is sufficient for the newly produced shoot biomass *LNC* to be maximal. The coefficient $\lambda_C(t)$ is thus obtained by equaling the nitrogen amount required by newly produced shoot and the amount of nitrogen extracted by the root, leading to the following expression for $\lambda_C(t)$:

$$\lambda_C(t) = \frac{(U_N(t) \cdot B_r(t) \cdot \Delta t + N_{res}(t)) \cdot \lambda_N}{\Delta B(t) \cdot LNC_{\max}} \quad \text{(A.26)}$$

This model ensures that $\lambda_C(t)$ is varying between 0 when the nitrogen supply is null and 1 when the nitrogen supply equals the demand of the newly produced shoot biomass. Moreover it implies that the leaf nitrogen content always equals $LNC_{\max}$. Following () we assumed that soil water availability do not affect the carbon allocation.

Nitrogen allocation. Following Dybzinski *et al*. (2011), it is assumed that a fixed fraction of assimilated nitrogen is allocated to the shoot: $\lambda_N(t) = \lambda_N$. This coefficient is used in the model to compute the LNC of newly produced shoot biomass from the amount of nitrogen extracted by the root (eq.A21 and A23).

Table A.7. Parameters, input and output variables required for the computation of the carbon allocation in individual plants.

Parameters	**Meaning**	**Units**	**Values**
LNC_{max}	Leaf nitrogen content for which photosynthesis is maximal	g. g^{-1}	0.01 - 0.05
λ_N	Fraction of captured nitrogen allocated to shoot	%	0.5 - 0.8
Input	**Meaning**	**Units**	**Values**
$B_r(t)$	Root biomass	g	-
$\Delta B(t)$	Newly produced biomass	g	-
$N_{res}(t)$	Nitrogen withdrawn during senescence	mg	-
$U_N(t)$	Effective nitrogen uptake rate	mg	-
Output	**Meaning**	**Units**	**Values**
$\lambda_C(t)$	Fraction of newly produced biomass allocated to shoot	%	0 - 1

A.1.8. Phenology

Plant development stages are not explicitly modelled but the shoot and root senescence is described with a continuous function of elapsed time. At each time step *t*, the amount of biomass produced in time *u*, $B(u)$ which has senesce during *t-u* is given by:

$$B_{sen}(u,t) = B(u).\exp(t-u-LL) \quad \text{(A.27)}$$

where LL is the lifespan of shoot or root. Consequently the remaining part of the biomass produced in time *u* at time *t+1*, $B(u,t+1)$ may be expressed according to $B(u,t)$:

$$B(u,t+1) = B(u,t) \cdot \left(\frac{1-\exp(t+1-u-LL)}{1-\exp(t-u-LL)} \right) \quad \text{(A.28)}$$

As the biomass produced in time *u* decreases due to senescence, the density in the cylinders surrounding the plant parts decreases whereas the cylinder volume does not change.

When shoot tissues are senescing, some portion of the constituting nitrogen is withdrawn and reused in newly produced tissues (Aerts, 1996). Here we assumed that the proportion of nitrogen withdrawn $N_{res}(t)$ via resorption is constant across time and environmental gradients. It only depends on the senescing tissues nitrogen content in time *t*, $LNC(t)$ and the nitrogen resorption efficiency of the species *NRE*:

$$N_{res}(t) = NRE \cdot LNC(t) \cdot \left(B_s(u,t) - B_s(u,t+1) \right) \quad \text{(A.29)}$$

The remaining fraction of nitrogen as well as the carbon contained in the senescing shoots are incorporated in the organic nitrogen and carbon pool of the litter respectively whereas all the nitrogen and carbon contained in the senescing roots are incorporated in organic nitrogen and carbon pools of the corresponding soil layer.

Table A.8. Parameters, input and output variables required for computation of root and shoot senescence and nitrogen resorption of individual plants.

Parameters	**Meaning**	**Units**	**Values**
NRE	Nitrogen resorption efficiency	%	0.1 - 0.5
RLL	Root life span	d	20 - 60
SLL	Shoot life span	d	20 - 60
Input	**Meaning**	**Units**	**Values**
$B_r(u,t)$	Remaining part of root biomass produced in time *u* at time *t*	g	-
$B_s(u,t)$	Remaining part of shoot biomass produced in	g	-

	time *u* at time *t*		
$LNC(t)$	Leaf nitrogen content	g. g^{-1}	0 - LNC_{max}
$RNC(t)$	Root nitrogen content	g. g^{-1}	-
Output	**Meaning**	**Units**	**Values**
$N_{res}(t)$	Nitrogen withdrawn via resorption	mg	-
$B_s(u,t+1)$	Remaining part of root biomass produced in time *u* at time *t+1*	g	-
$B_r(u,t+1)$	Remaining part of shoot biomass produced in time *u* at time *t+1*	g	-

A.2. Resources dynamics

A.2.1. Light

In order to take into account individuals competition for light, the space is divided in pixels of 0.01 cm^2. A pixel associated with a height *h* form a column. For each pixel, the mean PAR received by shoot included in the column of height *h* is computed using Beer's law (Monsi and Saeki, 1953):

$$I(h) = I_0 \cdot e^{-k \cdot LAI(h)} \quad \text{(A.30)}$$

where $I(h)$ and I_0 are the PAR at the height *h* and above the canopy respectively, *k* is the light extinction coefficient and $LAI(h)$ is the cumulative leaf area per unit ground area from the top of the canopy to the height *h* in the canopy. Following Pierce et al. (1994) a linear relationship is assumed between the LAI and the SLA, in such a way that:

$$LAI(h) = m \cdot SLA \cdot B_{shoot}(h) \quad \text{(A.31)}$$

where $B_{shoot}(h)$ is the amount of shoot biomass above the height *h*. When an individual do not have to compete for light, i.e. when a column only contains the shoot biomass of one individual, the mean PAR received by the shoot in the column $I_c(t)$ is computed by integrating the Beer's law between h=0 and h=h_{shoot}:

$$I_c(t) = \frac{I_0(t)}{k \cdot LAI(h=0)} \cdot \left[1 - \exp\left(-k \cdot LAI(h=0)\right)\right] \quad \text{(A.32)}$$

When competition for light occurs, i.e. when a column contains the shoot biomass of several species, the column is divided in layers. The size of one layer is determined by the difference in height between two consecutive individuals (Fig. A.4). For each layer l, the mean PAR received by the shoot $I_{c,l}(t)$ is computed as:

$$I_{c,l}(t) = \frac{I_0}{\sum_i k_i \cdot \left(LAI_i(h_1) - LAI_i(h_2)\right)} \cdot \left[\exp\left(-\sum_i k_i \cdot LAI_i(h_2)\right) - \exp\left(-\sum_i k_i \cdot LAI_i(h_1)\right)\right] \quad \text{(A.33)}$$

where h_1, respectively h_2, are the height at the top, respectively the bottom, of the layer l. The total PAR received by an individual equals the average PAR across the layers and columns:

$$I(t) = \frac{1}{N_p} \cdot \sum_{c=1}^{N_p} \frac{V_l(c)}{V_{shoot}(t)} \sum_{l=1}^{N_l(c)} I_{c,l}(t) \quad \text{(A.34)}$$

where N_p is the number of pixel occupied by the individual, $V_l(c)$ is the volume of the layer l in the column c and $V_{shoot}(t)$ is the volume of the cylinder surrounding the shoot biomass.

Figure A.2. Division of a column in layers according to the height of each individual.

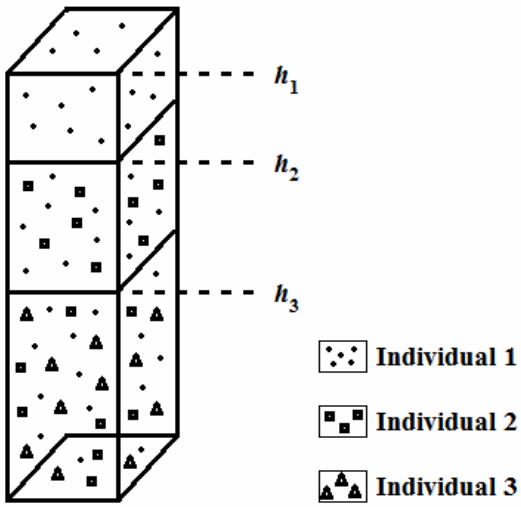

Table A.9. Parameters, input and output variables required for computation of the PAR received by individual plants.

Parameters	Meaning	Units	Values
k	Light extinction coefficient	m^{-1}	0.1 - 1.0
SLA	Specific leaf area	$m^2.g^{-1}$	0.01 - 0.05
m	Conversion coefficient from SLA to LAI	-	0.1 - 0.3
Input	**Meaning**	**Units**	**Values**
$B_s(t)$	Shoot biomass in time t	g	-
$h_s(t)$	Shoot height in time t	cm	-
$I_0(t)$	PAR above the canopy	$\mu mol.m^{-2}.s^{-1}$	0 - 1200
Output	**Meaning**	**Units**	**Values**
$I(t)$	PAR received by the shoot of individual plants	$\mu mol.m^{-2}.s^{-1}$	0 - $I_0(t)$

A.2.2. Soil water dynamics

Evaporation. The first soil layer has a depth of 2 cm and represents the litter. Water enters the litter through precipitations $P(t)$ and leave it through evaporation $E(t)$ towards the atmosphere. The evaporation rate is computed using the Penman-Monteith equation (Monteith, 1965):

$$E(t) = \frac{0.408 \cdot \Delta(t) \cdot \left(R_n(t) - G(t)\right) + \gamma \cdot \frac{900}{T(t)+273} \cdot u(t) \cdot VPD(t)}{\Delta(t) \cdot \left(1 + \frac{r_s(t)}{r_a(t)}\right)} \quad \text{(A.35)}$$

where $G(t)$ is ground heat flux, $u(t)$ is the wind speed at two meters height, γ is a psychometric constant and $\Delta(t)$ is the slope of the vapor pressure curve at air temperature $T(t)$ computed as:

$$\Delta(t) = \frac{4098 \cdot \left[0.6108 \cdot \exp\left(\frac{17.27 \cdot T(t)}{T(t)+237.3}\right)\right]}{\left(T(t)+237.3\right)^2} \quad \text{(A.36)}$$

The net radiation $R_n(t)$ is computed from the PAR $I(t)$ as:

$$R_n(t) = \frac{I(t) \cdot h \cdot c \cdot N_A}{\lambda_s} \quad \text{(A.37)}$$

with h the Plancks constant, c the speed of light, N_A the Avogadro number and λ_s the solar radiation wavelength. Although the amount of energy gained or lost by the soil through heat flux $G(t)$ should theoretically be subtracted or added to R_n it is small compared to R_n and is neglected when estimating evaporation.

Fluxes between the calculation node at soil surface and the height of the meteorological measurements are controlled by the aerodynamic resistance $r_a(t)$ between this two points, which is computed according to Daamen et al. (1996):

$$r_a(t) = \frac{\left(\ln(z_u) - \ln(z_0)\right)^2}{k_v^2 \cdot u(t)} \cdot \left(1 + \delta(t)\right)^{\varepsilon} \quad \text{(A.38)}$$

where z_u is the height at which wind speed is recorded, z_0 is roughness length, k_v is von Karman's constant, ε is a constant equals to -2 if $\delta(t)<0$ and -0.75 otherwise. Finally $\delta(t)$ is computed as:

$$\delta(t) = 5 \cdot g \cdot z_u \cdot \frac{T_s(t) - T(t)}{T(t) \cdot u(t)^2} \quad \text{(A.39)}$$

with g the acceleration due to gravity and $T_s(t)$ the soil temperature. The surface resistance $r_s(t)$ is an additional aerodynamic resistance to water vapor flux which reduces evaporation below potential rates. It is computed according to Kondo et al. (1990):

$$r_s(t) = \left(3 \cdot 10^{10}\right) \cdot \left(\theta_{sat} - \theta(t)\right)^{16.6} \quad \text{(A.40)}$$

with θ_{sat} the saturated soil water content and $\theta(t)$ the soil water content in the litter.

Table A.10. Parameters, input and output variables required for computation of the evaporation from bare soil.

Parameters	Meaning	Units	Values
γ	Psychometric constant	kPa.°C^{-1}	0.067

k_v	Von Karman's constant	-	0.41
z_0	Roughness length	M	0.01
θ_{sat}	Saturated soil water content	$cm^3.cm^{-3}$	0.4 - 0.5

Input	**Meaning**	**Units**	**Values**
$I(t)$	PAR received by the shoot of individual plants	$\mu mol.m^{-2}.s^{-1}$	0 - $I_0(t)$
$T(t)$	Atmospheric temperature	°C	0 - 40
$u(t)$	Wind speed at the heigth z_u	$m.s^{-1}$	0 - 1200
$VPD(t)$	Vapour pressure deficit	kPa	0.45 - 1.25
$\theta(t)$	Soil water content	$cm^3.cm^{-3}$	θ_r - θ_{sat}

Output	**Meaning**	**Units**	**Values**
$E(t)$	Evaporation rate	$cm.h^{-1}$	-

Vertical water flows. In each soil layer, water may be lost either because of drainage towards lower layers or capillary rise towards upper layers. When the soil water content in layer l, $\theta_s(l,t)$ is higher than the water content at field capacity θ_{fc}, a part of the excess water flows from the layer l to the layer $l+1$ with a velocity depending on the soil hydraulic conductivity K. When $\theta_s(l,t)$ is smaller than θ_{fc} and higher than the residual water content θ_{res}, a water flow may occur either upwards or downwards depending on the difference in layers water content. Water moves from layers of high- to low- water content with a velocity depending on K. Finally, the net water flow between layers l and $l+1$, $F_{l\rightarrow l+1}(t)$ is computed following:

$$F_{l\rightarrow l+1}(t)=\begin{cases} K\cdot\left(\theta_s(l,t)-\theta_{fc}\right) & if \quad \theta_s(l,t)>\theta_{fc} \\ K\cdot\left(\theta_s(l+1,t)-\theta_s(l,t)\right)\cdot 1_{\theta_s(l+1,t)>\theta_{res}} & if \quad \theta_s(l+1,t)>\theta_s(l,t) \\ K\cdot\left(\theta_s(l,t)-\theta_s(l+1,t)\right)\cdot 1_{\theta_s(l,t)>\theta_{res}} & if \quad \theta_s(l,t)>\theta_s(l+1,t) \end{cases} \tag{A.41}$$

where $1_{\theta s(l,t)>\theta res}$. is an indicator function, which equals 1 when $\theta_s(l,t)$ is higher than θ_{res} and 0 otherwise. The flow $F_{l\rightarrow l+1}(t)$ is positive when the water moves from layer l to layer $l+1$ and negative otherwise.

Radial water flows. In each soil layer l water may also be lost because of individual's i uptake $W_{up}(l,i,t)$. The individual's i water uptake creates a depletion of the water content in its rooting zone $\theta_r(l,i,t)$, leading to a radial flow from the soil to the rooting zone $f_i(l,t)$. At each time step we assumed that the radial diffusion equalizes the soil water content of layer l with that of rooting zones included in layer l. The radial flows $f_i(l,t)$ are then estimated by solving the following linear system for each soil layer:

$$\theta_s(l,t) + \frac{1}{V_s(l,t)} \cdot \left(F_{l-1\to l}(t) - F_{l\to l+1}(t) - \sum_{j=1}^{N} f_j(l,t) \right) = \theta_r(l,i,t) + \frac{1}{V_r(l,i,t)} \cdot \left(f_i(l,t) - W_{up}(l,i,t) \right) \qquad \forall i = 1,...,N \qquad \text{(A.42)}$$

where N is the number of individuals in the patch. $V_s(l,t)$ and $V_r(l,i,t)$ are the soil and individual's i rooting zone volume respectively.

Table A.11. Input and output variables required for simulating the water movement in the soil plant atmosphere continuum.

Parameters	**Meaning**	**Units**	**Values**
K	Saturated hydraulic conductivity	$cm.h^{-1}$	0.1 - 30
θ_{fc}	Soil water content at field capacity	$cm^3.cm^{-3}$	0.2 - 0.3
θ_{res}	Soil residual water content	$cm^3.cm^{-3}$	0.01 - 0.10
Input	**Meaning**	**Units**	**Values**
$E(t)$	Evaporation rate	$cm^3.h^{-1}$	-
$P(t)$	Precipitation rate	$cm^3.h^{-1}$	-
$W_{up}(l,i,t)$	Water uptake by individual i in layer l	$cm^3.h^{-1}$	-
$\theta_s(l,t)$	Soil water content in layer l	$cm^3.cm^{-3}$	-
$\theta_r(l,i,t)$	Water content in the l-th layer of the rooting zone of individual i	$cm^3.cm^{-3}$	-
Output	**Meaning**	**Units**	**Values**

$F_{l \to l+1}(t)$	Vertical flow from layer l to layer $l+1$	$cm^3.h^{-1}$	-
$f_i(l,t)$	Radial flow from the soil to the rooting zone of individual i in layer l	$cm^3.h^{-1}$	-

Plant water uptake. The water uptake rate of individual i at time t in layer l, $U_w(l,i,t)$ is constrained by the soil water content in the rooting zone of layer l, $\theta_r(l,i,t)$ (eq.A.19 and A.20). Moreover the water uptake in layer l, $W_{up}(l,i,t)$ depends on the amount of root biomass included in this layer $B_r(l,i,t)$. The amount of water extracted by plant roots is computed as the product between plant water uptake rate and root biomass in each layer:

$$W_{up}(l,i,t) = U_w(l,i,t) \cdot B_r(l,i,t) \quad \text{(A.43)}$$

Table A.12. Input and output variables required for computation of the amount of water incoming the soil.

Input	**Meaning**	**Units**	**Values**
$B_r(l,i,t)$	Root biomass in the l-th layer of the individual i rooting zone	g	-
$U_w(l,i,t)$	Water uptake rate in the l-th layer of individual i	$cm^3.g^{-1}.h^{-1}$	-
Output	**Meaning**	**Units**	**Values**
$W_{up}(l,i,t)$	Amount of water extracted by individual i in layer l	$cm^3.h^{-1}$	-

A.2.3. Nitrogen cycle

The model developed by Johnsson *et al.* (1987) was used to simulate nitrogen cycle in a 2-dimension layered soil. This model includes the major processes that determine inputs, transformation and outputs of nitrogen in soil (Fig. A.6). The soil is divided in two principal organic matter pools: a fast cycling pool (litter), and a slow-cycling pool (humus). The humus

is divided in layers of equal size, the number of layers being set by the user. At each time step, the nitrogen transformations and movements are simulated in each layer.

Figure A.3. Nitrogen cycling and movement in a 2-dimensions layered soil.

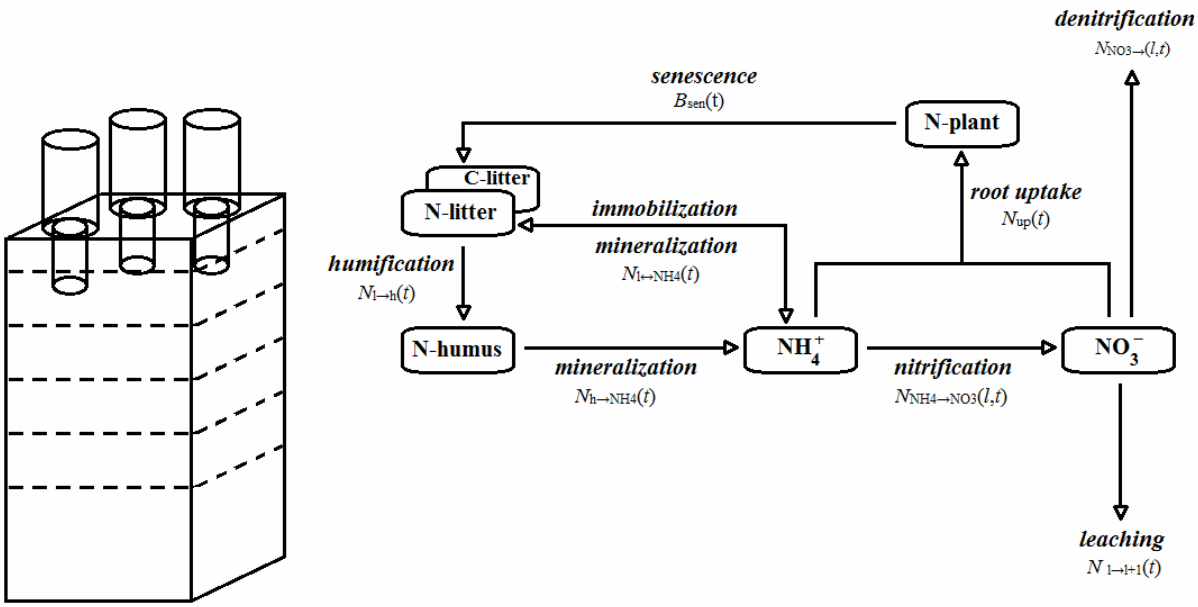

N*itrogen transformations in the litter.* The litter is a fast-cycling pool representing an organic matter-microbial biomass complex, which receives fresh organic material. The organic nitrogen in the litter may be humified during the litter decomposition, following:

$$N_{l\rightarrow h}(t) = r_0 \cdot f_e \cdot f_h \cdot \left(K_d \cdot e_T(t) \cdot e_M(t) \cdot C_l(t)\right) \quad \text{(A.44)}$$

where r_0 is the C-N ratio of decomposer biomass and humification products, f_e is a synthesis efficiency constant, f_h is the humification fraction, K_d is the specific decomposition rate of litter and $e_T(z)$ and $e_M(z)$ are response functions for soil temperature and moisture respectively.

Otherwise the organic nitrogen may be transformed in ammonium during the mineralization. This process is governed by two assumptions: (1) that the formation of humus (eq. A.44) has a nitrogen demand determined by a constant C-N ratio of decomposer biomass and humification products (r_0); (2) that nitrogen is released by decomposition of soil litter carbon

in proportion to the actual litter C-N ratio. As a result net mineralization or immobilization of nitrogen in litter is determined by the balance between the release of nitrogen during decomposition and the nitrogen immobilized during microbial synthesis and humification. The switch between net immobilization and mineralization of nitrogen in litter occurs et the C-N ratio equals r_0/f_e:

$$N_{l\leftrightarrow NH4}(t) = \left(\frac{N_l(t)}{C_l(t)} - \frac{f_e}{r_0}\right)\cdot\left(K_d \cdot e_T(t)\cdot e_M(t)\cdot C_l(t)\right) \quad \text{(A.45)}$$

Here the mineralization rate is proportional to the actual soil litter C-N ratio. When this latter equals r_0/f_e there is a switch between net immobilization and mineralization.

Table A.13. Parameters, input and output variables required for computation of the nitrogen transformation in the litter.

Parameters	**Meaning**	**Units**	**Values**
f_e	Synthesis efficiency constant	-	0.5
f_h	Carbon humification fraction	-	0.2
K_d	Litter specific decomposition rate for C	h^{-1}	0.0015
r_0	C-N ratio of microorganisms and humified products	-	10
Input	**Meaning**	**Units**	**Values**
$C_l(t)$	Soil litter carbon concentration	$mg.cm^{-3}$	-
$N_l(t)$	Soil litter organic nitrogen concentration	$mg.cm^{-3}$	-
Output	**Meaning**	**Units**	**Values**
$N_{l\rightarrow h}(t)$	Litter specific humifcation rate	$mg.cm^{-3}.h^{-1}$	-
$N_{l\leftrightarrow NH4}(t)$	Mineralization rate in the litter	$mg.cm^{-3}.h^{-1}$	-

Nitrogen transformation in the humus. In favorable conditions, the humified nitrogen is mineralized. For each humus layer, the mineralization is computed as a first order rate:

$$N_{h\to NH4}(l,t) = k_h \cdot e_T(l,t) \cdot e_M(l,t) \cdot N_h(l,t) \quad \text{(A.46)}$$

where k_h is the specific mineralization rate and $N_h(l,t)$ is the organic nitrogen concentration in the l-th layer of humus.

The ammonium cations are oxidized in nitrite, which are in turn oxidized in nitrate ion. Nitrification is not modelled explicitly as a microbial process, but the segregation of mineral nitrogen into ammonium and nitrate is made by assuming a nitrate-ammonium ratio characteristic for a particular soil, so that the nitrification rate in layer l at time t is given by:

$$N_{NH4\to NO3}(l,t) = k_n \cdot e_T(l,t) \cdot e_M(l,t) \cdot \left(NH_4(l,t) - \frac{NO_3(l,t)}{n_q} \right) \quad \text{(A.47)}$$

where k_n, the nitrification potential rate is reduced as the specific nitrate-ammonium ratio n_q is approached.

The nitrate ion may be reduced to form dinitrogen, which is released in the atmosphere in gaseous form. Denitrification is an anaerobic process and consequently is highly dependant on soil aeration. The model uses soil water content $\theta_s(l,t)$ as an indirect expression of soil oxygen status, and its impact on the denitrification rate is taken into account using a power function $e_{O2}(z)$:

$$N_{NO3\to}(l,t) = k_d \cdot e_{O2}(l,t) \cdot e_T(l,t) \cdot \left(\frac{NO_3(l,t)}{NO_3(l,t) + c_s} \right) \quad \text{(A.48)}$$

where k_d is the potential denitrification rate. The effect of nitrate concentration is controlled by the half-saturation constant c_s.

Table A.14. Parameters, input and output variables required for computation of the nitrogen transformation in the humus.

Parameters	Meaning	Units	Values
c_s	Half-saturation constant	$Mg.cm^{-3}$	10
k_d	Humus specific denitrifiction potential rate	$g.h^{-1}$	0.004
k_h	Humus specific mineralization rate	h^{-1}	3.10^{-6}
k_n	Humus specific nitrifiction rate	h^{-1}	0.008
n_q	Humus specific nitrate-ammonium ratio	-	8
Input	**Meaning**	**Units**	**Values**
$N_h(l,t)$	Organic nitrogen concentration in the *l*-th layer of humus	$Mg.cm^{-3}$	-
$NH4(l,t)$	Ammonium concentration in the *l*-th layer of humus	$Mg.cm^{-3}$	-
$NO3(l,t)$	Nitrate concentration in the *l*-th layer of humus	$Mg.cm^{-3}$	-
Output	**Meaning**	**Units**	**Values**
$N_{h\rightarrow NH4}(t)$	Mineralization rate in the *l*-th humus layer	$mg.cm^{-3}.\ h^{-1}$	-
$N_{NH4\rightarrow NO3}(l,t)$	Nitrification rate in the *l*-th humus layer	$mg.cm^{-3}.\ h^{-1}$	-
$N_{NO3\rightarrow}(l,t)$	Denitrification rate in the *l*-th humus layer	$mg.cm^{-3}.\ h^{-1}$	-

Abiotic response functions. Decomposition, mineralization and nitrification are regulated by the same abiotic response function involving soil temperature and moisture. A Q_{10} relationship is used to express the effect of temperature:

$$e_T(l,t) = Q_{10}^{\frac{1}{10}(T(l,t)-T_b)} \quad \text{(A.49)}$$

where $T(l,t)$ is the soil temperature in layer l at time t, T_b is the base temperature at which $e_T(l,t)$ equals 1 and Q_{10} is the factor change in rate with a 10-degree change in temperature.

Table A.15. Parameters, input and output variables required for computation of the soil temperature response function.

Parameters	Meaning	Units	Values
Q_{10}	Response to a 10-degree change	-	3
T_b	Optimal temperature	°C	20
Input	**Meaning**	**Units**	**Values**
$T(l,t)$	Soil temperature in the layer l	°C	-
Output	**Meaning**	**Units**	**Values**
$e_T(l,t)$	Soil temperature response function	-	-

The soil moisture factor decreases on either side of an optimum level, in drier soil or in excessively moist soil:

$$e_M(l,t) = \begin{cases} e_s + (1-e_s)\cdot\left(\dfrac{\theta_{sat}-\theta(l,t)}{\theta_{sat}-\theta_h}\right)^m & if \quad \theta_{sat} \geq \theta(l,t) > \theta_h \\ 1 & if \quad \theta_h \geq \theta(l,t) > \theta_l \\ \left(\dfrac{\theta(l,t)-\theta_w}{\theta_l-\theta_w}\right)^m & if \quad \theta_l \geq \theta(l,t) > \theta_{wl} \end{cases} \tag{A.50}$$

where θ_{sat} is the soil saturated water content, θ_w is the minimum water content for process activity and θ_h and θ_l are the high and low water content respectively. When the soil water content $\theta(l,t)$ is between these values, the soil moisture factor is optimal. A coefficient e_s defines the relative effect of moisture when the soil is completely saturated and m is an empirical constant

Table A.16. Parameters, input and output variables required for computation of the soil moisture response function.

Parameters	Meaning	Units	Values
e_s	Saturation activity	-	0.6

m	Empirical coefficient	-	1
θ_l	Lower limit for $e_M(l,t)$ to be optimal	$Cm^3.cm^{-3}$	0.22
θ_h	Upper limit for $e_M(l,t)$ to be optimal	$Cm^3.cm^{-3}$	0.32
θ_{sat}	Soil saturated water content	$Cm^3.cm^{-3}$	0.4
θ_w	Permanent wilting point	$Cm^3.cm^{-3}$	0.12
Input	**Meaning**	**Units**	**Values**
$\theta(l,t)$	Soil water content in the *l*-th layer of humus	$Cm^3.cm^{-3}$	-
Output	**Meaning**	**Units**	**Values**
$e_M(l,t)$	Soil moisture response function	-	-

The soil aeration factor is expressed as a power function which increases from a threshold point θ_d and is maximum at saturation

$$e_{O2}(l,t) = \left(\frac{\theta(l,t) - \theta_d}{\theta_{sat} - \theta_d} \right)^d \quad \text{(A.51)}$$

where θ_{sat} is the soil saturated water content and d is an empirical constant.

Table A.17. Parameters, input and output variables required for computation of the soil aeration response function.

Parameters	**Meaning**	**Units**	**Values**
d	Empirical coefficient	-	2
θ_d	Lower limit for process activity	$Cm^3.cm^{-3}$	0.1
θ_{sat}	Soil saturated water content	$Cm^3.cm^{-3}$	0.4
Input	**Meaning**	**Units**	**Values**
$\theta(l,t)$	Soil water content in the *l*-th layer of humus	$cm^3.cm^{-3}$	-
Output	**Meaning**	**Units**	**Values**

$e_M(l,t)$	Soil aeration response function	-	-

Nitrogen movements. Nitrate is considered to be wholly in solution and movement between layers and leaching from the profile in drainage flow are determined by water flow rates. The amount of nitrate outgoing the layer l, $F_N(l,t)$ is thus calculated as the product of the water flow $F(l,t)$ and the nitrate concentration in the soil layer from which the water flow originates:

$$F_N(l,t) = F(l,t) \cdot \theta_s(l,t) \cdot NO_3(l,t) \quad \text{(A.52)}$$

where $NO_3(l,t)$ is the soil concentration in nitrate and $\theta_s(l,t)$ is the soil water content in layer l. Moreover the horizontal water flows $f_i(l,t)$ also involve a movement of nitrate from the soil to the rooting zone. This process, called mass flow, is the main process driving nitrate anion NO_3^- flow from the soil to the root surface (Barber et al., 1963). The amount of NO_3^- entering the rooting zone of individual i in the layer l by mass-flow $M_f(l,i,t)$ is computed as the product of the water flow from the soil to the rooting zone $f_i(l,t)$ and the concentration of NO_3^- in the soil water:

$$M_f(l,i,t) = f_i(l,t) \cdot \theta_s(l,t) \cdot NO_3(l,t) \quad \text{(A.53)}$$

where $[NO_3^-]_s(l,t)$ is the soil concentration in nitrate and $\theta_s(l,t)$ is the soil water content in layer l. By contrast the ammonium cation NH_4^+ does not move with water and it is made available for plant uptake mainly by root interception.

Table A.18. Input and output variables required for simulation of nitrate movement in soil.

Input	Meaning	Units	Values
$F(l,t)$	Vertical flow outgoing layer l	$cm^3.h^{-1}$	-
$f_i(l,t)$	Radial flow from the soil to the rooting zone of individual i in layer l	$cm^3.h^{-1}$	-
$NO3(l,t)$	Nitrate concentration in the l-th layer of humus	$mg.cm^{-3}$	-

$\theta_s(l,t)$	Soil water content in layer l	$cm^3.cm^{-3}$	-

Output	**Meaning**	**Units**	**Values**
$M_f(l,i,t)$	Mass flow for individual i in layer l	Mg	-
$F_N(l,t)$	Nitrogen amount outgoing layer l	Mg	-

REFERENCES

Aerts R. 1996. Nutrient resorption from senescing leaves of pernnial: are there general patterns? *J. Ecol.* 84: 597-608.

Anten, N. P. R. et al. 1998. Nitrogen distribution and leaf area indices in relation to photosynthetic nitrogen use efficiency in savanna grasses. *Plant Ecol.* 138: 63-75.

Assman, S. M. 1999. The cellular basis of guard cell sensing of rising CO2. *Plant Cell Environ.* 22: 629-637.

Assman, S. M. and Shimazaki, K. 1999. The multisensory guar cell. Stomatal responses to blue light and abscisic acid. *Plant Physiol.* 119: 809-815.

Barber, S. A., Walker, J. M. and Vasey, E. H. 1963. Mechanisms for movement of plant nutrients from soil and fertilizer to plant root. *J. Agric. Food Chem.* 11(3): 204-207.

Caird, M.A., Richards, J.H., & Donovan, L.A. 2007. Nighttime stomatal conductance and transpiration in C3 and C4 plants. *Plant Physiol.* 143(1): 4-10.

Engels, C., Neumann, G., Gahoonia, T.S., George, E., & Schenk, M. 2000. Assessing the ability of roots for nutrient acquisition. In *Root Methods* (pp. 403-459). Springer Berlin Heidelberg.

Feddes, R.A. et al. 1988. Modelling soil water dynamics in the unsaturated zone - State of the art. *J. Hydro.* 100:69-11.

Gale, J. 1972. Availability of carbon dioxide for photosynthesis at high altitudes: theoritical considerations. *Ecology* 53(3): 494-497.

Harley P. C. and Baldocchi D. D. 1995. Scaling carbon dioxide and water vapour exchange from leaf to canopy in a deciduous forest. I. Leaf model parametrization. *Plant Cell Environ.* 18: 1146-1156.

Jarvis, P. G. 1976. The interpretation of the variations in leaf water potential and stomatal conductance found in canopies in the field. *Phil. Trans. R. Soc.* 273: 593-610.

Johnson I. R. and Thornley J. H. M. A model of instantaneous and daily canopy photosynthesis. *J. Theor. Biol.* 107(4): 531-545.

Johnson, P. S., Johnson, C. L. and West N. E. 1988. Estimtion of phytomass for ungrazed crested wheatgrass using allometric equations. *J. Range Manage.* 41(5): 421-425.

Johnsson, H. et al. 1987. Simulated nitrogen dynamics and losses in a layered agricultural soil. *Agric. Ecosyst. and Environ.* 18: 333-356.

Kikuzawa, K. and Lechowicz, M. 2006. Toward synthesis of relationships among leaf longevity, 3 instantaneous photosynthetic rate, lifetime leaf carbon gain, and the gross primary production 4 of forests. *Am. Nat.* 168: 373-383.

Lambers, H. et al. 2008. Photosynthesis, respiration and long-distance transport. In: *Plant Physiological Ecology*, Springer, p.21.

Lambers, H. et al. 2008. Plant water relations. Plant Physiological Ecology, Springer, p.163.

Lange, O. L et al. 1971. Responses of stomata to changes in humidity. *Planta* 100: 76-86.

Monsi M. and Saeki T. 1953. Uber den Lichtfacktor in den Pflanzengesellschaften und seine Bedeutung für die Stoffproduktion. *J. Ap. Bot.* 15:60-82.

Monteith, J.L. 1965. Evaporation and environment. *Symposia of the Society for Experimental biology* 19: 205-224.

Perchorowicz J. T., Raynes D. A. and Jensen R. G. 1981. Light limitation of photosynthesis and activation of ribulose bisphosphate carboxylase in wheat seedlings. *Proc. Nat. Acad. Sci.* 78(5): 2985-2989.

Schippers, P. and Kropff, M. J. 2001. Competition for light and nitrogen among grassland species a simulation analysis. *Fun. Ecol.* 15: 155-164.

Stalfelt M. G. 1962. The effect of temperature on opening of the stomatal cells. *Physiol. Plant.* 15: 772-779.

Taubert, F., Franck, K. and Huth, A. 2012. A review of grassland models in the biofuel context. *Ecol. Mod.* 245: 84-93.

Thornley, J.H.M. 1970. Respiration, growth and maintenance in plants.

APPENDIX B. PROCESS SUBMODELS IN GRASSLAND MODELS

This appendix details the equations used to describe the physiological processes integrated in 9 pasture models differing in their purpose and structure. The reference of models are given in Table B0. The parameterization cost of each submodel Φ is simply assessed through the number of parameters required by the submodels. The meaning and units of abbreviation are detailed in the table B11 of this appendix. Some models do not integrate every processes described here and are consequently off the table.

TABLE B0. List of the 9 pasture models reviewed.

Reference	Model	Literature
[1]	HP model	Thornley el al. (1989)
[2]	GEM	Hunt et al. (1991)
[3]	GRAZPLAN	Moore et al. (1997)
[4]	PaSim	Riedo et al. (1998)
[5]	Lingra	Schapendonck et al. (1998)
[6]	-	Schippers and Kropff (2001)
[7]	SGS	Johnson et al. (2008)
[8]	GRASSMIND	Taubert et al. (2012)
[9]	GEMINI	Soussana et al. (2012)

TABLE B1. Submodels describing the relationship between the photosynthetically active radiation (PAR) received by leaves and gross CO2 assimilation rate (A_g) used in pasture models, and their complexity Φ (assessed through the number of parameters).

Submodels	Models	Equations	Φ
Farquhar et al. (1980)	[9]	$A_g = \min(V_c, V_j) \cdot \left(\frac{1-\Gamma^*}{C_i}\right)$ $V_c = \frac{V_{c,pot} \cdot C_i}{C_i + K_c\left(1+\frac{O_i}{K_o}\right)}$ $V_j = \frac{1}{\left(1+\frac{2\Gamma^*}{C_i}\right)} \cdot \frac{\alpha \cdot I \cdot V_{j,pot}}{\sqrt{1+(4\cdot\alpha\cdot I)^2}}$	10
Light response curve (LRC)	[1], [4], [7]	$A_g = \frac{1}{2\cdot\beta}\left(\alpha\cdot I + A_{pot} - \sqrt{(\alpha\cdot I + A_{pot})^2 - 4\cdot\beta\cdot\alpha\cdot A_{pot}}\right)$	3
	[8]	$A_g = \frac{\alpha\cdot I\cdot A_{pot}}{\alpha\cdot I + A_{pot}}$	2
Radiation use efficiency (RUE)	[2], [3], [5], [6]	$A_g = RUE\cdot I$	1

TABLE B2. Response function describing the relationship between the leaf nitrogen content (LNC) and net CO2 assimilation rate (A_n) used in pasture model, and their complexity (assessed through the number of parameters).

Models	Equations	Φ
[1]	$f_N = b_N \cdot N_{plant}$	1
[2]	$f_N = \dfrac{1}{1 + \dfrac{PP2}{C_i} + \dfrac{PP8 - PP9}{RGN - PP9}}$	3
[4]	$f_N = 1 + b_{LNC} \cdot (LNC - a_{LNC})$	2
[6]	$f_N = \dfrac{LNC - LNC_{\min}}{LNC_{opt} - LNC_{\min}}$	2
[7]	$f_N = \min\left(1, \dfrac{LNC}{LNC_{opt}}\right) \cdot \dfrac{LNC_{opt}}{LNC_{ref}}$	2
[8]	$f_N = \dfrac{N_{pot}}{N_{demand}}$	2
[9]	$\begin{cases} V_{c,pot} = \left(k_3 + p_3 \cdot \left(C_{a,ref} - C_g\right)\right) \cdot N_{pa} \cdot f_T \\ V_{j,pot} = \left(\dfrac{V_{j,ref}}{V_{c,ref}} + p_1 \cdot \left(T_{K,ref} - T_g\right) + p_2 \cdot \left(C_{a,ref} - C_g\right)\right) \cdot V_{c,pot} \cdot f_T \end{cases}$	12

TABLE B3. Response function describing the relationship between atmospheric temperature (T) and net CO2 assimilation rate (A_n) used in pasture model, and their complexity (assessed through the number of parameters).

Models	Equations	Φ
[1]	$f_T = \frac{T - T_{\min}}{T_{ref} - T_{\min}}$	2
[2]	$f_T = \mu(\Psi_s) \cdot \left[\left(\frac{T_h(\Psi_s) - T}{T_h(\Psi_s) - T_o(\Psi_s)} \right) \cdot \left(\frac{T - T_{\min}}{T_o(\Psi_s) - T_{\min}} \right)^{\left(\frac{T_o(\Psi_s) - T_{\min}}{T_h(\Psi_s) - T_o(\Psi_s)} \right)} \right]^{k_1}$	6
[3]	$f_T = \min\left(SIG(T_{lag}, K_{T1}, K_{T2}), SIG(T_{lag}, K_{T3}, K_{T4})\right)$ $SIG(x,a,b) = \left(1 + \exp\left(-\frac{2(\ln(0.95) - \ln(0.05))}{b-a}\left(x - \frac{a+b}{2}\right)\right)\right)^{-1}$	4
[4]	$f_T = \frac{(T - T_{\min})(T - T_{\max})}{(T - T_{\min})(T - T_{\max}) - (T - T_{opt})^2}$	3
[5]	$f_T = \min\left(1, \frac{T - T_{\min}}{T_{opt} - T_{\min}}\right)$	2
[6], [8]	$f_T = \begin{cases} 0 & , \quad T < -5 \\ 0.02857 \cdot T + 0.142 & , \quad -5 < T < 2 \\ 0.1 \cdot T & , \quad 2 < T < 10 \\ 1 & , \quad T > 10 \end{cases}$	6
[7]	$f_T = \begin{cases} \frac{(T - T_{\min})^q (T_{\max} - T)}{(T_b - T_{\min})^q (T_{\max} - T_{ref})} & , \quad T_{\min} \le T \le T_{\max} \\ 0 & , \quad otherwise \end{cases}$	4
[9]	$f_T = \exp\left[\frac{\Delta Ha}{R \cdot T_{ref}} \cdot \left(1 - \frac{T_{ref}}{(273.15 + T)}\right)\right] \cdot \frac{1 + \exp\left[\frac{\Delta S \cdot T_{ref} - \Delta Hd}{R \cdot T_{ref}}\right]}{1 + \exp\left[\frac{\Delta S \cdot (273.15 + T) - \Delta Hd}{R \cdot (273.15 + T)}\right]}$	4 (x2) + 1

TABLE B4. Model describing the relationship between water availability and net CO2 assimilation rate (A_n) used in pasture model, and their complexity (assessed through the number of parameters).

Models	**Equations**	Φ
[3]	$f_W = f_{WC} \cdot f_{WL}$ $\begin{cases} f_{WC} = \max\left[0, \min\left(\frac{K_{W1}}{K_{W2}} \cdot \frac{TR}{PET \cdot AL}, 1\right)\right] \\ f_{WL} = \sum_m \pi_m \cdot \exp\left[K_{W3} \cdot \max\left(\frac{\theta}{\theta_s} - K_{W4}, 1\right)\right] \end{cases}$	7
[4]	$f_W = \frac{1}{1 + \exp(-\Psi_S \cdot (\Psi - \Psi_b))}$	3
[5], [8]	$f_W = \min\left(1, \frac{\theta - \theta_{wp}}{\theta_c - \theta_{wp}}\right)$	2
[7]	$f_W = \begin{cases} 0 & , \quad \theta \le \theta_{wp} \\ \frac{\theta - \theta_{wp}}{\theta_r - \theta_{wp}} & , \quad \theta_{wp} < \theta \le \theta_r \\ 1 & , \quad \theta_r < \theta \le \theta_{fc} \\ 1 + (f_{w,sat} - 1) \cdot \frac{\theta - \theta_{fc}}{\theta_s - \theta_{fc}} & , \quad \theta > \theta_{fc} \end{cases}$	5

TABLE B5. Submodel describing the maintenance respiration rate associated with photosynthetic activity (R_m).

Models	Equations	Φ
[1]	$R_m = C_{plant} \cdot \sum_{i=1}^{4} \left(m_{sh,i} \cdot W_{sh,i} + m_{r,i} \cdot W_{r,i} \right)$	8
[2]	$R_m = R_{m,\max} \cdot g_T \cdot B_s$ $g_T = 2.82 \cdot \exp\left(32.24 - \frac{10000}{273.15 + T} \right)$	5
[4]	$R_m = \frac{C_{plant}}{C_{plant} + K_{ma\,\mathrm{int}}} \cdot \sum_{i=1}^{4} \left(g_{sh,T} \cdot m_{sh,i} \cdot W_{sh,i} + g_{r,T} \cdot m_{r,i} \cdot W_{r,i} \right)$ $g_{sh,T} = 2^{(T - T_{SH,0})/10} \quad and \quad g_{r,T} = 2^{(T - T_{R,0})/10}$	11
[6]	$R_m = f_N \cdot g_T \cdot R_{m,\max} \cdot B_{tot}$ $g_T = \begin{cases} 0 & , \quad T < 0°C \\ 0.03333 \cdot T & , \quad 0 < T < 15°C \\ 2^{(T - T_0)/10} & , \quad T > 15°C \end{cases}$	3
[7]	$R_m = R_{m,ref} \cdot g_T \cdot \frac{N_{plant}}{N_{plant,ref}} \cdot B_{tot}$ $g_T = \frac{T}{T_{ref}}$	3
[8]	$R_m = g_T \cdot R_{m,\max} \cdot B_{tot}$ $g_T = \begin{cases} 0 & , \quad T < 0°C \\ 0.03333 \cdot T & , \quad 0 < T < 15°C \\ 2^{(T - T_0)/10} & , \quad T > 15°C \end{cases}$	3
[9]	$R_m = R_{m,sh} + R_{m,r}$ $\begin{cases} R_{m,sh} = SS \cdot I_{fac} \cdot R_{fac} \cdot k_3 \cdot N_{pa} \cdot g_{T,sh} \cdot LAI \\ R_{m,r} = R_{m,root} \cdot g_{T,r} \cdot B_r \end{cases}$	13

TABLE B6. Submodel describing the growth respiration rate associated with photosynthetic activity (R_g).

Models	**Equations**	Φ
[1], [4]	$R_g = \frac{1-Y}{Y} \cdot C_{plant} \cdot G \cdot C_{struct} \cdot N_{struct} \cdot \left(W_{sh} \cdot \lambda_C + W_r \cdot (1-\lambda_C)\right)$	1
[7]	$R_g = \frac{1-Y}{Y} \cdot GPP$	1
[8]	$R_g = k_g \cdot \left(A_g - R_m\right)$	1
[9]	$R_m = \frac{1-Y}{Y} \cdot \left(\lambda_P \cdot W_P \cdot f_{cp} + \lambda_C \cdot W_s \cdot f_{cs} + \left(1-\lambda_C-\lambda_P\right) \cdot W_r \cdot f_{cr}\right)$	1

TABLE B7. Submodels describing the transpiration rate (*TR*).

Models	**Equations**	Φ
[2]	$\begin{cases} TR = & S_{sh} \cdot PT3 \cdot G_{CO2} \cdot (W_i - W_a) \cdot PT4 \cdot f_T \\ U_W = & U_{W,ref} \cdot h_T \cdot h_W \cdot B_r \end{cases}$ $h_T = 1.3^{(T-T_0)/10} \quad and \quad h_W = \frac{\theta - \theta_{low}}{\theta_{hi} - \theta_{low}}$	4
[3]	$TR = \sum_l PET \cdot AL \cdot \left[\pi_l \cdot TR_l^* + \left(1 - \sum_m \pi_m \cdot TR_m^* \right) \cdot \frac{RW_l}{\sum_m RW_m} \right]$ $TR_l^* = \max\left(0, \min\left(\frac{\Theta_l}{K_{W1}}, 1\right)\right) \quad and \quad RW_l = \begin{cases} \pi_l & , \ \Theta_l \geq K_{W1} \\ 0 & , \ \Theta_l < K_{W1} \end{cases}$	5
[4]	$TR = \sum_l \frac{\Psi_l - Z_l - \Psi_r}{r_{s,rs}(l) + r_{rs,r}(l)}$	4
[5], [8]	$TR = f_W \cdot TR_p$	2
[7]	$TR = \sum_l \pi_l \cdot f_{W,l} \cdot TR_p$	3

TABLE B8. Submodels describing the root nitrogen uptake (U_N).

Models	Equations	Φ
[1]	$U_N = \frac{\sigma_N \cdot f_T}{1+\frac{K_{C,un}}{C_{plant}}\left(1+\frac{N_{plant}}{K_{N,un}}\right)} \cdot \left(N_{amm} + a_{N,T} \cdot N_{nit}\right) \cdot \sum_{i=1}^{4} \nu_i \cdot W_{r,i}$ $a_{N,T} = a_{N,20} - \left(a_{N,20} - a_{N,10}\right) \cdot \frac{20 - T_s}{20 - 10}$	9
[2]	Mcgill (1981)	
[4]	$U_N = \frac{\sigma_N \cdot f_T}{1+\frac{K_{C,un}}{C_{plant}}\left(1+\frac{N_{plant}}{K_{N,un}}\right)} \cdot \frac{N_{amm} + N_{nit}}{N_{amm} + N_{nit} + K_{Neff}} \cdot \sum_i \nu_i \cdot W_{r,i}$	8
[6]	$U_N = \min\left(U_{N,pot}, U_{N,dem}\right)$ $U_{N,dem} = F \cdot B_s \cdot \left(LNC_{\max} - LNC\right)$ $U_{N,pot} = N_s \cdot \frac{R_i}{\sum_j R_j}$	$2 + N_{sp}$
[7]	$U_{Nu} = LNC_{\max} \cdot \delta_{ref} \cdot \frac{\sum_l B_{r,l} \cdot Nu_l}{B_{r,ref} \cdot \chi_{Nu}}$	4
[8]	$U_N = f_W \cdot \min\left(U_{N,pot}, U_{N,dem}\right)$ $U_{N,dem} = \frac{A_g \cdot \mathrm{cov}}{NUE}$ $U_{N,pot} = \sum_l \left(\beta_l - \beta_{l+1}\right) \cdot N_l$	4
[9]	$U_N = D \cdot \min\left(U_{N,pot}, U_{N,dem}\right) \cdot B_r \cdot lwr \cdot f_{act}$ $\begin{cases} U_{N,dem} = \frac{1}{\left(1+Stol_{ratio}\right)} \cdot \left(\frac{U_{N,\max}}{\max\left(1, \frac{N_{plant}}{K_U}\right)} + \frac{F_{N,\max}}{\max\left(1, \frac{N_{plant}}{K_F}\right)} \right) \\ U_{N,pot} = N_s \cdot \frac{sk_N}{sd} \end{cases}$	10

TABLE B9. Submodels used to estimate the coefficient of carbon allocation to aboveground plant parts (λ_C).

Models	Equations	Φ
[1], [4]	$\lambda_C = \frac{1}{1+P\cdot\rho}$ $P = \frac{f_r \cdot N_{plant}}{N_{plant}+N_{struct}} \cdot \frac{C_{plant}+C_{struct}}{f_{sh}\cdot C_{plant}}$	4
[2]	$\lambda_C = A_n \cdot \max\left(ELN(LNC), ELW(G_{CO2})\right)$ $ELN(LNC) = \lambda_{C,\min} + (\lambda_{C,\max} - \lambda_{C,\min}) \cdot \frac{LNC - LNC_{\min}}{LNC_{\max} - LNC_{\min}}$ $ELW(G_{CO2}) = b(G_{CO2}) \cdot G_{CO2} + a(G_{CO2})$	10
[3]	$\lambda_C = (1-\lambda_{C,seed}) \cdot \frac{RS}{RS + RS_{tar}^2}$ $RS_{tar} = K_{A1} + (K_{A2} - K_{A1}) \cdot SIG(DD, 0, K_{F1})$ $\lambda_{C,seed} = K_{A3} \cdot \frac{FL}{K_{F2}}$	6
[5]	$\lambda_C = a_{part} + b_{part} \cdot f_W$	4
[6]	$\lambda_C = \lambda_{C,\min} + (\lambda_{C,\max} - \lambda_{C,\min}) \cdot \frac{LNC - LNC_{\min}}{LNC_{\max} - LNC_{\min}}$	4
[7]	$\lambda_C = \frac{f_N \cdot f_W \cdot \rho_{\max}^2}{\rho + f_N \cdot f_W \cdot \rho_{\max}^2}$	8
[8]	$B_s = \alpha \cdot (B_r)^{\beta}$	2
[9]	$\lambda_C = \min(\lambda_{C,pot}, \lambda_{C,\max})$ $\lambda_{C,pot} = \frac{P\cdot Q}{P+Q+P\cdot Q}$ *and* $\lambda_{C,pot} = \frac{Q \cdot CR_{sh,pot}}{k_{cn}\cdot(Q\cdot B_s + W_p)}$ $P = \left(\frac{C_{plant}}{N_{plant}} \cdot \frac{\sigma_N \cdot B_r \cdot lwr \cdot f_{act}}{\sigma_C \cdot LA}\right)^q$ *and* $Q = \left(\frac{NP_{plant}\cdot W_p \cdot D}{\sum_z N_{pac,z}\cdot LAI_z}\right)^q$	14

TABLE B10. Submodels used to estimate the coefficient of nitrogen allocation to aboveground plant parts (λ_N).

Models	**Equations**	Φ
[1], [4]	$\lambda_N = \lambda_C$	0
[2]	$\lambda_N = \lambda_{N,\max} \cdot RNC \cdot h_T \cdot h_W \cdot ELR \cdot ELS$ $ELR = \frac{N_r - N_{r,\min}}{N_{r,\max} - N_{r,\min}} \quad ; \quad ELS = \frac{N_{s,\max} - N_s}{N_{s,\max} - N_{s,\min}}$	9
[6], [8]	$\lambda_N = 1$	0
[7]	$\lambda_N \propto \rho$	0

TABLE B11. Pasture model parameters and variables

Symbol	Description	Unit
	PAR submodels	
A_g	Gross CO2 assimilation rate	µmol CO2.m^{-2}.s^{-1}
A_{pot}	Potential gross CO2 assimilation rate	µmol CO2.m^{-2}.s^{-1}
K_c	Constant of Michaelis-Menten for carboxylase activity of the Rubisco	Pa
K_o	Constant of Michaelis-Menten for oxygenase activity of the Rubisco	Pa
I	Photosynthetically active radiation received by leaves	µmol PPFD.m^{-2}.s^{-1}
RUE	Radiation use efficiency	µmol CO2. µmol^{-1} PPFD.m^{-2}.s^{-1}
$V_{c,pot}$	Potential carboxylation rate of Rubisco according to environmental conditions	µmol CO2.m^{-2}.s^{-1}
$V_{j,pot}$	Potential rate of RuBP regeneration according to environmental conditions	µmol CO2..m^{-2}.s^{-1}
Γ^*	CO2 compensation point	-
α	Apparent quantum yield of net photosynthesis at saturating CO2	µmol CO2. µmol^{-1} PPFD
β	Curvature parameter	-
	Nitrogen submodels	
a_{LNC}	Ordinate of the linear relationship relating LNC to A_g	-
b_{LNC}	Slope of the linear relationship relating LNC to A_g	g^{-1} N
b_N	Slope of the linear relationship relating N_{plant} to A_g	g^{-1} N
$C_{a,ref}$	Reference atmospheric CO_2 partial pressure	Pa
C_g	Mean atmospheric CO_2 partial pressure during the preceding month	Pa
C_i	Leaf intercellular carbon concentration	g CO2. cm^{-3} air
k_3	Slope of the linear relationship relating N_{pa} to $V_{c,ref}$	µmol CO2. mmol^{-1} N.s^{-1}
LNC	Leaf nitrogen content	g N. g^{-1} leaf DM

LNC_{min}	Critical LNC below which the photosynthetic activity stops	g N. g^{-1} leaf DM
LNC_{opt}	LNC for which the photosynthetic activity may be optimal	g N. g^{-1} leaf DM
LNC_{ref}	LNC associated with the reference gross assimilation rate $A_{g,ref}$	g N. g^{-1} leaf DM
N_{pa}	Leaf photosynthetic protein content per unit area	g Np. m^{-2} leaf
N_{plant}	Plant nitrogen content	kg N. kg^{-1} DM
N_{demand}	Nitrogen demand of the plant	g N
N_{pot}	Amount of nitrogen that root are potentially able to extract	g N
p_1	Coefficient representing the extent to which the to ratio is modified by the CO_2 partial pressure	-
p_2	Coefficient representing the extent to which the to ratio is modified by the temperature	-
p_3	Coefficient representing the effect of CO_2 partial pressure on k_3	µmol CO2. g^{-1} $N.s^{-1}$
*PP*2	Half saturation constant for CO2 fixation	g CO2.cm^{-3} air
*PP*8	Half saturation constant	g N. g^{-1} C
*PP*9	Minimal level of shoot N:C ratio for CO2 fixation	g N. g^{-1} C
RGN	Shoot actual N:C ratio	g N. g^{-1} C
$T_{K,ref}$	Reference air temperature	K
T_g	Mean air temperature of the preceding month	°C
$V_{c,ref}$	Maximal rate of RuBP regeneration at reference temperature and CO_2 partial pressure	µmol CO2..$m^{-2}.s^{-1}$
$V_{j,ref}$	Maximal rate of Rubisco at reference temperature and CO_2 partial pressure	µmol CO2..$m^{-2}.s^{-1}$
Temperature submodels		
K_{T1}	Lower temperature for 5% of maximum growth	°C
K_{T2}	Lower temperature for 95% of maximum growth	°C
K_{T3}	Upper temperature for 95% of maximum growth	°C
K_{T4}	Upper temperature for 5% of maximum growth	°C

q	Curvature coefficient	-
R	Whole plant respiration	µmol CO2. $m^{-2}.s^{-1}$
T	Atmospheric temperature	°C
T_{lag}	Lagged temperature used as a surrogate for soil temperature	°C
T_{min}	Minimum air temperature for photosynthetic activity	°C
T_{max}	Maximum air temperature for photosynthetic activity	°C
T_{opt}	Optimal air temperature for photosynthetic activity	°C
T_{ref}	Temperature at which the reference CO_2 assimilation rate $A_{g,ref}$ is measured	°C
$T_h(\Psi_s)$	Maximum air temperature for photosynthetic activity according to the soil water potential (Φ=2)	°C
$T_o(\Psi_s)$	Optimum air temperature for photosynthetic activity according to the soil water potential (Φ=2)	°C
ΔHa	Activation energy	$J.mol^{-1}$
ΔHd	Deactivation energy	$J.mol^{-1}$
ΔS	Entropy factor	$J.K^{-1}.mol^{-1}$
$\mu(\Psi_s)$	Maximum of the response function according to the soil water potential (Φ=1)	-
Water submodels		
AL	Proportion of radiation intercepted by established and seedling plants	-
$f_{W,sat}$	Parameter for f_W	-
K_{W1}	Soil water content threshold for water use	-
K_{W2}	Soil water content threshold for growth	-
K_{W3}	Water-filled pore space (computed as $\theta/\ \theta_s$) threshold for waterlogging	-
K_{W4}	Curvature of growth limitation by waterlogging	-
PET	Potential evapotranspiration	mm
TR	Actual transpiration rate	mm

Ψ	Soil water potential	m
Ψ_b	Parameter for f_W	m
Ψ_s	Parameter for f_W	m^{-1}
θ	Soil volumetric water content	$cm^3.cm^{-3}$
θ_c	Volumetric soil water content below which transpiration decreases	$cm^3.cm^{-3}$
θ_{fc}	Volumetric soil water content at field capacity	$cm^3.cm^{-3}$
θ_r	Residual volumetric water content	$cm^3.cm^{-3}$
θ_s	Volumetric soil water content at saturation	$cm^3.cm^{-3}$
θ_{wp}	Volumetric soil water content at wilting point	$cm^3.cm^{-3}$
Maintenance respiration submodels		
B_r	Root biomass	g
B_s	Shoot biomass	g
B_{tot}	Total biomass	g
C_{plant}	Plant nitrogen content	kg C. kg^{-1} DM
$g_{T,r}$	Temperature dependence of root respiration (Φ=3)	-
$g_{T,sh}$	Temperature dependence of shoot respiration (Φ=3)	-
I_{fac}	Degree of inhibition of mitochondrial respiration during day time (Φ=4)	-
K_{maint}	Maintenance respiration parameter	kg $C.kg^{-1}$
LAI	Leaf area index	m^{-2} leaf.m^{-2} soil
$m_{r,i}$	Maintenance costs for different age categories i of the root	kg $C.m^{-2}.d^{-1}$
$m_{sh,i}$	Maintenance costs for different age categories i of the shoot	kg $C.m^{-2}.d^{-1}$
$N_{plant,ref}$	Reference plant nitrogen content	kg N. kg^{-1} DM
R_{fac}	Dependence of maintenance respiration to $V_{c,max}$	-

$R_{m,max}$	Maximal respiration rate	g C.g^{-1} shoot.d^{-1}
$R_{m,ref}$	Reference respiration rate in controlled conditions	d^{-1}
$R_{m,root}$	Root maintenance respiration coefficient	g C.(g DM) $^{-1}$.d^{-1}
SS	Conversion coefficient from instantaneous (µmol CO2.m^{-2}.s^{-1}) to daily (g C.m^{-2}.d^{-1}) photosynthesis	g C.s. (µmol CO2) $^{-1}$. d^{-1}
$T_{sh,0}$, $T_{r,0}$	Reference temperature for Q10 response function	°C
$W_{r,i}$	Root structural dry matter components	kg C. m^{-2}
$W_{sh,i}$	Shoot structural dry matter components	kg C. m^{-2}
Transpiration submodels		
G_{CO2}	Stomatal conductance for CO_2	cm.s^{-1}
PT3	Diffusivity of water vapor relative to that of CO_2	-
PT4	Number of second of transpiration per day	-
$r_{s,rs}(l)$	Resistance for radial flow across the roots in soil layer *l*	d
$r_{s,rs}(l)$	Resistance for radial flow to root surfaces in soil layer *l*	d
$U_{w,ref}$	Nitrogen uptake rate at reference temperature and soil moisture	mg N. g^{-1} root.h^{-1}
S_{sh}	Shoot surface	cm^2.m^{-2}
T_0	Reference temperature for Q10 function	°C
TR_p	Potential transpiration rate	mm.d^{-1}
W_i	Water vapor pressure in the shoot	g H_2O.cm^{-3} air
W_a	Water vapor pressure in the air	g H_2O.cm^{-3} air
Z_l	Depth of soil layer *l*	m
π_l	Effective root density profile in layer *l*	-
θ_{hi}	Highest soil water content allowing nitrogen extraction	cm^3.cm^{-3}
θ_{low}	Lowest soil water content allowing nitrogen extraction	cm^3.cm^{-3}

Θ_l	Absolute soil water content in layer *l* computed as $(\theta_l - \theta_{wp})/(\theta_{fc} - \theta_{wp})$	-
Ψ_l	Soil water potential in layer *l*	m
Ψ_r	Root water potential (assumed homogeneous)	m
Nitrogen uptake submodels		
$a_{N,T}$	Relative availability of ammonium and nitrate to the plant at soil temperature *T*	-
$B_{r,ref}$	Root biomass corresponding to δ_{ref}	Kg
cov	Individual shoot cover	m^2
D	Axes density	axes.m^{-2} soil
F	Factor accounting for the fact that plant cannot entirely restore their N level in a day	-
f_{act}	Part of active root for N uptake	active root.$root^{-1}$
$F_{N,max}$	Maximal root nitrogen fixation capacity	gN.m^{-2} root.d^{-1}
$K_{C,un}$	Root activity parameter	kg C. kg^{-1}
K_{Neff}	Michaelis-Menten constant	kg N.m^{-2}
$K_{N,un}$	Root activity parameter	kg N. kg^{-1}
K_U	Michaelis-Menten coefficient of inhibition of root absorption activity (N in soil solution)	-
K_F	Michaelis-Menten coefficient of inhibition of root absorption activity (N2 fixation)	-
lwr	Surface:weight root ratio	m^2.g^{-1} root
N_{amm}	Ammonium nitrogen in soil	kg N. m^{-2}
N_{nit}	Nitrate nitrogen in soil	kg N. m^{-2}
N_l	Soil nitrogen content in layer *l*	
N_s	Total available N in the soil	g N.m^{-2}
Nu_l	Concentration in nutrient *Nu* in layer *l*	kg Nu. m^{-2}
NUE	Nitrogen use efficiency	µmol CO_2. g^{-1} $N.s^{-1}$
R_i	Root length of species *i*	m.m^{-2}

sd	Soil depth	Cm
sk_{N}	Soil N diffusion rate	m^3 soil.m^{-2} root.d^{-1}
$Stol_{ratio}$	Fraction of stolons, rhizomes or tap roots which are assumed to be metabolically inactive for N acquisition	-
T_s	Soil temperature	°C
$U_{N,max}$	Maximal root nitrogen uptake capacity	gN.m^{-2} root.d^{-1}
β_l	Root distribution factor for layer l	-
δ_{ref}	Reference growth rate	kg DM.ha^{-1}
σ_N	Root activity parameter	kg N. kg^{-1}.d^{-1}
v_i	Root activity weighting parameters	-
χ_{Nu}	Root activity parameter for nutrient Nu	-
Submodels for carbon allocation		
$a(G_{CO2})$	Ordinate of the relationship between carbohydrates allocation and stomatal conductance	-
a_{part}	Ordinate of the relationship between carbohydrates allocation and water availability	-
$b(G_{CO2})$	Slope of the relationship between carbohydrates allocation and stomatal conductance	m^2.s.mol^{-1}
b_{part}	Slope of the relationship between carbohydrates allocation and water availability	-
C_{struct}	Concentration of C substrate in plant structural dry matter	kg C. kg^{-1} struct. DM
$CR_{sh,pot}$	Potential growth of all growing leaves	g DM. $axis^{-1}$.d^{-1}
DD	Degree-days since the beginning of the current developmental stage	°days
f_r	Fraction of the structural dry matter in the root	-
f_{sh}	Fraction of the structural dry matter in the shoot	-
FL	Length of the flowering part of the reproductive stage	days
K_{A1}	Target root:shoot ratio during vegetative growth	-
K_{A2}	Target root:shoot ratio after flowering	-

K_{A3}	Maximum allocation to reproductive structure	-
K_{F1}	Degree-day sum for commencement of flowering	°days
K_{F2}	Maximum length of flowering period	days
k_{cn}	Inherent rate of maximal relative growth modulated by C and N substrates availability	d^{-1}
LA	Leaf area per axis	m^2 leaf $axis^{-1}$
$N_{pac,z}$	Coordinated leaf photosynthetic protein content in layer z	g Np. m^{-2}
N_{struct}	Concentration of N substrate in plant structural dry matter	kg N. kg^{-1} struct. DM
NP_{plant}	N fraction in shoots proteins	g $N.g^{-1}$ DM
P	Allocation rate between shoot and root system	-
Q	Allocation rate between aerial structure and leaf proteins	-
q	Degree of allocation control	-
RS	Root:shoot ratio	$g.g^{-1}$
RS_{tar}	Genetically determined "target" root:shoot ratio	$g.g^{-1}$
α, β	Allometric coefficients	-
$\lambda_{C,max}$	Maximal fraction of carbohydrates allocated to aboveground biomass	-
$\lambda_{C,min}$	Minimal fraction of carbohydrates allocated to aboveground biomass	-
$\lambda_{C,seed}$	Fraction of carbohydrates allocated to reproductive organs	-
ρ	Shoot:root ratio	$g.g^{-1}$
ρ_{max}	Shoot:root ratio when there is neither nitrogen nor water limitation	$g.g^{-1}$
σ_C	Net photosynthesis per axis	gC. $axis^{-1}.d^{-1}$
Submodels for nitrogen allocation		
N_r	N:C ratio of root	g N. g^{-1} C
$N_{r,min}$	Minimum root C:N ratio for N translocation	g N. g^{-1} C

$N_{r,max}$	Root C:N ratio for which N translocation is maximal	g N. g^{-1} C
N_s	N:C ratio of shoot	g N. g^{-1} C
$N_{s,min}$	Minimum shoot C:N ratio for N translocation	g N. g^{-1} C
$N_{s,max}$	Shoot C:N ratio for which N translocation is maximal	g N. g^{-1} C
RNC	Root nitrogen content	g $N.m^{-2}$
$\lambda_{N,max}$	Maximal fraction of root N translocated to shoot	d^{-1}

REFERENCES

Johnson, I.R. 2013. PlantMod: exploring the physiology of plant canopies. IMJ Software, Dorrigo, NSW, Australia. *www.imj.com.au/software/plantmod*.

Hunt, H.W., Trlica, M.J., Redente, E.F., Moore, J.C., Delting, J.K. Kittel, T.G.F., Walter, D.E., et al. 1991. Simulation model for the effects of climate change on temperate grassland ecosystems. *Ecol. Mod.* 53, 205-246.

Moore, A.D., Donnelly, J.R., Freer, M. 1997. GRAZPLAN: decision support systems for Australian grazing entreprises. III. Pasture growth and soil moisture submodels, and the GrassGro DSS. *Agricult. Sys.* 55 (4), 535-582.

Riedo, M., Grub, A., Rosset, M., Fuhrer, J. 1998. A pasture simulation model for dry matter production, and fluxes of carbon, nitrogen, water and energy. *Ecol. Mod.* 105, 141-183.

Schapendonk, A.H.C.M., Stol, W., van Kraalingen, D.W.G., Bouman, B.A.M. 1998. LINGRA, a sink/source model to simulate grassland productivity in Europe. *Eur. J. Agron.* 9, 87-100.

Schippers, P., Kropff, M.J. 2001. Competition for light and nitrogen among grassland species: a simulation analysis. *Fun. Ecol.* 15, 155-164.

Soussana J.-F., Maire, V., Gross, N. et al. 2012. Gemini: a grassland model simulating the role of plant traits for community dynamics and ecosystem functioning. Parameterization and evaluation. *Ecol. Mod.* 231: 134-145.

Taubert, F., Frank, K., Huth, A. 2012. A review of grassland models in the biofuel context. *Ecol. Mod.* 245, 84-93.

Thornley, J.H.M., Verberne, EL.J. 1989. A model of nitrogen flows in grassland. *Plant Cell Environ.* 12, 863-886.

VI. Utilisation de Nemossos pour explorer les mécanismes à l'origine de la coexistence.

Manuscrit correspondant:

Lohier, T., Jabot, F., & Deffuant, G. (in prep). Storage effect and intransitivity in plant communities: A virtual experiment with the mechanistic trait-based model Nemossos.

Storage effect and intransitivity in plant communities: a virtual experiment with the mechanistic trait-based model Nemossos.

Théophile Lohier[1*], Franck Jabot[1,] and Guillaume Deffuant[1]

Forthcoming submission in *Ecological Modelling*

[1]LISC - Laboratoire d'Ingénierie pour les Systèmes complexes, IRSTEA, 9 avenue Blaise Pascal, CS 20085, 63178 Aubière, France.

*Corresponding author: theophile.lohier@gmail.com

ABSTRACT

Local coexistence of non-neutral species competing in spatially homogeneous environmental conditions can be explained by three main processes: immigration from the surrounding regional pool of inferior competitors, temporal environmental variability and the associated storage effect, and intransitive competition. We here investigate the potential and mechanics of the last two processes in grassland communities with a series of virtual experiments based on a realistic trait-based model of plant community dynamics and on realistic time-series of environmental conditions. We specifically address the following questions: (1) Are species competitive hierarchies perfectly transitive in constant and temporally variable environmental conditions, as often assumed in plant community ecology? (2) Does temporal environmental variability prevents competitive exclusion, as predicted by storage effect theory, and with which magnitude? (3) What is the respective influence of intra-seasonal and inter-seasonal variability on species coexistence? (4) Are functional distances among species good predictors of species competitive outcomes? Our virtual experiments evidence 1) that intransitivity can occur in temporally variable environments; 2) that strong storage effects are likely, leading to the coexistence of very dissimilar plant strategies on long time periods, with realistic levels of environmental temporal variability; 3) that intra-seasonal variability seems to be the major driver of the storage effect; 4) that functional distances among species are good predictors of their coexistence. This study more generally highlights the formidable potential of mechanistic ecological models to test the relevance of ecological theory for real systems.

1. INTRODUCTION

Classical competition theory predicts that competitive exclusion occurs when species with similar resource requirements are competing for shared and limited resources (Gause, 1934). Plant species have very similar resource requirements and a limited number of ways to acquire them (Lambers et al., 2008). Competitive exclusion should therefore prevent the maintenance of large diversity levels in plant communities (Tilman & Pacala, 1993). Yet most natural plant communities exhibit large species richness (Kreft and Jetz, 2007).
Multiple processes and theories have been proposed to reconcile the predictions of competition theory with empirical observations (Chesson, 2000). To explain the local coexistence of plant species in spatially homogeneous environmental conditions, three major processes can be invoked: the recurrent immigration of inferior competitors (Pulliam, 1988; Mouquet and Loreau, 2003), the temporal environmental variability and the associated storage effect (Warner and Chesson, 1985), and the intransitivity in competitive hierarchies (Aarssen, 1992; Kerr et al., 2002; Laird and Schamp, 2006).

While immigration of inferior competitors does play a role in community dynamics (Eriksson, 1996), this process cannot explain alone all cases of local plant coexistence, especially in systems like grasslands in which reproduction is principally vegetative (Benson and Hartnett, 2006), and immigration is consequently strongly limited (Turnbull et al., 2000). The storage effect in plant communities has received a detailed attention in arid systems dominated by annual plants (eg., Angert et al., 2009), but less so in temperate systems dominated by perennial species (but see Adler et al., 2006). The potential of competitive intransitivity to explain local plant coexistence has neither received much attention in plant systems (but see e.g., Lankau et al., 2011; Soliveres et al., 2015). Most importantly, a careful examination of the importance of these last two processes in real plant systems is difficult, since competitive

trials between subsets of species become quickly numerous as species richness increases, and even more so if one wants to assess the interaction of these competitive trials with environmental variability.

The aim of this study is therefore to assess the potential importance of the storage effect and of competitive intransitivity in grassland plant systems thanks to virtual experiments. These virtual experiments are based on the model Nemossos, a recently developed mechanistic model of plant community dynamics that is based on plant functional traits and integrates the carbon, water and nitrogen cycles (Lohier et al., manuscript 3). This virtual experimental approach presents the double advantage of providing results associated to realistic settings, while being as flexible as more theoretical approaches.

More specifically, we assess four main questions: (1) are species competitive hierarchies perfectly transitive in constant and temporally variable environmental conditions, as often assumed in plant community ecology? (2) Does temporal environmental variability prevents competitive exclusion, as predicted by storage effect theory, and with which magnitude? (3) What is the respective influence of intra-seasonal and inter-seasonal variability on species coexistence? (4) Are functional distances among species good predictors of species competitive outcomes?

2. METHODS

2.1. Model description

Nemossos is a spatially-explicit individual-based model designed to simulate the vegetative growth of grassland communities within a plot of finite dimension with toroidal boundary conditions. It runs on a daily time step and integrates the carbon, water, and nitrogen cycles

All the process modules are based on commonly measured plant functional traits in a parsimonious fashion. Competition between individuals occurs through resource depletion in the soil and through shading between plants.

Individual positions in the plot are described by their two dimensional coordinates. Each individual is described by its above- and below-ground biomass and the spatial extension of these two compartments is represented by two distinct cylinders. The height and radius of these cylinders increase with compartment biomass according to species-specific allometric rules. In total, Nemossos contains 30 parameters per individual corresponding to measurable plant functional traits. 22 of these traits are used to compute basic physiological processes including photosynthesis, transpiration, resource uptake and allocation of assimilates. The 8 remaining parameters enable to determine above- and below-ground plant geometry. Moreover it needs as inputs 34 atmospheric and soil variables. The model structure and the representation of the physiological processes driving individual plant vegetative growth are described in details in Lohier et al. (manuscript 3).

2.2. Design of the virtual experiment

We generated 10 realistic virtual perennial grass species with strategies ranging from exploitative to conservative. The exploitative strategies are defined by high resource acquisition made possible through high photosynthetic capacity (A_{max}), high specific leaf area (SLA) and high leaf nitrogen content (LNC_{max}), which is positively correlated with high nitrogen resource uptake rate (U_{max}, Maire et al., 2009). Moreover these strategies are associated with high tissue turnover realized through low shoot lifespan (SL) and high respiration rates of the roots ($R_{d,r}$) and shoots ($R_{d,sh}$). The species with conservative strategies present opposite suite of traits (Tab. 1). Other trait values were assumed constant across

simulations and were set according to empirical observations drawn from the literature (Table S1).

From this pool of virtual species, we assembled 45 2-species mixtures in a full factorial design. Each mixture included 10 individuals of each species, weighting 70 mg (Table S1). The dynamics of these mixtures were simulated for ten years in a plot of 20x20 cm^2 with soil depth of 50 cm. Each year consisted in a growing season of 6 months between mid-April and mid-October, followed by a mowing event at a height of 3 cm. Plant growth during winter was neglected so that plant biomass at the beginning of a growing season equaled its biomass after harvest at the end of the previous one. Soil nitrogen content at the beginning of the growing seasons was set to 0.05 $mg.cm^{-3}$, which is in the range of reported values for the Cedar Creek Ecosystem Science Reserve (Tilman et al., 2012). The day length as well as the daily precipitation amount, temperature and relative humidity were parameterized from the climate data available for the Cedar Creek Ecosystem Science Reserve (http://www.cedarcreek.umn.edu/research/weather). As these temporal series do not include the daily solar irradiance, we used the model developed by Winslow et al. (2001) to estimate it from temperature and precipitation data.

We implemented three scenarios to test the impact of environmental variability on species coexistence. In scenario S1, climate was constant across and within seasons with daily values of climate variables equal to the average values across the season 1995. In scenario S2, climate varied within the season but not across seasons. The intra-seasonal variability was obtained by using the daily values observed in Cedar Creek during the year 1995, and this climatic trajectory was looped 10 times. In scenario S3, climate varied both within and across

seasons with daily values equal to the empirical values reported between years 1995 and 2005 in Cedar Creek.

2.3. Data analysis

The relative abundance of a species was computed as its aerial biomass divided by the total aerial biomass of the mixture at the end of the 10 simulated years. For each scenario, the number of mixtures N_{dom} for which a species achieved a relative abundance larger than 0.5 served as a measure of its overall competitive efficiency. This measure was further used to compute the "relative variance" index of competitive intransitivity proposed by Laird and Schamp (2006) in the three environmental scenarios.

Species proportions in mixture were further computed at the end of each growing season, and the time duration before competitive exclusion occurs t_{ex} was defined as the number of years during which the dominant species proportion remained smaller than 0.9. Functional distance between species was quantified through the difference in shoot lifespans, ΔSL, which is a good proxy for the position of the species on the exploitation-conservation axis (Wright et al. 2004). And the influence of this functional distance between species on their coexistence was assessed.

3. RESULTS

3.1. Optimal strategy according to climatic variability

The optimal strategy in constant climatic conditions was found to be rather conservative (SL=140 days, Fig. 1A). It shifted towards a more intermediary strategy (SL=110 days), when intra-seasonal climatic variability was added (Fig. 1B) and even more so (SL=100 days) when both intra and inter-seasonal climatic variability were considered (Fig. 1C).

3.2. Nestedness and intransitivty in competitive trials

We observed a perfectly nested competitive hierarchy in scenario S1 with constant environmental conditions (Fig. 1A, Fig. 2B) with an intransitivity index equal to 1 (meaning that the competition matrix is completely transitive). This was also the case in scenario S3 with both intra and inter-seasonal variability (Fig. 1C). In contrast, the competitive matrix was partially intransitive in scenario S2 with intra-seasonal variability only (Fig. 1B), with an intransitive index equal to 0.85. More precisely, we observed competitive loops among the virtual species in this scenario, for instance species 5 > species 6 > species 4 > species 5 (Fig 2D, Fig S2).

3.3. Effects of environmental variability on species coexistence

In constant environmental conditions (scenario S1), competitive exclusion was observed in 82% of the mixtures, and coexistence after 10 years of simulations was achieved only among the most conservative species (Fig. 2A). In contrast, in both scenarios S2 and S3, species mixtures were still coexisting after 10 years in the vast majority of cases (87 and 76% respectively, Fig. 2C,E). This was further evidenced in the fact that dominance in species abundances was lower in scenarios S2 and S3 than in scenario S1 (Fig. 3, p-values $< 10^{-7}$ for both scenarios). In these coexisting mixtures, dominance was lower in mixtures with more similar species, leading to a pattern of darker cell values along the diagonal in the competitive dominance matrices (Fig. 2D,F). In these mixtures, we further recovered the often assumed bell shape dominance pattern when plotting dominance against functional distance (Fig. 4, Fig. S2), implying that dominance increases when functional distance among competitive species increases (Fig. 4). Interestingly, these various effects of environmental variability on species coexistence was recovered in both scenarios S2 and S3, with little difference among

these two scenarios (Figs. 2 and 3), meaning that inter-seasonal environmental variability had little effects on top of intra-seasonal variability on mixture dynamics.

4. DISCUSSION

This study points that in both constant and temporally-variable environmental conditions, competition between plants species mainly leads to a perfectly nested hierarchy (Fig. 2), although some level of intransitivity seems possible (Fig. 2C). From the literature, the importance of intransitivity for plant coexistence is uncertain, with experimental studies mainly reporting the absence of intransitivity (e.g., Aarssen 1992) while recent indirect evidence based on static observational data suggests that intransitivity may be more important than previously thought in grassland plant communities (Soliveres et al. 2015). The fact that we recovered intransitivity in the second scenario with intra-seasonal variability suggests that experiments performed in controlled environmental conditions may not be able to detect the presence of intransitivity, thereby underestimating its importance in real settings. Besides, we used in our experiments ten virtual species evenly spaced along the exploitation-conservation axis (Table 1). More similar species should be even more likely to present some levels of competitive intransitivity.

The second main result of our study is that storage effect is very strong under these realistic experimental settings, enabling the coexistence for more than ten years of widely functionally dissimilar species (Fig. 3). Our finding that this storage effect mainly stems from intra-seasonal variability is striking. Most ecological studies on the storage effect document environmental variability at yearly time scales (Adler et al., 2006; Angert et al., 2009). Our results highlight the potentially key importance of finer scale temporal variability.

The third main result of our study is that we recover a bell-shape relationship between plant functional traits and their competitive ability (Fig. 4). Such a relationship is assumed in most theoretical studies of community ecology (e.g., Gravel et al., 2006) and is at the heart of the concept of environmental filtering in functional ecology (Keddy, 1992; Weiher and Keddy, 1995). Our virtual experiments bring concrete support for these widely shared visions of community assembly.

It is worth noting that the mechanistic model Nemossos does not include any phenological differences between species. Such phenological effects are likely to interact with temporal environmental variability, and may further increase the magnitude of the storage effect in real plant communities, and maybe also the importance of competitive intransitivity. More generally, although there is room for further progress in the mechanistic description of plant dynamics, this study points out the formidable potential of virtual experiments to tackle empirical challenges and fertilize progress in our understanding of community dynamics.

AKNOWLEDGEMENTS

T.L was funded by the Institut national de Recherche en Sciences et Technologie pour l'Environnement et l'Agriculture (IRSTEA) and the Regional Council of Auvergne.

REFERENCES

Aarssen, L. W. (1992). Causes and consequences of variation in competitive ability in plant communities. *Journal of Vegetation Science*, *3*(2), 165-174.

Adler, P. B., HilleRisLambers, J., Kyriakidis, P. C., Guan, Q., & Levine, J. M. (2006). Climate variability has a stabilizing effect on the coexistence of prairie grasses. *Proceedings of the National Academy of Sciences*, *103*(34), 12793-12798.

Angert, A. L., Huxman, T. E., Chesson, P., & Venable, D. L. (2009). Functional tradeoffs determine species coexistence via the storage effect. *Proceedings of the National Academy of Sciences*, *106*(28), 11641-11645.

Benson, E. J., & Hartnett, D. C. (2006). The role of seed and vegetative reproduction in plant recruitment and demography in tallgrass prairie. *Plant Ecology*, *187*(2), 163-178.

Chesson, P. L., & Warner, R. R. (1981). Environmental variability promotes coexistence in lottery competitive systems. *American Naturalist*, 923-943.

Chesson, P. L. (1985). Coexistence of competitors in spatially and temporally varying environments: a look at the combined effects of different sorts of variability. *Theoretical Population Biology*, *28*(3), 263-287.

Chesson, P. L., & Grubb, P. J. (1990). Geometry, heterogeneity and competition in variable environments [and discussion]. *Philosophical Transactions of the Royal Society B: Biological Sciences*, *330*(1257), 165-173.

Chesson, P. (2000). Mechanisms of maintenance of species diversity. *Annual review of Ecology and Systematics*, 343-366.

Diaz, S., Cabido, M., & Casanoves, F. (1998). Plant functional traits and environmental filters at a regional scale. *Journal of Vegetation Science*, *9*(1), 113-122.

Ellner, S. (1987). Alternate plant life history strategies and coexistence in randomly varying environments. *Vegetatio*, *69*(1-3), 199-208.

Eriksson, O. (1996). Regional dynamics of plants: a review of evidence for remnant, source-sink and metapopulations. *Oikos*, 248-258.

Fargione, J., Brown, C. S., & Tilman, D. (2003). Community assembly and invasion: an experimental test of neutral versus niche processes. *Proceedings of the National Academy of Sciences*, *100*(15), 8916-8920.

Gause, G. F. (1934). The struggle for existence Williams and Wilkins. *Baltimore, Maryland*.

Gravel, D., Canham, C. D., Beaudet, M., & Messier, C. (2006). Reconciling niche and neutrality: the continuum hypothesis. *Ecology Letters*, *9*(4), 399-409.

Grime, J. P. (1977). Evidence for the existence of three primary strategies in plants and its relevance to ecological and evolutionary theory. *American naturalist*, 1169-1194.

Grubb, P. J. (1977). The maintenance of species-richness in plant communities: the importance of the regeneration niche. *Biol. Rev*, *52*(1), 107-145.

Hector, A., & Bagchi, R. (2007). Biodiversity and ecosystem multifunctionality. *Nature*, *448*(7150), 188-190.

Hutchinson, G. E. (1959). Homage to Santa Rosalia or why are there so many kinds of animals?. *American naturalist*, 145-159.

Keddy, P. A. (1992). Assembly and response rules: two goals for predictive community ecology. *Journal of Vegetation Science*, *3*(2), 157-164.

Kerr, B., Riley, M. A., Feldman, M. W., & Bohannan, B. J. (2002). Local dispersal promotes biodiversity in a real-life game of rock–paper–scissors. *Nature*, *418*(6894), 171-174.

Kraft, N. J., Valencia, R., & Ackerly, D. D. (2008). Functional traits and niche-based tree community assembly in an Amazonian forest. *Science*, *322*(5901), 580-582.

Kreft, H., & Jetz, W. (2007). Global patterns and determinants of vascular plant diversity. *Proceedings of the National Academy of Sciences*, *104*(14), 5925-5930.

Lambers, H., Chapin III, F. S., & Pons, T. L. (2008). *Plant Physiological Ecology*. Springer Science & Business Media.

Lankau, R. A., Wheeler, E., Bennett, A. E., & Strauss, S. Y. (2011). Plant–soil feedbacks contribute to an intransitive competitive network that promotes both genetic and species diversity. *Journal of Ecology*, *99*(1), 176-185.

Laird, R. A., & Schamp, B. S. (2006). Competitive intransitivity promotes species coexistence. *The American Naturalist*, *168*(2), 182-193.

Lohier, T., Jabot, F. & Deffuant, G. (in prep). Mechanistic trait-based plant community dynamics: the Nemossos model.

McKane, R. B., Johnson, L. C., Shaver, G. R., Nadelhoffer, K. J., Rastetter, E. B., Fry, B., ... & Murray, G. (2002). Resource-based niches provide a basis for plant species diversity and dominance in arctic tundra. *Nature*, *415*(6867), 68-71.

Maire, V., Gross, N., da Silveira Pontes, L., Picon‐Cochard, C., & Soussana, J.F. 2009. Trade−off between root nitrogen acquisition and shoot nitrogen utilization across 13 co−occurring pasture grass species. *Fun. Ecol.* 23(4): 668-679.

Mouquet, N., & Loreau, M. (2003). Community patterns in source‐sink metacommunities. *The american naturalist*, *162*(5), 544-557.

Newman, E. I. (1982). Niche separation and species diversity in terrestrial vegetation. *Special publications series of the British Ecological Society*.

Pulliam, H. R. (1988). Sources, sinks, and population regulation. *American naturalist*, 652-661.

Reineking, B., Veste, M., Wissel, C., & Huth, A. (2006). Environmental variability and allocation trade-offs maintain species diversity in a process-based model of succulent plant communities. *Ecological Modelling*, *199*(4), 486-504.

Soliveres, S., Maestre, F. T., Ulrich, W., Manning, P., Boch, S., Bowker, M. A., ... & Gallardo, A. (2015). Intransitive competition is widespread in plant communities and maintains their species richness. *Ecology letters*, *18*(8), 790-798.

Thompson, K., Askew, A. P., Grime, J. P., Dunnett, N. P., & Willis, A. J. (2005). Biodiversity, ecosystem function and plant traits in mature and immature plant communities. *Functional Ecology*, *19*(2), 355-358.

Tilman, D., & Pacala, S. (1993). The maintenance of species richness in plant communities. *Species diversity in ecological communities*, 13-25.

Tilman, D., Reich, P. B., Knops, J., Wedin, D., Mielke, T., & Lehman, C. (2001). Diversity and productivity in a long-term grassland experiment. *Science*, *294*(5543), 843-845.

Tilman, D., Reich, P. B., & Isbell, F. (2012). Biodiversity impacts ecosystem productivity as much as resources, disturbance, or herbivory. *Proceedings of the National Academy of Sciences*, *109*(26), 10394-10397.

Turnbull, L. A., Crawley, M. J., & Rees, M. (2000). Are plant populations seed‐limited? a review of seed sowing experiments. *Oikos*, *88*(2), 225-238.

Warner, R. R., & Chesson, P. L. (1985). Coexistence mediated by recruitment fluctuations: a field guide to the storage effect. *American Naturalist*, 769-787.

Warren, J., & Topping, C. (2004). A trait specific model of competition in a spatially structured plant community. *Ecological modelling*, *180*(4), 477-485.

Weiher, E., & Keddy, P. A. (1995). Assembly rules, null models, and trait dispersion: new questions from old patterns. *Oikos*, 159-164.

Winslow, J. C., Hunt, E. R., & Piper, S. C. (2001). A globally applicable model of daily solar irradiance estimated from air temperature and precipitation data. *Ecological Modelling*, *143*(3), 227-243.

Wright, I.J., et al. (2004). The worldwide leaf economics spectrum. *Nature, 428*(6985), 821-827.

TABLES

Tab.1. Plant functional traits of the 10 virtual species. The values of the other traits used in the model Nemossos are given in Table S1.

Sp	**SL** (day)	$\boldsymbol{A_{max}}$ ($\mu mol.m^{-2}.s^{-1}$)	***SLA*** ($cm^2.g^{-1}$)	$\boldsymbol{LNC_{max}}$ ($mg.g^{-1}$)	$\boldsymbol{R_{d,r}}$ ($nmol.g^{-1}.s^{-1}$)	$\boldsymbol{R_{d,sh}}$ ($nmol.g^{-1}.s^{-1}$)	$\boldsymbol{U_{N,max}}$ ($mg.g^{-1}.d^{-1}$)
1	60	15.3	286	348	30.9	31.8	0.61
2	70	14.4	267	325	28.3	30.8	0.456
3	80	13.7	248	307	25.8	29.6	0.36
4	90	13.0	229	291	23.1	28.5	0.29
5	100	12.5	210	278	20.6	27.4	0.23
6	110	12.1	191	267	18.0	26.3	0.20
7	120	11.7	172	257	15.4	25.1	0.17
8	130	11.3	153	248	12.8	24.0	0.14
9	140	11.0	134	240	10.2	22.9	0.12
10	150	10.7	115	233	7.7	21.7	0.11

FIGURES

Fig. 1. Number of mixtures N_{dom} for which a species is dominant as a function of its shoot lifespan (*SL*) in the three scenarios simulated.

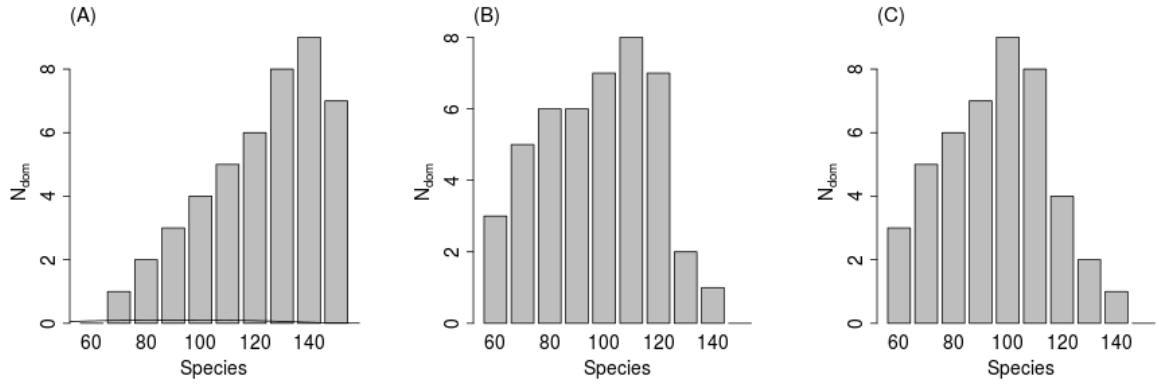

Fig. 2. Time to exclusion (panels A, C, E) and dominance (panels B, D, F) in the three scenarios respectively. For each species mixture, the color of the corresponding case depicts: in panels A, C, E, the time to exclusion, ranging from no exclusion (in white) to very quick exclusion (two years, in black); in panels B, D, F, the relative abundance of species 1, ranging from 0 (in white) to 1 (in black).

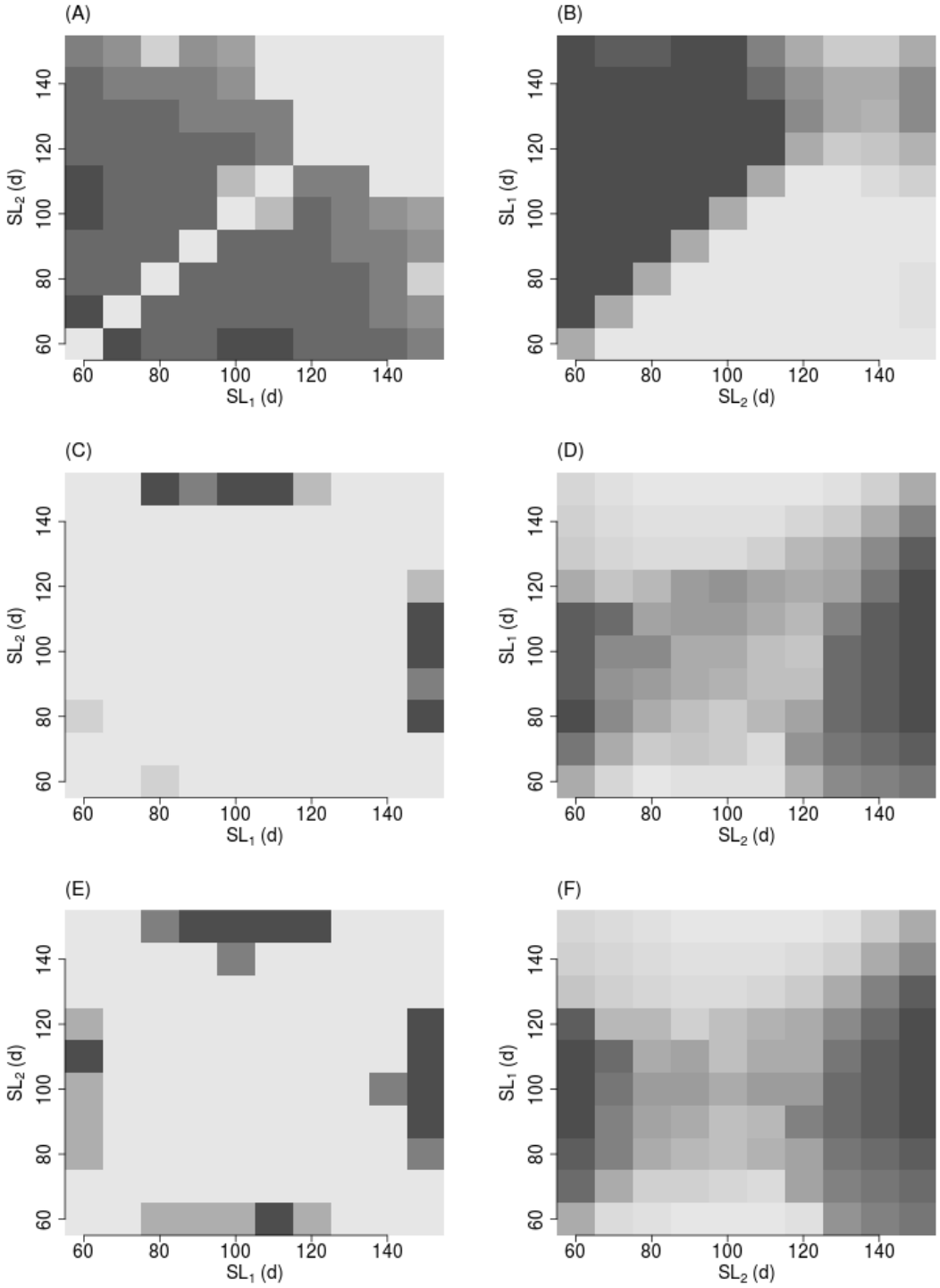

Fig. 3. Effects of intra and inter-seasonal variability of environmental conditions on species coexistence quantified through the final relative abundance of the dominant species in the 2-species mixtures.

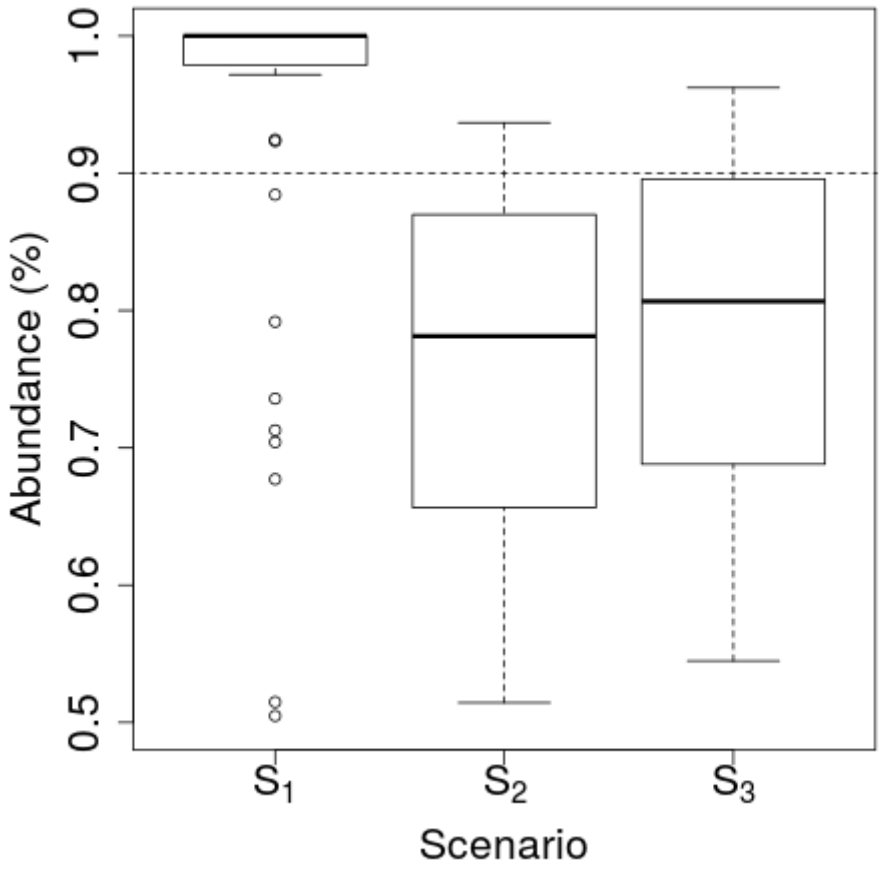

Fig. 4. Relationship between the final relative abundance of a species *i* and its functional distance (ΔSL) with the best competitor in the three environmental scenarios.

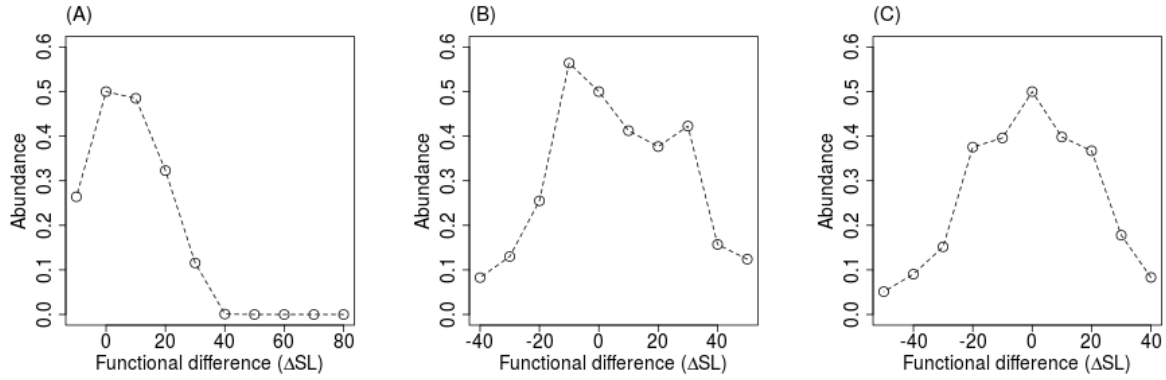

SUPPLEMENTARY INFORMATION

Tab. S1. Average plant functional traits remaining constant across the ten species referenced in Table 1. The chosen values and their justification are provided.

Symbols	Meaning	Mean values	References
	Plant structural traits		
$B_{r,0}$	Initial root biomass	0.02 g	Shipley & Meziane (2002)
SRR_0	Initial shoot-root ratio	2.5	Shipley & Meziane (2002)
ρ_r, ρ_s	Root and shoot density	0.15; 0.40 g.cm^{-3}	Craine et al. (2002)
a_r, b_r	Allometric coefficients for rooting zone volume	4; 1	Fox et al. (1984)
a_s, b_s	Allometric coefficients for shoot volume	10; 1	Andariese & Covington (1986)
	Aboveground plant traits		
A_{max}	Gross CO2 assimilation rate in optimal conditions	13.5 µmol.m^{-2}.s^{-1}	Reich et al. (2003)
g_{low}	Conductance threshold below which the ratio $C_i(t)/C_a(t)$ decreases	0.010 mol. m^{-2}.s^{-1}	Baldocchi (1994)
k	Light extinction coefficient	0.5	Anten et al. (1998)
LNC_{max}	LNC inducing optimal photosynthesis	3.85 %	Reich et al. (2003)
LNC_{min}	LNC below which photosynthetic activity stops	2.25 %	Sage & Pearcy (1987)
$R_{d,r}$	Root maintenance respiration rate	36 nmol.g^{-1}.s^{-1}	Reich et al. (2003)
$R_{d,sh}$	Shoot maintenance respiration rate	34.5 nmol.g^{-1}.s^{-1}	Reich et al. (2003)
SLA	Specific leaf area	320 cm^2.g^{-1}	Reich et al. (2003)
SLL	Shoot lifespan	60 d	Ryser & Urbas (2000)
T_{min}	Temperature threshold below which photosynthesis efficiency is null	0 °C	-
T_{opt}	Temperature threshold above which photosynthesis efficiency is maximal	20 °C	-
Y	Growth efficiency	0.8	Johnson (2008)
α	Photosynthetic efficiency	0.05 µmol.µmol^{-1}	Ehleringer & Pearcy (1983)
β	Curvature parameter for the light response curve	0.85	Jones (1988)
λ_N	Nitrogen fraction allocated to aboveground organs	0.6	Reich et al. (2003)
χ	Value of the ratio $C_i(t)/C_a(t)$ when $g_{CO2}(t)$ is larger than g_{low}	0.6	Baldocchi (1994)
χ_{up}	Value of the ratio $C_i(t)/C_a(t)$ when $g_{CO2}(t)$ equals g_{min}	2	Baldocchi (1994)

	Belowground plant organs traits		
K_N	Michaelis-Menten constant for nitrogen uptake	$3.5.10^{-4}$ mg.cm^{-3}	Leadley et al. (1997)
RLL	Root lifespan	650 d	Tjoelker et al. (2005)
NRE	Nitrogen resorption efficiency	60%	Huang et al. (2008)
$U_{N,max}$	Nitrogen uptake rate in optimal conditions	0.515 mg.g^{-1}.h^{-1}	Maire et al. (2009)
$U_{W,max}$	Water uptake rate in optimal conditions	6 cm^3.g^{-1}.d^{-1}	Hunt et al. (1991)

Fig. S2. Relationship between the final relative abundance of a species *i* and its functional distance (ΔSL) with a reference species *j* in the three environmental scenarios. First, second and third column panels correspond to the three environmental scenarios respectively. Each line corresponds to a different reference species *j*, from virtual species 1 to virtual species 10 (see Tab. 1).

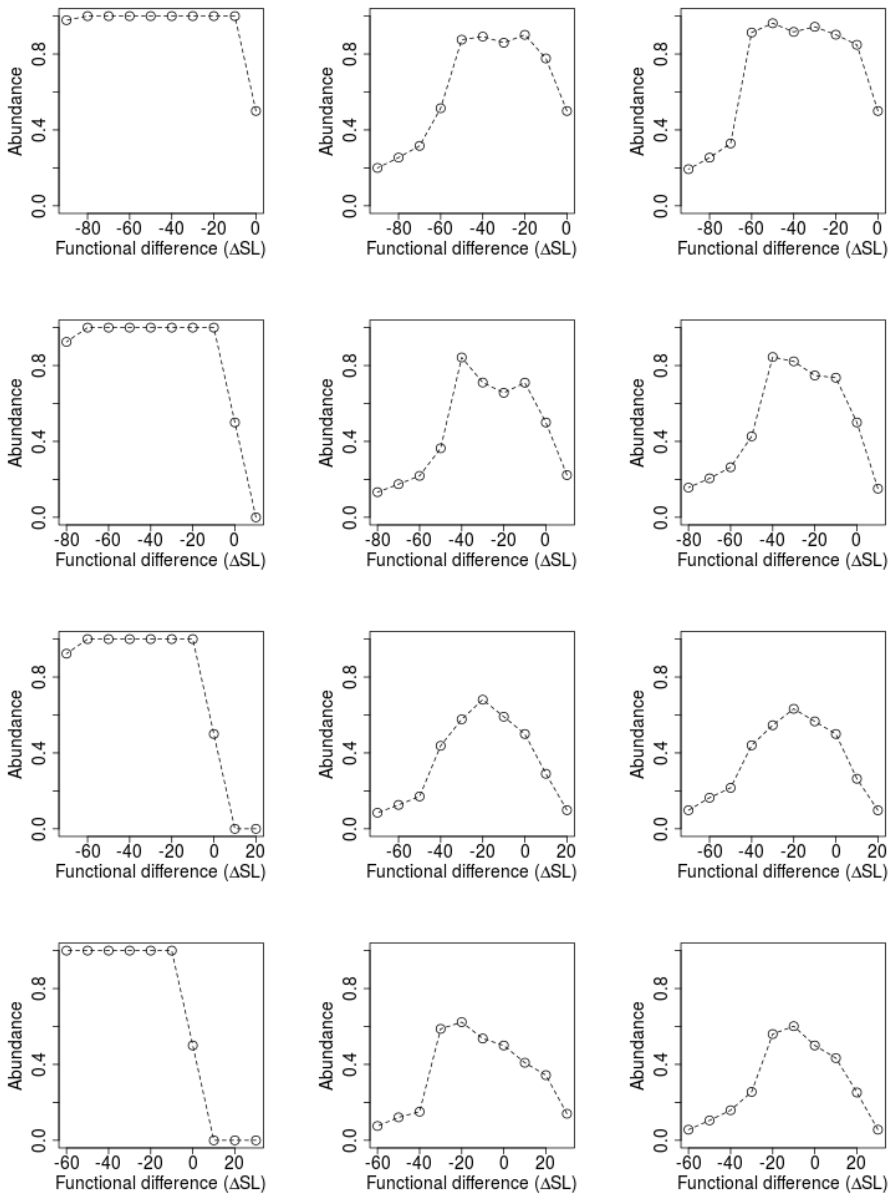

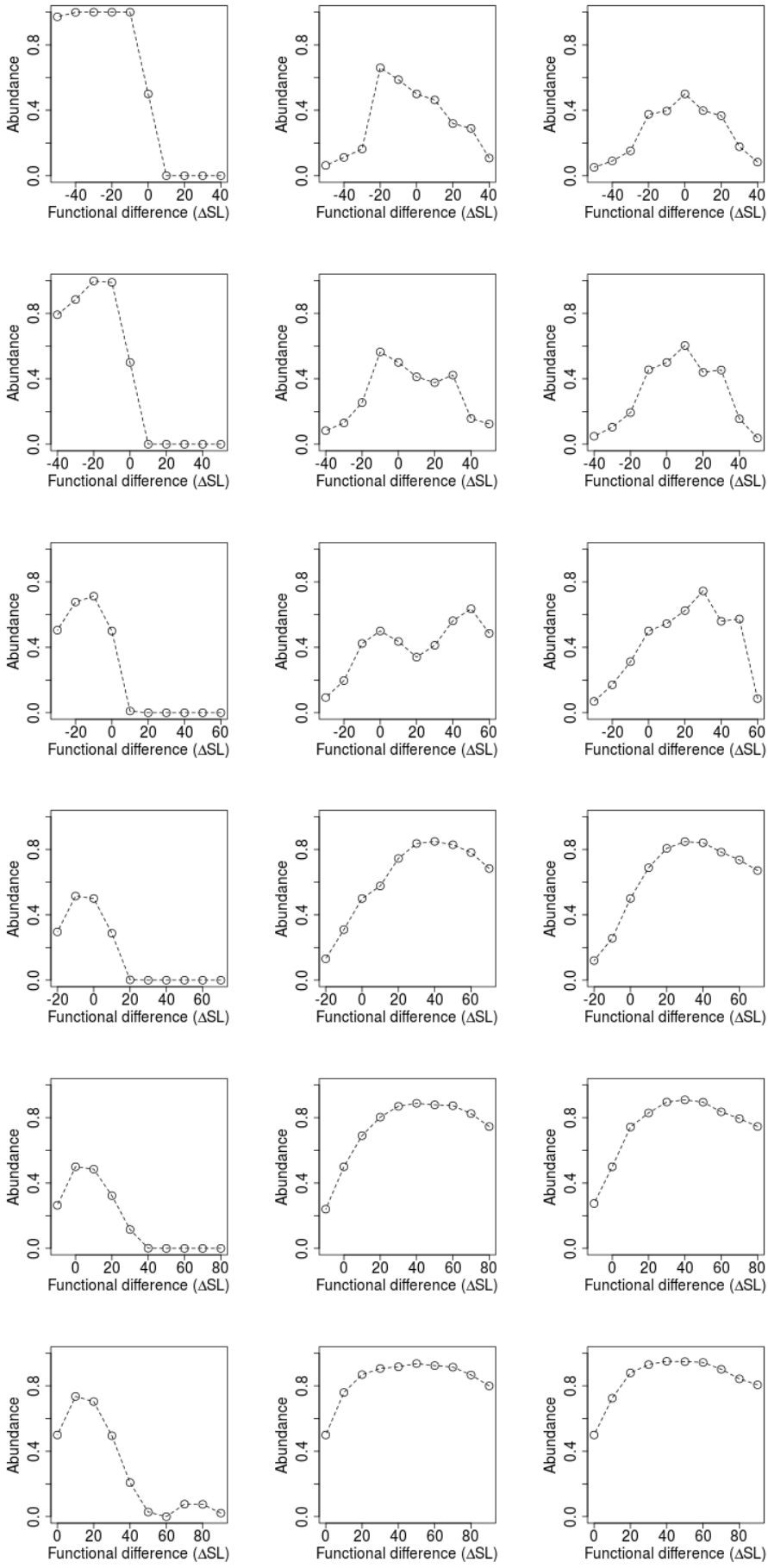
Abundance
Functional difference (ΔSL)

VII. Discussion

L'objectif scientifique de cette thèse est de montrer que l'information contenue dans les traits fonctionnels des espèces végétales prairiales peut être intégrée au sein de modèles mécanistes et que ces nouvelles approches de modélisation peuvent être utilisées pour améliorer notre compréhension des mécanismes gouvernant les dynamiques des communautés végétales. Deux approches ont été mises en oeuvre: la première décrit les dynamiques des populations végétales formant une communauté en intégrant l'impact des variations environnementales et démographiques à travers des termes stochastiques et les interactions intra- et interspécifiques à l'aide de coefficients empiriques. Cette approche a été appliquée aux communautés prairiales expérimentales mises en place dans le cadre de l'expérience sur la biodiversité de Jena en Allemagne (Weigelt et al. 2010) pour quantifier l'impact des variabilités environnementale et démographique ainsi que des interactions compétitives sur les dynamiques temporelles de ces communautés (Chapitre III). La seconde s'appuie sur une représentation individu-centrée des communautés végétales, chaque individu étant défini à travers un ensemble de traits fonctionnels qui détermine sa réponse aux variations des conditions environnementales. Cette approche s'appuie sur la théorie de l'allocation optimale (Poorter et al., 2012) pour définir la répartition des carbohydrates entre les différentes parties de la plante. La première étape a été de vérifier que cette théorie pouvait effectivement servir de base à un modèle de croissance végétal réaliste. Une version préliminaire du modèle Nemossos a été utilisée pour simuler la croissance de différentes espèces et les relations allométriques ainsi prédites ont été comparées à des données empiriques (Shipley & Meziane,

2002) (Chapitre IV). Le modèle a ensuite été spatialisé, enrichi de processus supplémentaires et relié à un modèle de sol. Dans la suite c'est cette version complète du modèle que nous appellerons Nemossos. D'abord nous nous sommes assurés que le modèle individu-centré Nemossos reproduisait fidèlement la réponse d'une communauté monospécifique virtuelle à divers facteurs environnementaux. Puis nous avons vérifié que les prédictions du modèle concernant la relation entre la composition fonctionnelle d'une communauté polyspécifique et la productivité de son habitat était conforme aux observations empiriques (Chapitre V). Enfin le modèle Nemossos a été utilisé pour quantifier l'impact de la variabilité environnementale temporelle sur les dynamiques de communautés polyspécifiques variant par leur composition fonctionnelle (Chapitre VI).

Grâce à la méthode d'inférence développée pour l'estimation des paramètres démographiques du modèle stochastique, il a été possible de calibrer le modèle à partir de séries temporelles de biomasse décrivant la dynamique de communautés monospécifiques. Ainsi paramétré, le modèle reproduit fidèlement les dynamiques des communautés monospécifiques tandis que la précision des prédictions relatives aux dynamiques de communautés polyspécifiques est altérée par l'hypothèse simplificatrice de compétition symétrique. Pour pouvoir relâcher cette hypothèse et utiliser notre cadre de modélisation stochastique pour prédire et analyser les dynamiques de communautés polyspécifiques, il est nécessaire de développer un méthode permettant d'estimer les paramètres de compétition. Les méthodes d'inférence Bayésienne de type ABC ("Approximate Bayesian Computation", Beaumont et al., 2002) fournissent une excellente base pour mettre en place ce type de procédure. De plus l'estimation des paramètres de compétition permettrait d'explorer la relation entre l'intensité des interactions interspécifiques et les traits fonctionnels des espèces (Gross et al., 2009).

Grâce à sa relative simplicité, le modèle stochastique peut facilement être appliqué à des systèmes réels. Cependant comme les processus physiologiques gouvernant la croissance des végétaux et leur modification par les facteurs externes ne sont pas explicitement représentés, certains mécanismes ne peuvent être élucidés à l'aide de ce modèle. Pour aller plus loin dans la compréhension des dynamiques des communautés, nous avons donc développé un modèle individu-centré basé sur les traits fonctionnels appelé Nemossos. Après s'être assuré que les sous-modèles sélectionnés pour représenter la mécanique de la plante permettaient une reproduction fidèle de la croissance végétale, nous avons utilisé Nemossos pour étudier les mécanismes favorisant la coexistence d'espèces fonctionnellement différentes. Ces travaux ont notamment permis de mettre en évidence l'importance de la variabilité temporelle intra-sainsonnière dans le maintien de la diversité.

Malgré la grande diversité des processus physiologiques et des facteurs abiotiques intégrés dans le modèle Nemossos, certains mécanismes susceptibles de significativement affecter les dynamiques des communautés végétales ne sont pas pris en compte. Ainsi, contrairement à de nombreux modèles de dynamiques des communautés qui concentrent leur attention sur l'établissement et la reproduction des espèces végétales (Maarel & Sykes, 1993; Hubbell, 2001; Tilman, 2004), Nemossos accorde une place centrale à la phase végétative. Par ailleurs la phénologie des espèces n'est pas prise en compte dans Nemossos et il ne peut donc pas être utilisé pour étudier l'impact de phénomènes tels que la différentiation temporelle de niche (Grubb, 1977; Wolkovich & Cleland, 2010) sur les dynamiques des communautés végétales. Enfin Nemossos suppose que toutes les ressources extraites par les plantes sont directement investies dans la croissance et ne peut donc capturer l'impact du stockage de ces ressources (Stitt & Schulze, 1994; Suzuki & Stuefer, 1999) sur les dynamiques des communautés. Malgré les limites actuelles du modèle, les travaux s'appuyant sur Nemossos mettre en

évidence le potentiel explicatif d'un modèle individu-centré exclusivement basé sur les traits fonctionnels des végétaux. De plus le cadre de modélisation développé est très flexible et peut facilement être enrichie par de nouveaux sous-modèles. Il constitue ainsi une base solide pour l'exploration des mécanismes gouvernant les dynamiques des communautés végétales.

Les analyses menées sur les communautés expérimentales de l'expérience sur la biodiversité de Jena ont montré qu'il n'existait pas de relation simple entre les attributs fonctionnels des espèces et leurs paramètres démographiques. Ce résultat suggère que les processus physiologiques gouvernant la croissance des individus composant les populations interagissent de manière non linéaire. Cela ne signifie pas pour autant que les relations entre les traits fonctionnels et les paramètres démographiques d'une espèce ne peuvent pas être décrites à l'aide de modèle plus complexes. Mais plutôt que l'approche empirique classique consistant à ajuster des relations relativement simples (e.g. linéaire, loi de puissance) en s'appuyant sur des données de terrains n'est pas suffisante pour les mettre en évidence. Parce qu'il permet de faire le lien entre les attributs fonctionnels individuels et les dynamiques des populations, le modèle Nemossos pourra être utilisé pour explorer ces relations. Par ailleurs c'est un outil qui pourra servir à valider ou infirmer des hypothèses couramment admises en modélisation stochastique des dynamiques de populations, telles que la normalité de la distribution des variables environnementales ou encore la forme logistique de la fonction de croissance. Ainsi au lieu de nourrir le débat sur le rapport entre la complexité des modèle et la généralité de leur prédictions (Grimm, 1999; DeAngelis & Mooji, 2005; Evans et al., 2013), nous proposons de réconcilier les deux types d'approche pour développer des modèles de complexité intermédiaire plus réalistes, notamment grâce à la mise en relation directe des paramètres du modèle avec le fonctionnement des plantes.

De manière plus générale, la variété des processus physiologiques et des facteurs abiotiques pris en compte dans Nemossos ainsi que le nombre réduit de traits fonctionnels nécessaire à sa paramétrisation en font un outil idéal pour aborder diverses questions théoriques en écologie des communautés. L'étude des mécanismes favorisant la coexistence d'espèces fonctionnellement différentes (Chapitre VI) constitue une bonne illustration des expériences numériques pouvant être mis en oeuvre pour répondre à ces questions à l'aide de Nemossos. Il existe de nombreux autres patterns dont les mécanismes sous-jacents n'ont pas encore été élucidés, comme la variation de l'intensité des interactions compétitives avec la productivité de l'habitat (Goldberg & Barton, 1992; Carlyle, 2010), le rôle de la variabilité fonctionnelle intraspécifique dans les dynamiques des communautés (Jung et al., 2010; Violle et al., 2012) ou encore la relation entre diversité fonctionnelle et productivité de la communauté (Cardinale et al., 2007; Cadotte et al., 2009). Par ailleurs Nemossos possède toutes les caractéristiques nécessaires pour produire des prévisions relatives aux variations de la composition fonctionnelle des communautés végétales induites par des changements climatiques tels que l'augmentation de la température, la diminution des précipitations ou encore l'augmentation de la concentration atmosphérique en dioxyde de carbone (Woodward & Cramer, 1996; McMahon et al., 2011). Enfin Nemossos fournit un cadre de modélisation flexible au sein duquel divers mécanismes supplémentaires peuvent être intégrés en vu de tester leur impact sur les dynamiques des communautés. On peut par exemple envisager d'utiliser Nemossos comme base pour étudier l'impact des différences phénologiques interspécifiques sur la coexistence des espèces (Fargione & Tilman, 2005).

Bibliographie

Abrahams, C. (2008). Climate change and lakeshore conservation: a model and review of management techniques. In *Ecological Effects of Water-Level Fluctuations in Lakes* (pp. 33-43). Springer Netherlands.

Abrams, P. A. (1988). Resource productivity-consumer species diversity: simple models of competition in spatially heterogeneous environments. *Ecology*, 1418-1433.

Adler, P. B., HilleRisLambers, J., Kyriakidis, P. C., Guan, Q., & Levine, J. M. (2006). Climate variability has a stabilizing effect on the coexistence of prairie grasses. *Proceedings of the National Academy of Sciences*, *103*(34), 12793-12798.

Aerts, R., & Chapin III, F. S. (2000). The mineral nutrition of wild plants revisited. *Adv Ecol Res*, *30*, 1-67.

Albert, C. H., Thuiller, W., Yoccoz, N. G., Douzet, R., Aubert, S., & Lavorel, S. (2010). A multi‐trait approach reveals the structure and the relative importance of intra‐vs. interspecific variability in plant traits. *Functional Ecology*, *24*(6), 1192-1201.

Alonso, D., Etienne, R. S., & McKane, A. J. (2006). The merits of neutral theory. *Trends in ecology & evolution*, *21*(8), 451-457.

Amarasekare, P. (2003). Competitive coexistence in spatially structured environments: a synthesis. *Ecology Letters*, *6*(12), 1109-1122.

Armstrong, R. A., & McGehee, R. (1980). Competitive exclusion. *American Naturalist*, 151-170.

Atkin, O. K., Scheurwater, I., & Pons, T. L. (2006). High thermal acclimation potential of both photosynthesis and respiration in two lowland Plantago species in contrast to an alpine congeneric. *Global Change Biology*, *12*(3), 500-515.

Austin, M. P., Nicholls, A. O., & Margules, C. R. (1990). Measurement of the realized qualitative niche: environmental niches of five Eucalyptus species. *Ecological monographs*, *60*(2), 161-177.

Barot, S. (2004). Mechanisms promoting plant coexistence: can all the proposed processes be reconciled?. *Oikos*, *106*(1), 185-192.

Beadle, N. C. W. (1966). Soil phosphate and its role in molding segments of the Australian flora and vegetation, with special reference to xeromorphy and sclerophylly. *Ecology*, 992-1007.

Bengtsson, J., Fagerström, T., & Rydin, H. (1994). Competition and coexistence in plant communities. *Trends in ecology & evolution*, *9*(7), 246-250.

Bertness, M. D., & Callaway, R. (1994). Positive interactions in communities. *Trends in Ecology & Evolution*, *9*(5), 191-193.

Bertness, M. D., & Hacker, S. D. (1994). Physical stress and positive associations among marsh plants. *American Naturalist*, 363-372.

Björkman, O. (1981). Responses to different quantum flux densities. In *Physiological plant ecology I* (pp. 57-107). Springer Berlin Heidelberg.

Boatman, N. D., Jones, N. E., Conyers, S. T., & Pietravalle, S. (2011). Development of plant communities on set-aside in England. *Agriculture, ecosystems & environment*, *143*(1), 8-19.

Bowes, M. D., & Sedjo, R. A. (1993). Paper 3. impacts and responses to climate change in forests of the mink region. *Climatic Change*, *24*(1-2), 63-82.

Bowes, G. (1996). Photosynthetic responses to changing atmospheric carbon dioxide concentration. In *Photosynthesis and the Environment* (pp. 387-407). Springer Netherlands.

Braun-Blanquet, J., Mayor, E., Fischer, E., & Cruchet, P. (1918). *Eine pflanzengeographische Exkursion durchs Unterengadin und in den schweizerischen Nationalpark*. Rascher.

Braun-Blanquet, J. (1932). Plant sociology. The study of plant communities. *Plant sociology. The study of plant communities. First ed.*

Bray, J. R., & Curtis, J. T. (1957). An ordination of the upland forest communities of southern Wisconsin. *Ecological monographs*, *27*(4), 325-349.

Brooker, R. W., & Callaghan, T. V. (1998). The balance between positive and negative plant interactions and its relationship to environmental gradients: a model. *Oikos*, 196-207.

Bruno, J. F., Stachowicz, J. J., & Bertness, M. D. (2003). Inclusion of facilitation into ecological theory. *Trends in Ecology & Evolution*, *18*(3), 119-125.

Bugmann, H. (2001). A review of forest gap models. *Climatic Change*, *51*(3-4), 259-305.

Caccianiga, M., Luzzaro, A., Pierce, S., Ceriani, R. M., & Cerabolini, B. (2006). The functional basis of a primary succession resolved by CSR classification. *Oikos*, *112*(1), 10-20.

Callaway, R. M. (1998). Competition and facilitation on elevation gradients in subalpine forests of the northern Rocky Mountains, USA. *Oikos*, 561-573.

Carey, P. D. (1996). DISPERSE: a cellular automaton for predicting the distribution of species in a changed climate. *Global Ecology and Biogeography Letters*, 217-226.

Cannell, M. G., & Dewar, R. C. (1994). Carbon allocation in trees: a review of concepts for modelling. *Advances in ecological research*, *25*, 59-104.

Carlyle, C. N., Fraser, L. H., & Turkington, R. (2010). Using three pairs of competitive indices to test for changes in plant competition under different resource and disturbance levels. *Journal of Vegetation Science*, *21*(6), 1025-1034.

Caswell, H. (2001). *Matrix population models*. John Wiley & Sons, Ltd.

Cerabolini, B. E., Brusa, G., Ceriani, R. M., De Andreis, R., Luzzaro, A., & Pierce, S. (2010). Can CSR classification be generally applied outside Britain?. *Plant Ecology*, *210*(2), 253-261.

Chapin III, F. S. (1980). The mineral nutrition of wild plants. *Annual review of ecology and systematics*, 233-260.

Charles-Edwards, D. A. (1976). Shoot and root activities during steady-state plant growth. *Annals of Botany*, *40*(4), 767-772.

Chave, J. (2004). Neutral theory and community ecology. *Ecology letters*, *7*(3), 241-253.

Chazdon, R. L., & Field, C. B. (1987). Determinants of photosynthetic capacity in six rainforest Piper species. *Oecologia*, *73*(2), 222-230.

Chesson, P. L., & Warner, R. R. (1981). Environmental variability promotes coexistence in lottery competitive systems. *American Naturalist*, 923-943.

Chesson, P. (1990). MacArthur's consumer-resource model. *Theoretical Population Biology*, *37*(1), 26-38.

Chesson, P. (1994). Multispecies competition in variable environments. *Theoretical Population Biology*, *45*(3), 227-276.

Chesson, P. (2000). Mechanisms of maintenance of species diversity. *Annual review of Ecology and Systematics*, 343-366.

Cleveland, C. C., Townsend, A. R., Schimel, D. S., Fisher, H., Howarth, R. W., Hedin, L. O., ... & Wasson, M. F. (1999). Global patterns of terrestrial biological nitrogen (N2) fixation in natural ecosystems. *Global biogeochemical cycles*, *13*, 623.

Coffin, D. P., & Lauenroth, W. K. (1990). A gap dynamics simulation model of succession in a semiarid grassland. *Ecological Modelling*, *49*(3), 229-266.

Colasanti, R. L., & Grime, J. P. (1993). Resource dynamics and vegetation processes: a deterministic model using two-dimensional cellular automata. *Functional Ecology*, 169-176.

Coley, P. D. (1988). Effects of plant growth rate and leaf lifetime on the amount and type of anti-herbivore defense. *Oecologia*, *74*(4), 531-536.

Condit, R., Pitman, N., Leigh, E. G., Chave, J., Terborgh, J., Foster, R. B., ... & Muller-Landau, H. C. (2002). Beta-diversity in tropical forest trees. *Science*, *295*(5555), 666-669.

Cornelissen, J. H. C., Lavorel, S., Garnier, E., Diaz, S., Buchmann, N., Gurvich, D. E., ... & Pausas, J. G. (2003). A handbook of protocols for standardised and easy measurement of plant functional traits worldwide. *Australian journal of Botany*, *51*(4), 335-380.

Craine, J. M., Froehle, J., Tilman, D. G., Wedin, D. A., & Chapin III, F. S. (2001). The relationships among root and leaf traits of 76 grassland species and relative abundance along fertility and disturbance gradients. *Oikos*, *93*(2), 274-285.

Craine, J. M., Tilman, D., Wedin, D., Reich, P., Tjoelker, M., & Knops, J. (2002). Functional traits, productivity and effects on nitrogen cycling of 33 grassland species. *Functional Ecology*, *16*(5), 563-574.

Craine, J. M. (2005). Reconciling plant strategy theories of Grime and Tilman. *Journal of ecology*, *93*(6), 1041-1052.

Craine, J. M., Morrow, C., & Fierer, N. (2007). Microbial nitrogen limitation increases decomposition. *Ecology*, *88*(8), 2105-2113.

Crawley, M. J., & May, R. M. (1987). Population dynamics and plant community structure: competition between annuals and perrenials. *Journal of theoretical Biology*, *125*(4), 475-489.

Cunningham, S. A., Summerhayes, B., & Westoby, M. (1999). Evolutionary divergences in leaf structure and chemistry, comparing rainfall and soil nutrient gradients. *Ecological Monographs*, *69*(4), 569-588.

Curtis, J. T., & McIntosh, R. P. (1951). An upland forest continuum in the prairie-forest border region of Wisconsin. *Ecology*, 476-496.

Darwin, C. (1859). *On the origin of the species by natural selection*.

Daubenmire, R. (1966). Vegetation: identification of typal communities. *Science*, *151*(3708), 291-298.

De Mazancourt, C., Isbell, F., Larocque, A., Berendse, F., Luca, E., Grace, J. B., ... & Tilman, D. (2013). Predicting ecosystem stability from community composition and biodiversity. *Ecology Letters*, *16*(5), 617-625.

Diaz, S., Cabido, M., & Casanoves, F. (1998). Plant functional traits and environmental filters at a regional scale. *Journal of Vegetation Science*, *9*(1), 113-122.

Diaz, S., Hodgson, J. G., Thompson, K., Cabido, M., Cornelissen, J. H. C., Jalili, A., ... & Band, S. R. (2004). The plant traits that drive ecosystems: evidence from three continents. *Journal of vegetation science*, *15*(3), 295-304.

Dytham, C. (1995). The effect of habitat destruction pattern on species persistence: a cellular model. *Oikos*, 340-344.

Easterling, M. R., Ellner, S. P., & Dixon, P. M. (2000a). Size-specific sensitivity: applying a new structured population model. *Ecology*, *81*(3), 694-708.

Easterling, M. R., & Ellner, S. P. (2000b). Dormancy strategies in a random environment: comparing structured and unstructured models. *Evolutionary Ecology Research*, *2*(4), 387-407.

Elton, C. (1927). Animal ecology. 207 pp. *Sidgwick & Jackson, LTD. London*.

Engels, C., Neumann, G., Gahoonia, T. S., George, E., & Schenk, M. (2000). Assessing the ability of roots for nutrient acquisition. In *Root Methods* (pp. 403-459). Springer Berlin Heidelberg.

Enquist, B. J., Brown, J. H., & West, G. B. (1998). Allometric scaling of plant energetics and population density. *Nature*, *395*(6698), 163-165.

Enquist, B. J., Economo, E. P., Huxman, T. E., Allen, A. P., Ignace, D. D., & Gillooly, J. F. (2003). Scaling metabolism from organisms to ecosystems. *Nature*, *423*(6940), 639-642.

Enquist, B. J., West, G. B., & Brown, J. H. (2009). Extensions and evaluations of a general quantitative theory of forest structure and dynamics. *Proceedings of the National Academy of Sciences*, *106*(17), 7046-7051.

Enquist, B. J., Norberg, J., Bonser, S. P., Violle, C., Webb, C. T., Henderson, A., ... & Savage, V. M. (2015). Scaling from traits to ecosystems: Developing a general Trait Driver Theory via integrating trait-based and metabolic scaling theories. *Advances in Ecological Research*.

Epstein, E. (1972). *Mineral nutrition of plants: principles and perspectives*.

Evans, J. R. (1989). Photosynthesis and nitrogen relationships in leaves of C3 plants. *Oecologia*, *78*(1), 9-19.

Evans, M. R., Grimm, V., Johst, K., Knuuttila, T., de Langhe, R., Lessells, C. M., ... & Wilkinson, D. J. (2013). Do simple models lead to generality in ecology?. *Trends in ecology & evolution*, *28*(10), 578-583.

Fargione, J., & Tilman, D. (2006). Plant species traits and capacity for resource reduction predict yield and abundance under competition in nitrogen‐limited grassland. *Functional Ecology*, *20*(3), 533-540.

Farquhar, G. D., von Caemmerer, S. V., & Berry, J. A. (1980). A biochemical model of photosynthetic CO2 assimilation in leaves of C3 species. *Planta*, *149*(1), 78-90.

Farquhar, G. D., & Sharkey, T. D. (1982). Stomatal conductance and photosynthesis. *Annual review of plant physiology*, *33*(1), 317-345.

Fischlin, A., Bugmann, H., & Gyalistras, D. (1995). Sensitivity of a forest ecosystem model to climate parametrization schemes. *Environmental Pollution*, *87*(3), 267-282.

Field, C. H., & Mooney, H. A. (1986). photosynthesis--nitrogen relationship in wild plants. In *On the economy of plant form and function: proceedings of the Sixth Maria Moors Cabot Symposium, Evolutionary Constraints on Primary Productivity, Adaptive Patterns of Energy Capture in Plants, Harvard Forest, August 1983*. Cambridge: Cambridge University Press.

Fonseca, C. R., Overton, J. M., Collins, B., & Westoby, M. (2000). Shifts in trait‐combinations along rainfall and phosphorus gradients. *Journal of Ecology*, *88*(6), 964-977.

Franklin, O., Johansson, J., Dewar, R. C., Dieckmann, U., McMurtrie, R. E., Brännström, Å., & Dybzinski, R. (2012). Modeling carbon allocation in trees: a search for principles. *Tree Physiology*, tpr138.

Freckleton, R. P., Matos, D. M., Bovi, M. L. A., & Watkinson, A. R. (2003). Predicting the impacts of harvesting using structured population models: the importance of density‐dependence and timing of harvest for a tropical palm tree. *Journal of Applied Ecology*, *40*(5), 846-858.

Frenette‐Dussault, C., Shipley, B., Meziane, D., & Hingrat, Y. (2013). Trait‐based climate change predictions of plant community structure in arid steppes. *Journal of ecology*, *101*(2), 484-492.

Fridley, J. D. (2003). Diversity effects on production in different light and fertility environments: an experiment with communities of annual plants. *Journal of Ecology*, *91*(3), 396-406.

Garnier, E., Cortez, J., Billès, G., Navas, M. L., Roumet, C., Debussche, M., ... & Neill, C. (2004). Plant functional markers capture ecosystem properties during secondary succession. *Ecology*, *85*(9), 2630-2637.

Gignoux, J., Noble, I. R., & Menaut, J. C. (1995). Modelling tree community dynamics in savannas: effects of competition with grasses and impact of disturbance. *Functioning and dynamics of natural and perturbed Ecosystems. Paris: Lavoisier Intercept. p*, 219-30.

Génard, M., Dauzat, J., Franck, N., Lescourret, F., Moitrier, N., Vaast, P., & Vercambre, G. (2008). Carbon allocation in fruit trees: from theory to modelling. *Trees*, *22*(3), 269-282.

Gleason, H. A. (1926). The individualistic concept of the plant association. *Bulletin of the Torrey Botanical Club*, 7-26.

Goldberg, D. E., & Barton, A. M. (1992). Patterns and consequences of interspecific competition in natural communities: a review of field experiments with plants. *American naturalist*, 771-801.

Goldberg, D. E., Rajaniemi, T., Gurevitch, J., & Stewart-Oaten, A. (1999). Empirical approaches to quantifying interaction intensity: competition and facilitation along productivity gradients. *Ecology*, *80*(4), 1118-1131.

Goodall, D. W. (1954). Objective methods for the classification of vegetation. III. An essay in the use of factor analysis. *Australian Journal of Botany*, *2*(3), 304-324.

Greenlee, J. T., & Callaway, R. M. (1996). Abiotic stress and the relative importance of interference and facilitation in montane bunchgrass communities in western Montana. *American Naturalist*, 386-396.

Grime, J. P. (1977). Evidence for the existence of three primary strategies in plants and its relevance to ecological and evolutionary theory. *American naturalist*, 1169-1194.

Grime, J. P. (1979). *Plant strategies, vegetation processes, and ecosystem properties*. John Wiley & Sons.

Grime, J. P. (1998). Benefits of plant diversity to ecosystems: immediate, filter and founder effects. *Journal of Ecology*, *86*(6), 902-910.

Grime, J. P., Brown, V. K., Thompson, K., Masters, G. J., Hillier, S. H., Clarke, I. P., ... & Kielty, J. P. (2000). The response of two contrasting limestone grasslands to simulated climate change. *Science*, *289*(5480), 762-765.

Grime, J. P. (2001). Plant strategies. *Vegetation processes and Ecosystem Properties. 2nd edition, Chichester*.

Gross, N., Kunstler, G., Liancourt, P., De Bello, F., Suding, K. N., & Lavorel, S. (2009). Linking individual response to biotic interactions with community structure: a trait‐based framework. *Functional Ecology*, *23*(6), 1167-1178.

Grubb, P. J. (1977). The maintenance of species-richness in plant communities: the importance of the regeneration niche. *Biol. Rev*, *52*(1), 107-145.

Guisan, A., & Thuiller, W. (2005). Predicting species distribution: offering more than simple habitat models. *Ecology letters*, *8*(9), 993-1009.

Hector, A., Bazeley‐White, E., Loreau, M., Otway, S., & Schmid, B. (2002). Overyielding in grassland communities: testing the sampling effect hypothesis with replicated biodiversity experiments. *Ecology Letters*, *5*(4), 502-511.

Hodgson, J. G., Wilson, P. J., Hunt, R., Grime, J. P., & Thompson, K. (1999). Allocating CSR plant functional types: a soft approach to a hard problem. *Oikos*, 282-294.

Holling, C. S. (1966). The strategy of building models of complex ecological systems. In: *Systems Analysis in Ecology* (Watt, K.E.F., ed.), pp. 195–214, Academic Press.

Holt, R. D. (1983). Optimal foraging and the form of the predator isocline. *American Naturalist*, 521-541.

Holt, R. D. (1984). Spatial heterogeneity, indirect interactions, and the coexistence of prey species. *American Naturalist*, 377-406.

Holt, R. A., & Lawton, J. H. (1994). The ecological consequences of shared natural enemies. *Annual review of Ecology and Systematics*, 495-520.

Holzapfel, C., & Mahall, B. E. (1999). Bidirectional facilitation and interference between shrubs and annuals in the Mojave Desert. *Ecology*, *80*(5), 1747-1761.

Hubbell, S. P. (1979). Tree dispersion, abundance, and diversity in a tropical dry forest. *Science*, *203*(4387), 1299-1309.

Hubbell, S. P. (1997). A unified theory of biogeography and relative species abundance and its application to tropical rain forests and coral reefs. *Coral reefs*, *16*(1), S9-S21.

Hubbell, S. P. (2001). *The unified neutral theory of biodiversity and biogeography (MPB-32)* (Vol. 32). Princeton University Press.

Humphries, H. C., Coffin, D. P., & Lauenroth, W. K. (1996). An individual-based model of alpine plant distributions. *Ecological modelling*, *84*(1), 99-126.

Hutchinson, G. E. (1957). Concluding remarks. In *Cold Spring Harbor symposia on quantitative biology* (Vol. 22, pp. 415-427). Cold Spring Harbor Laboratory Press.

Ives, A. R., Klug, J. L., & Gross, K. (2000). Stability and species richness in complex communities. *Ecology Letters*, *3*(5), 399-411.

Ives, A. R., Dennis, B., Cottingham, K. L., & Carpenter, S. R. (2003). Estimating community stability and ecological interactions from time-series data. *Ecological monographs*, *73*(2), 301-330.

Jabot, F., & Pottier, J. (2012). A general modelling framework for resource‐ratio and CSR theories of plant community dynamics. *Journal of Ecology*, *100*(6), 1296-1302.

Jassby, A.D., & Platt, T. (1976). Mathematical formulation of the relationship between photosynthesis and light for phytoplankton. *Limnology and Oceanography, 21*, 540-547.

Kattge, J., Diaz, S., Lavorel, S., Prentice, I. C., Leadley, P., Bönisch, G., ... & Cornelissen, J. H. (2011). TRY–a global database of plant traits. *Global change biology*, *17*(9), 2905-2935.

Keane, R. E., Arno, S. F., & Brown, J. K. (1990). Simulating cumulative fire effects in ponderosa pine/Douglas-fir forests. *Ecology*, 189-203.

Keddy, P. A. (1992). Assembly and response rules: two goals for predictive community ecology. *Journal of Vegetation Science*, *3*(2), 157-164.

Kellomäki, S., & Kolström, M. (1992). Simulation of tree species composition and organic matter accumulation in Finnish boreal forests under changing climatic conditions. *Vegetatio*, *102*(1), 47-68.

Lamarck, J. (1809). *Philosophie zoologique: ou exposition des considérations relatives a lahistoire naturelle des animaux*.

Lambdon, P. W., Lloret, F., & Hulme, P. E. (2008). Do alien plants on Mediterranean islands tend to invade different niches from native species?. *Biological Invasions*, *10*(5), 703-716.

Lambers, H., Chapin III, F. S., & Pons, T. L. (2008). *Plant Physiological Ecology*. Springer Science & Business Media.

Landhäusser, S. M., & Lieffers, V. J. (2001). Photosynthesis and carbon allocation of six boreal tree species grown in understory and open conditions. *Tree physiology*, *21*(4), 243-250.

Laughlin, D. C., Fule, P. Z., Huffman, D. W., Crouse, J., & Laliberte, E. (2011). Climatic constraints on trait‐based forest assembly. *Journal of Ecology*, *99*(6), 1489-1499.

Laughlin, D. C., Joshi, C., Bodegom, P. M., Bastow, Z. A., & Fulé, P. Z. (2012). A predictive model of community assembly that incorporates intraspecific trait variation. *Ecology Letters*, *15*(11), 1291-1299.

Lavorel, S., & Garnier, E. (2002). Predicting changes in community composition and ecosystem functioning from plant traits: revisiting the Holy Grail. *Functional ecology*, *16*(5), 545-556.

Lehsten, V., & Kleyer, M. (2007). Turnover of plant trait hierarchies in simulated community assembly in response to fertility and disturbance. *Ecological Modelling*, *203*(3), 270-278.

Leibold, M. A. (1998). Similarity and local co-existence of species in regional biotas. *Evolutionary Ecology*, *12*(1), 95-110.

Leishman, M. R., & Murray, B. R. (2001). The relationship between seed size and abundance in plant communities: model predictions and observed patterns. *Oikos*, *94*(1), 151-161.

Linares, C., Coma, R., & Zabala, M. (2008). Restoration of threatened red gorgonian populations: an experimental and modelling approach. *Biological Conservation*, *141*(2), 427-437.

Lindner, M., Lasch, P., & Erhard, M. (2000). Alternative forest management strategies under climatic change-prospects for gap model applications in risk analyses. *Silva Fennica*, *34*(2), 101-111.

Loreau, M., & de Mazancourt, C. (2008). Species synchrony and its drivers: neutral and nonneutral community dynamics in fluctuating environments. *The American Naturalist*, *172*(2), E48-E66.

Lotka, A. J. (1932). The growth of mixed populations: two species competing for a common food supply. *Journal of the Washington Academy of Sciences*, 22, 461-469.

MacArthur, R. H., & Wilson, E. O. (1967). *The theory of island biogeography* (Vol. 1). Princeton University Press.

MacArthur, R., & Levins, R. (1967). The limiting similarity, convergence, and divergence of coexisting species. *American naturalist*, 377-385.

MacArthur, R. H. (1972). *Geographical ecology: patterns in the distribution of species*. Princeton University Press.

Marks, C. O., & Lechowicz, M. J. (2006). Alternative designs and the evolution of functional diversity. *The American Naturalist*, *167*(1), 55-66.

Marks, C.O, & Muller-Landau, H.C. (2007). Comment on "From plant traits to plant communities: A statistical mechanistic approach to biodiversity". *Science, 316*(5830), 1425.

May, R. M., & Leonard, W. J. (1975). Nonlinear aspects of competition between three species. *SIAM Journal on Applied Mathematics*, *29*(2), 243-253.

McGill, B. J. (2003). A test of the unified neutral theory of biodiversity. *Nature*, *422*(6934), 881-885.

McGill, B. J., Enquist, B. J., Weiher, E., & Westoby, M. (2006). Rebuilding community ecology from functional traits. *Trends in ecology & evolution*, *21*(4), 178-185.

McIntosh, R. P. (1967). The continuum concept of vegetation. *The Botanical Review*, *33*(2), 130-187.

McNickle, G. G., & Dybzinski, R. (2013). Game theory and plant ecology. *Ecology Letters*, *16*(4), 545-555.

Menges, E. S. (2000). Population viability analyses in plants: challenges and opportunities. *Trends in Ecology & Evolution*, *15*(2), 51-56.

Messier, J., McGill, B. J., & Lechowicz, M. J. (2010). How do traits vary across ecological scales? A case for trait‐based ecology. *Ecology letters*, *13*(7), 838-848.

Miller, T. E., Burns, J. H., Munguia, P., Walters, E. L., Kneitel, J. M., Richards, P. M., ... & Buckley, H. L. (2005). A critical review of twenty years' use of the resource‐ratio theory. *The American Naturalist*, *165*(4), 439-448.

Mohren, G. M., & van de Veen, J. R. (1995). Forest growth in relation to site conditions. Application of the model FORGRO to the Solling spruce site. *Ecological Modelling*, *83*(1), 173-183.

Monk, C. D. (1966). An ecological significance of evergreenness. *Ecology*, *47*(3), 504-505.

Mouquet, N., Moore, J. L., & Loreau, M. (2002). Plant species richness and community productivity: why the mechanism that promotes coexistence matters. *Ecology Letters*, *5*(1), 56-65.

Mouquet, N., Lagadeuc, Y., Devictor, V., Doyen, L., Duputié, A., Eveillard, D., ... & Jabot, F. (2015). Predictive ecology in a changing world. *Journal of Applied Ecology*, 20.

Muko, S., & Iwasa, Y. (2000). Species coexistence by permanent spatial heterogeneity in a lottery model. *Theoretical Population Biology*, *57*(3), 273-284.

Niinemets, Ü. (1999). Research review. Components of leaf dry mass per area–thickness and density–alter leaf photosynthetic capacity in reverse directions in woody plants. *New Phytologist*, *144*(1), 35-47.

Norberg, J., Swaney, D. P., Dushoff, J., Lin, J., Casagrandi, R., & Levin, S. A. (2001). Phenotypic diversity and ecosystem functioning in changing environments: a theoretical framework. *Proceedings of the National Academy of Sciences*, *98*(20), 11376-11381.

Ögren, E., & Evans, J. R. (1993). Photosynthetic light-response curves. *Planta*, *189*(2), 182-190.

Oren, R., Sperry, J. S., Katul, G. G., Pataki, D. E., Ewers, B. E., Phillips, N., & Schafer, K. V. R. (1999). Survey and synthesis of intra-and interspecific variation in stomatal sensitivity to vapour pressure deficit. *Plant Cell and Environment*, *22*(12), 1515-1526.

Pacala, S. W., & Tilman, D. (1994). Limiting similarity in mechanistic and spatial models of plant competition in heterogeneous environments. *American naturalist*, 222-257.

Pierce, S., Luzzaro, A., Caccianiga, M., Ceriani, R. M., & Cerabolini, B. (2007). Disturbance is the principal α‐scale filter determining niche differentiation, coexistence and biodiversity in an alpine community. *Journal of Ecology*, *95*(4), 698-706.

Pierce, S., Brusa, G., Vagge, I., & Cerabolini, B. E. (2013). Allocating CSR plant functional types: the use of leaf economics and size traits to classify woody and herbaceous vascular plants. *Functional Ecology*, *27*(4), 1002-1010.

Poorter, H., Remkes, C., & Lambers, H. (1990). Carbon and nitrogen economy of 24 wild species differing in relative growth rate. *Plant Physiology*, *94*(2), 621-627.

Poorter, H., Niklas, K. J., Reich, P. B., Oleksyn, J., Poot, P., & Mommer, L. (2012). Biomass allocation to leaves, stems and roots: meta‐analyses of interspecific variation and environmental control. *New Phytologist*, *193*(1), 30-50.

Pugnaire, F. I., & Luque, M. T. (2001). Changes in plant interactions along a gradient of environmental stress. *Oikos*, *93*(1), 42-49.

Pysek, P., Prach, K., & Smilauer, P. (1995). Relating invasion success to plant traits: an analysis of the Czech alien flora. *Plant invasions: general aspects and special problems*, 39-60.

Pyšek, P., Sádlo, J., Mandák, B., & Jarošík, V. (2003). Czech alien flora and the historical pattern of its formation: what came first to Central Europe?. *Oecologia*, *135*(1), 122-130.

Pywell, R. F., Bullock, J. M., Roy, D. B., Warman, L. I. Z., Walker, K. J., & Rothery, P. (2003). Plant traits as predictors of performance in ecological restoration. *Journal of applied Ecology*, *40*(1), 65-77.

Ramula, S., Toivonen, E., & Mutikainen, P. (2007). Demographic consequences of pollen limitation and inbreeding depression in a gynodioecious herb. *International journal of plant sciences*, *168*(4), 443-453.

Ramula, S., Knight, T. M., Burns, J. H., & Buckley, Y. M. (2008). General guidelines for invasive plant management based on comparative demography of invasive and native plant populations. *Journal of Applied Ecology*, *45*(4), 1124-1133.

Ramula, S., Rees, M., & Buckley, Y. M. (2009). Integral projection models perform better for small demographic data sets than matrix population models: a case study of two perennial herbs. *Journal of Applied Ecology*, *46*(5), 1048-1053.

Reich, P. B., Walters, M. B., & Ellsworth, D. S. (1997). From tropics to tundra: global convergence in plant functioning. *Proceedings of the National Academy of Sciences*, *94*(25), 13730-13734.

Reich, P. B., Ellsworth, D. S., Walters, M. B., Vose, J. M., Gresham, C., Volin, J. C., & Bowman, W. D. (1999). Generality of leaf trait relationships: a test across six biomes. *Ecology*, *80*(6), 1955-1969.

Reich, P. B., Wright, I. J., Cavender‐Bares, J., Craine, J. M., Oleksyn, J., Westoby, M., & Walters, M. B. (2003). The evolution of plant functional variation: traits, spectra, and strategies. *International Journal of Plant Sciences*, *164*(S3), S143-S164.

Reynolds, H. L., Packer, A., Bever, J. D., & Clay, K. (2003). Grassroots ecology: plant-microbe-soil interactions as drivers of plant community structure and dynamics. *Ecology*, *84*(9), 2281-2291.

Reynolds, J. F., & Chen, J. (1996). Modelling whole-plant allocation in relation to carbon and nitrogen supply: coordination versus optimization: opinion. *Plant and soil*, *185*(1), 65-74.

Rigler, F. H. (1982). Recognition of the possible: an advantage of empiricism in ecology. *Canadian Journal of Fisheries and Aquatic Sciences*, *39*(9), 1323-1331.

Roscher, C., Weigelt, A., Proulx, R., Marquard, E., Schumacher, J., Weisser, W. W., & Schmid, B. (2011). Identifying population‐and community‐level mechanisms of diversity–stability relationships in experimental grasslands. *Journal of Ecology*, *99*(6), 1460-1469.

Roxburgh, S.H., & Mokany, K. (2007). Comment on "From plant traits to plant communities: A statistical mechanistic approach to biodiversity". *Science, 316*(5830), 1425.

Savage, V. M., Webb, C. T., & Norberg, J. (2007). A general multi-trait-based framework for studying the effects of biodiversity on ecosystem functioning. *Journal of theoretical biology*, *247*(2), 213-229.

Sale, P. F. (1977). Maintenance of high diversity in coral reef fish communities. *American Naturalist*, 337-359.

Schenk, H. J., & Mahall, B. E. (2002). Positive and negative plant interactions contribute to a north-south-patterned association between two desert shrub species. *Oecologia*, *132*(3), 402-410.

Schenk, H. J. (2008). Soil depth, plant rooting strategies and species' niches. *New Phytologist*, *178*(2), 223-225.

Schulze, E.-D. (1991). Water and nutrient interactions with plant water stress. In: Response of plants to multiple stresses. H. A. Mooney, W. E. Winner, & E. J. Pell (eds.). Academic Press, San Diego, pp. 89-101.

Schoener, T. W. (1974). Resource partitioning in ecological communities. *Science*, *185*(4145), 27-39.

Shipley, B., Keddy, P. A., Moore, D. R. J., & Lemky, K. (1989). Regeneration and establishment strategies of emergent macrophytes. *The Journal of Ecology*, 1093-1110.

Shipley, B., Vile, D., & Garnier, É. (2006). From plant traits to plant communities: a statistical mechanistic approach to biodiversity. *science*, *314*(5800), 812-814.

Shipley, B., Laughlin, D. C., Sonnier, G., & Otfinowski, R. (2011). A strong test of a maximum entropy model of trait-based community assembly. *Ecology*, *92*(2), 507-517.

Shugart, H. H., & Smith, T. M. (1996). A review of forest patch models and their application to global change research. *Climatic Change*, *34*(2), 131-153.

Silvertown, J., & Law, R. (1987). Do plants need niches? Some recent developments in plant community ecology. *Trends in ecology & evolution*, *2*(1), 24-26.

Silvertown, J., Holtier, S., Johnson, J., & Dale, P. (1992). Cellular automaton models of interspecific competition for space--the effect of pattern on process. *Journal of Ecology*, 527-533.

Silvertown, J. (2004). Plant coexistence and the niche. *Trends in Ecology & Evolution*, *19*(11), 605-611.

Smith, M., Caswell, H., & Mettler-Cherry, P. (2005). Stochastic flood and precipitation regimes and the population dynamics of a threatened floodplain plant. *Ecological Applications*, *15*(3), 1036-1052.

Soares-Filho, B. S., Cerqueira, G. C., & Pennachin, C. L. (2002). DINAMICA—a stochastic cellular automata model designed to simulate the landscape dynamics in an Amazonian colonization frontier. *Ecological modelling*, *154*(3), 217-235.

Soussana, J. F., Maire, V., Gross, N., Bachelet, B., Pagès, L., Martin, R., ... & Wirth, C. (2012). Gemini: A grassland model simulating the role of plant traits for community dynamics and ecosystem functioning. Parameterization and evaluation. *Ecological Modelling*, *231*, 134-145.

Southwood, T. R. E. (1988). Tactics, strategies and templets. *Oikos*, 3-18.

Specht, R. L., & Specht, A. (1989). Canopy structure in Eucalyptus-dominated communities in Australia along climatic gradients. *Acta oecologica. Oecologia plantarum*, *10*(2), 191-213.

Stewart, F. M., & Levin, B. R. (1973). Partitioning of resources and the outcome of interspecific competition: a model and some general considerations. *American Naturalist*, 171-198.

Stein, A., Gerstner, K., & Kreft, H. (2014). Environmental heterogeneity as a universal driver of species richness across taxa, biomes and spatial scales. *Ecology letters*, *17*(7), 866-880.

Suding, K.N., Goldberg, D. E., & Hartman, K. M. (2003). Relationships among species traits: separating levels of response and identifying linkages to abundance. *Ecology*, *84*(1), 1-16.

Swenson, N. G. (2013). The assembly of tropical tree communities–the advances and shortcomings of phylogenetic and functional trait analyses. *Ecography*, *36*(3), 264-276.

Thornley, J. H. M. (1998). Modelling Shoot [ratio] Root Relations: the Only Way Forward?. *Annals of Botany*, *81*(2), 165-171.

Tilman, D. (1980). Resources: a graphical-mechanistic approach to competition and predation. *American Naturalist*, 362-393.

Tilman, D. (1982). *Resource Competition and Community Structure. (Mpb-17)*. Princeton, NJ: Princeton University Press.

Tilman, D. (1988). *Plant strategies and the dynamics and structure of plant communities* (No. 26). Princeton University Press.

Tilman, D. (1990). Constraints and tradeoffs: toward a predictive theory of competition and succession. *Oikos*, 3-15.

Tilman, D. (2004). Niche tradeoffs, neutrality, and community structure: a stochastic theory of resource competition, invasion, and community assembly. *Proceedings of the National Academy of Sciences of the United States of America*, *101*(30), 10854-10861.

Twolan-Strutt, L., & Keddy, P. A. (1996). Above-and belowground competition intensity in two contrasting wetland plant communities. *Ecology*, 259-270.

Valladares, F., Martinez-Ferri, E., Balaguer, L., Perez-Corona, E., & Manrique, E. (2000). Low leaf‐level response to light and nutrients in Mediterranean evergreen oaks: a conservative resource‐use strategy?. *New Phytologist*, *148*(1), 79-91.

van Wijk, M. T., & Rodriguez‐Iturbe, I. (2002). Tree‐grass competition in space and time: Insights from a simple cellular automata model based on ecohydrological dynamics. *Water Resources Research*, *38*(9), 18-1.

Van Wijk, M. T. (2007). Predicting ecosystem functioning from plant traits: results from a multi-scale ecophysiological modeling approach. *Ecological modelling*, *203*(3), 453-463.

Veneklaas, E. J., & Poorter, L. (1998). Growth and carbon partitioning of tropical tree seedlings in contrasting light environments. *Inherent variation in plant growth. Physiological mechanisms and ecological consequences. Leiden, the Netherlands: Backhuys Publishers*, 337-361.

Violle, C., Navas, M. L., Vile, D., Kazakou, E., Fortunel, C., Hummel, I., & Garnier, E. (2007). Let the concept of trait be functional!. *Oikos*, *116*(5), 882-892.

Volkov, I., Banavar, J. R., Hubbell, S. P., & Maritan, A. (2003). Neutral theory and relative species abundance in ecology. *Nature*, *424*(6952), 1035-1037.

Volterra, V. (1928). Variations and fluctuations of the number of individuals in animal species living together. *J. Cons. Int. Explor. Mer*, *3*(1), 3-51.

Walter, D. E., Halliday, R. B., & Lindquist, E. E. (1993). A review of the genus Asca (Acarina: Ascidae) in Australia, with descriptions of three new leaf-inhabiting species. *Invertebrate Systematics*, *7*(6), 1327-1347.

Warren, J., & Topping, C. (2004). A trait specific model of competition in a spatially structured plant community. *Ecological modelling*, *180*(4), 477-485.

Watkinson, A. R. (1980). Density-dependence in single-species populations of plants. *Journal of Theoretical Biology*, *83*(2), 345-357.

Wedin, D. A., & Tilman, D. (1990). Species effects on nitrogen cycling: a test with perennial grasses. *Oecologia*, *84*(4), 433-441.

Weiner, J., & Thomas, S. C. (1986). Size variability and competition in plant monocultures. *Oikos*, 211-222.

Westoby, M. (1998). A leaf-height-seed (LHS) plant ecology strategy scheme. *Plant and soil*, *199*(2), 213-227.

Westoby, M., & Wright, I. J. (2006). Land-plant ecology on the basis of functional traits. *Trends in Ecology & Evolution*, *21*(5), 261-268.

Whitfield, J. (2002). Ecology: neutrality versus the niche. *Nature*, *417*(6888), 480-481.

Whittaker, R. H. (1951). A criticism of the plant association and climatic climax concepts. *Northwest Sci*, *25*, 17-31.

Whittaker, R. H. (1956). Vegetation of the great smoky mountains. *Ecological Monographs*, *26*(1), 1-80.

Whittaker, R. H. (1960). Vegetation of the Siskiyou mountains, Oregon and California. *Ecological monographs*, *30*(3), 279-338.

Whittaker, R. H. (1975). *Communities and ecosystems*. MacMillan Publ. Co., New York.

Wilkie, D. S., & Finn, J. T. (1988). A spatial model of land use and forest regeneration in the Ituri forest of northeastern Zaire. *Ecological Modelling*, *41*(3), 307-323.

Williams, K., Field, C. B., & Mooney, H. A. (1989). Relationships among leaf construction cost, leaf longevity, and light environment in rain-forest plants of the genus Piper. *American naturalist*, 198-211.

Wright, I. J., & Westoby, M. (1999). Differences in seedling growth behaviour among species: trait correlations across species, and trait shifts along nutrient compared to rainfall gradients. *Journal of Ecology*, *87*(1), 85-97.

Wright, I. J., & Westoby, M. (2003). Nutrient concentration, resorption and lifespan: leaf traits of Australian sclerophyll species. *Functional Ecology*, *17*(1), 10-19.

Wright, I. J., Reich, P. B., Westoby, M., Ackerly, D. D., Baruch, Z., Bongers, F., ... & Flexas, J. (2004). The worldwide leaf economics spectrum. *Nature*, *428*(6985), 821-827.

Yıldırım, C., Karavin, N., & Cansaran, A. (2012). Classification and evaluation of some endemic plants from Turkey using Grime's CSR strategies. *EurAsian Journal of BioSciences*, *6*, 97-104.

Yoda, K. (1963). Self-thinning in overcrowded pure stands under cultivated and natural conditions. *Journal of Biology Osaka City University*, *14*, 107-129.